GEOLOGICA ULTRAIECTINA

Mededelingen van de
Faculteit Aardwetenschappen der
Rijksuniversiteit te Utrecht

No. 71

EARLY DIAGENESIS AND AUTHIGENIC MINERAL FORMATION IN ANOXIC SEDIMENTS OF KAU BAY, INDONESIA

JACOBUS B. M. MIDDELBURG

GEOLOGICA ULTRAIECTINA

Mededelingen van de
Faculteit Aardwetenschappen der
Rijksuniversiteit te Utrecht

No. 71

EARLY DIAGENESIS AND AUTHIGENIC MINERAL FORMATION IN ANOXIC SEDIMENTS OF KAU BAY, INDONESIA

CIP-GEGEVENS KONINKLIJKE BIBLIOTHEEK, DEN HAAG.

Middelburg, Jacobus Bernardus Maria

Early diagenesis and authigenic mineral formation in anoxic sediments of Kau Bay, Indonesia / Jacobus Bernardus Maria Middelburg. - [Utrecht: Instituut voor Aardwetenschappen der Rijksuniversiteit Utrecht]. - (Geologica Ultraiectina, ISSN 0072-1026 ; no. 71)
Proefschrift Utrecht. - Met lit. opg. - Met samenvatting in het Nederlands.
ISBN 90-71577-24-4
SISO 566.1 UDC 553.06:551.3.051(594)(043.3)
Trefw.: sedimentologie; Indonesië/ mineralen; Indonesië.

EARLY DIAGENESIS AND AUTHIGENIC MINERAL FORMATION IN ANOXIC SEDIMENTS OF KAU BAY, INDONESIA

VROEGE DIAGENESE EN AUTHIGENE MINERAAL VORMING IN ANOXISCHE SEDIMENTEN VAN DE KAU BAAI, INDONESIË

(MET EEN SAMENVATTING IN HET NEDERLANDS)

PROEFSCHRIFT

TER VERKRIJGING VAN DE GRAAD VAN DOCTOR AAN DE RIJKSUNIVERSITEIT TE UTRECHT OP GEZAG VAN DE RECTOR MAGNIFICUS, PROF. DR. J.A. VAN GINKEL, INGEVOLGE HET BESLUIT VAN HET COLLEGE VAN DEKANEN IN HET OPENBAAR TE VERDEDIGEN OP MAANDAG 26 NOVEMBER 1990 DES NAMIDDAGS TE 2.30 UUR

DOOR

JACOBUS BERNARDUS MARIA MIDDELBURG
GEBOREN OP 6 MEI 1963 TE TWELLO

PROMOTOR: PROF. DR. C.H. VAN DER WEIJDEN
CO-PROMOTOR: DR. G.J. DE LANGE

Aan mijn ouders

Aan Petra

Es ist ein einförmiges Ding um das Menschengeschlecht. Die meisten verarbeiten den grössten Teil der Zeit, um zu leben, und das bisschen, das ihnen von Freiheit übrig bleibt, ängstigt sie so, dass sie alle Mittel aufsuchen, um es loszuwerden.

from: Die Leiden des jungen Werther
by: J.W. Goethe

VOORWOORD

Graag wil ik iedereen bedanken die aan de totstandkoming van dit proefschrift heeft bijgedragen.

Allereerst ben ik dank verschuldigd aan de deelnemers van cruise G4 van de Snellius II expeditie naar de Kau Baai: W. van der Linden, J.W. Zachariasse, A. Meertens, D. M. Barmawidjaja, S. Latiff, H. Sukardjono, S. Hartosukohardjo, G. de Lange, C. van der Weijden, R. van der Weijden, T. Bouten, G. Eussen, S. Shofiyah, D. Hoede, A. Balk, H. van Veen, H. de Porto, T. Buisman en kapitein Blok en de bemanning van de Tyro.

Daarnaast bedank ik de medewerkers van het IVAU die mij hebben bijgestaan bij de praktische kant van het onderzoek: P. Anten, A. van Dijk, M. Haller, R. Kreulen, J. Meesterburrie, G. Nobbe, G. Peters, S. Scholten, A. Tolboom, V. Govers, P. Boderie, B. van Os, E. Henneke, P. Pruysers, T. van Zessen, B. 't Hart, R. Meyer, F. Trappenburg en F. Quint.

Mijn dank gaat verder uit naar dr. van der Plicht (RU Groningen) voor de analyse van enige monsters op ^{210}Pb, dr. J. Woittiez (ECN/TU Delft) voor INA en $\delta^{34}S$ analyses, en D. Hoede (ECN), dr. H.A. van der Sloot (ECN), G. Hamburg (ECN) en P. van Emburg (RU Leiden) voor de prettige samenwerking tijdens de bestudering van gesuspendeerd materiaal in de Kau Baai.

Some chapters benefitted greatly from reviews, comments and contributions by R.A. Berner, E. Suess, R.C. Aller, S.E. Emerson, W. Martin, K. Kelts, J. Compton, G. Luther, G.J. de Lange, C.H. van der Weijden, S.E. Calvert, R.E. Karlin, R. Kreulen, R.D. Schuiling, B. van Os, P. Pruysers, P.D. van Steenbergen and a number of anonymous reviewers. Miss S. McNab is thanked for linguistic and stylistic advice that made some chapters more readable.

Ik ben in het bijzonder dank verschuldigd aan Prof. dr. L.M.J.U. van Straaten (RU Groningen) en dr. W. Salomons (RU Groningen; IB/WL Haren). Door de boeiende colleges van Prof. van Straaten ben ik me gaan interesseren voor de processen die plaatsvinden in de oceanen en sedimenten. Wim Salomons maakte me enthousiast voor de quantitatieve beschrijving van deze processen.

Mijn promotor, Prof. dr. C.H. van der Weijden, wil ik bedanken voor het genoten vertrouwen en de vrijheid om tijd te besteden aan onderzoek niet direct gerelateerd aan de Kau Baai. Rob Comans bedank ik voor de voortreffelijke samenwerking en talrijke wetenschappelijke discussies tijdens de koffie, in de bus, op het station en aan de telefoon. Gert de Lange, co-promotor en co-auteur van enkele artikelen, dank ik voor de uitstekende samenwerking, het delen van een kamer (en telefoon) en de vele wetenschappelijke discussies.

Tenslotte dank ik Petra voor inspiratie en mijn ouders voor de steun die zij mij tijdens mijn opleiding hebben gegeven.

Het onderzoek beschreven in dit proefschrift is gesteund door de Nederlandse Organisatie voor Wetenschappelijk Onderzoek, d.m.v. de stichting Aardwetenschappelijk Onderzoek (AWON 751.355.012) en de werkgroep van analytisch-chemisch onderzoek van mineralen en gesteenten (WACOM), de Stichting Onderzoek der Zee (voorheen NRZ) en Shell Nederland B.V.

CONTENTS

Some chapters or parts of chapters have already been published; some other chapters have been or will be submitted for publication in international journals.

Chapter 2: Marine Chemistry, v. 23, 353-364.
Marine Geology, v. 82, 251-259.
Neth. J. Sea Res., v. 24, 607-613.
Neth. J. Sea Res., v. 24, 583-589.
Chapter 3: Neth. J. Sea Res., v. 24, 615-622.
Chapter 5: Geochim. Cosmochim. Acta, v. 53, 1577-1581.
Chapter 6: Geology, v. 18, 399-402.

ABSTRACT

Kau Bay (island of Halmahera, Eastern Indonesia) is a 470 m deep basin separated from the Pacific Ocean by a sill that is at present only 40 m below sea-level. The presence of this sill has two major implications. Firstly, during Weichselian time, the sea-level dropped below the depth of the sill, Kau Bay became isolated and fresh-water sediments were deposited. Secondly, the exchange of water between Kau Bay and the adjacent Pacific Ocean is limited. As a consequence, Kau Bay is at present a semi-euxinic marine basin wherein low oxygen, but non-sulphidic, bottom waters alternate with anoxic sulphidic bottom waters. These two interesting features are reflected in the composition of the interstitial waters of the sediments.

The fact that fresh-water sediments are underlying marine sediments has resulted in the downward diffusion of chloride and the other major components of seawater. It also initiated ion-exchange reactions between the fresh-water clays and the brackish-to-saline pore waters.

The distinct hydrography and chemistry of Kau Bay has resulted in the accumulation of organic-carbon-rich sediments. The anoxic decomposition of organic matter causes the release of ammonium, alkalinity, phosphate and sulphide to the interstitial waters. This liberation of nutrients drives various diagenetic reactions such as ion-exchange between dissolved ammonium and exchangeable cations and the formation of authigenic minerals. It also causes changes in the salinity and the speciation of the major components in pore waters.

Sediments in Kau Bay can be divided into three distinct units: a Holocene semi-euxinic marine facies (Unit 1), a transitional facies (Unit 2) and a Weichselian fresh-water unit (Unit 3). These different units represent the response of Kau Bay to the Holocene sea-level change. Within these sediments a range of authigenic minerals has been identified and include dolomite, calcite, pyrite and apatite. Dolomite appears to be forming in specific intervals by direct precipitation from solution at a rate of a few centimetres per 1 kyr. The formation of dolomite is believed to be initiated in the zone of anoxic methane oxidation. The sediments contain about 1 wt% pyrite-sulphur and 0.5 wt% acid-volatile sulphur. The reactive iron content of the sediment limits the amount of iron that is sulphidized. Reactive iron contents are shown to be correlated with the amount of terrigenous organic matter. The marine sediments from unit 1 show no relation between organic carbon and sulphur and have Degree of Sulfidization values that vary from 0.36 to 0.78.

SAMENVATTING

De Kau Baai (Halmahera, Oostelijk Indonesië) is een 470 m diep bekken dat door een drempel met een diepte van maximaal 40 m gescheiden wordt van de Pacifische Oceaan. De aanwezigheid van deze drempel brengt met zich mee dat door de Weichseliense zeespiegeldaling tot beneden het drempel niveau de Kau Baai geïsoleerd werd en sedimentatie in een zoetwater milieu plaatsvond. Bovendien wordt hierdoor de huidige uitwisseling van water tussen de Kau Baai en de Pacifische Oceaan beperkt. Het gevolg hiervan is dat de Kau Baai heden ten dage een semi-euxinisch marien bekken is, waarin zuurstof arm, maar niet sulfidisch, bodemwater afwisselt met anaëroob sulfidisch bodemwater. Deze twee interessante verschijnselen hebben hun invloed op de samenstelling van het poriënwater van de sedimenten.

De aanwezigheid van zoetwater sedimenten onder mariene sedimenten heeft diffusief transport van chloride en andere hoofdcomponenten van zeewater van de mariene naar de zoetwater sedimenten veroorzaakt. Dit verschijnsel heeft tevens tot ion-uitwisselings-reacties tussen de zoetwater kleien en het brak tot zoute poriënwater geleid.

Ten gevolge van de karakteristieke hydrografie en chemie van de Kau Baai zijn er sedimenten afgezet, die rijk zijn aan organisch materiaal. De anoxische afbraak van organisch materiaal resulteert in verrijking van het poriënwater aan ammonium, alkaliteit, fosfaat en zwavelwaterstof. Als gevolg van dit vrijkomen van nutriënten vinden er vele diagenetische veranderingen plaats zoals ion-uitwisselings reacties tussen opgelost ammonium en uitwisselbare kationen, en de vorming van authigene mineralen. Veranderingen in de saliniteit en de speciatie van de hoofdelementen in het poriënwater zijn hier eveneens een gevolg van.

In de sedimenten van de Kau Baai kunnen drie karakteristieke eenheden worden onderscheiden: een Holocene semi-euxinische facies (Unit 1), een overgangs facies (Unit 2) en een Weichselien zoetwater facies (Unit 3). Deze eenheden vertegenwoordigen de response van de Kau Baai op de Holocene zeespiegel stijging. In deze sedimenten wordt een scala van authigene mineralen gevonden waaronder dolomiet, calciet, pyriet en apatiet. Dolomiet blijkt gevormd te worden in specifieke laagjes door middel van precipitatie uit oplossing met een snelheid van een paar centimeter per 1000 jaar. De vorming van dolomiet is waarschijnlijk begonnen in de zone van anaërobe methaan oxidatie. De sedimenten bevatten ongeveer 1 gew% pyriet-zwavel en 0.5 gew% AVS (zuur-vluchtig-zwavel). Het reactieve ijzergehalte van het sediment limiteert de hoeveelheid ijzer die wordt omgezet in een sulfidische vorm. Reactief ijzer is gecorreleerd met de hoeveelheid terrestrisch organisch materiaal. Er is geen relatie tussen het gehalte aan organisch materiaal en zwavel in de mariene sedimenten van Unit 1. Deze sedimenten hebben een verzwavelingsgraad (DOS) waarvan de waarden liggen tussen 0.36 en 0.78.

CHAPTER 1: INTRODUCTION

Various marine basins are semi-isolated from the open ocean due to the presence of a sill. The restricted nature of these basins has two major implications. Firstly, these sills restrict water exchange between the enclosed sea and adjacent areas of the open ocean. As a consequence, these basins are known to have a distinctive hydrography, chemistry and biology (e.g. DEUSER, 1975; GRASSHOFF, 1975; ANDERSON and DEVOL, 1987). Secondly, the presence of these sills makes these basins very sensitive to eustatic sea-level fluctuations. During periods of low global sea level, the sea level may drop below the sill depth. Hence, some silled basins will become isolated from the open ocean.

On the basis of the water balance, silled basins can be divided into two main groups (GRASSHOFF, 1975), namely those basins located in arid zones having a negative water balance and those located in humid zones having a positive water balance.

Typical examples of the first group are the Mediterranean and the Red Sea. These basins are usually well oxygenated and nutrient depleted. Isolation of these basins during periods of low global sea level will cause an increase in salinity and eventually the deposition of evaporites. The Messinian salinity crisis in the Mediterranean is a supreme example (HSÜ et al., 1977).

Typical examples of the second category are the Black Sea (ROSS et al., 1970; ROSS and DEGENS, 1974), the Baltic Sea (SUESS, 1976) and Kau Bay. This type of basin may act as nutrient trap which may thus stimulate higher primary productivity. As a result anoxic conditions are a general feature of these basins. Isolation of these basins may result in a decrease in salinity or even the conversion of the marine basin into a fresh-water lake.

Both the Black Sea and the Baltic Sea have been studied extensively, because of these interesting features (e.g. the Black Sea: BERNER, 1970b, 1974a; ROSS et al., 1970; DEGENS and ROSS, 1972; ROSS and DEGENS, 1974; GLENN and ARTHUR, 1985; RAISWELL and BERNER, 1985; CALVERT et al., 1987; CALVERT and FONTUGNE, 1987; MURRAY et al., 1989; CALVERT, 1990; CALVERT and KARLIN, 1990; LYONS and BERNER, 1990; CAGATAY et al., 1990; the Baltic Sea: MANHEIM, 1961, 1982; SUESS, 1976, 1979, 1982; BLOOMQUIST, 1977; SHAFFER, 1987; KÖGLER and LARSEN, 1979; BOESEN and POSTMA, 1988; JAKOBSEN and POSTMA, 1989; WULFF and STIGEBRANDT, 1989; KOOP et al., 1990; and many others). In contrast to the wealth of information that is available for the Black Sea and the Baltic Sea, there are almost no data for Kau Bay. It is the purpose of this thesis to provide these data. Prior to this

study, the only data available for Kau Bay were the results of the SNELLIUS I expedition (KUENEN, 1943; NEEB, 1943; VAN RIEL ,1943).

The results reported in this study are based on samples that have been obtained during a scientific expedition with the R.V. Tyro to Kau Bay as part of cruise G4 of the Snellius II expedition. Due to the remoteness of Halmahera, and the limited time scheduled for cruise G4 (16 days), only 8 days were available for research in Kau Bay proper.

The main objectives of this expedition were **(1)** to study diagenesis and authigenic mineral formation in anoxic sediments, **(2)** to establish the Late Quaternary history of Kau Bay, **(3)** to determine the behaviour of redox-sensitive elements and **(4)** to study the hydrography and ventilation of Kau Bay. It will be clear that an 8 days survey incorporating physical oceanographic, marine geochemical, micro-paleontological and marine geophysical research is not enough to cover all aspects of this interesting natural laboratory. Nevertheless the survey was very successful.

This thesis is mainly limited to objective 1: the study of early diagenetic processes taking place in Kau Bay. Some aspects of objectives 2-4 can be found in Chapter 2 and BARMAWIDJAJA et al. (1989, 1990); VAN DER LINDEN et al. (1989); VAN AKEN and VERBEEK (1988); VAN DER WEIJDEN et al. (1989); VAN DER SLOOT et al. (1988) and MIDDELBURG et al. (1988a, 1989).

Chapter 2 contains a collection of auxiliary data pertinent to the understanding of diagenetic processes taking place in Kau Bay. It provides **(1)** an overview of the setting and hydrography of Kau Bay, **(2)** information on the composition of water, suspended matter and sediments in Kau Bay and **(3)** estimates for sediment accumulation rates based on ^{14}C and ^{210}Pb.

Chapters 3, 4 and 5 deal with early diagenetic processes. The subject of early diagenesis can be approached on three levels (BERNER, 1980a). The first level is that of qualitative generalizations based on natural observations. The second level is qualitative predictions based on laboratory measurements and thermodynamic calculations. The third level is quantitative descriptions in terms of mathematical rate expressions. The approach to diagenesis in this thesis is, where possible, at all three levels.

In chapter 3 the distribution of chloride in interstitial water of Kau Bay is used as evidence for the isolation of Kau Bay during the last glaciation. The observed chlorinity versus depth profiles can be described using a transient diffusion-advection model.

The interstitial water chemistry of Kau Bay sediments is the subject of chapter 4. Its composition is shown to be influenced by both the presence of fresh-water sediments at greater depth and the anoxic decomposition of organic matter. Ion-exchange reactions, the anoxic decomposition of organic

matter by sulphate reduction and methane generation and the formation of authigenic minerals are recognized as the major processes involved. The distributions of calcium, strontium, ammonium, sulphate, phosphate and alkalinity are modelled using diffusion-advection-reaction models with linear kinetics.

The use of linear kinetics for early diagenetic reactions may perhaps not be the best approach as shown for organic matter in chapter 5. In this chapter a new model, i.e. the Power model, is proposed for the decomposition of marine sedimentary organic matter. In this model the rate constant, k, is treated as a continuously varying parameter.

Chapters 6 and 7 are devoted to the formation of authigenic minerals. In chapter 6 evidence is presented for the formation of authigenic dolomite layers. Dolomite seems to have formed by direct precipitation from solution at a rate of few centimetres per 1 kyr. The formation of dolomite is believed to be initiated in the zone of anoxic methane oxidation.

The iron, sulphur and organic carbon contents of Kau Bay sediment are discussed in chapter 7. Special attention is given to **(1)** the formation of iron sulphides, **(2)** the interpretation of relationships in the C-S-Fe system as indicators of depositional environments and **(3)** the relation between reactive iron and organic carbon.

Finally, in chapter 8 a comparison is made between Kau Bay and the Black Sea. For both Kau Bay and the Black Sea the sedimentary record can be divided into three geochemical distinct units: a Pleistocene fresh/brackish water (Unit 3), a Holocene transitional (Unit 2) and a recent fully marine semi-euxinic facies (Unit 1). These different units represent the response of these silled basins to the Holocene sea-level change.

CHAPTER 2. KAU BAY

2.1. INTRODUCTION

The purpose of this chapter is to provide information on the geology, oceanography and geochemistry of Kau Bay. This serves to set the stage for the detailed discussion of diagenetic processes that follows in the next six chapters. After description of the environmental setting of Kau Bay and the sampling sites, a comprehensive overview of the chemistry of Kau Bay water is presented. This is followed by a discussion on the limitations and reliability of sediment accumulation rate determinations. At the end of this chapter, the major, minor and trace element composition of Kau Bay is discussed.

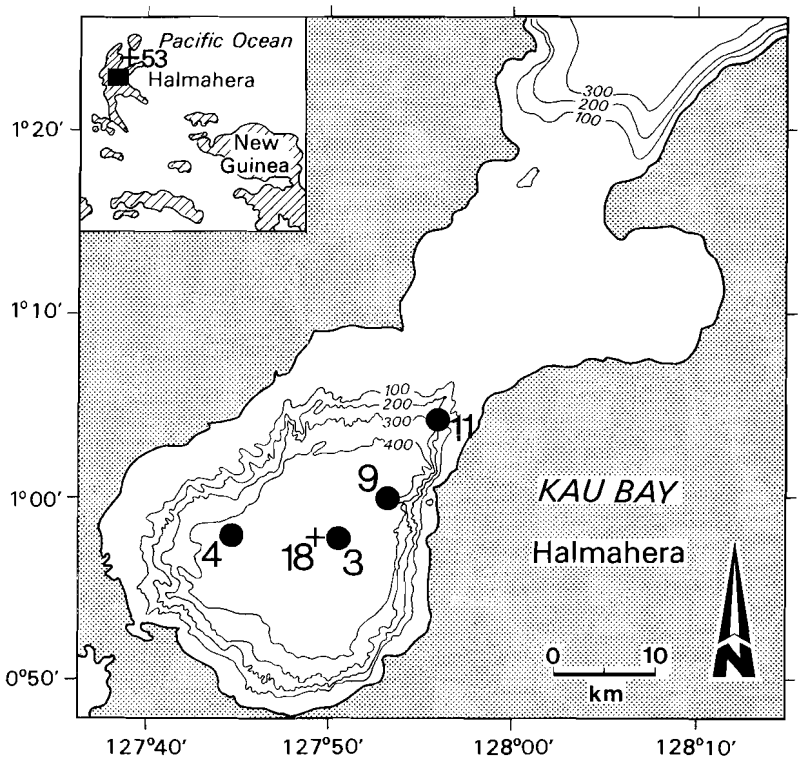

Figure 2.1 Map of Kau Bay showing the positions of the cores used in this study (dots) and the positions of hydrographic casts (crosses).

2.2. KAU BAY SETTING

Kau Bay is enclosed by the northern and northeastern arms of the island of Halmahera (northern Maluku, Indonesia). The Kau Basin is 470 m deep and covers and area of 60 by 30 km (Fig. 2.1). It is separated from the Pacific Ocean by a flat-floored, 30-km-wide sill that is only 40 m below sea-level. The northern arm of the island is a part of a gently curving volcanic arc that can be followed from northern Halmahera, through Ternate and Tidore, to Bacan. The volcanic rocks are predominantly andesites. The northeastern arm of Halmahera belongs to a tectonic melange, accretionary wedge or subduction complex, consisting of ultramafic, volcanic, metamorphic and sedimentary rocks (VAN DER LINDEN et al., 1989).

The western and northern edges of Kau Bay are fringed by broad shelf areas. The coastline is practically reef-free and is occupied by mangrove swamps and a number of sandy beaches. To the south and east the shelf is much narrower and the coastline is often rocky with scattered occurrences of sandy beaches and mangrove swamps. From the shelf break Kau Bay deepens rapidly to about 400 m, whereafter the basin floor flattens out. The steep slopes are intersected by submarine canyons through which shallow-water sediments are transported to the basin floor (470 m).

The average annual precipitation of about 2 m per year is sufficient to support a dense tropical vegetation (TERRAIN HANDBOOK 31, 1944). River runoff into the bay comes principally from the Kau river.

2.3 SAMPLING SITES

During the international Snellius II expedition on R.V. Tyro, high quality cores of up to 9 m in length were taken in Kau Bay. In order to have enough material for all investigations (i.e. sedimentological, micro-paleontological and geochemical) and for reference purposes at least two cores were taken for some sites.

The cores on which this thesis is based are listed in Table 2.1 and their location is given in Fig. 2.1. The hydrographic casts used in this chapter are also indicated in this figure.

TABLE 2.1 Cores used in this thesis.

Core	Waterdepth (m)
K3P2	457
K4P3	414
K4P1	440
K9B1	410
K9P1	410
K11P1	260

Kxx : Station number
Py: Piston core number
Bz: Box core number

2.4. HYDROGRAPHY

This discussion will be mainly limited to two stations: one in the center of Kau Bay (st. 18) and one just outside Kau Bay (st.53). A more detailed description of the hydrography of Kau Bay can be found in VERBEEK (1987), VAN AKEN and VERBEEK (1988) and VAN DER WEIJDEN et al. (1989). Figure 2.2 shows profiles of temperature, salinity, density and oxygen of the water column inside (solid line) and outside Kau Bay (dashed line).

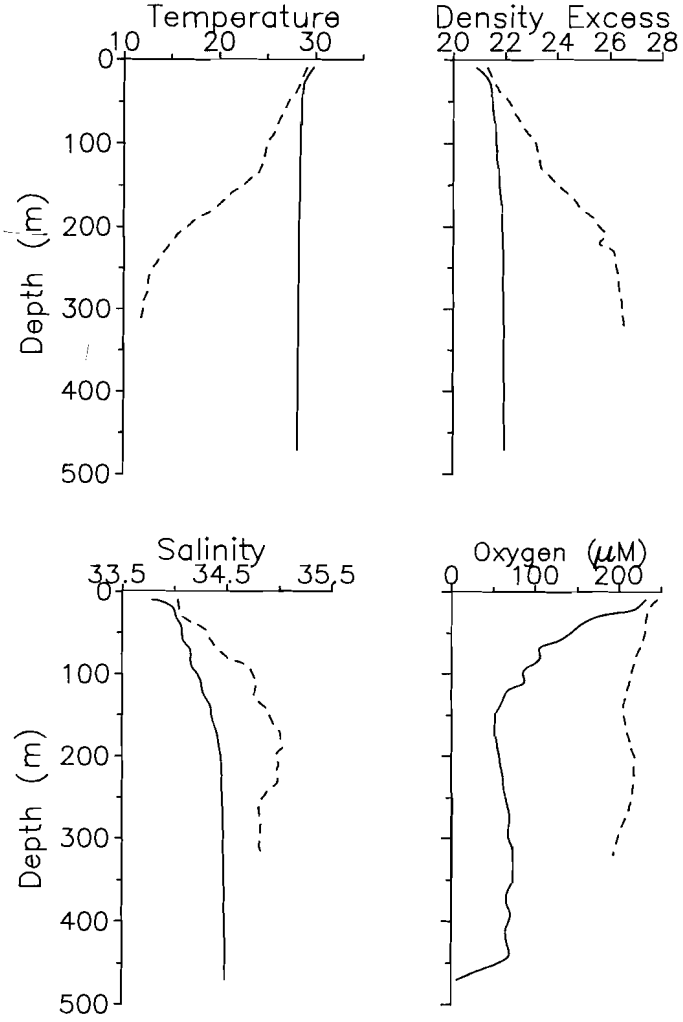

Figure 2.2 Profiles of temperature, salinity, density and oxygen at station 18 within Kau Bay (solid line) and at station 53 outside Kau Bay (dashed line).

2.4.1 T-S-density inside Kau Bay

Near the sea surface a thin mixed layer overlying a shallow pycnocline is found. In this pycnocline the potential temperature decreases and salinity increases to a depth of about 50 m. At depths between 50 and 150 m small-scale fine structures in salinity are found with a vertical length scale of about 20 m. These fine structures are indicative for the occurrence of intrusions of outside water into the Kau Bay. At depths below 150 m profiles of temperature, salinity and density become smoother because most thermohaline structures disappear there. Towards the bottom the temperature slowly decreases and salinity slowly increases.

2.4.2. T-S-density outside Kau Bay

The water properties outside Kau Bay are influenced by the Pacific Ocean and local upwelling along the island. There is a strong halocline at 40 m and a small thermocline at 50 m. At depths between 50 and 200 m the temperature gradient is rather constant with only a few steps, whereas there is substantial salinity fine structure with a maximum salinity over 35 $^{o}/_{oo}$ at a depth of 170 to 190 m. At depths greater than 200 m the salinity and temperature decrease to 34.8 $^{o}/_{oo}$ and 12.0 °C respectively.

2.4.3. Temperature-salinity diagram

Temperature-salinity diagrams can be used to recognize certain local water types. The T-S diagram for water inside (dots) and water outside (crosses) Kau Bay is shown in Figure 2.3. On the basis of this diagram, Kau Bay deep and surface waters can be identified with (T,S)=(28.1,34.5) and (T,S)=(30.0,33.7) respectively. The connection between Kau Bay deep, Kau Bay surface and outside water is at about (T,S)=(28.5,34.0). The water outside Kau Bay is going through (T,S)=(18.0,35.0) down to (T,S)=(12.0,34.8).

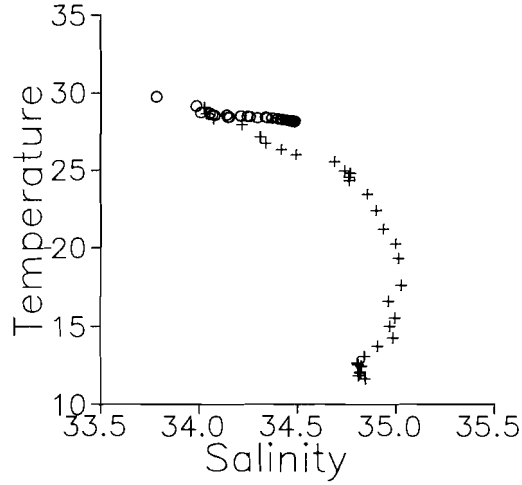

Figure 2.3 Temperature-salinity diagram for samples inside Kau Bay (dots) and outside Kau Bay (crosses).

Accordingly, the main body of Kau Bay water has a temperature excess of about 2° C compared to adjacent ocean water masses with the same salinity. Surface water in Kau Bay is fresher and warmer than surface water outside the basin due to solar heating and fresh-water inflow by rivers on the island. It is important to notice that the water-mass properties found within the bay below about 50 m (i.e. 34.1 isohaline) have not been observed outside the sill area.

2.4.4. Oxygen

In Kau Bay there is an oxygen maximum in the surface water of over 220 μM. From the surface to 150 m depth oxygen concentrations decrease to about 60 μM. At depths between 50 and 150 m there is significant fine structure in the oxygen profile with a typical vertical length scale of about 20 m, the same scale as is found for the thermohaline fine structure. From a depth of 150 m towards 350 m the oxygen profile shows a slightly increasing trend while below 350 m the oxygen concentration decreases to about 60 μM at 440 m. In the depth range between 150 and 440 m, fine structure is observed with a typical vertical length scale of about 50 m and with a typical magnitude of 10 μM. These steps in the oxygen profile probably reflect intrusions of outside water into the bay at intermediate levels. At depths below 440 m oxygen concentrations decrease very rapidly to values of the order of 5 to 10 μM near the bottom.
At all depths below 20 m within the bay, the water has a strong oxygen deficit compared to the Pacific water outside the bay at the same depth. At this station oxygen concentrations are of the order of 200 μM.

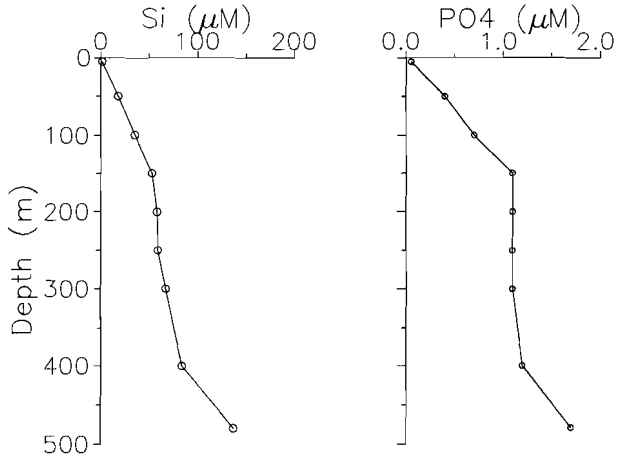

Figure 2.4 Profiles of phosphate and silicate in Kau Bay.

2.4.5. Nutrients

Figure 2.4 shows profiles that are typical for silica and phosphate in the water column of Kau Bay. Silica and phosphate are essential nutrients for biota and their concentrations are consequently below the detection limits (Si: 3μM; PO_4: 0.1 μM) in the surface layer. Below this surface layer nutrient concentrations are relatively high for the depth levels involved. Since inflow into the bay occurs as nutrient depleted surface waters, almost all silica and phosphate present in Kau Bay originates from the dissolution of silica tests and the degradation of organic matter. The vertical gradients of phosphate and silica in the upper 150 m of the bay may be explained by a turbulent flux into the photic zone where these nutrients are consumed by biota. The relatively constant concentrations of silica at depths between 200 and 350 m and of phosphate at depths below 150 m are caused by local dissolution of silica tests and local degradation of organic matter. At depths below 350 m silica and phosphate concentrations are increasing as a consequence of large benthic fluxes.

2.4.6. Temporal variability

Temporal variations in the hydrography are important to assess since they may provide information on the stability of the water column and on the representativity of the data sets available. Observations on the hydrography of Kau Bay have been made during the Snellius I (May 1930) and Snellius II (April 1985) expeditions. Such a small dataset precludes a detailed study of temporal variability.

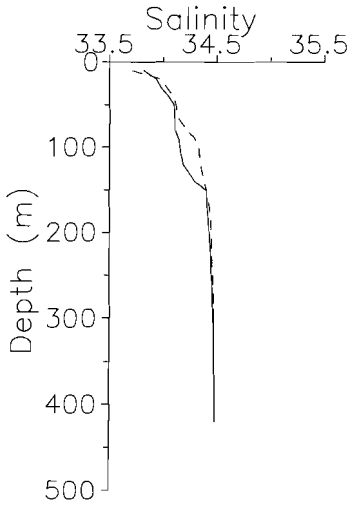

Figure 2.5 The salinity profile from two stations in the centre of Kau Bay that have been recorded 68 hours after each other at a mutual distance of less than 400 m m.

However, evidence exists of temporal variability during a single expedition. Figure 2.5 shows the salinity profiles from two stations that have been recorded 68 hours after each other at a mutual distance of less than 400 m. There is a strong difference in the salinity profiles in the upper 150 m. This indicates that hydrographic characteristrics at depths less than 150 m may show significant variability in time.

Evidence of temporal variability is also found for water at depths more than 150 m. Comparison of temperature, salinity and phosphate data from May 1930 with the April 1985 data (Fig 2.6) reveals that since 1930 the

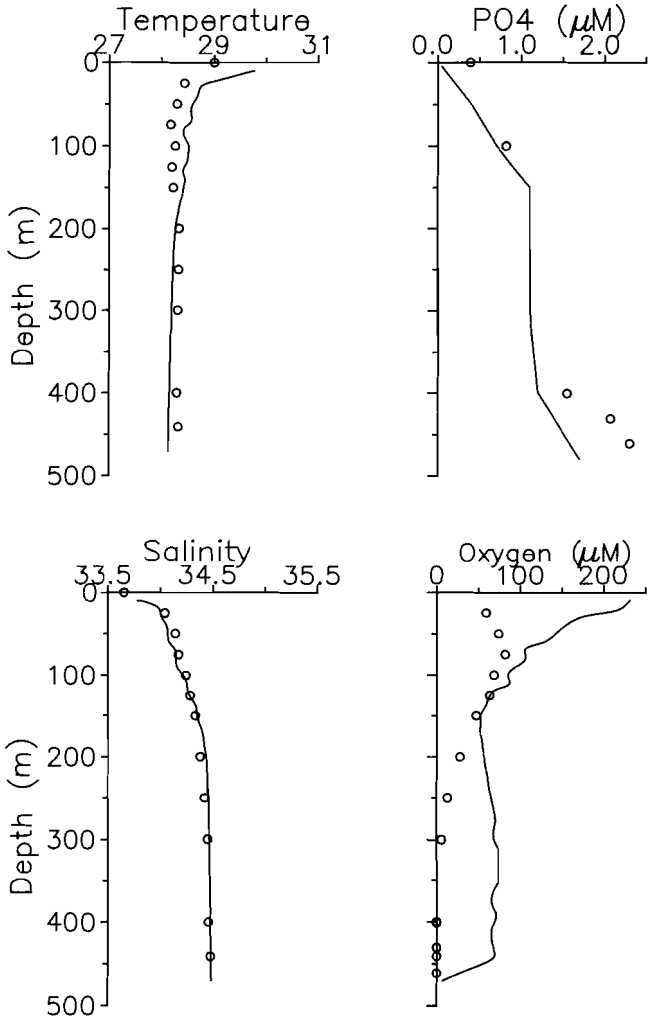

Figure 2.6 Comparison between the temperature, salinity, oxygen and phosphate distributions in 1985 (solid line) and 1930 (dots).

temperature and phosphate concentration have decreased with about 0.04 ° C and 0.8 μM respectively and that salinity has increased about 0.03 units. Moreover, in May 1930 oxygen was not found in the water deeper than about 350 m, and hydrogen sulphide concentrations of up to 13 μM were observed, whereas in April 1985 oxygen was present at all depths (Fig. 2.6). Accordingly, we have to conclude that the deep water in Kau Bay has been ventilated by inflow of Pacific surface water at least once. This indicates that the renewal time of Kau Bay water is less than 55 yr. In the next two sections we will provide estimates for the ventilation of Kau Bay.

2.4.7 Renewal estimates based on temperature and salinity

Water-mass analysis by means of the temperature-salinity diagram has shown that water-mass properties found within the deep parts of Kau Bay have not been observed outside the basin in April 1985 (Fig.2.3). VAN AKEN and VERBEEK (1988) have suggested that surface water outside Kau Bay must have had a salinity of at least 34.5 $^{o}/_{oo}$ during the last flushing event. This is about 0.5 units higher than that actually found in April 1985. Surface water salinities near Halmahera vary from 33.85 in March to 34.55 in October with an annual mean of 34.2 $^{o}/_{oo}$ (VAN AKEN and VERBEEK, 1988).

As a consequence of this temporal variation in initial properties, inflowing water will reach a level in the bay where its density is adapted to the density stratification in the bay. That level is not necessarily the bottom. Important for the present discussion is that each inflow event may cause a distinct thin layer which can be observed as a fine structure in salinity, temperature and oxygen (Fig.2.2).

After each flushing event these fine structures will be eroded by turbulent diffusion. The typical time scale τ for which structures with a length scale L will be reduced by a factor e (2.7183) by turbulent diffusion can be estimated as (cf. VAN AKEN and VERBEEK, 1988):

$$\tau = L^2/K$$

where K is the eddy diffusion coefficient. VAN AKEN and VERBEEK (1988) suggested that for Kau Bay the eddy diffusion coefficient K may vary from $4*10^{-6}$ to $4*10^{-5}$ $m^2\ s^{-1}$ in the pycnocline to $4*10^{-5}$ to $4*10^{-4}$ $m^2\ s^{-1}$ in the deep water. Since τ provides a timescale for diffusive elimination of structures, it will be clear that stationary structures will have a time scale much smaller than τ and that transient structures will have a time scale smaller than, but of about the same order as τ.

In order to quantify the flushing frequency of Kau Bay we will apply this equation to some of the length scales observed: e.g. 480, 50, 30 and 20 m. The typical time scale for diffusive elimination of the large scale stratification (L=480 m) appears to be 18 to 180 yr. Since there is significant vertical structure observable, renewal events are expected to occur much more often than every 18 to 180 yr. The observed fine structure between 50 and 150 m depth with a length scale of 20 m will be eliminated by diffusion on a timescale of 100 to 1000 days. Similarly, the oxygen structure in the deep water with a depthscale of 50 m will be smoothed by diffusion on a timescale of 70 to 700 days. Finally, the oxygen minimum layer at the bottom, with a characteristic depth scale of 30 m, should be eliminated by diffusion after 25 to 250 days. These rough estimates indicate the maximum time during which fine structure can be observed. Flushing events are therefore expected to occur on a smaller timescale: i.e. in the order of months.

2.4.8 Renewal estimates based on Si-excess and O_2-depletion

The water inside Kau Bay is enriched in silica and depleted in oxygen compared to water outside the basin. This is due to dissolution of opaline silica and oxygen consumption by decomposing organic matter.

This Si-excess allows us to calculate a residence time by division of the integrated excess of Si in the water column by the annual flux out of the sediments. The total integrated excess of silica in the water column of Kau Bay is about 17.4 mol m^{-2}. Sediment-water fluxes calculated from dissolved Si pore water profiles indicate an average dissolved Si-flux of 0.8 mol m^{-2} yr^{-1} with a maximum of 1.3 mol m^{-2} yr^{-1}. These fluxes are probably underestimations since the depth resolution of our pore-water samples is not sufficient to describe gradients properly. Moreover, part of the Si-excess originates from dissolution in the watercolumn. Nevertheless our estimates for Si-fluxes are in line with data reported for eastern Indonesian basins: Eastern Banda Sea (0.5 to 0.95 mol m^{-2} yr^{-1}: VAN BENNEKOM, 1988), Aru Basin (1.1 to 1.6 mol m^{-2} yr^{-1}: VAN BENNEKOM, 1988) and Savu Basin (1.4 to 2.7 mol m^{-2} yr^{-1}: HELDER, 1989). On the basis of a depth integrated Si-excess of 17.4 mol m^{-2} and Si-fluxes of 0.8 and 1.3 mol m^{-2} yr^{-1}, a residence time of 13 to 22 years can be calculated. This residence time estimate based on excess silica is in line with that based on the thermohaline structures (20 to 200 yr).

It is in principle possible to use a similar approach for oxygen by relating the depth integrated oxygen deficit with the oxygen flux into the sediments and so calculate a residence time. Unfortunately, there are no

measurements available for the oxygen consumption rate in Kau Bay. However, if we assume a certain residence time, it is possible to calculate an average oxygen consumption rate. This oxygen consumption rate can then be used to calculate time scales for the fine structure in the oxygen profile. On the assumption of a residence time of 20 years, and on the basis of a depth integrated oxygen deficit of 62 mol m^{-2}, an oxygen consumption rate of 3.1 mol m^{-2} yr^{-1} (8.5 mmol m^{-2} d^{-1}) is estimated. This estimate is consistent with some auxiliary data. Firstly, JØRGENSEN (1983) proposed that sediments at depths of 400-500 m should have oxygen consumption rates in the range of 2 to 10 mmol m^{-2} d^{-1}. Secondly, for the sediments of Savu Basin at depths of 3200-3500 m HELDER (1989) found an average oxygen consumption rate of 1.36 mmol m^{-2} d^{-1}. Finally, depth integrated sulphate reduction rates in Kau Bay average 1.7 mmol m^{-2} d^{-1} (chapter 7).

Having an estimate for the oxygen consumption rate in Kau Bay we will determine the time scale of oxygen fine structure in Kau Bay. The oxygen minimum layer at the bottom of the basin has an oxygen deficit of about 1 mol m^{-2} and appears to have a time scale of about 120 days. Similarly, the oxygen fine structures with a length scale of 50 m at depths between 150 and 440 m have oxygen deficits of the order of 0.5 mol m^{-2} and hence timescales of about 60 days.

TABLE 2.2 Estimates for ventilation in Kau Bay

Feature	Temperature/ Salinity	silica	oxygen
Large Scale Stratification (L= 480 m)	18-180 yr	13-22 yr	
Fine Structure (L= 50 m)	70-700 days	--	60 days
Bottom Layer (L= 30 m)	25-250 days	--	120 days

The timescale estimates based on chemical and thermohaline characteristics are compared in Table 2.2. Agreement is quite good considering the many assumptions made and the limited data set available.

Finally, during the Snellius I expedition the depth integrated oxygen deficit was about 83 mol m^{-2} and there was a 150 m thick layer at the bottom

with no oxygen (Fig 2.6). These data indicate that the residence time at that time was about 27 yr and that the zero oxygen bottom layer could have developed in less than 3 years. These tentative calculations show that anoxic conditions in Kau Bay may develop relatively rapidly.

2.5 REDOX-SENSITIVE SPECIES IN KAU BAY

One of the objectives of the expedition to Kau Bay was to determine the responsiveness of a number of redox sensitive dissolved chemical species. In order to cover the whole range of redox potentials occurring in anoxic basins the following redox couples were investigated: iodate/iodide (pe = 10), manganese(IV/III)/manganese(II) (pe=4.4), antimonate/ antimonite (pe=1.6), iron(III)/iron(II) (pe=1.1), U(VI)/U(IV) (pe=-2.3), arsenate/arsenite (pe=-2.7), V(V)/V(IV) (pe=-4.1) and sulphate/sulphide (pe=-4.9). These pe values are representative for a pH of 8.2 (TURNER et al., 1981).

This selection of redox-sensitive species was made on the basis of information available from the Snellius I expedition. However, large temporal variations in hydrography of Kau Bay occur and oxygen was found at all depths (Figs. 2.2/2.6). As a consequence, for all redox couples but iodate/iodide, no reductive transformations have been found to occur in the water column. Conversely, there is considerable evidence for oxidation of reduced manganese and iron species that are released by reductive dissolution of manganese and iron oxides at the sediment-water interface (e.g., see section 2.6 and Fig. 2.9).

In this section we will first discuss the profiles of arsenic, antimony, vanadium and uranium since they are among the first ever reported. After that the distribution of I-species within and outside Kau Bay will be discussed. The analytical methods applied can be found in VAN DER SLOOT (1976), MIDDELBURG et al. (1988b), VAN DER WEIJDEN et al. (1989, 1990) and WOITTIEZ et al. (1991).

2.5.1 Arsenic

Arsenic forms oxyanions based on a tetrahedral coordination of As by oxygen. In oxygenated sea water arsenic primarily exists as the $HAsO_4^{2-}$ anion which chemically closely resembles the corresponding species formed by phosphorus; i.e. HPO_4^{2-}. In the euphotic zone arsenic occurs not only in the form of arsenate but also as the species arsenite ($HAsO_2$), methylarsonate ($CH_3AsO(OH)OH$) and dimethylarsinate ($(CH_3)_2AsOOH$) (ANDREAE, 1978). The latter species are positively correlated with

indicators of primary production (ANDREAE, 1978) and are believed to be formed by biochemical interactions (ANDREAE, 1978, 1979; IRGOLIC and STOCKTON, 1987).

The profiles of dissolved arsenate and arsenite are shown in Fig 2.7a. The methylated forms are analyzed together with arsenite under the conditions used. Particulate arsenic concentrations are negligible compared to dissolved concentrations (MIDDELBURG et al, 1988b). Concentrations

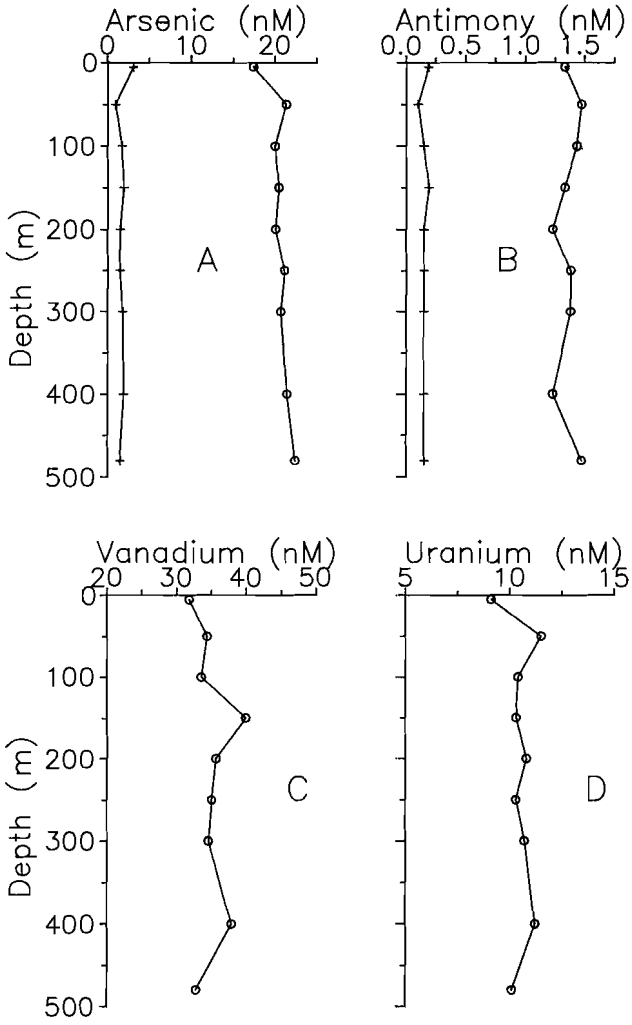

Figure 2.7 Profiles of dissolved trace elements versus depth. A: arsenate (dots), arsenite (crosses); B: antimonate (dots), antimonite (crosses); C: vanadium; D: uranium.

of both arsenate and arsenite are relatively constant with depth except for a small decrease of arsenate and increase of arsenite in the surface waters. Surface depletions for arsenate have been reported for Saanich Inlet (PETERSON and CARPENTER, 1983), the North Atlantic (MIDDELBURG et al., 1988b), the South Atlantic (STATHAM et al., 1987), the Mediterranean (VAN DER WEIJDEN et al., 1990) and the Pacific (ANDREAE, 1979).

This depletion of arsenate in surface waters is a function both of biologic uptake and release, and of the rate of upward mixing and eolian supply. The observed surface depletion of arsenate (about 3 nM) is consistent with a $\Delta As/\Delta P$ molar ratio of $3 * 10^{-3}$, which is close to the ratio proposed for the global ocean ($2.5 * 10^{-3}$; MIDDELBURG et al., 1988b). Considering the differences in time and space scales of oceanic cycling and cycling in Kau Bay, some caution is needed comparing the Kau Bay removal ratio with the ratio proposed for the global ocean. Moreover, part of the surface depletion may perhaps be due to the lower surface salinities.

2.5.2 Antimony

In oxygenated waters the antimonate ion ($Sb(OH)_6^-$) should be the thermodynamical stable form of Sb (TURNER et al., 1981). Thermodynamic predictions suggest that antimonate is subject to scavenging (WHITFIELD and TURNER, 1987) although experiments have shown that this element has a relatively weak affinity for natural particles (LI et al., 1984).

Measurements in natural waters revealed the presence of four species, namely antimonate ($Sb(OH)_6^-$), antimonite ($HSbO_2$), methylstibonic acid ($CH_3SbO(OH)OH$) and dimethylstibonic acid ($(CH_3)_2SbOOH$) (ANDREAE et al., 1981; ANDREAE, 1983; BERTINE and LEE, 1983). The presence of the thermodynamically non-equilibrium species antimonite and the methylantimony acids is probably due to biological activity (ANDREAE, 1983).

The profiles of dissolved antimonate and antimonite are shown in Fig. 2.7b. The methylated forms of antimony are analyzed together with antimonite. Particulate antimony concentrations (Table 2.3) are two orders of magnitude lower than dissolved concentrations.

Concentrations of both antimonate and antimonite are relatively constant with depth. Similar observations have been made in Saanich Inlet (BERTINE and LEE, 1983), the North Atlantic (MIDDELBURG et al., 1988b) and the Mediterranean (VAN DER WEIJDEN et al., 1990).

2.5.3 Vanadium

In oxygenated sea water vanadium occurs in the + 5 oxidation state, primarily as HVO_4^{2-}, $H_2VO_4^-$ and as the complex $NaHVO_4^-$ (TURNER et al., 1981; WEHRLI, 1987; SADIQ, 1988). As a consequence, the vanadium species involved in adsorption processes appear to be anionic, resulting in a relatively low affinity for natural particles (WHITFIELD and TURNER, 1987; SHILLER and BOYLE, 1987). Laboratory experiments by VAN DER SLOOT (1976), JEANDEL et al. (1987) and SHILLER and BOYLE (1987) have shown that complexation with organic matter is not a major factor in determining the aquatic behaviour of vanadate.

The profile of dissolved vanadium is shown in Fig.2.7c. Particulate vanadium concentrations are almost two orders of magnitude lower and decrease significantly with depth (Table 2.3). Concentrations of dissolved vanadium are relatively constant with depth. This has been found in various other marine environments (MORRIS, 1975; JEANDEL et al., 1987; SHERREL and BOYLE, 1988; MIDDELBURG et al., 1988b; VAN DER WEIJDEN et al., 1990) suggesting that the flux of vanadium by transport from the euphotic zone into deeper water is small relative to the concentration of vanadium in marine waters.

2.5.4 Uranium

Uranium is unique among the natural elements in seawater in being present as an oxo-cation (UO_2^+) which interacts strongly with carbonate to form large, relatively inert, negatively charged complexes. As a result the uranium species interact only weakly with mineral phases and differences in uranium concentration with depth and location are only small. The major removal of uranium takes places at ocean margins and in anoxic basins where it may become involved in coupled reduction precipitation processes given sufficient time (ANDERSON et al., 1989; BARNES and COCHRAN, 1990; VAN DER WEIJDEN et al., 1990).

The concentration of dissolved uranium in Kau Bay is relatively constant with depth (Fig.2.7d) in agreement with observations made elsewhere for oxygenated waters (WHITFIELD and TURNER, 1987).

2.5.5 Iodine

It has been well established that the main species of iodine in seawater are iodate (IO_3^-) and iodide (I^-), although small quantities of molecular iodine (I_2) and iodine containing organic compounds may exist

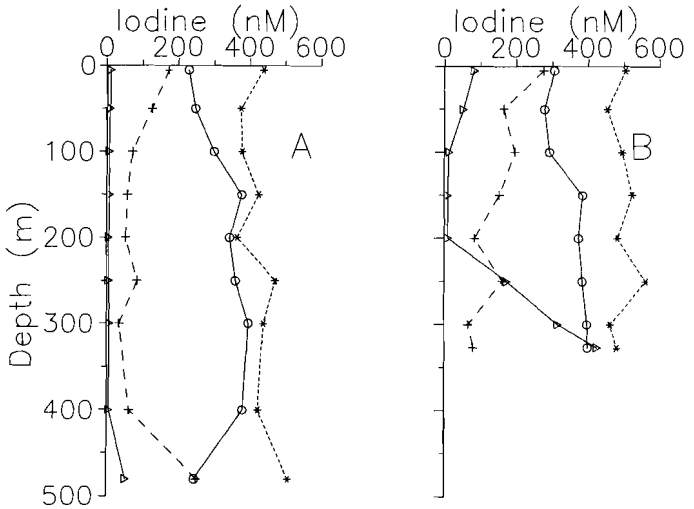

Figure 2.8 A: Profiles of total inorganic iodine (stars), iodate (dots), iodide (crosses) and charcoal extractable iodine (triangles) inside Kau Bay. B: idem outside Kau Bay.

(e.g. WINKLER, 1916; TSUNOGAI, 1971; WONG and BREWER, 1977; ELDERFIELD and TRUESDALE, 1980; LUTHER and COLE, 1988; ULLMAN et al., 1990; WOITTIEZ et al., 1991). In oxygenated seawater iodate is the thermodynamically stable form of dissolved iodine. The equilibrium ratio of iodate and iodide for oxygenated seawater is of the order of $10^{13.5}$, but this ratio is not generally observed due to the presence of metastable iodide. Iodide is often relatively enriched in surface waters (e.g. TSUNOGAI, 1971), bottom waters and pore waters (ULLMAN and ALLER, 1980; KENNEDY and ELDERFIELD, 1987), anoxic water (e.g. WONG and BREWER, 1977; ULLMAN et al., 1990) or near oxic-anoxic boundaries (EMERSON et al., 1979; WONG and BREWER, 1977).

There is little information available on the distribution of organic iodine and molecular iodine since these species are normally assumed to be unimportant and not analyzed separately (e.g. LUTHER et al., 1988). Molecular iodine is thought to be an insignificant species except in zones of high productivity or near the oxic-anoxic boundary (ULLMAN et al., 1990). Organic iodine is considered to be a significant species in coastal water only (e.g. TRUESDALE, 1975).

For Kau Bay independent measurements have been made for iodate, iodide, charcoal extractable iodine and total iodine (WOITTIEZ et al., 1991). Charcoal extractable iodine is thought to represent molecular iodine and some organic-I compounds. Results for iodide, iodate, total inorganic iodine and charcoal extractable iodine are shown in Fig. 2.8 for a station outside Kau Bay (st.53) and a station (st.18) in the middle of Kau Bay. Total inorganic iodine is essentially constant with depth and has a concentration level (495 nM at st. 53; 424 nM at st. 18) in agreement with the level of

world ocean (440 ± 20 nM). At both stations the dominant iodine species through the water column is iodate, the thermodynamically stable form in oxygenated seawater. At depths less than 150 m, there is a depletion in iodate and an increase in both iodide and charcoal extractable iodine. This interconversion of iodine species in the surface layer is a common feature and is related to the biophilic nature of iodine in seawater (ELDERFIELD and TRUESDALE, 1980).

Outside Kau Bay, there is a significant increase in the concentration of charcoal extractable iodine at depths more than 200 m. This increase is not due to an interconversion of iodine species since the concentrations of iodate, iodide and total inorganic iodine do not significantly change. Instead, this increase in charcoal extractable iodine, hence total iodine, is indicative for a source of iodine near the bottom at st. 53. The observed enrichment may perhaps reflect the release of iodine from the sediments. This charcoal extractable iodine is very reactive because it could not be found after storage of the sample for one year (WOITTIEZ et al., 1991).

Within Kau Bay there is an interconversion of iodate to iodide at depths more than 400 m. At the very same depths, there is a decrease in the oxygen contents. Hence, the iodate/iodide redox couple does respond sufficiently fast. The reductive transformation of iodate to iodide (Fig. 2.8) and the oxidation of Mn(II) in the bottom layer of Kau Bay (Fig. 2.9), which has an oxygen content of about 10 μM, are in accordance with thermodynamic expectations.

2.6 SUSPENDED MATTER

Suspended particulate matter plays a major role in the geochemical cycling of elements. The important role of these particles in regulating the composition of sea water has been recognized (e.g. WANGERSKY, 1986; WHITFIELD and TURNER, 1987), but the intimate interplay between biological and inorganic processes remains an enigma. Microbial catalysis of phase changes and redox transformations have been shown to occur (e.g. TEBO, 1983), but our knowledge of these particular interactions is still very limited.

Suspended particulate matter is composed mainly of three phases: terrigenous aluminosilicates, organic or biogenic, and authigenic phases (SPENCER et al., 1972; PRICE and CALVERT, 1973). Since aluminum in particulate matter is almost entirely associated with aluminosilicates (SPENCER and SACHS, 1970), aluminum concentrations in suspended matter can be used to assess the amount of terrigenous aluminosilicates and the partitioning of elements between aluminosilicates and other phases.

TABLE 2.3 Composition of suspended matter in Kau Bay

Element/Depth	5m		200m		480m	
	C	F	C	F	C	F
Al (wt%)	2.71	1.82	3.01	3.65	1.89	2.80
Mn/Al	0.07	0.09	0.33	0.13	5.72	1.42
Fe/Al	2.0	2.9	2.4	1.6	3.5	2.1
Sc/Al (*10^4)	3.5	3.7	3.3	1.9	6.8	4.4
La/Al (*10^4)	1.8	---	2.2	2.0	1.5	1.1
Sm/Al (*10^4)	0.70	0.71	0.63	0.30	0.63	0.39
Sb/Al (*10^4)	1.1	---	3.5	1.87	4.6	2.9
Au/Al (*10^4)	---	---	2.33	1.51	1.32	1.29
V/Al (*10^4)	75	84	39	43	---	26
I/Al (*10^4)	41	48	34	37	---	---
Br/Al (*10^4)	244	324	70	134	---	---
Al (nM)	120	12	128	19	132	17
Mn (nM)	3.8	0.5	20.7	1.2	374	12
Fe (nM)	115	17	146	10	227	17
Sc (pM)	24.9	2.7	25.3	2.1	54.2	4.4
La (pM)	4.3	---	5.5	0.7	3.9	0.3
Sm (pM)	1.50	0.16	1.45	0.10	1.51	0.12
Sb (pM)	2.9	---	10.0	0.7	13.5	1.1
Au (pM)	---	---	4.1	0.4	2.4	0.3
V (pM)	474	54	264	43	---	23
I (pM)	104	12	92	15	---	6
Br (pM)	983	7	302	86	---	---

2.6.1 Chemical composition

Suspended matter was obtained by continuous-flow centrifugation (e.g. see VAN DER SLOOT et al., 1988) and separated into two size/density fractions, namely a 'coarse' fraction (90% > 5 μm) and a 'fine' fraction (90% < 10 μm). Concentrations of total suspended matter are in the range of 95-250 μg/l and agree well with reported data for other basins with restricted circulation (e.g. SHILLER et al., 1985). Concentrations of particulate trace elements were determined by INAA and are given in Table 2.3 (see also MIDDELBURG et al., 1988a). Trace element results are reported both as concentration of particulate trace elements in seawater and as element/aluminum mass ratios. Results for low density or fine and high density or coarse fraction are tabulated separately.

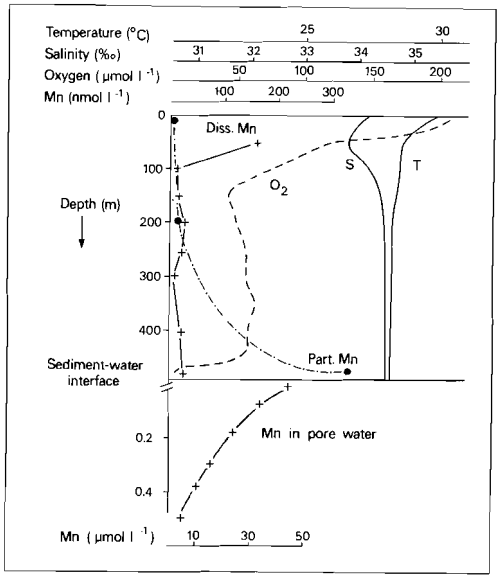

Figure 2.9 Temperature, salinity, oxygen and dissolved and particulate Mn profiles versus depth for station 18 in Kau Bay, and the dissolved Mn profile in the porewater for the same location. Note a different depth and Mn concentration scale above and below the sediment-water interface respectively.

In suspended particulate matter iron is partitioned between aluminosilicates and other constituents such as oxides, sulphides and biogenic phases (SPENCER et al., 1972; PRICE and CALVERT, 1973). The high Fe/Al mass ratio of samples within this basin is striking. Iron enrichment of suspended matter is likely since all samples have Fe/Al mass ratios greater than the sedimentary ratio. However, the adaptation of any Fe/Al mass ratio for reference, such as the sedimentary ratio (0.77), is somewhat arbitrary and may produce erroneous results and conclusions (PRICE and SKEI, 1975).

The Mn/Al mass ratios increase with depth and show large differences between the size/density fractions (Table 2.3). In general the concentration of Mn is higher in the 'coarse' fraction than in the 'fine' fraction. This is probably due to the relatively high density of Mn-rich particles. On the basis of Mn/Al mass ratio of 0.02 for Kau Bay surface sediments, we assign the total particulate Mn concentration to non-silicate Mn (i.e. excess Mn).

Pronounced enrichments of particulate Mn in the near-bottom water of land-locked basins are not uncommon (e.g. PRICE and SKEI, 1975; SKEI and MELSOM, 1982). In general, these particulate manganese maxima arise either through resuspension of Mn-rich surface sediments and preferential resettling of aluminosilicates (PRICE and SKEI, 1975) or by the release of dissolved Mn and subsequent oxidation and precipitation in oxic water (e.g. SPENCER et al., 1972). In Kau Bay the former mechanism is not likely

because the oxygen stratification is pronounced (Fig. 2.2/2.6). A dynamic environment with enhanced resuspension must be accompanied by a decreased oxygen stratification. In addition, the surface sediments of Kau Bay do not deviate chemically from the subsurface sediments; the top few mm of the cores might, however, be lost during coring. Finally, the high density or coarse fraction is richer in Mn than the low density or fine fraction, whereas the Al concentrations are almost equal; this is in contradiction with the preferential resettling hypothesis.

Therefore, we believe that the particulate Mn enrichment is the result of reprecipitation of Mn that is released by dissolution of Mn-oxides at the sediment-water interface. At present, the O_2/H_2S interface seems to coincide with this interface and as a result Mn-oxides at the surface of the sediments are being mobilized. The resulting enhanced concentration of Mn(II) in the surficial sedimentary pore water will cause Mn to migrate along a concentration gradient both into the sediment and into the bottom water (Fig. 2.9). The Mn diffusing into the bottom water of Kau Bay is oxidized and subsequently reprecipitated. In similar land-locked basins, field studies have shown that Mn(II) is oxidized both by inorganic reactions and by bacterial catalysation (e.g. EMERSON et al., 1979, 1982; TEBO, 1983; TEBO et al., 1984).

2.6.2 Electron microscopy

Since we wanted to know whether there was any microbial catalysation and direct measurements were not feasible, we examined the morphology and ultrastructure of Mn-rich particles. Although this indirect method is not definitive, it is useful (e.g. TEBO, 1983).

Scanning electron microscopy (SEM) revealed the presence of three different forms of Mn-rich particles (VAN DER SLOOT et al., 1988; MIDDELBURG et al., 1988a): **(1)** Mn deposits on diatom fragments, **(2)** ring-shaped structures and **(3)** spherical particles. The spherical particles are the most abundant (90 % of the Mn-rich particles) and these will be discussed in some more detail. The major elements detected in these particles are Mn(90 %) and Fe(10%); the H, C, N and O contents were ignored since they cannot be determined by SEM-EDAX. The most striking feature of the particles is their fairly uniform size (2 - 5 μm) and the very unilateral cavity which is 0.7 μm wide and approximately 1.5 μm deep (Fig. 2.10a). This uniformity probably points to a common source. Since the remains of a cell wall were found in one cavity (VAN DER SLOOT et al., 1988), it is tempting to speculate that bacteria lived inside this cavity. Extensive SEM examination also revealed the presence of morphologically

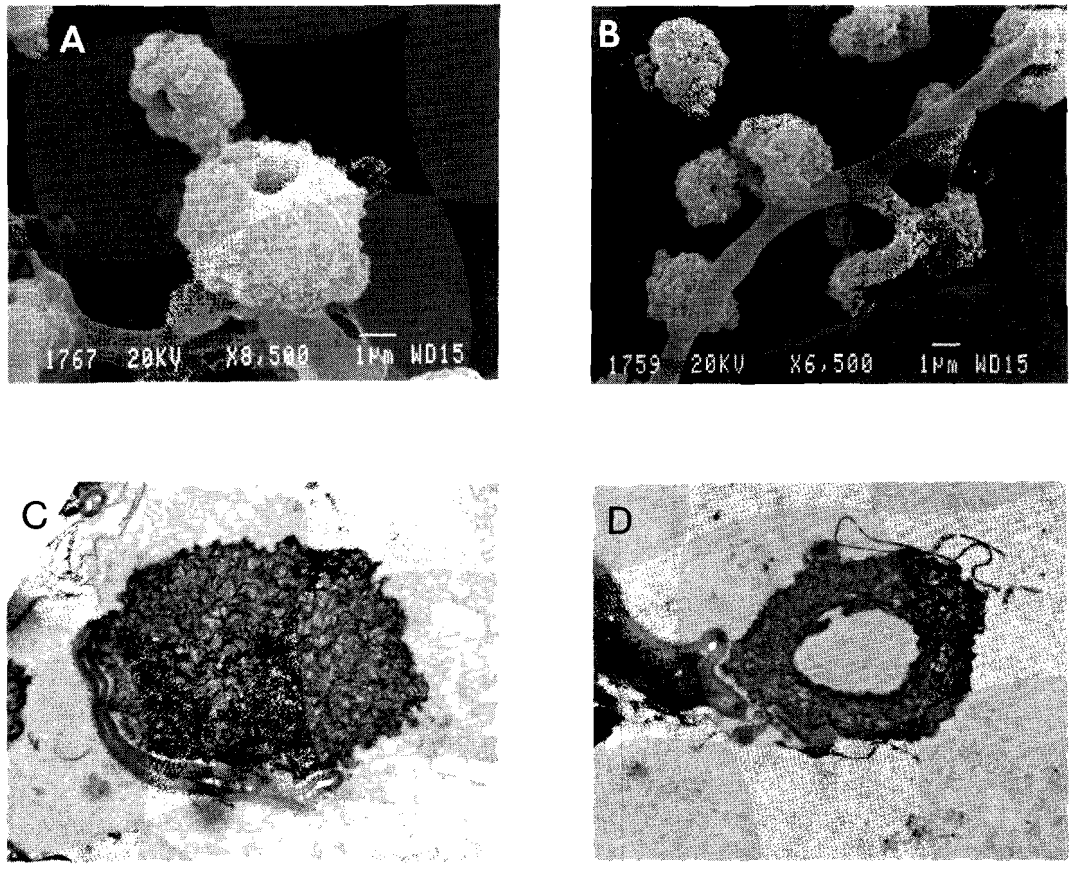

Figure 2.10 SEM micrographs and transmission electron micrographs of Mn-rich spheres. a) single sphere (4,600 X); b) organic string with adhering Mn-rich spheres (3,600 X); c,d) ultrastructure of Mn-rich spheres with organic string (8,000 and 8,000 X).

similar particles adhering directly, or by means of hyphae, to an organic string (Fig. 2.10b). However, these cavities and hyphae did not form a consistent configuration. This might be due to the centrifugation during sampling. Although these observations point to a microbially catalysed phase transformation (i.e. Mn oxidation and precipitation), only direct measurements can give absolute certainty of microbial activity (TEBO, 1983).

Transmission electron micrographs of spherical particles are shown in Fig. 2.10 c,d. Because of their morphology these particles, depending on the actual cut position, yield circular, U-shaped or ring-shaped cross-sections. The manganese precipitates occur mainly as fibrous material with various densities. High densities are expected for inorganic manganates whereas low densities may result from the presence of biological organic matrices (TEBO, 1983). The stalks, which seem to be associated with the spherical particles (Fig. 2.10 c,d), are only visible after staining. These stalks probably contain an organic matrix and they lack electron dense atoms as of metals. Although both SEM and TEM support an association of stalks and spherical particles (Fig. 2.10 b,c,d), a relation cannot be proved because of the many preparatory steps required prior to examination (e.g. centrifugation and sugar gradient separation). It will be clear that spatial relations will remain speculative, until these organisms are studied in vivo using preparative procedures for their visualization which cause minimal disturbance of structural patterns.

2.7 SEDIMENT ACCUMULATION RATES

Knowledge of sediment accumulation rates is mandatory for the interpretation of sediments as records of the past and for the interpretation of diagenetic phenomena. Sediment accumulation rates can be determined using (micro)faunal/floral, magnetic, volcanic, isotope or lithological events of known age, by counting varves, by methods based on the rate of chemical processes and by radiometric dating (e.g. ROTH and POTY, 1989). The choice of a particular method depends on both the equipment and tools available to the investigator, and the presence or absence of certain events.

For sediments of Kau Bay there are no indications for distinct (micro)faunal/flora events (BARMAWIDJAJA et al., 1989, 1990), volcanic ash layers that can be correlated between cores, or varves or related laminations that represent seasonal cycles in sediment deposition. This absence of annual rhythm in sediments is a common phenomena for deposits in Indonesia (KUENEN, 1943), but it is unlike mid-latitudinal anoxic environments such as the Black Sea (DEGENS and ROSS, 1974; CALVERT

et al., 1987) and the California Borderland Basins (LANGE et al., 1987). In addition, in Kau Bay sediments there are no clear-cut lithological events but the presence of dark-coloured dehydrated clays deposited in fresh-water conditions. However, only cores P1 and P3 at station K4 penetrated deep enough to recover this lithological horizon at depths of 771 and 750 cm below the sediment-water interface respectively. Therefore, the only methods applicable to Kau Bay sediments are those based on radiometric dating or rates of chemical processes.

2.7.1 Carbon-14

Carbon-14 is produced in the atmosphere by reactions of neutrons with ^{14}N among others. The ^{14}C atoms so produced rapidly mix with the other carbon isotopes (^{12}C and ^{13}C) throughout the atmosphere and hydrosphere. Living organisms incorporate ^{14}C due to carbon dioxide assimilation. Upon their death, exchanges of ^{14}C no longer occur and the ^{14}C activity declines by radioactive decay. By comparing the ^{14}C activity of a sample with the ^{14}C activity reference level, it is possible to assign an age. This ^{14}C age rests on the assumption that the ^{14}C activity has been constant during the last 60.000 years. It is now well established that the ^{14}C reference level has changed with time (DELIBRIAS, 1989), but correction tables for the last 8.000 years are available. For ages before 8.000 years only a few intercalibration studies exist and these show that ^{14}C ages may be younger than true ages (BARD et al., 1990).

Sediment accumulation rates can be obtained using the ^{14}C method by plotting the ^{14}C age versus depth. The carbon required for dating can be obtained from carbonate or organic carbon. There are two assumptions underlying the use of ^{14}C ages in sediment accumulation rate studies: **(1)** newly-deposited material should have a zero ^{14}C age, and **(2)** there should be no exchange between solid phase carbonate/organic carbon and dissolved bicarbonate/organic carbon. These constraints can be compared with those used in petrological studies: initial isotopic homogeneity and closed system behaviour.

For sediments at station K3, K4, K9 and K11 a total number of 32 radiocarbon ages are available (Table 2.4). These data were obtained on samples of about 10 mg of biogenic carbonate derived from pteropods using the Accelerator Mass Spectrometry (AMS) facility at the University of Utrecht (VAN DER BORG et al., 1987). The ^{14}C age of sample UtC-535, a wood fragment, is based on organic carbon rather than carbonate carbon.

The carbonate carbon ^{14}C ages of samples from cores K3P2, K4P3, K9P1 and K11P1 are plotted versus depth in Figure 2.11. This figure shows

TABLE 2.4 Radiocarbon data for Kau Bay sediments

Depth (cm)	Code Number	$\delta^{13}C$ (‰)	Age (years)
K3P2			
27	UtC-518	-0.84	780
152	UtC-533	-0.17	650
543	UtC-535	-28.56	1180
651	UtC-534	0.63	2340
781	UtC-481	0.39	1820
877	UtC-517	-1.34	1940
K4P3			
36	UtC-478	-0.11	780
75	UtC-475	0.38	1480
203	UtC-480	0.75	2710
303	UtC-476	0.14	3790
417	UtC-474	-1.17	5960
505	UtC-479	-0.40	7600
606	UtC-472	-4.18	9900
628	UtC-477	-4.06	9920
659	UtC-473	-4.04	9670
K4P1			
746	UtC-644	-3.40	9940
751	UtC-645	-3.00	10400
756	UtC-646	-2.93	9890
761	UtC-647	-3.36	10030
K9P1			
2	UtC-484	-0.62	1300
91	UtC-516	-1.29	1270
161	UtC-515	-0.48	1560
210	UtC-514	-0.92	1570
353	UtC-519	-0.98	1450
417	UtC-483	-0.02	1580
554	UtC-482	-0.07	1970
K11P1			
194	UtC-614	0.01	2530
297	UtC-615	0.15	4210
381	UtC-616	-0.16	5520
487	UtC-617	-0.32	6260
511	UtC-618	-0.28	6410
609	UtC-619	-0.78	7610

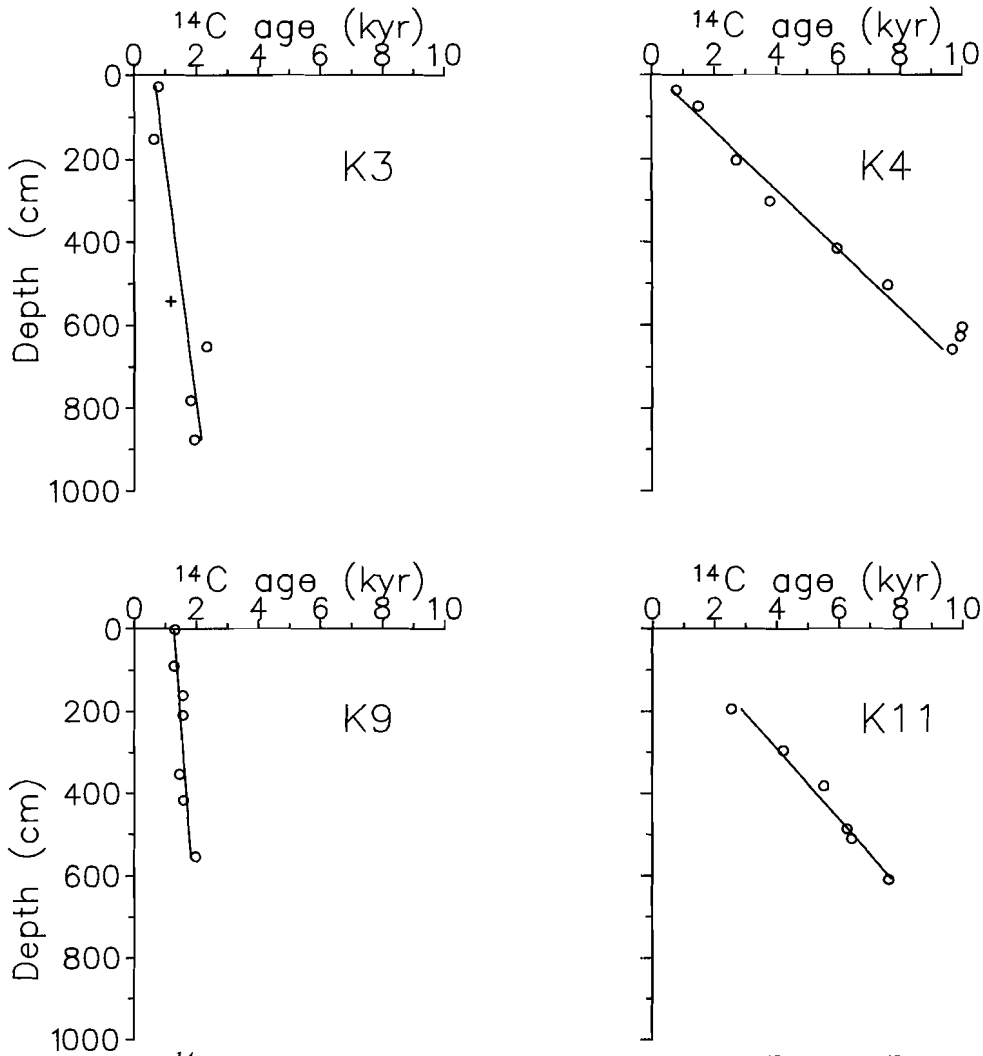

Figure 2.11 ^{14}C ages versus depth in cores at stations K3, K4, K9 and K11 respectively. Dots: carbonate carbon-14 age; Cross: organic carbon-14 age.

two important features. Firstly, the age/depth slopes are relatively constant, but different for various cores. From these slopes average sediment accumulation rates of 0.6 (±0.2), 0.071 (±0.005), 1 (±0.3) and 0.085 (±0.006) cm yr^{-1} are calculated for station K3, K4, K9 and K11 respectively (Figure 2.11). Secondly, the ^{14}C ages of the surficial sediments are significantly different from zero. Radiocarbon ages of modern surface sediments are commonly not zero because of the finite age of the carbon reservoir in the ocean and the mixing of subsurface sediment into the surface layers by benthic organism (BROECKER and PENG, 1983). For Kau Bay, benthic mixing can be neglected because of the low oxygen content of the bottom

waters. The finite surface ^{14}C ages (K3: 644 (±399) yr; K4: 132 (±413) yr; K9 1272 (±139) yr; K11: 582 (±312) yr) must therefore be due to the finite age of the carbon reservoir in Kau Bay. The ^{14}C age estimate of about 650 yr for carbon in Kau Bay is not unreasonable, because the average apparent ^{14}C age of seawater is about 400 year but can reach 700 to 800 years in upwelling zones (DELIBRIAS, 1989). For comparison the age of carbon reservoirs in the Black Sea is about 2000 yr (CALVERT et al., 1987).

The most important aspect of non-zero age of newly-deposited material is that ^{14}C dating yields an age older than that would correspond to the track of sediments surface in time. Estimates based on ^{14}C age/depth curves are representative for sediment accumulation rates, provided that we assume a constant initial age (i.e. initial isotopic homogeneity).

The single organic carbon ^{14}C age available is consistent with the carbonate ^{14}C ages (Table 2.4, Fig 2.11). However, care should be taken in interpreting this consistency since this ^{14}C age is based on a wood fragment with a very low $\delta^{13}C$ value (- 28.6 °/$_{oo}$) reflecting its terrestrial origin (see chapter 7).

The second basic assumption of ^{14}C dating of sediments (i.e. closed system behaviour) is not easy to verify. Although the ^{14}C ages are based on carefully selected pteropods, there are some indications for recrystallization, hence ^{14}C age resetting, at depths more than 550 cm at station K4. Firstly, at these depths, pore waters are slightly undersaturated or close to saturation with respect to aragonite (Figs. 4.9/6.1). Secondly, there is a decrease in the concentration of solid phase calcium at depths more than 550 cm (see Fig 6.1). Thirdly, the $\delta^{13}C$ values of bulk carbonate are indicative for authigenic carbonate precipitation or recrystallization (Fig. 6.1). Fourthly, all pteropods sampled at depths more than 550 cm at station 4 have a uniform ^{14}C age of about 10.000 years and $\delta^{13}C$ values of -3 to -4 °/$_{oo}$. These numbers suggest that 10 to 20 % old carbon is involved in the recrystallization process and that the ^{14}C ages are reset. This is a reasonable estimate since about 25 to 30 % of old carbon is incorporated in the dolomite layer that is presently forming at a depth of 350 cm (MIDDELBURG et al., 1990; see also chapter 6). Therefore care should be taken in interpreting ^{14}C ages of carbonate samples with low $\delta^{13}C$ values (cf., RITGER et al., 1987; PAULL et al., 1989).

2.7.2 Lead-210 dating

^{210}Pb, a member of the ^{238}U-decay series with a half-life of 22.3 yr, is both produced in the sediments by radioactive decay of ^{226}Ra (supported ^{210}Pb) as well as supplied by deposition (unsupported ^{210}Pb or excess ^{210}Pb). Within the sediment unsupported ^{210}Pb activity will decline with depth in

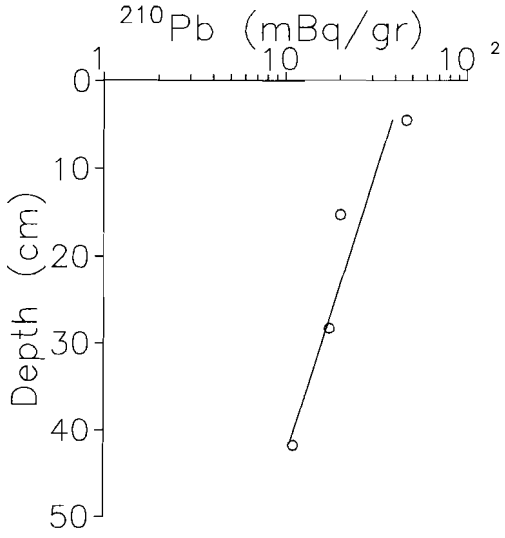

Figure 2.12 Semi-logarithmic plot of ^{210}Pb in boxcore K9B1 versus depth. Lead-210 data were kindly provided by dr. van der Plicht (R.U. Groningen).

accordance with its radioactive decay. If we assume a constant flux of unsupported ^{210}Pb to the sediment (i.e. initial homogeneity) and no significant post-depositional migration of ^{210}Pb (i.e. closed system behaviour), a ^{210}Pb age can be assigned. These assumptions form the concept of the Constant Rate of Supply model (APPLEBY and OLDFIELD, 1978). The ^{210}Pb dating method is only applicable to rapidly accumulating recent sediments. In sediments with a low sedimentation rate (e.g. less than 1 cm / 1000 yr) there is no excess ^{210}Pb measurable below the surface layer.

In order to have an independent estimate of the sediment accumulation rate 4 samples from boxcore K9B1 were selected for ^{210}Pb dating. Figure 2.12 shows a semi-logarithmic plot of total ^{210}Pb activities versus depth. If we assume a constant sedimentation rate (i.e. Constant Initial Concentration model) sediment accumulation rates of 0.9 ± 0.2 and 0.65 ± 0.15 cm yr^{-1} are obtained using the total ^{210}Pb activity and an excess ^{210}Pb activity based on a supported activity of 5 mBq gr^{-1}, respectively. The first estimate is based on the assumption that unsupported ^{210}Pb >>> supported ^{210}Pb and provides an upper limit for the true sediment accumulation rate, whereas the second estimate provides the lower limit for the true sediment accumulation rate.

Given the limited data available there is fair agreement between sediment accumulation rates estimates based on ^{14}C (1.0 ± 0.3 cm yr^{-1}) and ^{210}Pb (0.65 to 0.9 cm yr^{-1}) for sediments at station K9.

2.7.3 Differences between cores

Sediment accumulation rates based on ^{14}C dating reveal large differences between various cores. Average sedimentation rates are high at stations K3 and K9 (0.6 and 1.0 cm yr^{-1}, respectively) and relatively low at stations K4 and K11 (0.071 and 0.085 cm yr^{-1}, repectively). These differences in accumulation rates are supported by differences in interstitial water chlorinity (chapter 3) and sulphate (chapters 4 and 7) gradients with depths.

Differences in sedimentation rate are related to differences in sediment supply, submarine morphology and shallow structures (VAN DER LINDEN et al., 1989; BARMAWIDJAJA et al., 1989, 1990). The presence of numerous turbidites, ash layers and high percentages of reworked planktonic foraminifers at station K3 indicate that high amounts of mass transported sediments are trapped in the deepest part of the basin. Although sediments at station K9 accumulate faster than those at station K3, they contain less turbidites and almost no reworked foraminifers. Station K9 is situated at the foot of a relatively steep slope (Fig 2.1) and may receive various slumps of fine-grained slope sediments. Sedimentation rates at station K4 and K11 are much lower since these stations are positioned on top of a tilted block and on a local ridge respectively (VAN DER LINDEN et al., 1989). Mass-transported sediments are therefore expected to be less important at these sites.

2.8 COMPOSITION OF KAU BAY SEDIMENTS

2.8.1 Sediment petrography

A few samples from the Snellius I expedition have been investigated by NEEB (1943) using a variety of techniques (microscopic examination, mechanical analyses, wet-chemical techniques). Samples from Kau Bay contain basic to intermediate volcanic material and glass, andesite particles, plagioclase, serpentine, pyroxenes, micas, chromite and are dominated by clays. In addition to these lithogenic components, she reported various biogenic components such as pelagic and benthic foraminifera, abundant pteropods, radiolaria, diatoms, faecel pellets and wood fragments. Kau Bay sediments were found to contain 12-21 % $CaCO_3$, 3.2 to 4.1 % organic C and more than 1 % of pyrite (NEEB, 1943). Results from the Snellius II expedition are consistent with these observations. A detailed description of biogenic components can be found in BARMAWIDJAJA et al. (1989, 1990).

TABLE 2.5 Chemical composition of the sediments (mean, std. dev.)

	Al (wt%)	K (wt%)	Mg(wt%)	Ca (wt%)
K3P2	5.78 ±0.29	0.62 ±0.07	5.06 ±0.34	6.18 ±0.89
K4P1	6.41 ±0.54	0.83 ±0.32	4.20 ±0.92	4.80 ±1.19
K4P3	6.28 ±0.69	0.66 ±0.11	4.37 ±0.57	4.82 ±0.96
K9B1	5.13 ±0.25	0.70 ±0.05	4.46 ±0.26	5.70 ±0.78
K9P1	4.83 ±0.36	0.68 ±0.09	4.79 ±0.21	6.04 ±0.85
K11	4.37 ±0.38	0.48 ±0.06	5.27 ±0.95	9.98 ±1.18
	Fe (wt%)	S (wt%)	Na (wt%)	Ti
K3P2	4.70 ±0.60	1.26 ±0.21	2.75 ±0.29	2437 ±236
K4P1	4.49 ±0.85	1.84 ±0.38	2.93 ±0.33	3036 ±394
K4P3	4.19 ±0.57	1.48 ±0.31	3.42 ±0.62	2541 ±301
K9B1	4.23 ±0.29	1.20 ±0.14	3.95 ±0.79	2223 ±124
K9P1	4.14 ±0.48	1.17 ±0.13	3.81 ±0.26	2124 ±190
K11	3.58 ±0.33	1.02 ±0.15	2.17 ±0.36	2025 ±188
	Sr	P	Mn	Ba
K3P2	409 ±69	647 ± 91	952 ±146	32 ± 6
K4P1	293 ±53	687 ±156	1566 ±340	69 ±68
K4P3	302 ±46	679 ±152	1204 ±245	58 ±34
K9B1	392 ±63	783 ± 59	1154 ±197	26 ± 3
K9P1	425 ±80	701 ± 39	1177 ±198	22 ± 1
K11	544 ±69	768 ± 67	704 ± 73	29 ± 9
	Zr	Y	Li	V
K3P2	48 ± 6	14 ±1	43 ± 4	126 ±24
K4P1	65 ±27	16 ±6	47 ±11	149 ±31
K4P3	63 ±14	15 ±4	42 ± 8	137 ±24
K9B1	49 ± 2	12 ±1	43 ± 3	96 ±16
K9P1	41 ± 3	12 ±1	40 ± 4	105 ±22
K11	41 ± 6	14 ±2	35 ± 4	87 ± 9
	Cr	Ni	Zn	Co
K3P2	317 ±127	304 ±60	67 ±12	28 ±4
K4P1	251 ±109	272 ±89	73 ± 7	23 ±6
K4P3	233 ± 75	274 ±72	65 ± 9	30 ±5
K9B1	315 ± 34	247 ±20	59 ±10	21 ±3
K9P1	258 ± 77	256 ±30	53 ± 5	24 ±5
K11	173 ± 22	198 ±31	54 ± 8	18 ±3

All concentrations in ppm, unless stated otherwise. These data are based on the following number of samples: K3P2: 85; K4P1: 36; K4P3: 95; K9B1: 50; K9P1: 18; K11: 27.

2.8.2 Inorganic geochemical composition

The primary composition of sediments is in general determined by a biogenic, an atmospheric and a terrestrial lithogenic input. After deposition,

this primary composition may be altered by various diagenetic reactions.

The mean composition and standard deviation of 20 elements in 6 cores is listed in Table 2.5. Major and trace elements were determined by routine Inductively Coupled Plasma Emission Spectrometry following digestion in a mixture of hydrofluoric, nitric and perchloric acids. The bulk geochemical composition of Kau Bay sediments is rather constant, both in a single core and between different cores. The sediments from Kau Bay have a composition that is significantly different from that of average shale (Table 2.6).

TABLE 2.6 Comparison between Kau Bay and average shale

Element	Aver. Sh.[1]	Kau Bay
Li	60	35-47
Na	1.56	2.17-3.95
Mg	1.57	4.2-5.3
Al	8.8	4.4-6.4
P	700	647-783
S	0.24	1.02-1.84
K	3.00	0.48-0.83
Ca	1.58	4.8-10.0
Sc*	13	18
Ti	4600	2000-3000
V	130	87-149
Cr	90	173-317
Mn	850	704-1566
Fe	4.82	3.6-4.7
Co	19	18-30
Ni	68	198-304
Zn	95	53-73
Rb*	140	25
Sr	300	293-544
Y	41	12-16
Zr	160	41-65
Cs*	5.5	1.4
Ba	580	22-69
Hf*	2.8	1.7
W*	1.8	2.2
Th*	12	1.3
U*	3.7	5.9

* Determined by INAA rather than ICPES
All concentrations in ppm, except for Na, Mg, Al, S, K, Ca and Fe (%).
1 WEDEPOHL (1968)

Sediments from Kau Bay are significantly depleted in Li, K, Rb, Cs, Ba, Al, Zr, Ti and REE (see section 2.8.3), but significantly enriched in Mg, Ca, Sr, S, Ni and Cr.

This deviating composition of Kau Bay sediments is related to a variety of factors. Firstly, Kau Bay sediments contain between 7 and 20 % calcium carbonate. Carbonates are very poor in most elements. Hence, most elements are depleted up to a factor 1.25 due to the presence of carbonates. Secondly, Kau Bay sediments are organic-carbon rich (see chapters 7, 8).

Organic-carbon-rich sediments and sedimentary rocks are known to be enriched in S and a number of trace elements (HOLLAND, 1984; CALVERT, 1976). The S enrichment of Kau Bay sediments may therefore be a diagenetic phenomena. The sediment chemistry of S, organic C and a number of trace elements will be discussed in chapters 7 and 8.

Finally, it is unlikely that on a relatively small island like Halmahera, sedimentary recycling processes are efficient enough to mask the influence of local rock-type (e.g. andesites and ultramafic rocks). Hence, the sediments of Kau Bay have characteristics similar to rocks on the island of Halmahera, namely they are rich in Mg, Ni and Cr and depleted in K, Rb, Cs and Ba.

2.8.3 Rare Earth Elements in Kau Bay sediments

In order to remove the natural saw-tooth variation in REE characteristics as the atomic number alternates from odd to even, REE are usually normalized. Three normalizations schemes are mostly used: average chondritic meteorites (EVENSEN et al., 1978), North American Shale Composite or Post-Archean Australian Average Shale (McLENNAN, 1989) and average marine shale (SHOLKOVITZ, 1988). The choice of any normalization scheme depends on the discipline (e.g. solid-earth geochemist or marine chemist) and the question being addressed, but may influence interpretations considerably (e.g. SHOLKOVITZ, 1988). In this study REE are normalized relative to chondrite.

The chondrite normalized pattern for Kau Bay sediments is shown in Fig. 2.13. The patterns of PAAS, NASC (McLENNAN, 1989) and average

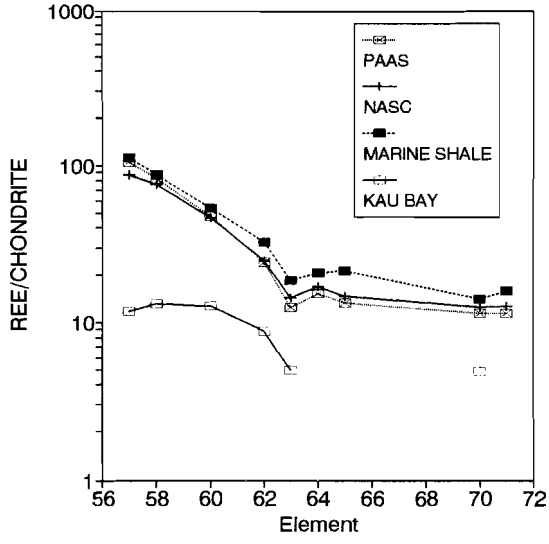

Figure 2.13 Chondrite normalized pattern for Kau Bay sediments. The patterns for PAAS, NASC and average marine shale are included for comparison.

marine shale (SHOLKOVITZ, 1988) are included for comparison. This figure shows **(1)** that LREE are only slightly enriched in Kau Bay sediments and **(2)** that the chondrite normalized pattern for Kau Bay sediments differs from that of average sedimentary rocks. The chondrite-normalized REE pattern of Kau Bay sediments is similar to that of andesites (McLENNAN, 1989). Hence, REE patterns are also indicative for the importance of local rock-type for the overall composition of Kau Bay sediments.

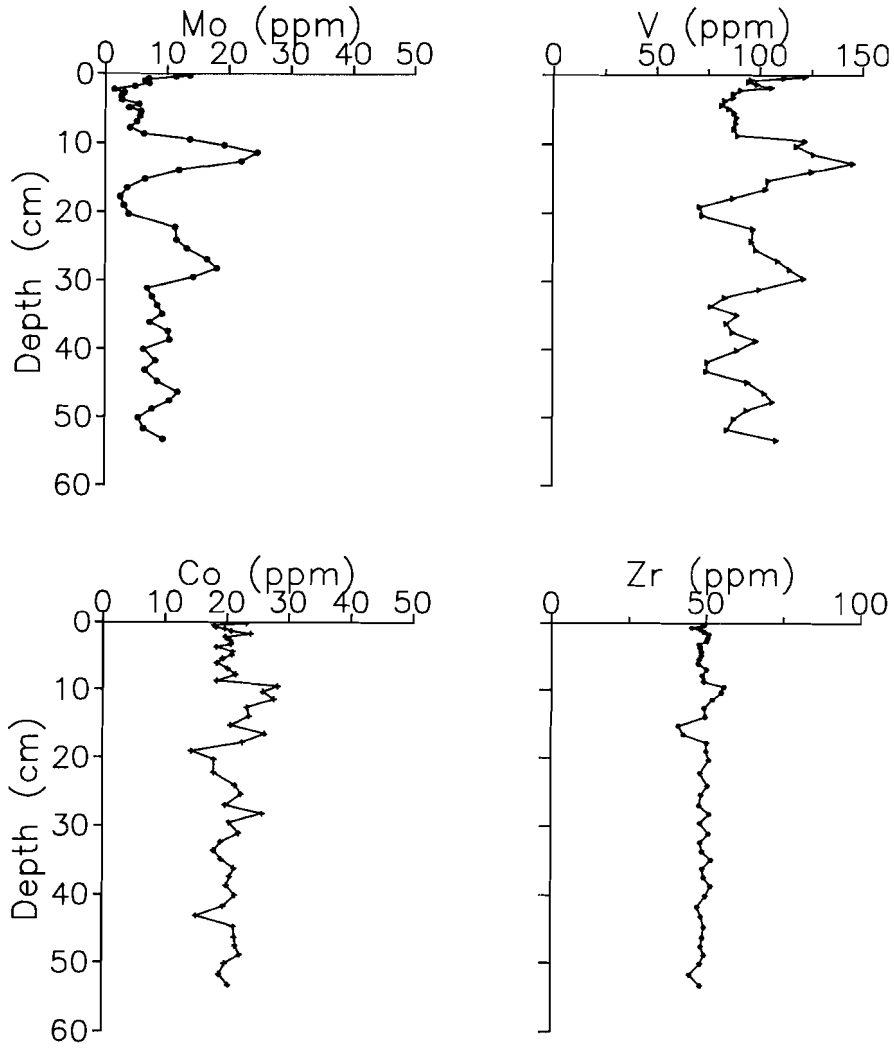

Figure 2.14 Concentration versus depth profiles for Mo (dots), V (triangles), Co (crosses) and Zr (stars) in core K9B1.

2.8.4 Do trace elements in sediments reflect environmental conditions at the time of burial?

In section (2.3) it was proposed that flushing events have a periodicity on the order of years. Such a periodicity can only be detected in the sedimentary record by taking a sampling time interval that is much smaller than the time interval to be detected.

In order to get a sufficient high resolution, a core with the highest sedimentation rate, i.e. K9B1, was sectioned into slices of a few mm. The time resolution obtained in this way, 4 to 7 months, represents a maximum since bioturbation may have lowered the extractable resolution.

The Mo, V, Co and Zr contents of bulk sediments in core K9B1 are shown in Fig. 2.14. Depth profiles for Mo and V are remarkably similar at all depths and show periodic enrichments with a cyclicity of 12 to 15 cm (i.e. 13 to 23 yr). The depth profile for Co shows limited fluctuations, whereas that for Zr is rather constant, indicating that no major fluctuations in the lithogenic input have occurred.

These parallel enrichments in Mo and V are interpreted to reflect anoxic or productivity events. SHAW et al. (1990) have shown that variations in bottom water oxygen content or surface water productivity may produce distinct changes in the trace metal signature in the sedimentary record. These authors found that near anoxic bottom water conditions lead to an increased accumulation of Cr, V and Mo. Hence, the intervals enriched in Mo and V (Fig. 2.14) may represent periods of anoxic conditions, whereas intervals depleted in these elements may represent periods with oxygenated bottom waters.

On the basis of these enrichments in Mo and V it is possible to calculate the time between periods of anoxia to be 13 to 23 yr. This estimate based on the sedimentary record is consistent with estimates based on the present-day Si-excess (13 - 22 yr) or thermohaline characteristics of Kau Bay (18 - 180 yr). This consistency suggests that multi-element signatures of the sedimentary record may be of great value in paleoceanographic studies.

CHAPTER 3: THE ISOLATION OF KAU BAY DURING THE LAST GLACIATION: DIRECT EVIDENCE FROM INTERSTITIAL WATER CHLORINITY

ABSTRACT

The pore water in the sediments of all piston cores shows a decrease in chlorinity with depth. The decrease of chloride with depth is the first direct evidence to support the theory that the Kau Bay salinity changed markedly during the Quaternary Era. These salinity changes are related to a sea level drop (relative to the present situation) of more than 40 m causing the isolation of Kau Bay. Calculations based on a transient diffusion-advection model support the existence of fresh-water conditions during the last isolational phase.

3.1 INTRODUCTION

Sea level is the most important reference surface on earth. In a geological context, however, sea levels are continually changing. It is now accepted that the sea level rose an incredible 100 to 130 m between 18,000 and 6,000 years ago, after which time the sea level has remained at about the same level (KENNETT, 1982).

Certain marginal marine basins are semi-isolated from the world ocean because of narrow gateways or high sills. These basins tend to amplify certain paleoenvironmental events of global significance. For instance, isolation of such basins due to a drop in global sea level may result in marked salinity changes, increases or decreases depending on the actual climatic setting. Kau Bay is a supreme example of such a semi-isolated basin. Kau Bay, which is enclosed by the two northern arms of the island of Halmahera (eastern Indonesia), is 470 m deep and covers an area of 60 by 30 km. It is separated from the Pacific Ocean by a sill that is only 40 m below sea-level. This peculiar submarine morphology inspired KUENEN (1943) to hypothesize:

'It appears almost certain that during the low sea levels of the Ice Age, the threshold was laid dry and the Kau Bay gradually converted into a fresh water lake. Somewhere below the recent marine sediments must be buried deposits bearing the mark of fresh water conditions. If these could be detected in our bottom samples, not only the lowering of glacial sea level could be proved, but the rate of subsequent sedimentation determined'.

Unfortunately, Kuenen and co-workers having rather limited technical possibilities, were unable to recover any sediments that had the characteristics

of fresh water deposits (KUENEN, 1943). Moreover, four decades ago not much was known about the Late Quaternary sea-level history.

Fortunately, at present the Late Quaternary sea-level history is better documented (for a summary see KENNETT, 1982). On the basis of a sill depth of about 40 m and the sea-level curve of BLOOM et al. (1974) or BARD et al. (1990), we can easily deduce that Kau Bay was probably isolated from the Pacific Ocean for at least 30,000 years. Rather than use an indirect approach by studying the sediments, we will determine the Kau Bay salinity history directly by studying the composition of fossil waters originally buried with the sediment.

Interstitial waters are interesting for the following reasons:
(1) they may retain some of the composition of the buried water; **(2)** they allow distinctions to be made between the principal modes of solute transport, i.e. between advection and diffusion; **(3)** they provide the most sensitive indicators of diagenetic reactions. For instance, the dissolution of only 0.02 % $CaCO_3$ results in a measurable increase of 20 % in the Ca concentration of the interstitial water (BERNER, 1980a); **(4)** they allow the determination of fluxes of dissolved components between sediments and overlying waters. This chapter will cover the first two aspects only; the last two will be discussed in succeeding chapters.

3.2 MATERIAL AND METHODS

In this study we discuss results obtained from cores taken during the Snellius II Expedition (Figure 2.1). The shipboard routine has been described in detail elsewhere (DE LANGE, 1984, 1988) and will be summarized briefly below.

Immediately after the core is collected, the pvc liner is cut into 1 m sections which are tightly sealed and stored horizontally at the in-situ temperature. The core sections are split lengthwise into two parts; one part for geochemical studies and the other part for detailed subsampling and for micropaleontological studies. The pressure filtration of the sediment in Reeburgh-type squeezers (REEBURGH, 1967) takes place in a nitrogen-filled glove-box. The recovered pore-water samples are sub-divided into three separate portions which are subsequently acidified (1), used for the determination of alkalinity (2), and used for other shipboard analyses (3) respectively. In the University laboratory, chloride was analysed by potentiometric titration using $AgNO_3$, the results having a standard deviation of less than 0.1 % (DE LANGE, 1986b).

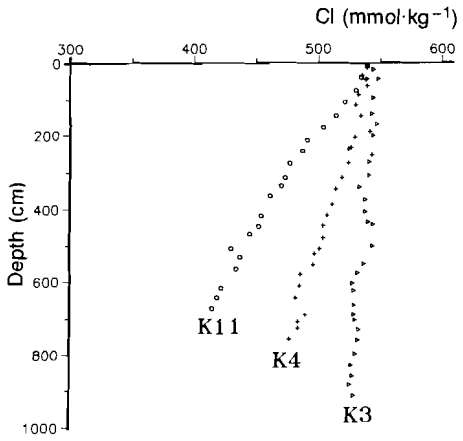

Figure 3.1 The interstitial water chloride concentration versus depth for cores K3, K4 and K11.

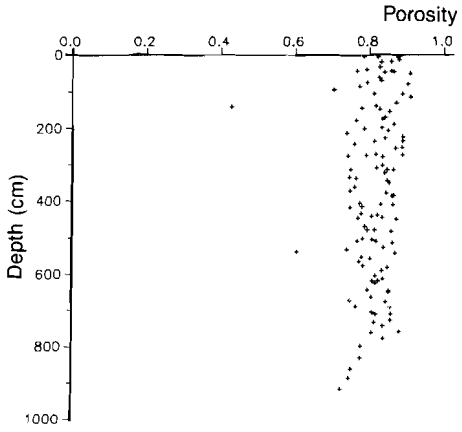

Figure 3.2 Plot showing the porosity versus depth for all cores. Porosity is calculated from water content data according to BERNER (1980a).

3.3 RESULTS AND DISCUSSION

During periods of low sea level Kau Bay is isolated from the Pacific Ocean and can be considered as a closed lake. Such a closed lake, with no outflow, normally becomes saline; salt brought in by rivers and atmospheric precipitation remains in the lake while the water is being continuously recycled. A semi-closed lake with ephemeral outflow may, however, become less saline. For Kau Bay the net annual precipitation is rather high and ephemeral outflow probably occurred. Therefore during the 30,000 yr period of isolation Kau Bay may gradually have converted into a fresh water lake. After this isolation saline conditions were re-established. As a consequence, we expect pore water chlorinities to decrease with depth down to the fresh water deposits and subsequently to increase again, because of underlying inter-glacial marine deposits.

Concentration versus depth profiles of chloride do indeed indicate that chlorinities decrease with depth in all cores (Figure 3.1). This chlorinity decrease with depth is different for various cores because of varying sediment accumulation rates. Figure 3.1 also shows that the top few samples of all cores have the same chlorinity as the bottom waters. This signifies the excellent quality of the cores: i.e. the uppermost part of the piston cores has not been distorted because there has been no significant loss of surface

sediments during the coring operation. The decrease of chloride with depth is the first direct evidence to support the theory that the Kau Bay salinity fluctuated markedly during the Quaternary Era. The presence of gas hydrates, which are ice-like substances that form in organic-rich sediments with strong bacterial methane production, could also cause a decrease in chlorinity with depth, but the P-T-conditions prevailing in Kau Bay are outside the stability fields of hydrates.

Although the salt concentrations in pore waters can yield the limits and direction of salinity changes, they cannot be used to establish former bottom salinities because diffusion has smoothed concentration gradients. In order to remove the influence of smoothing by diffusion and to obtain some ideas of dominating transport processes, we use a mathematical model for the distribution of Cl^- in Kau Bay sediment cores.

3.3.1 Description of model

At the end of Kau Bay's period of isolation (time t=0) we consider interstitial water to have had constant chlorinities to a depth of several metres and to have had the same chlorinity (C_i) as the overlying water. Hereafter (i.e. at time t > 0), sea levels were higher than the height of the Kau Bay sill and Kau Bay bottom water chlorinities are considered to be constant in time and similar to the actual chlorinity (C_o). As a result of the concentration jump at the sediment-water interface, the concentration of solute in the interstitial brine changes as a function of time and depth according to the differential equation:

$$R\frac{\delta C}{\delta t} = \frac{\delta(D[\delta C/\delta x])}{\delta x} - \frac{\delta(vC)}{\delta x} + \sum R_i \qquad (E1)$$

where R is the retardation factor, C is the concentration of the diffusing species in interstitial water, t is time, D is the diffusion coefficient, v is the rate of water flow relative to the sediment-water interface, ΣR_i is a term accounting for chemical reactions involved and x is the vertical dimension scaled to increase downwards from the sediment-water interface, set at x = 0.

Equation E1 is difficult to solve in its present form, but a solution is not necessary in view of the given conditions. To the best of our knowledge, no chemical reactions (ΣR_i - term) or equilibrium sorption processes (retardation factor R) are quantitatively important for chloride and these terms can consequently be omitted; i.e. $\Sigma R_i = 0$ and $R = 1$.

In addition, there is no porosity (i.e. diffusivity) change with depth (Figure 3.2) and we can adopt a constant and depth independent interstitial water diffusion coefficient (D).

The rate of water flow (v) is normally considered to equal the sediment

The rate of water flow (v) is normally considered to equal the sediment accumulation rate (w); i.e. interstitial water is buried along with the sediment. However, if there are very sharp porosity gradients that cause water-loss or if there is an externally imposed water flow, the rate of water flow upwards is a negative quantity. In section 2.6 it was shown that the average rate of sediment accumulation is relatively constant with depth for each core (Fig. 2.11). In the following we shall substitute the sediment accumulation rate for the water flow rate unless stated otherwise.

Adopting the above-mentioned simplifications we arrive at (see LERMAN and WEILER, 1970; LERMAN and JONES, 1973; MANHEIM and CHAN, 1974):

$$\frac{\delta C}{\delta t} = D\frac{\delta^2 C}{\delta x^2} - v\frac{\delta C}{\delta x} \qquad (E2)$$

where D is the depth independent interstitial water diffusion coefficient and v is the pore water advection rate.

Before equation E2 can be solved the initial, upper and lower boundary conditions need to be specified.

The initial condition appropriate to the presented model is that the interstitial water chlorinities are constant to a depth of several metres and similar to the chlorinity of the overlying bay water:

$$\text{at } t = 0 \qquad C = C_i \qquad (B1)$$

where C_i is the concentration of solute in both the Kau Bay pore and bottom water during the isolation period.

For the upper boundary, the concentration at the sediment-water interface after re-establishment of saline conditions is taken as the present-day concentration in the Kau Bay bottom water and is assumed to have been constant with time:

$$\text{at } t > 0; \text{ at } x = 0 \quad C = C_o \qquad (B2),$$

where C_o is the present-day chlorinity of the Kau Bay bottom waters. This sudden (jump-type) increase in bottom water salinity is very likely in view of the Kau Bay morphology and the high density of sea water, and is supported by fauna data of BARMAWIDJAJA et al. (1989) derived from post-isolation sediments.

Finally, the appropriate lower boundary condition is:

$$\text{at } t > 0; \text{ for } x \dashrightarrow \infty \quad \delta C/\delta x = 0 \qquad (B3).$$

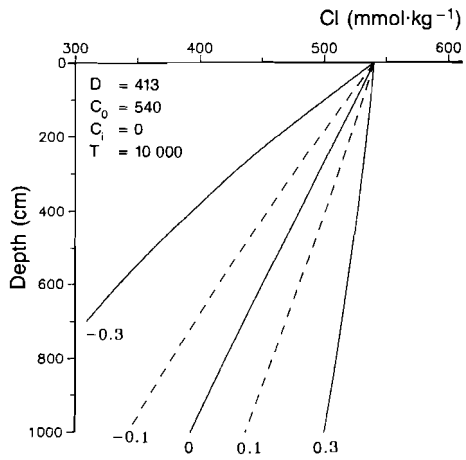

Figure 3.3 The calculated chlorinity versus depth for various sediment accumulation rates; D = 413 cm²/yr; T = 10.000 yr, C_o = 540 mmol/kg, C_i = 0 and v varies between -0.3 and 0.3 cm/yr.

A solution for E2 satisfying the initial and boundary conditions (B1, B2 and B3) is:

$$C = C_i + (C_0 - C_i)A(x,t) \qquad (E3)$$

where

$$A(x,t) = 0.5\,erfc[(x-vt)/(2\sqrt{(Dt)})] + 0.5\exp(vx/D)\,erfc[(x+vt)/(2\sqrt{(Dt)})]$$

where erfc is the error function complement (CARSLAW and JAEGER, 1959; CRANK, 1975). The error function complements (erfc) are approximated with a Taylor series of order ten.

Equation E3 contains five variables which characterize chlorinity versus depth profiles. All calculations will be based on a fixed interstitial water diffusion coefficient (D) of 413 cm²/yr (or 13.1E-6 cm²/sec) which is obtained from the temperature-corrected free diffusion coefficient of LI and GREGORY (1974), formation factor estimates of ULLMAN and ALLER (1983) and a mean porosity of 0.81. The chlorinity of Kau Bay bottom waters (C_0) is fixed at 540 mM. For the other three variables (t, v and C_i) no a priori value can be given. Therefore, we shall start by presenting figures showing the sensitivity of the curves to v, t and C_i respectively. Finally, curves will be given representing the most likely values for these parameters, namely zero chlorinity during the isolational phase, ^{14}C-determined sediment accumulation rates and post-isolational periods beginning 10,000 and 15,000 yr ago.

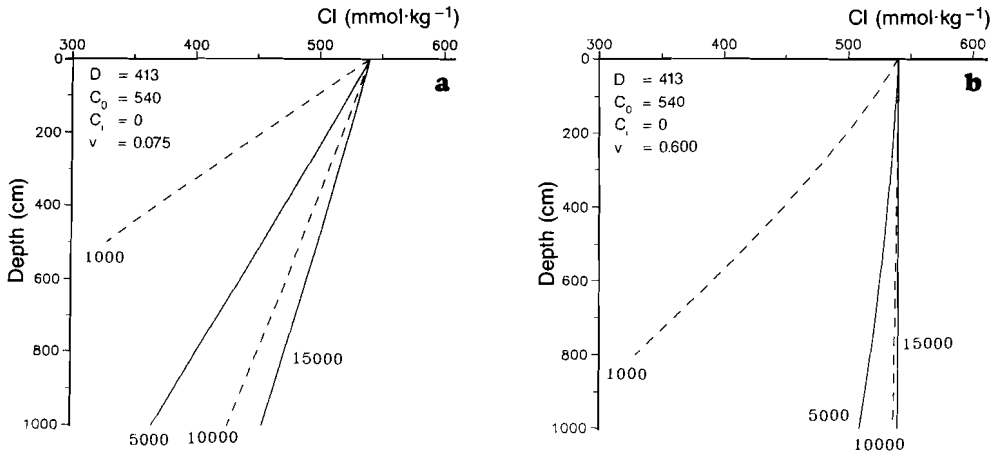

Figure 3.4 Calculated chlorinity versus depth profiles for various times; a) T varies between 1.000 and 15.000 yr and v = 0.075cm/yr; b) idem but v = 0.600. Other parameters are similar to those in Figure 3.3.

3.3.2 Sensitivity of the model

Figure 3.3 shows the sensitivity of some calculated curves to varying water flow rates. In the case of no water flow (v=0), diffusion is the only transport mechanism and the curves approximate a straight line. High sediment accumulation rates yield curves below the curve for diffusion only; the chlorinity at a certain depth is higher because of the burial of bottom water. In contrast, net water flow upwards (i.e. negative rates) yields curves above the diffusion-dominated curves.

Various time scenarios for sediment accumulation rates of 75 and 600 cm/kyr are shown in figures 3.4a and 3.4b respectively. For relatively short times the curves are very sensitive to the amount of time that has passed, whereas for longer times the curves for different times begin to converge; i.e. steady-state is approached. The effect of the length of time that has passed is relatively small for high sediment accumulation rates. Figure 3.4 suggests that the time required to reach steady-state concentrations is dependent on the water flow rate (i.e. sediment accumulation rate). This dependence can be given approximately by the transcendental equation

$$[(x+vt)/(2\sqrt{(Dt)})] \cong -2 \qquad (E4)$$

The rationale behind this approximation in E4 is as follows (see also LERMAN and JONES, 1973). When t tends to infinity, i.e. steady state is reached, the terms in square brackets in E3 approach the limits of the error function complement: erfc[∞] = 0 and erfc[-∞] = 2. However, for [(x+vt)/2(Dt)] = -2 and [(x-vt)/2(Dt)] = 2 the values for the error function complement are erfc[2] = 0.0047 and erfc[-2] = 1.9953, which are for practical purposes sufficiently close to their limiting value at t = ∞. Note that for these conditions E3 reduces to:

TABLE 3.1 APPROXIMATE TIME-REQUIRED-TO-REACH-STEADY STATE (depth of 500 cm; D = 413 cm^2yr^{-1})

v (cm yr^{-1})	time (kyr)
0.01	66200
0.075	1200
0.1	700
0.3	77
0.6	20
1.0	8
2.0	2

$$C = C_i + (C_0 - C_i)\exp(vx/D) \qquad (E5)$$

which is obviously the steady state solution for the boundary conditions (B2 and B3). Table 3.1 gives some time-to-steady-state estimates for various sediment accumulation rates. This table shows that there is a clear relation between the time-required-to-reach steady-state and the sediment accumulation rate.

Figure 3.5 Calculated chlorinity versus depth profiles for various initial chlorinities; a) C_i varies between 0 and 300 mmol/kg and v = 0.075 and T = 5.000 yr. b) idem, but T = 10.000 yr. Other parameters are similar to those in Figure 3.3.

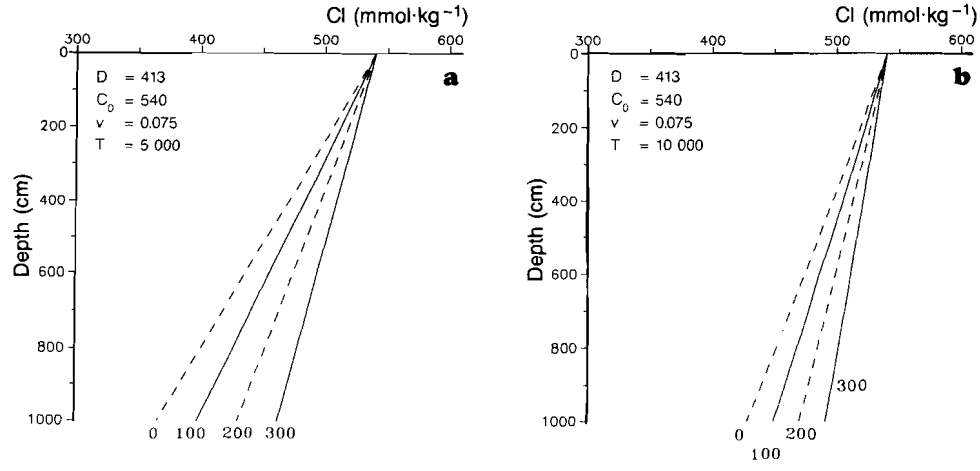

The sensitivity of the curves to varying initial chlorinity levels (C_i) is shown in Figures 3.5a and 3.5b. For non-zero initial concentrations the curves are shifted towards higher concentrations, but this increase is relatively small for larger times such as those applying to the present study.

Figure 3.6. a) The calculated and observed chlorinity versus depth profiles for cores K3 and K4. T = 10.000 yr, v = 0.075 cm/yr for K4 and v = 0.600 for K3; b) idem, but for T = 15.000 yr; c) Observed and calculated chlorinity versus depth profiles for K11. Two lines representing a best fit are also included, T = 10.000 yr and v = 0.075 cm/yr.; d) idem, but for T = 15.000 yr. Other parameters are similar to those in Figure 3.3.

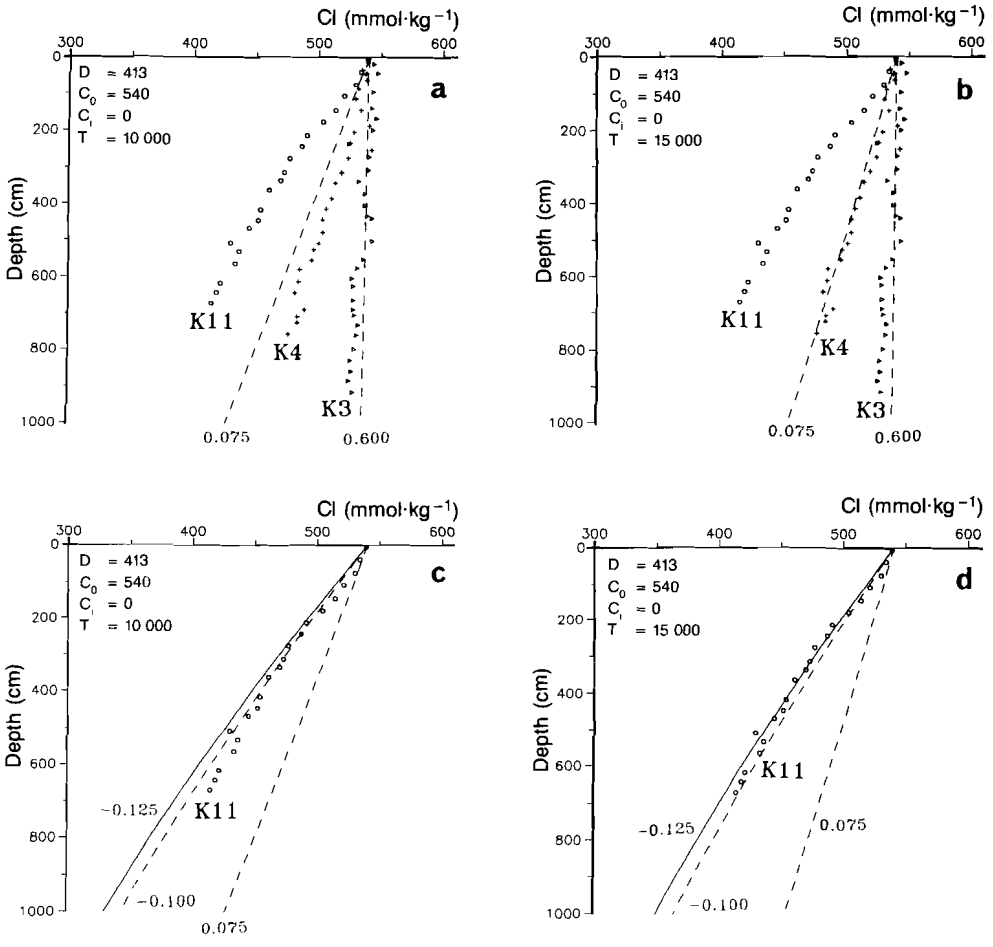

3.3.3 Application of the model

Because we do not know the actual time that has elapsed since isolation, we will present two end-member scenarios: one for 10 kyr and the other for 15 kyr. Initial chlorinities are taken to equal zero; this is supported by diatom data (BARMAWIDJAJA et al., 1989). Water flow rates are taken to equal sediment accumulation rates. Figures 3.6a and 3.6b shows the chlorinity data for cores K3, K4 and K11 and curves representing a sediment accumulation rate of 600 cm/kyr (K3) and 75 cm/kyr (K4 and K11). The curves describe the data excellently for cores K3 and K4, but not for K11. Perhaps it should be mentioned that we did not fit the data but applied appropriate independent data such as measured sediment accumulation rates, temperatures and porosities. The small scale curvature in the observed chlorinity versus depth profiles may reflect some variations in sediment accumulation rates. The lack of correspondence between the calculated curve for K11 and the observed data must be attributed to an advective flow. Figures 3.6c and 3.6d show, in addition to the curve expected if the measured sediment accumulation rate is used, two curves representing a best-fit estimate. From these curves we can calculate the pore water advection rate relative to the solid phase to be about -200 cm/kyr (i.e. best fit advection rate (-115 cm/kyr) minus sediment accumulation rate (85 cm/kyr)).

Slow advective flow of solutions through marine sediments is a subject that has received considerable attention over the last few years (e.g. WILSON, 1986). The movement of pore water relative to the solid phase has been explained by various processes such as flow induced by porosity change (i.e. compaction), submarine discharge of fresh (artesian) water, convective flow due to exchange between new crust and overlying seawater, and escape of water due to tectonic squeezing. All these processes - except compaction - are possible explanations. It is perhaps interesting to note that core K11 was recovered from the sill (see Fig. 2.1), just near a tectonic fault.

3.4 CONCLUSIONS

All piston cores show a decrease in interstitial chlorinity with depth. This decrease of chloride with depth is the first direct evidence supporting the isolation of Kau Bay during the last glaciation. During this isolation Kau Bay converted gradually into a fresh water lake.

The presented transient diffusion-advection model adequately describes the observed concentration versus depth profiles. Sensitivity analysis has shown that these profiles are influenced most by the sediment accumulation rate. Model calculations support fresh water conditions during the last isolational phase.

CHAPTER 4:INTERSTITIAL WATER CHEMISTRY IN SEDIMENTS OF KAU BAY

ABSTRACT

Measurements of Cl, Na, K, Mg, Ca, Sr, sulphate, ammonium, phosphate, alkalinity and pH are used to examine the processes controlling their distribution in the interstitial waters of Kau Bay, Indonesia. Two factors dominate the interstitial-water chemistry, namely the presence of fresh-water sediments below marine sediments and the anoxic decomposition of organic matter by bacterial sulphate reduction and methane generation. The presence of fresh-water sediments below marine sediments has resulted in the downward diffusion of Cl and other major components of seawater. In addition, it has initiated ion-exchange reactions between fresh-water clays and the brackish-to-saline pore waters. The anoxic decomposition of organic matter caused the release of ammonium, alkalinity and phosphate and the consumption of sulphate. This liberation of nutrients drives various diagenetic reactions such as ion-exchange between dissolved ammonium and exchangeable cations, and the formation of authigenic minerals. Thermodynamic calculations indicate that the pore waters approach equilibrium with calcite, dolomite, struvite, apatite and alike substances. The distribution of dissolved calcium, strontium, ammonium, sulphate and phosphate can be described by simple mathematical models.

4.1 INTRODUCTION

Kau Bay is a 470 m deep basin that is separated from the Pacific Ocean by a flat-floored 30-km-wide sill which is only 40 m below sea level. The presence of this sill has two major implications. Firstly, during the low global sea level associated with the Weichselian glaciation Kau Bay was isolated from the Pacific Ocean, and fresh-water sediments were deposited. Secondly, the sill restricts water exchange between Kau Bay and the Pacific Ocean. As a consequence, Kau Bay has a distinct hydrography and chemistry (see chapter 2). In Kau Bay organic matter is deposited at a rate exceeding the supply of dissolved oxygen and the oxic-anoxic boundary is located at, and sometimes above, the sediment-water interface. These two interesting features are not curiosities unique to Kau Bay, but are a general characteristic of silled basins (e.g. the Black Sea; ROSS et al., 1970; DEGENS and ROSS, 1974; the Baltic Sea; SUESS, 1976).

In this chapter we describe the chemistry of interstitial water in sediments of Kau Bay. The two characteristic features of Kau Bay both have a significant influence on the composition of pore water. Their effects will be

referred to as "sea-level related" and "organic-matter related" changes.

Sea-level related changes include the downward diffusion of most major elements in response to the marine transgression over the Pleistocene fresh-water sediments (see chapter 3). They also involve ion-exchange reactions between the downward diffusing ions and the fresh-water clays.

Organic-matter related changes include all processes involved in and related to the anoxic decomposition of organic matter. An important consequence of anoxic diagenesis is the release of metabolites to interstitial waters (e.g., BERNER et al., 1970; HARTMANN et al., 1973; SHOLKOVITZ, 1973; MURRAY et al., 1978; ELDERFIELD et al., 1981, and many others). This liberation of nutrients may **(1)** initiate changes in the speciation of the major components of pore water (e.g. VON BREYMANN et al., 1991), **(2)** cause changes in salinity (e.g., GIESKES, 1983; PEDERSEN and SHIMMIELD, 1990); **(3)** induce ion-exchange reactions (e.g. COMANS et al., 1989) and **(4)** result in the formation of authigenic minerals (e.g. SUESS, 1979).

The relative importance of "sea-level related" and "organic-matter related" changes for the composition of interstitial water is different for each element. Some elements are influenced only by "sea-level related" diagenetic features (e.g. Cl), whereas others are influenced only by the decomposition of organic matter (e.g. NH_4). Most of the components are, however, influenced by both resulting in a very complex behaviour of these components. It is the purpose of this chapter to trace the processes involved and to quantify them, if possible.

4.2 MATERIAL AND METHODS

In this chapter results will be discussed of the analyses of cores recovered during the Snellius II expedition in April 1985 (Fig. 2.1). The shipboard routine has been described in detail elsewhere (DE LANGE, 1986a, 1988) and will be summarized briefly below.

Cores were stored at in situ temperature (28 °C) until analysis, which was started within 24 hours of core collection. The core sections of 1 m were split lengthwise into two parts: one part was stored at 4 °C for detailed subsampling at the University laboratory and the other part was immediately transferred to a high-purity nitrogen atmosphere (O_2 < 0.003%). Samples for pore-water extraction were taken with a bone spatula after removal of the top mm of sediment in order to prevent the inclusion of oxidized/ contaminated material. The pressure filtration of the sediment in Reeburgh-type squeezers took place in a nitrogen-filled glovebox. The sediment cakes remaining after squeezing were stored under nitrogen in air-tight jars and

kept in the dark at 4 °C during transport and subsequent storage.

The recovered pore-water samples were subdivided into three separate portions which were subsequently (1) acidified, (2) used for the determination of alkalinity by potentiometric titration and (3) used for the analyses of ammonium according to the phenol-hypochlorite method (HELDER and DE VRIES, 1979) and of phosphate according to automated STRICKLAND and PARSONS (1968) methods. The acidified portion of pore water was stored at 4 °C and analysed for major elements by Inductively Coupled Plasma Emission Spectrometry (ICPES; ARL 34000). Total sulphur measured in this way is attributed to sulphate.

Prior to analysis, sediment samples for bulk determination were dried at 105 °C and finely ground in an agate mortar. Following digestion in a mixture of hydrofluoric, nitric and perchloric acids, final solutions were made up in 1 N HCl and analysed by ICPES.

The exchangeable and fixed nitrogen content of selected samples were determined using methods described in DE LANGE (1988).

A selection of sediment samples remaining after squeezing, and stored under nitrogen at 4 °C, was subjected to an acid-gradient extraction technique. These sediment samples were used directly without any pre-treatment. About 1.5 gr of sediment in Teflon (FEP) centrifuge tubes was sequentially leached for 3 hours with 20 ml each of : (1) distilled water, (2) 0.1 N NH_4Ac, (3) 10% 0.1 N HAc/90% 0.1 N NaAc, (4) 20% 0.1 N HAc/80% 0.1 N NaAc, (5) 35% 0.1 N HAc/65% 0.1 N NaAc, (6) 65% 0.1 N HAc/35% 0.1 N NaAc, (7) 80% 0.1 N HAc/20% 0.1 N NaAc, (8) 90% 0.1 N Hac/10% 0.1 N NaAc, (9) 0.1 N HAc, (10) 1 N Hac, (11) 3.3 N HAc, (12) 0.05 N HCl, (13) 0.1 N HCl, (14) 0.5 N HCl, (15) 1 N HCl, (16) 2 N HCl and (17) 6 N HCl. After each step the samples were centrifuged, and the supernatant was carefully removed and stored after addition of appropriate amounts of HCl. The residue was subsequently extracted for 24 hours with 20 ml of 10 N HF (18) and concentrated nitric acid (19). After each of these two steps the samples were centrifuged and the supernatant was carefully transferred into a teflon vessel. In the teflon vessel the solutions were evaporated to dryness and the final solutions were made up in 1 N HCl. The final residue left after these 19 steps was digested in a mixture of hydrofluoric, nitric and perchloric acids, subsequently evaporated and taken up in 1 N HCl. All 20 fractions were analysed by ICPES. The sum of the various fractions for Al,Mg,Fe,Ca,Sr and Mn was compared with the independently determined total contents and the difference was found to be less than 10%, with no systematic deviation. This agreement indicates that there was no significant sample loss due to the sequential nature of the extraction procedure.

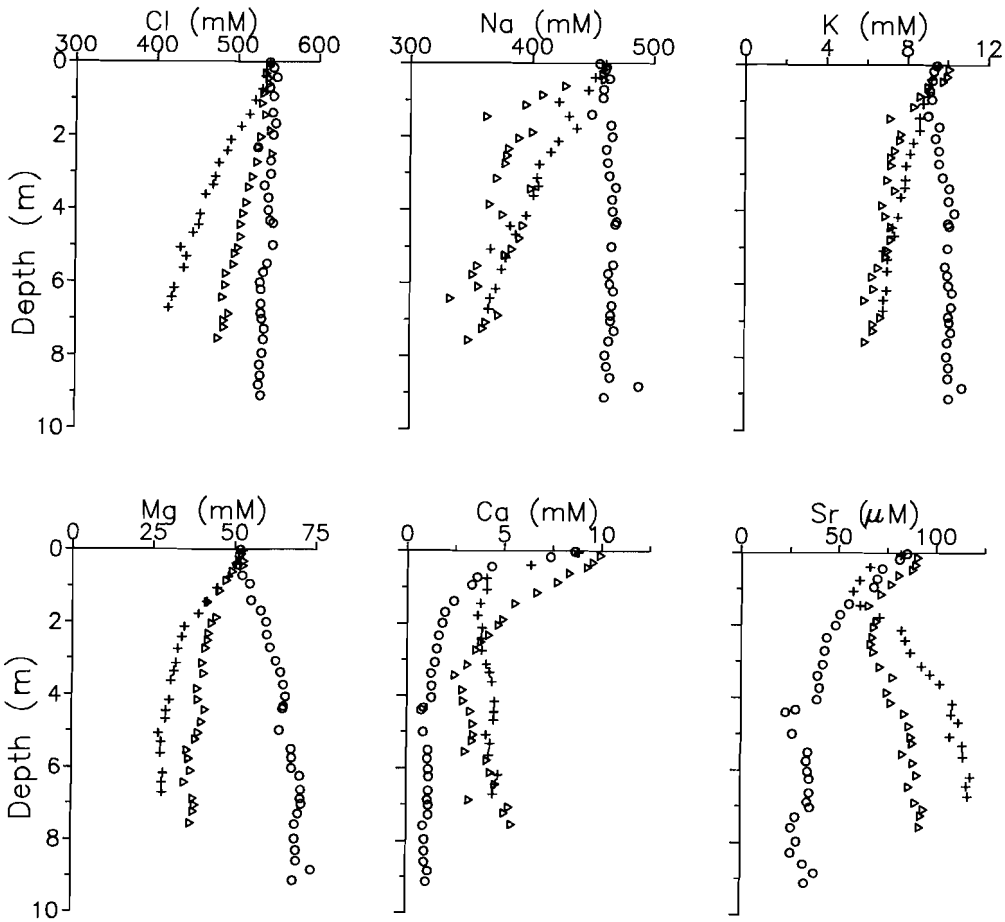

Figure 4.1 The concentration of chloride, sodium, potassium, magnesium, calcium and strontium in interstitial waters versus depth. Dots: K3; Triangles: K4 ; Crosses: K11.

4.3 RESULTS

In this chapter results will be presented from three sites in Kau Bay, namely K3, K4 and K11 (Fig. 2.1). Station K3 is positioned in the deepest part of the basin. The sediment accumulation rate at station K3 is 0.6 cm/yr. In contrast to station K3 sediment accumulation rates at stations K4 and K11 are only 0.071 and 0.085 cm/yr respectively. These differences in sediment accumulation rates are related to differences in sediment supply and submarine morphology (see Chapter 2).

The sediments in Kau Bay can be divided into three distinct units: a Holocene semi-euxinic marine facies (Unit 1), a transitional facies (Unit 2) and a Weichselian fresh-water unit (Unit 3) (see chapters 7 and 8). Sediments from unit 2 and 3 have been recovered at station K4 only. On the basis of the sediment accumulation rates for the top few meters it can be calculated by extrapolation that the fresh-water sediments of Unit 3 at stations K3 and K11 will be at depths of about 60 and 8.5 m respectively; i.e. at depths of about 50 and 1.5 m below the depths that were recovered by our cores. Accordingly, pore waters at stations K4 and K11 are likely to show features related to the presence of fresh-water deposits, whereas the interstitial water at station K3 is not expected to be influenced by "sea-level related" diagenetic features. This difference between stations will be used to unravel the processes that affect the composition of interstitial waters.

4.3.1 MAJOR ELEMENTS AND SALINITY

Figure 4.1 shows dissolved chloride, sodium, potassium, magnesium, calcium and strontium as a function of depth. This figure shows that the top few samples of all cores have the same concentrations as the bottom waters (i.e. sea water). This signifies the excellent quality of the cores: i.e. the uppermost part of the piston cores has not been distorted or was not lost during the coring operation. Concentration versus depth profiles are different for each core and for the different components.

Pore water at station K3 shows major depletions with depth for Ca and Sr, a minor depletion with depth for Cl, a minor enrichment with depth for K, a major enrichment with depth for Mg and no significant change in Na concentrations (Fig. 4.1).

Concentration versus depth profiles at stations K4 and K11 show major depletions with depth for all components but not for Ca and Sr. Concentrations of Ca initially decrease to minima at depths of about 3.5 and 1.1 m for stations K4 and K11 respectively and then increase. Similarly, concentrations of Sr initially decrease to minima at depths of about 1.5 and 1.1 m for stations K4 and K11 respectively and then increase to values above or similar to that of sea water (Fig. 4.1).

Figure 4.2 shows the content of total dissolved salts (TDS) and the TDS/Cl ($^{o}/_{oo}/^{o}/_{oo}$) ratio as a function of depth. At station K3 there are increases with depth for the TDS content and the TDS/Cl ratio. At the other two stations there are significant depletions with depth for the TDS content and the TDS/Cl ratio. Changes in the TDS/Cl ratio are considered to be due to diagenetic reactions rather than historical changes in salinity.

The distribution of chloride can be used as a measure for downward

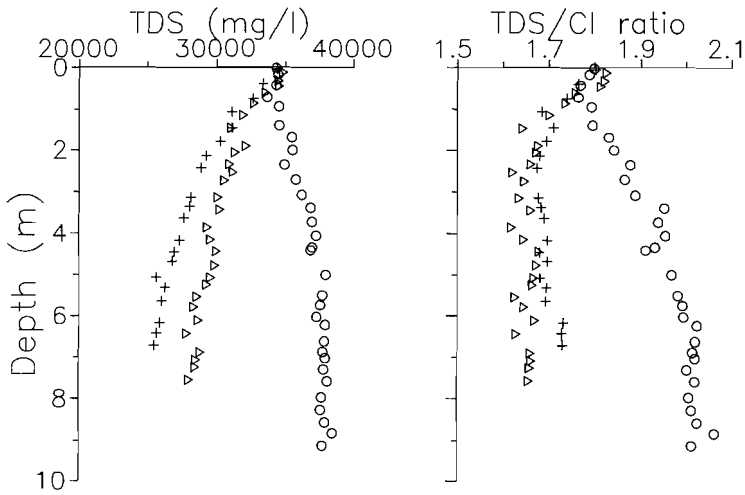

Figure 4.2 The total dissolved salt content and total-dissolved-salt/chlorinity ($^o/_{oo}/^o/_{oo}$) ratio of pore water versus depth. Dots: K3; Triangles: K4; Crosses: K11.

diffusive transport of seawater ions to the fresh-water deposits since chloride is not involved in chemical reactions (see chapter 3). On the basis of chloride versus depth profiles it can, therefore, be concluded that the downward diffusive transport of seawater ions to the fresh-water sediments is a major factor controlling pore-water gradients at stations K4 and K11, but not at station K3. It may also be concluded that the salinity increase at station K3 and part of the salinity decrease at stations K4 and K11 are not related to historical changes in the salinity, but to diagenetic reactions (Fig. 4.2).

4.3.2 SULPHATE, NUTRIENTS AND PH

Results of sulphate, ammonium, phosphate, alkalinity and pH measurements are shown versus depth in Figures 4.3 to 4.7. Interstitial water sulphate concentrations decrease to zero at depths of about 0.6, 2.2 and 1.2 m for stations K3, K4 and K11 respectively (Figure 4.3). These decreases in sulphate are accompanied by large enrichments in ammonium (Fig. 4.4), phosphate (Fig. 4.5) and titration alkalinity (Fig. 4.6).

Anaerobic decomposition of organic matter by sulphate reduction and methane generation are the dominant diagenetic processes inferred from the pore-water chemistry. The process of organic matter decomposition during sulphate reduction is usually represented by the following simple stoichiometric reaction:

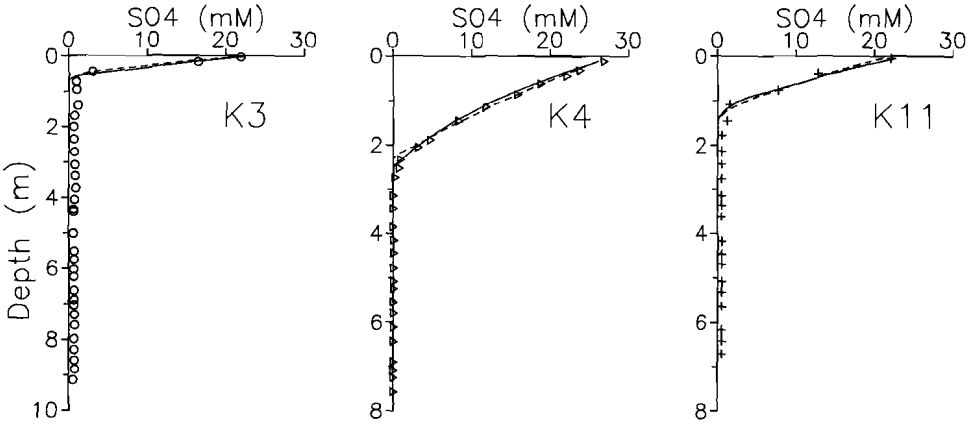

Figure 4.3 The pore water concentration of sulphate versus depth. Solid line: finite-layer model (E15); Dashed line: modified-Berner model (E16). For fit parameters see Table 4.4.

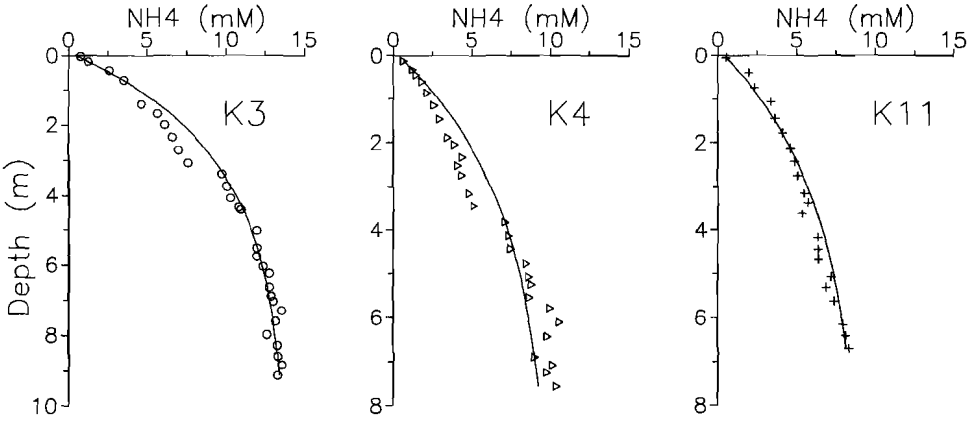

Figure 4.4 The pore water concentration of ammonium versus depth. The solid lines represent the fit to data using equation E11. For fit parameters see Table 4.3.

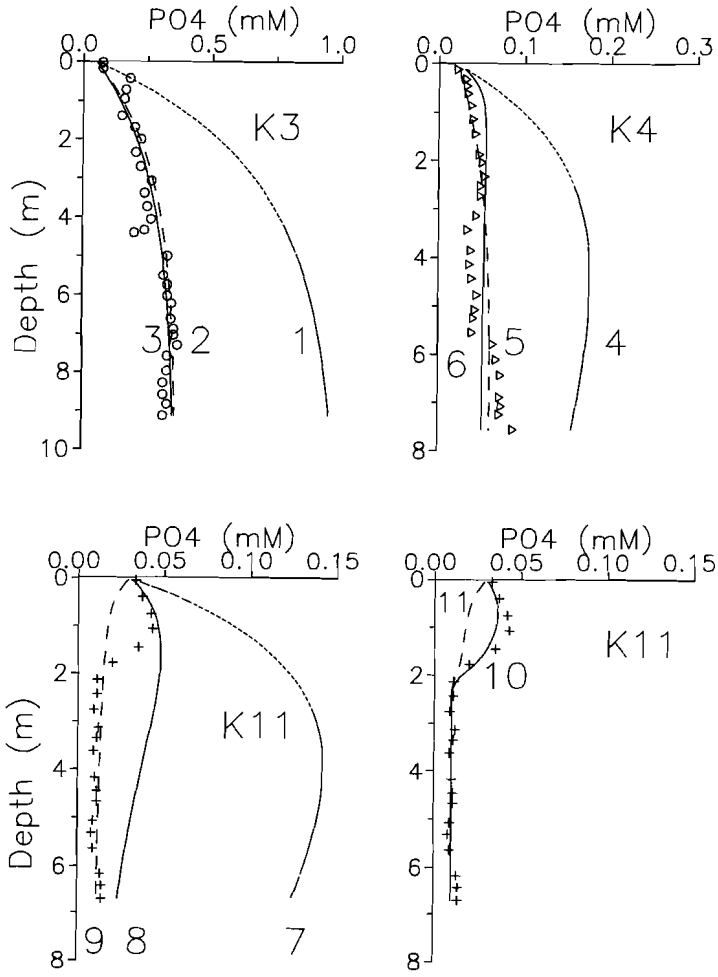

Figure 4.5 The pore water concentration of phosphate versus depth. The lines represent model curves as presented in Table 4.5.

$(CH_2O)_x(NH_3)_y(H_3PO_4)_z + 0.5x\ SO_4^{2-} \rightarrow$ (R1)

$x\ CO_2 + y\ NH_4^+ + z\ HPO_4^{2-} + (-0.5x - y + 2z)\ H^+ + 0.5x\ HS^- + x\ H_2O$

where x, y, z are stoichiometric coefficients depending on the composition of organic matter involved. The overall reaction for organic matter decomposition by methane generation can be represented by a similar simple stoichiometric equation:

$(CH_2O)_x(NH_3)_y(H_3PO_4)_z \rightarrow 0.5x\ CO_2 + 0.5x\ CH_4 + y\ NH_4^+ + z\ HPO_4^{2-} + (-y + 2z)\ H^+$ (R2).

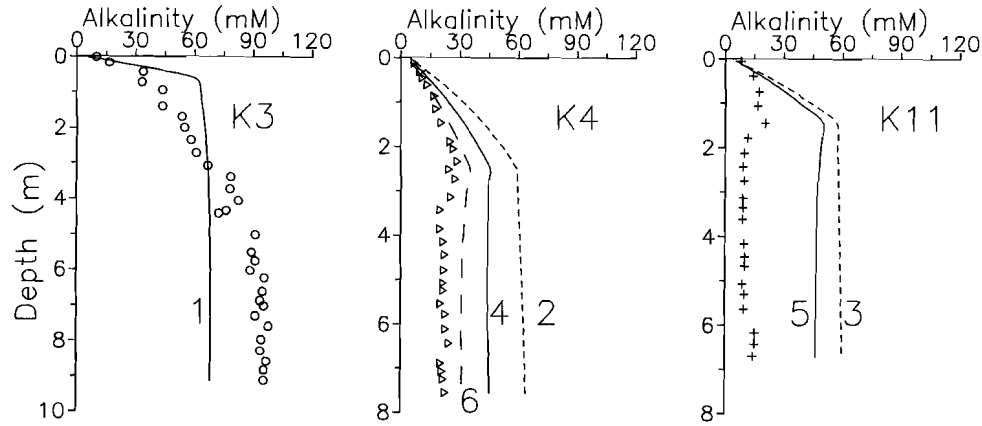

Figure 4.6 Pore water alkalinity versus depth. The lines represent model curves (E20). 1: St = 2, K3; 2: St = 2, K4; 3: St = 2, K11; 4: St = 4, K4; 5: St = 4; K11; 6: St = 5.5, K4 (see text).

Figures 4.3 to 4.6 show that significant amounts of ammonium, phosphate and alkalinity are produced in Kau Bay sediments due to anoxic organic matter decomposition according to reactions R1 and R2. Despite these large changes in concentrations of ammonium, phosphate and alkalinity, the punch-in pH of Kau Bay sediments is surprisingly constant (Fig. 4.7). At all depths at station K3, and in the sulphate reduction zone at stations K4 and K11, the pH is confined within very narrow limits; i.e. 7.2 and 7.5. In the zone of methanogenesis at stations K4 and K11 the pH observations center on values of 6.9 and 7.05 respectively. (Fig. 4.7).

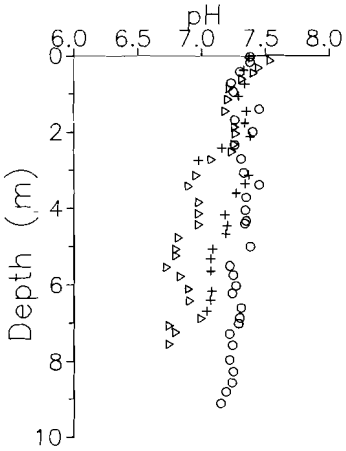

Figure 4.7 Punch-in pH versus depth. Dots: K3; Triangles: K4; Crosses: K11.

4.4 DISCUSSION

4.4.1 THERMODYNAMIC CONSIDERATIONS

4.4.1.1 CHANGES IN THE SPECIATION OF CA, MG, NA AND K IN PORE WATER

Knowledge of the speciation of the major components is a prerequisite before interpreting ion-exchange or solubility equilibria. The speciation of an ion in sea water can be determined: (1) using thermodynamic association constants and estimates for the activity coefficients of free ions and ion pairs (i.e. geochemical approach); (2) using stoichiometric association constants experimentally determined in sea water (i.e. marine chemist approach). The first method relies on reasonable estimates for the activity coefficients of ions and ion pairs, whereas the second method does not require these (e.g. MILLERO and SCHREIBER, 1982).

The first approach has been chosen for this study since (1) reliable estimates for activity coefficients of ions and ion pairs at higher ionic strength are available (MILLERO and SCHREIBER, 1982), and (2) the stoichiometric approach may not be correct for pore waters that have compositions deviating considerably from that of seawater. The ion-association model WATEQ (PLUMMER et al., 1976; VAN GAANS, 1989) was used to calculate the chemical composition of pore water. Activity coefficients for all aqueous species were calculated with the ion-pairing model of MILLERO and SCHREIBER (1982). The results of calculations for Na, K, Ca and Mg at station K3 are shown in Fig. 4.8. Results for CO_3^{2-} and HCO_3^-, and SO_4^{2-} and HSO_4^- complexes are merged and referred to as carbonate and sulphate species respectively. The speciation results as presented in Fig. 4.8 for station K3 are also representative for stations K4 and K11 although at these stations the changes were smaller due to lower alkalinities.

No significant changes in ion pairing occur for Na or K, which is not surprising since these cations exist mainly as free species in seawater (e.g. see GARRELS and THOMPSON, 1962) and form only weak complexes with carbonate and sulphate. Calcium and magnesium form, however, strong complexes with both sulphate and carbonate. This is reflected in their speciation versus depth profiles. The consumption of sulphate and production of alkalinity in the sulphate reduction zone results in an increase of Ca and Mg-carbonate complexes at the expense Ca and Mg-sulphate complexes (Fig. 4.8). This transfer of Ca and Mg between sulphate and carbonate complexes is almost quantitative. In the sulphate reduction zone

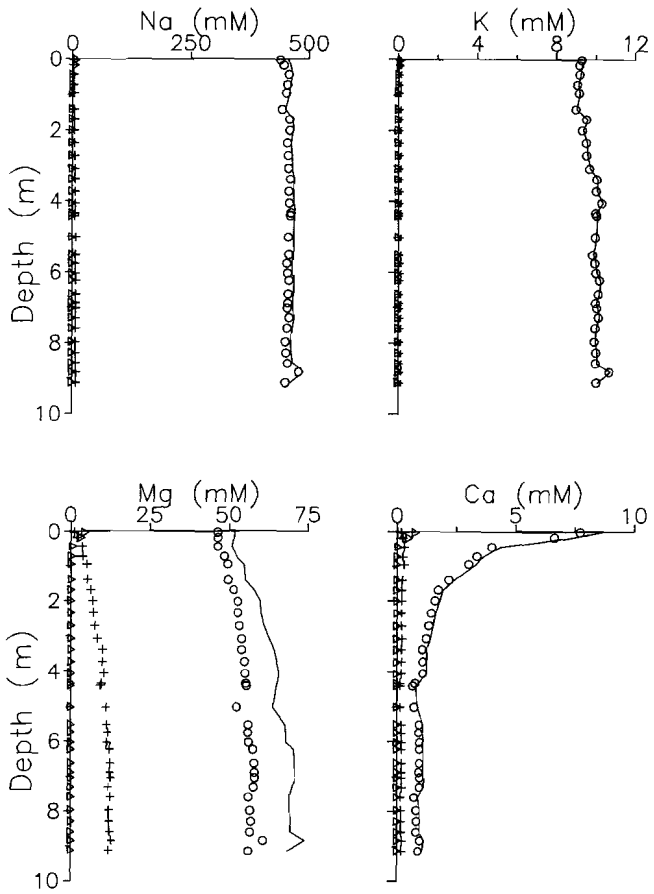

Figure 4.8 Changes in the speciation of Na, K, Mg and Ca in interstitial water at station K3. Solid lines represent the total concentration. Dots: concentration of free cation; Triangles: concentration of sulphate complexes; Crosses: concentration of carbonate complexes; Stars: concentration of chloride complexes (only for K).

there are no significant changes in concentration of free Ca^{2+} or Mg^{2+}. Similar results have been obtained by VON BREYMANN et al. (1991). Below the sulphate reduction zone the titration alkalinity continues to increase with depth (Fig. 4.6). This is followed by an increase in the concentration of Mg- and Ca- carbonate complexes (Fig. 4.8).

The percentage of Ca as free Ca^{2+} decreases from about 89 % in seawater, and in the sulphate reduction zone, to about 83 % at depths below 5 m. Similarly, the percentage of Mg as free Mg^{2+} decreases from about 89 % in seawater to about 82 % at depths below 5 m. It seems that the pore-water/sediment system is buffered rather well for changes in the constituents.

4.4.1.2 THERMODYNAMIC EQUILIBRIUM CALCULATIONS

It has been well established that anoxic decomposition of organic matter may lead to the formation of various authigenic minerals (e.g. SUESS, 1979; BERNER, 1981). Evidence of the formation of authigenic minerals can be obtained in two ways: **(1)** directly by analysing the solid phase or **(2)** indirectly by calculating the equilibrium saturation state of pore water with respect to various solid phases. Direct analysis of authigenic minerals by X-ray diffraction or wet-chemical techniques is often not possible due to factors such as the dispersive nature of newly formed minerals and their poorly defined chemical composition and X-ray diffraction patterns (see also section 4.4.9).

There are several limitations to the indirect approach based on thermodynamic equilibrium calculations (e.g. ALLER, 1980; MIDDELBURG et al., 1987; MORSE and CASEY, 1988). Firstly, the saturation state of the pore water with respect to authigenic mineral phases should be expressed properly for the solid solution present in the sediment. Since the actual phases formed are not known, it is as a first approximation instructive to calculate ion activity products (IAP) for pure minerals. Secondly, magnification of analytical uncertainties during calculation, the lack of thermodynamic data on any but a few pure well crystallized end-member phases, the exclusion of organic complexes and the lack of grain-size data for authigenic minerals preclude detailed comparison between calculated IAP and solubility products. Thirdly, there may be kinetic effects which inhibit nucleation and precipitation (e.g. MORSE and CASEY, 1988 and references therein). Nevertheless, this indirect approach has been successfully applied to predict the presence and formation of authigenic minerals (e.g. POSTMA, 1982; ALLER et al., 1986 and others).

Ion activity products were calculated with the ion-association model WATEQ. Figure 4.9 shows the ion activity products for calcium carbonate, dolomite, hydroxy-apatite and struvite versus depth. The solubility products for pure calcite (pK=8.48), aragonite (pK=8.3), dolomite (pK=17.0), hydroxy-apatite (pK=54.5) and struvite (pK=13.2) are included for comparison. Results for the IAP of siderite, vivianite, rhodochrosite, kutnohorite and reddingite are not shown because the results were highly variable and generally much lower than those expected for equilibrium with respect to pure phases.

Pore waters at all depths at station K3 and in the upper few meters at stations K4 and K11 are highly supersaturated with respect to aragonite, calcite and dolomite. Pore water at stations K4 and K11 approach equilibrium with respect to aragonite or calcite at depths below 3 and 2 m

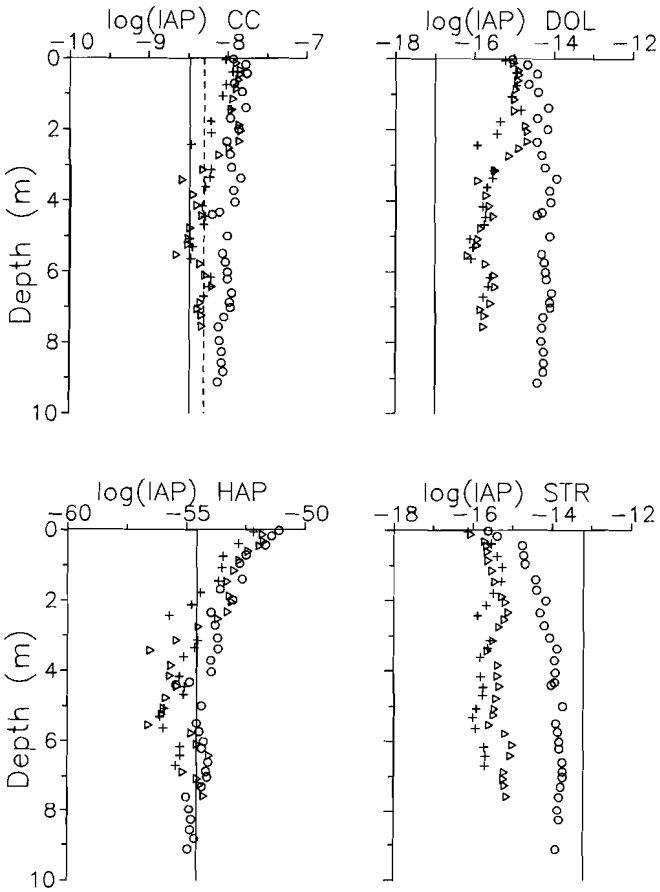

Figure 4.9 Ion activity product of calcium carbonate, dolomite, hydroxyapatite and struvite versus depth. Lines represent thermodynamic solubility products: calcite (pK = 8.48); aragonite (pK = 8.3: dashed line); dolomite (pK = 17.0); hydroxy-apatite (pK = 54.5) and struvite (pK = 13.2). Dots: K3; Triangles: K4 ; Crosses: K11.

respectively. The ion activity product for dolomite at stations K4 and K11 is remarkably constant below 3 and 2 m respectively. Dolomite is actively forming at station K4 (see chapter 6 or MIDDELBURG et al., 1990 for details), and possibly at station K11. The relatively constant IAP level reached may perhaps reflect the solubility product of the dolomite actually formed, i.e. 10^{-16}. Estimates for the solubility product of dolomite vary from $10^{-16.5}$ to $10^{-18.0}$ (e.g. CARPENTER, 1980). The variation in the reported values for dolomite can be attributed to differences in the crystallinity of and degree of substition in the dolomites. It is obvious that these discrepancies are critical for the interpretation of equilibrium on a thermodynamic basis.

The IAP for hydroxy-apatite show similar profiles at all stations, surface maxima are followed by a steady decrease with depth and virtual

constant values at depths below about 3 m (Fig. 4.9) The relatively constant value of IAP below about 3 m suggests that equilibrium with hydroxy-apatite or a similar substance has been attained. The approach of a relatively constant IAP level with depth is consistent with the removal of phosphate from the interstitial water (see section 4.4.7) and the presence of authigenic P-bearing phases (see section 4.4.9). A detailed comparison between the calculated IAP and reported solubility products is not warranted since the solubility product of apatite is strongly dependent on impurities and on crystallinity (e.g. JAHNKE, 1984; JAHNKE et al., 1983; CHANDER and FUERSTENAU, 1984).

Pore waters at stations K4 and K11 are undersaturated with respect to struvite ($MgNH_4PO_4.6H_2O$) at all depths. The interstitial water at station K3 has, however, a remarkably constant IAP of about $10^{-13.8}$ at depths below 4 m. This suggests that equilibrium with struvite or a similar substance has been attained. The asymptotic IAP level for struvite at station K3 ($10^{-13.7}$ to $10^{-14.0}$) is surprisingly similar to that found in anoxic pore water of Long Island Sound sediments ($10^{-14.1}$ to $10^{-14.6}$) by MARTENS et al. (1978). It is also consistent with reported values for the solubility product of struvite: $10^{-13.2}$ (TAYLOR et al., 1963), $10^{-13.1}$ to $10^{-14.3}$ (MARTENS et al., 1978) and $10^{-12.9}$ (STUMM and MORGAN, 1981).

4.4.2 ION-EXCHANGE REACTIONS

Clay minerals adapt very rapidly to changes in the chemical composition of the environment by loosing or gaining certain components (e.g. GARRELS and CHRIST, 1965; SPOSITO, 1984; MAES and CREMERS, 1986). These exchange reactions occur when clay minerals are transferred from a water of one composition to another of a different composition. In the marine environment the two major factors promoting ion-exchange reactions are: **(1)** the exposure of fresh-water clays to seawater and **(2)** the transport of sediment (through burial) from an environment low to an environment high in ammonium.

Both types of ion-exchange reactions may be important factors affecting the composition of pore water in sediments at stations K4 and K11. However, at station K3 the fresh-water sediments are at depths far below those recovered and it is fair to assume that the effects of ion-exchange between seawater and fresh-water clays are negligible. Hence, for sediments at station K3 it is possible to study the effects of ammonium induced ion-exchange reactions.

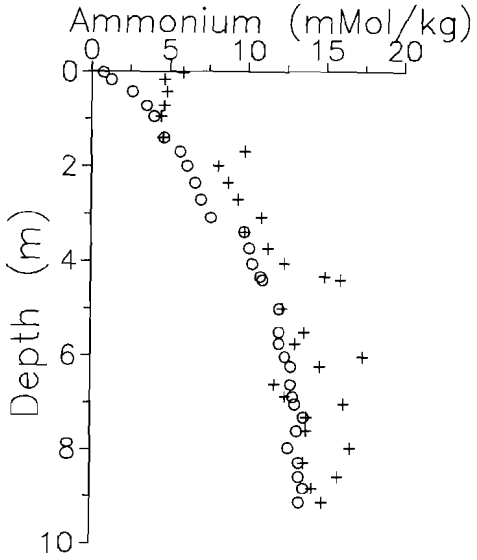

Figure 4.10 Dissolved (dots) and exchangeable (crosses) ammonium versus depth at station K3.

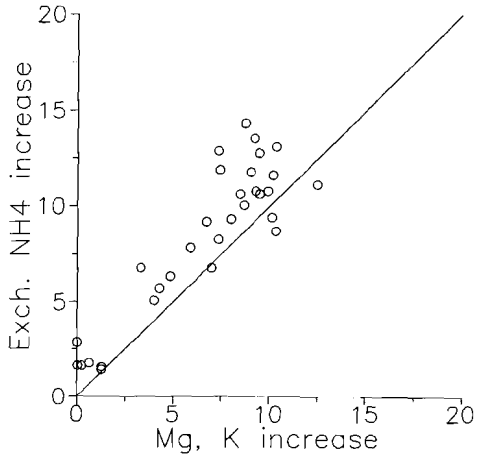

Figure 4.11 Agreement of the increase in exchangeable NH_4 (mM/kg) and the increase in dissolved cations (mM) as represented by $0.5\Delta Mg$ and ΔK. Solid line represents 1:1 stoichiometric exchange.

4.4.2.1. AMMONIUM INDUCED ION-EXCHANGE REACTIONS

Ammonium driven ion-exchange reactions may have a significant influence on the pore-water composition of rapidly accumulating anoxic sediments. In such environments ammonium can reach levels comparable to or even higher than those of Ca and K (e.g., Figure 4.4). These high concentrations of ammonium result in a significant transfer of ions from the solid phase to solution since ammonium has a high affinity for ion-exchange sites (e.g. SPOSITO, 1984; MAES and CREMERS, 1986; COMANS et al., 1989).

Figure 4.10 shows dissolved and exchangeable ammonium as a function of depth at station K3. This figure shows that a significant amount of the ammonium produced occupies exchangeable positions. The major

reactions involved are of the type:

$$NH_4^+ + M_{ex} \text{ ---> } NH_{4ex} + M^+ \qquad (R3)$$

and

$$2\,NH_4^+ + D_{ex} \text{ ---> } 2\,NH_{4ex} + D^{2+} \qquad (R4)$$

where M is Li, Na, K, Rb or Cs and D is Mg, Ca, Sr or Ba. Accordingly, an increase in the concentration of these elements is expected. Pore waters at station K3 do indeed show an enrichment in Mg and K, but are depleted in Ca and Sr (Figures 4.1, 4.12, 4.13). Data for Li, Rb, Cs and Ba are not available. The depletions in Ca and Sr are probably due to the precipitation of authigenic carbonates (see sections 4.4.1.2 and 4.4.3).

If ionic exchange is the major reaction responsible for changes in Mg and K then an increase in exchangeable ammonium should be balanced by an increase in dissolved magnesium and potassium:

$$NH_{4ex} = \Delta K + 0.5 * \Delta Mg \qquad (E1)$$

The balance between exchangeable ammonium and increases in dissolved Mg and K (Fig. 4.11) is quite good considering the omission of other exchangeable cations such as Ca, Sr, Na and H^+. This agreement suggests that the increase in the concentrations of Mg and K are due to ion-exchange with NH_4. This interpretation is consistent with the fact that maxima for dissolved magnesium, potassium and rubidium in pore water are found together with maxima in dissolved ammonia at various DSDP and ODP sites (e.g. GIESKES, 1983 and references therein).

Recently, VON BREYMANN et al. (1991) suggested that maxima in dissolved Mg are related not only to ammonium exchange reactions, but also to ligand competition. Their arguments are based on a reduction of free Mg^{2+} concentration due to formation of Mg-carbonate complexes. These lowered concentrations of free Mg^{2+} induce desorption of Mg adsorbed onto solid surfaces and may so cause an increase in total dissolved magnesium.

Pore water data at station K3 show, however, that this ligand competition mechanism is relatively unimportant in sediments of Kau Bay. Although the increase of Mg-carbonate complexes causes a depletion in the relative concentration of free Mg^{2+} (e.g. from 89 % to about 82 %), there is an increase in the absolute concentration of free Mg^{2+} (see Figure 4.8). The primary cause for enhanced Mg concentrations in sediments of K3 is therefore NH_4-exchange rather than Mg-desorption due to lowered free Mg^{2+}. The formation of Mg-carbonate complexes does, however, indirectly favour Mg-NH_4 exchange by lowering the concentrations of free Mg^{2+}.

The relative importance of an ammonium exchange versus a ligand-competition mechanism for release of Mg from the solid phase is dependent on the Alkalinity/NH_4 ratio of the pore waters (e.g. VON BREYMANN et al., 1991). The pore waters in Kau Bay have rather low C/N (i.e. HCO_3/NH_4) ratios due to the removal of alkalinity through the formation of authigenic carbonates (see sections 4.4.1.2 and 4.4.8; chapter 6).

4.4.2.2 ION-EXCHANGE REACTIONS IN THE FRESH-WATER SEDIMENTS

When riverine particles are carried to the marine environment they will react with seawater. This type of ion-exchange reactions mainly involves the release of Ca and H^+ and the uptake of Na and sometimes Mg and K (e.g. SAYLES and MANGELSDORF, 1977). Ion-exchange reactions are known to be very fast (e.g. KINNIBURGH and JACKSON, 1981) and reach therefore virtual completion before sedimentation. The effects of this type of ion-exchange on the composition of interstitial water is generally limited (e.g. see SAYLES, 1979; DE LANGE, 1986b). However, in areas where fresh/brackish water sediments are underlying marine sediments ion-exchange reactions may influence the composition of interstitial water significantly (e.g. the Black Sea: MANHEIM and CHAN, 1974; the Baltic Sea: SUESS, 1976, 1982; MANHEIM, 1982; JAKOBSEN and POSTMA, 1989; the southern Norwegian Sea: DE LANGE, 1983).

In the southern Norwegian Sea, where a fresh-to-brackish sediment slab is underlying marine sediment, DE LANGE (1983) observed an approximately linear decrease with depth for Cl, Na, K and Mg and an increase with depth of Ca and Sr. He explained the behaviour of Na, K, Mg and Cl by diffusive exchange between the fresh/brackish sediment and seawater and attributed the increase in Ca and Sr to ion-exchange reactions with the clay minerals in the fresh-to-brackish sediments. Similarly, in the Baltic Sea SUESS (1976, 1982) observed significant depletions with depth for Cl, Na, K and Mg and an enrichment with depth for Ca. The chloride concentration gradient was interpreted to be the result of diffusive downward flux of seawater ions. He explained the increase in Ca by desorption of Ca from exchangeable sites on fresh-water clays with simultaneous uptake of Na, K and Mg. SUESS (1976, 1982) was able to make a charge balance between the Ca added and Na, K and Mg lost from solution to confirm ion-exchange as the major reaction involved.

The exchange reactions described by SUESS (1976, 1982) and DE LANGE (1983) are likely to affect the composition of pore waters at stations K4 and K11. The data shown in Figures 4.1, 4.12, 4.13 do indeed show

depletions with depth for Cl, Na, K and Mg and enrichments with depth for Ca and Sr at stations K4 and K11. However, the trends are not very clear due to the occurrence of two other reactions that counterbalance some of the features related to ion-exchange between saline pore water and fresh-water clays. Firstly, the ion-exchange and desorption reactions induced by enhanced levels of ammonium and alkalinity may have caused the liberation of Ca, Sr, Mg, Na and K as has been observed at station K3 (see section 4.4.2.1). Secondly, the formation of authigenic calcium carbonate, dolomite and apatite may have resulted in the removal of Ca, Sr (Figs. 4.12 and 4.13; chapter 6) and Mg (chapter 6). Depending on the rate of removal by authigenic mineral formation, the rate of uptake or release by ion-exchange with ammonium and the rate of uptake or release by ion-exchange between saline pore water and fresh-water sediments, any of these three processes may be dominating and hence be deduced from the pore water profiles. The observation that both Ca and Sr increase at greater depth at stations K4 and K11 suggest that ion-exchange reactions between pore-water and fresh-water clays may be the most important process at these depths. A more quantitative description of removal and liberation rates for Ca and Sr will be given in the next section.

4.4.3 CALCIUM AND STRONTIUM

In the previous section it was shown that Ca and Sr are involved in a number of processes. These elements are added to pore water through ion-exchange reactions, but are removed from pore water through the precipitation of aragonite, calcite, dolomite and apatite. The net rate of removal or addition of dissolved Ca and Sr results from the competition between supply and precipitation processes. It is possible to obtain estimates for reaction rates by the use of diagenetic equations (e.g. LERMAN, 1979; BERNER, 1980a).

The general diagenetic equation for a dissolved component in pore water

$$\frac{\delta C}{\delta t} = \frac{\delta(D\delta C/\delta x)}{dx} - \frac{\delta(vC)}{\delta x} + \sum R \qquad (E2)$$

includes three major processes, namely diffusion, advection and chemical reactions respectively (BERNER, 1980a). In this equation: C is the concentration, t is time, x is the depth below the sediment-water interface, D is the sediment diffusion coefficient, v is the advection rate and ΣR is the rate of each chemical reaction affecting the component described.

The distribution of Ca and Sr in pore water of sediments in Kau Bay

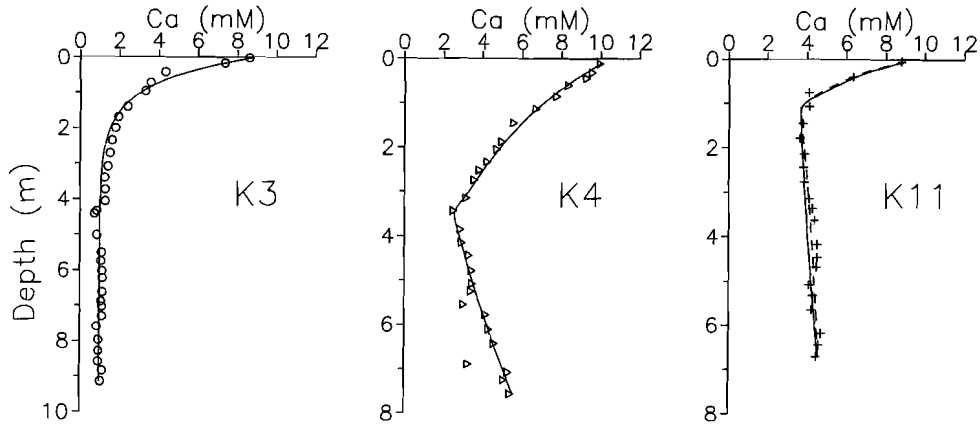

Figure 4.12 The pore water concentration of calcium versus depth. Solid lines represent model fits (see Table 4.1). Dashed line at station K11 represent model fit for v = -0.1 cm yr^{-1}.

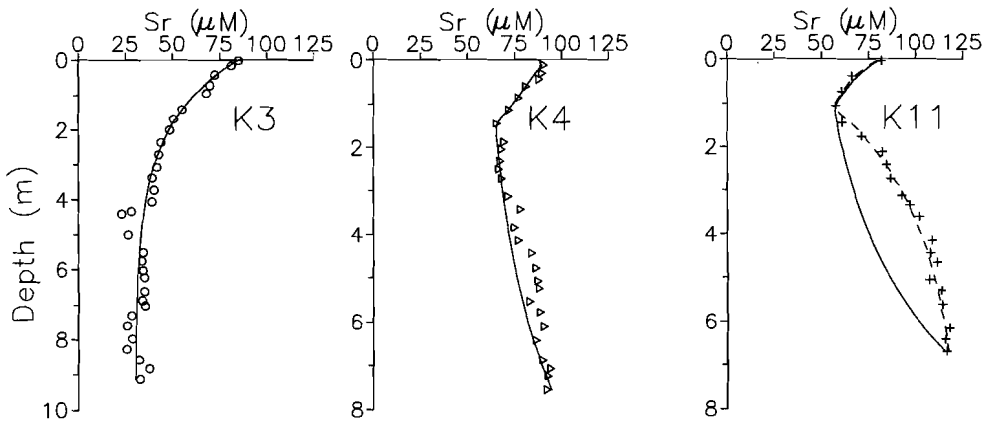

Figure 4.13 The pore water concentration of strontium versus depth. Solid lines represent model fits (see Table 4.1). Dashed line at station K11 represent model fit for v = -0.1 cm yr^{-1}.

can be modelled using:

$$D\frac{\delta^2 C}{\delta x^2} - v(1+K)\frac{\delta C}{dx} - k_m(C - C_{eq}) = 0 \qquad (E3)$$

where C is the concentration of dissolved Ca or Sr (mM or μM respectively), C_{eq} is the concentration at saturation with the authigenic precipitate (mM or μM), D is the sediment diffusion coefficient for Ca or Sr ($cm^2\ yr^{-1}$), v is the advection rate ($cm\ yr^{-1}$), K is the dimensionless linear adsorption constant for Ca and Sr and k_m is the first-order rate constant for Ca or Sr removal (yr^{-1}). The basic assumptions of this model are:

(1) steady state diagenesis is present

(2) diffusion occurs via molecular processes only

(3) there are no porosity gradients with depth (see Figure 3.2; MIDDELBURG and DE LANGE, 1989)

(4) equilibrium adsorption is present and follows a simple linear isotherm

(5) authigenic mineral formation is the major removal process involved

(6) precipitation of Ca and Sr to form authigenic minerals takes place via the simple linear rate law $R_{ptn} = k_m(C-C_{eq})$.

This assumption of linear kinetics for Ca and Sr removal is probably the major restriction to the model. No attempt has been made to describe the removal of Ca and Sr with more complex reaction kinetics since very little is known about the precipitation kinetics of these minerals at conditions relevant to those found in marine pore waters. Precipitation rates for aragonite, calcite and hydroxyapatite are known to depend strongly on factors such as the degree of supersaturation, the temperature and the presence of inhibitors (e.g. BERNER, 1980a; MORSE, 1983; MUCCI, 1988; MIDDELBURG et al., 1990). In addition, the removal of Ca and Sr occurs through the precipitation of a mineral assemblage rather than a single mineral. Given this lack of information on the number of minerals involved and their precipitation kinetics, it is not warranted to adopt higher-order kinetics to describe the overall rates of removal of Ca and Sr.

Before equation E3 can be solved the boundary conditions need to be specified. For the upper boundary condition the concentration of Ca and Sr are set equal to their concentration in bottom water:

$$x = 0;\ C = C_o \qquad (B1).$$

It is possible to consider pore-water profiles either as semi-infinite columns or as columns with a finite thickness (e.g. see BERNER, 1974b, 1980a; VAN GENUCHTEN, 1981; LERMAN, 1975; TOTH and LERMAN, 1977). For a semi-infinite pore-water medium with the lower boundary

condition:

$$x \dashrightarrow \infty;\ C = C_{eq} \qquad \text{(B2)}$$

the solution of equation E3 is:

$$C = C_{eq} - (C_{eq} - C_0)\exp\left(\frac{[v(1+K) - \sqrt{v^2(1+K)^2 + 4k_m D}]x}{2D}\right) \qquad (E4a)$$

or

$$C = C_{eq} + (C_0 - C_{eq})\exp\left(\frac{[v(1+K)]x}{2D} - Rx\right) \qquad (E4b)$$

where

$$R = \sqrt{\frac{v^2(1+K)^2}{4D^2} + \frac{k_m}{D}}$$

For a sediment layer of finite thickness (L) with the lower boundary condition:

$$x = L;\ C = C_1 \qquad \text{(B3)}$$

the solution of equation E3 is:

$$C = C_{eq} + (C_0 - C_{eq})\exp\left(\frac{[v(1+K)]x}{2D}\right)\frac{\sinh(R(L-x))}{\sinh(RL)} \qquad (E5)$$

$$+ (C_1 - C_{eq})\exp\left(\frac{v(1+K)(x-L)}{2D}\right)\frac{\sinh(Rx)}{\sinh(RL)}$$

where C_1 is the concentration of Ca or Sr at depth x = L and sinh is the hyperbolic sine: sinh{z} = 0.5(exp{z}-exp{-z}). It is often found that the concentrations of Ca and Sr are at their equilibrium value at the lower boundary:

$$x = L;\ C = C_{eq} = C_1 \qquad \text{(B4).}$$

TABLE 4.1 Parameters for modelling of Ca and Sr

	K3		K4		K11	
	Ca	Sr	Ca	Sr	Ca	Sr
D^1 ($cm^2\ yr^{-1}$)	162	162	162	162	162	162
K^2	1.6	5	1.6	5	1.6	5
v^3 ($cm\ kyr^{-1}$)	600	600	71	71	85	85
$C_o{}^4$ (mM/μM)	9	85	10.5	92	9.5	82
$C_{eq}{}^4$ (mM/μM)	1	30	2.5	65	3.6	57
$C_1{}^4$ (mM/μM)	--	--	5.5	94	4.6	118
L^4 (cm)	900	900	750	750	670	670
Lay1-2 ^{4} (cm)			350	150	110	110
$k_m{}^5$ ($*10^{-2}\ yr^{-1}$)	5	2.5	0.5	0.5	5	5

1 Diffusion coefficient in sediment for Ca and Sr were obtained from the temperature/salinity corrected diffusion coefficient of LI and GREGORY (1974), formation factor estimates of ULLMAN and ALLER (1983) and a mean porosity of 0.81.
2 BERNER (1980a)
3 ^{14}C determined sediment accumulation rates
4 Estimated from data: Lay1-2 means the boundary between layer 1 and layer 2 in two-layer models.
5 Obtained by curve fitting

The solution is then given by:

$$C = C_{eq} + (C_0 - C_{eq})\exp\left(\frac{[v(1+K)]x}{2D}\right)\frac{\sinh(R(L-x))}{\sinh(RL)} \qquad (E6)$$

At station K3 concentrations of dissolved Ca and Sr decrease continually with depth due to precipitation. However, at stations K4 and K11 the initial decrease in dissolved Ca and Sr due to precipitation is followed by an increase related to the diffusion of Ca and Sr from the fresh-water sediment to the overlying marine sediment. In the fresh-water sediments, there are relatively high concentrations of Ca and Sr due to ion-exchange reactions between fresh-water clay and saline pore water (see section 4.4.2.2).

Pore water profiles at station K3 have been modelled using equations E4 and E6. Pore water profiles for Ca and Sr at stations K4 and K11 could only be described using two-layer models based on appropriate modifications of equations E5 and E6. In the upper layer Ca and Sr are removed from the

pore water, whereas in the lower layer no such removal processes are considered. The behaviour of Ca and Sr in the lower layer is assumed to be governed by diffusion, advection and ion-exchange only. Results of the modelling efforts are shown in Figures 4.12 and 4.13. The parameters used for modelling the distribution of Ca and Sr are summarized in Table 4.1.

The data at station K3 could be described equally well, and with the same parameters, using a semi-infinite or finite layer model. This is probably due to the high rate of Ca and Sr removal. If the layer thickness (L) is large or the rate of Ca or Sr removal is very fast (k_m), then the finite layer model (E6) becomes nearly identical to the semi-infinite model (E4).

Two curves are presented for Ca and Sr at station K11; one on the basis of sediment accumulation rates (solid line) and another one using an advection rate of -0.1 cm yr^{-1} (dashed line). Figures 2.12 and 2.13 show that the latter curves (v = -0.1 cm yr^{-1}) provides a better description for the distribution of Ca, and in particular Sr, in the lower layer. This advection rate of -0.1 cm yr^{-1} is not merely introduced to provide a better fit to the data, but has been determined independently using the distribution of dissolved chloride (see chapter 3; MIDDELBURG and DE LANGE, 1989).

Rate parameters for Ca and Sr removal from pore waters were estimated by fitting the appropriate equations to the data. The values obtained are rather high and vary from 0.005 to 0.05 yr^{-1} (Table 4.1). For linear kinetics, the half-life of the removal reactions can be calculated as $t_{1/2} = \ln\{2\}/k_m$ = 14 - 140 yr. These rate parameters for Ca and Sr removal are not independent from those of alkalinity and phosphate since they are coupled through the principle of solubility equilibrium. Accordingly, the rate of Ca and Sr removal is indirectly coupled to the rate of organic matter decomposition. A quantitative description of the rate of organic matter decomposition will be given in the next few sections.

4.4.4 STOICHIOMETRIC MODELLING OF NUTRIENT REGENERATION

The simplest model for nutrient regeneration is the stoichiometric model. In this model, the changes in the concentrations of dissolved sulphate, ammonium and phosphate are used to predict the average chemical composition of decomposing organic matter: i.e. the stoichiometric coefficients x, y, z in reactions R1 and R2 are determined (see section 4.3.2).

The changes in dissolved sulphate, ammonium and phosphate are plotted against each other in Figure 4.14. This figure shows some interesting features. Firstly, at low concentrations of sulphate there is considerable change in the relationships between sulphate and ammonium. This implies

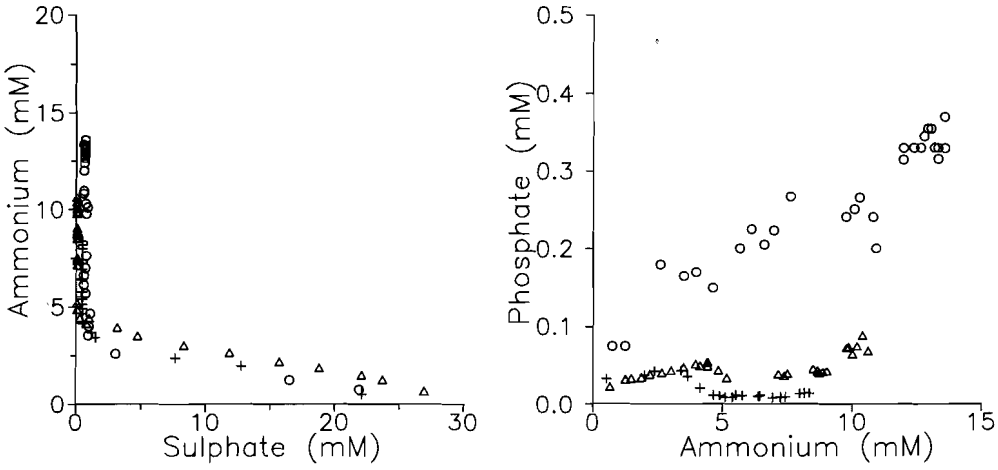

Figure 4.14 Pore water ammonium versus sulphate and phosphate versus ammonium. Dots: K3; Triangles: K4 ; Crosses: K11.

that ammonium is produced not only during sulphate reduction (reaction R1), but also during methane generation (reaction R2). Secondly, in the zones of sulphate reduction there are linear relationships between sulphate depletions and ammonium enrichments with slopes varying between 6.5 and 8 (see also chapter 7). Thirdly, there is a linear relationship between ammonium and phosphate enrichments with a slope of about 53 at station K3, but not at stations K4 and K11. This linear relationship between ammonium and phosphate enrichments at station K3 may imply that the same organic material is being decomposed by sulphate reducing and methane generating bacteria. However, care should be taken to pursue this linear relationship since pore waters at station K3 approach saturation with respect to phosphate and ammonium bearing phases such as struvite and hydroxy-apatite (see Fig. 4.9). The lack of relationship between phosphate and ammonium at stations K4 and K11 is probably due to removal of phosphate through authigenic mineral formation.

It has been shown by BERNER (1977) that the slope of the straight line between sulphate depletions and ammonium or phosphate enrichments can be used to estimate the C:N:P stoichiometry provided that corrections are made for differential diffusion and adsorption of the various ions and provided that steady-state diagenesis is present. The appropriate equations for determination of the C/N and N/P ratios are:

$$\frac{C}{N} = \frac{2\Delta SO_4}{\Delta NH_4} \frac{(v^2 + kD_s)}{(v^2(1+K_N) + kD_n)} \qquad (E7)$$

$$\frac{N}{P} = \frac{\Delta NH_4}{\Delta PO_4} \frac{(v^2(1+K_N) + kD_n)}{(v^2(1+K_P) + kD_p)} \qquad (E8)$$

where ΔSO_4 is the sulphate depletion, ΔNH_4 and ΔPO_4 are the ammonium and phosphate enrichments, D_s, D_n and D_p are the diffusion coefficients of sulphate, ammonium and phosphate corrected for tortuosity, salinity and temperature effects, K_N and K_P are the linear sorption coefficients of ammonium and phosphate respectively and k is the first-order rate constant for organic matter decomposition.

The C/N molar ratio of decomposing organic matter in Kau Bay varies from 6.5 to 8.4 (e.g. see Table 7.1), whereas the N/P molar ratio of decomposing organic matter at station K3 is about 58 (Table 4.2). No such estimates could be made for the decomposing organic matter at stations K4 and K11 since there are non-linear relationships between phosphate and the other metabolites at these stations. It is however fair to assume that the N/P ratio deduced at station K3 is applicable to the other stations since the C/N ratios are very much alike (see Table 7.1). Accordingly, the composition of organic matter decomposing in Kau Bay sediments can as a first approximation be represented by: $(CH_2O)_{106}(NH_3)_{12.6\text{-}16.3}(H_3PO_4)_{0.22\text{-}0.28}$.

TABLE 4.2 N/P ratio of decomposing organic matter at station K3

D_n (cm^2yr^{-1})	436
D_{p_1} (cm^2yr^{-1})	218
K_P [2]	1.8
K_N [2]	0.9
v	0.6
k ($*10^3$ yr^{-1}) [3]	2.1
dNH_4/dPO_4	52.8
N/P	57.6

1 KROM and BERNER (1980)
2 Determined from plot of exchangeable versus dissolved ammonium.
3 Table 4.3

4.4.5 KINETIC MODELLING OF AMMONIUM

Ammonium is formed through decomposition of nitrogen-bearing organic compounds. Decomposition of these compounds occurs not only by sulphate reduction but also by methane generation. This is indicated by the continued increase of ammonium in the pore water below the depth where sulphate is depleted (Figures 4.4 and 4.14). This has been observed not only in Kau Bay, but also in Loch Duich in Scotland (PRICE, 1976), Somes Sound (BERNER et al., 1970) , Long Island Sound (ROSENFELD, 1981), Saanich Inlet (MURRAY et al., 1978) and various DSDP and ODP sites (e.g.

GIESKES, 1983). The distribution of dissolved ammonium can be described using (BERNER, 1980a):

$$D_N \frac{\delta^2 C}{\delta x^2} - v(1+K)\frac{\delta C}{dx} + FkN = 0 \qquad (E10)$$

where C is the concentration of dissolved ammonium, F is a concentration conversion factor and N is the concentration of non-diffusable metabolizable organic nitrogen. In order to derive equation E10 from E2 the following assumptions have been made:

(1) steady state diagenesis is present

(2) diffusion occurs via molecular processes only

(3) there are no porosity gradients with depth (see Figure 3.2; MIDDELBURG and DE LANGE, 1989)

(4) equilibrium adsorption is present and follows a simple linear isotherm

(5) the advection rate is taken equal to the sediment accumulation rate

(6) precipitation of ammonium in authigenic minerals does not occur. This may perhaps not be strictly true at station K3 since pore waters at this station are in equilibrium with a struvite or alike compound (Figure 4.9)

(7) decomposition of nitrogen-bearing organic matter occurs via first-order kinetics

(8) the first-order rate constant for ammonium release and the C/N ratio of decomposing organic matter do not change when the overall decomposition changes from sulphate reduction to methane production.

The latter two assumptions require some more attention.

It is known that organic matter is characterized by a continuum of reactivities rather than a single rate constant (e.g. chapter 5; WESTRICH and BERNER, 1984; MIDDELBURG, 1991; BOUDREAU and RUDDICK, 1991). However, the adoptation of first-order kinetics for organic matter decomposition was guided not only by conceptual and mathematical simplicity, but also by the fact that this approach has enjoyed succes in describing data from a variety of environments (e.g. BERNER, 1974b, 1980a and references therein). Moreover, a 2-G model for the dissolved ammonium data was tested and found to be not significantly better than the simple approach adopted here.

This lack of improvement while using a multi-G model indicates also that the same rate parameter can be used for ammonium production in the sulphate reduction and methane generating zones. This lack of difference in ammonium generation rates is supported by the constant N/P ratio at station K3 (Fig. 4.14). Similar observations have been made by BERNER et al. (1970) and ROSENFELD (1981). In contrast, MURRAY et al. (1978) found, however, an inflection in the dissolved ammonium-versus-depth profile at

about the same depth where sulphate disappears in sediments from Saanich Inlet, British Columbia.

Appropriate boundary conditions for the solution of E10 are:

$$x = 0;\ N = N_0;\ C = C_0 \qquad (B6)$$

and

$$x \dashrightarrow \infty;\ N \dashrightarrow 0 \text{ and } C \dashrightarrow C_\infty \qquad (B7),$$

where C_0 is the concentration of ammonium at the sediment-water interface, N_0 is the initial amount of metabolizable organic N and C_∞ is the asymptotic concentration of ammonium.

The solution for these boundary conditions is:

$$C = C_0 + \frac{(v^2 F N_0)}{(D_n k + (1+K_N)v^2)} [1-\exp(-\frac{k}{v}x)] \qquad (E11a)$$

or

$$C = C_0 + (C_\infty - C_0) [1-\exp(-\frac{k}{v}x)] \qquad (E11b)$$

The measured profiles of dissolved ammonium were fitted to equation 11. Results of the modelling efforts are shown in Figure 4.4 and tabulated in Table 4.3.

Figure 4.4 shows that dissolved ammonium data can be described adequately using equation E11. The discontinuities in ammonium concentrations at depths of about 3.5 m at stations K3 and K4 are not related to changes in the production rate of ammonium since they do not concur with the change from sulphate reduction to methane generation or with any known change in the characteristics of organic matter (see chapters 7 and 8). These discontinuities are attributed to analytical artefacts since they correspond with the change from one analytical batch to another.

The value found for the first-order rate constant (k) at station K3 is an order of magnitude higher than those found at stations K4 and K11 (Table 4.3). For a wide range of marine depositional environments, it has been shown that the reactivity of organic matter is positively correlated with the sediment accumulation rate (TOTH and LERMAN, 1977; BERNER, 1978, 1980a; ALLER and MACKIN, 1984). In particular, TOTH and LERMAN (1977) and BERNER (1978) proposed that:

$$k = Aw^2 \qquad (E12)$$

TABLE 4.3 Parameters used to describe ammonium profiles

	K3	K4	K11
D_N (cm^2 yr^{-1})	436	436	436
K_N[1]	0.9	1.6	0.8
v (cm kyr^{-1})	600	71	85
F (gr cm^{-3})	0.65	0.65	0.65
N_o[2] (μmol N gr^{-1})	87	321	238
k^2 ($*10^{-3}$ yr^{-1})	2.1	0.21	0.255
k_e[3] ($*10^{-3}$ yr^{-1})	14.4	0.20	0.29

1 Determined from plots of exchangeable versus dissolved ammonium
2 Obtained by curve fitting
3 First order rate constant predicted from Toth-Lerman relationship (E12)

where A is an empirical constant (0.04 cm^{-2} yr) and w is the sediment accumulation rate. On the basis of this equation it is possible to predict the first order rate constants at a certain sediment accumulation rate. Table 4.3 shows that there is excellent agreement between the values found by fitting equation E11 and the values predicted by equation E12 for stations K4 and K11, but not for station K3. At this station the reactivity of organic matter is about seven times smaller than expected.

Organic matter in Kau Bay sediments is of mixed terrigenous and marine origin (see chapter 7). Organic matter at station K3 is very similar to that found at stations K4 and K11, but may perhaps have a somewhat higher contribution of terrestrial organic matter as revealed by $\delta^{13}C_{org.}$ values (Fig. 7.5). Because of the presence of relatively refractory organic matter, Kau Bay organic matter may have an apparent initial reactivity that is smaller than that found at similar sediment accumulation rates in the open ocean. Similar observations have been made in the Mississippi Delta, Gulf of Mexico (BERNER, 1978). However, care should be taken to make comparisons between different depositional environments since the relationship between k and w (eq. E12) is determined by a variety of factors (ALLER and MACKIN, 1984).

4.4.6. KINETIC MODELLING OF SULPHATE

Sulphate in the interstitial waters of anoxic marine sediments is not only consumed by sulphate reducing bacteria, but also by anoxic methane oxidation. Methane oxidation takes place via the reaction (e.g. REEBURGH, 1976, 1980; DEVOL et al., 1984):

$$CH_4 + SO_4^{2-} \text{---}> HS^- + HCO_3^- + H_2O \qquad (R5).$$

HENRICHS and REEBURGH (1987) proposed that in highly anoxic environments about 20 % of the downward flux of sulphate is consumed by anoxic methane oxidation. Unfortunately, there are no data available for dissolved methane or methane oxidation rates in sediments of Kau Bay. As a first approximation it is therefore assumed that sulphate consumption by anoxic methane oxidation is only of little importance.

The distribution of dissolved sulphate can be described by (BERNER, 1964):

$$D_S\frac{\delta^2 C}{\delta x^2} - v(1+K)\frac{\delta C}{dx} - FLkG = 0 \qquad (E13)$$

where C is the concentration of dissolved sulphate, G is the concentration of non-diffusable metabolizable organic carbon and L is a stoichiometric coefficient (L = 0.5; see reaction R1). The assumptions made to derive this equation for dissolved sulphate (E13) from the general diagenetic equation (E2) are similar to those made to derive the equation for dissolved ammonium (E10), except that two further assumptions have been made:

1 Adsorption of sulphate is negligible

2 The rate of sulphate reduction is independent of the dissolved sulphate concentration. BOUDREAU and WESTRICH (1984) have shown that the concentration of sulphate limits the rate of sulphate reduction only when the dissolved sulphate concentration drops below about 3 mM. This effect is only of minor importance in anoxic sediments since any decrease in sulphate reduction rates due to low dissolved sulphate concentrations, will be masked by increased rates of sulphate reduction through methane oxidation.

The upper boundary condition of equation E13 is similar to that for ammonium:

$$x = 0;\ G = G_o;\ C = C_o \qquad (B8)$$

where C_o is the concentration of sulphate at the sediment-water interface and G_o is the initial amount of metabolizable organic carbon.

The choice of the lower boundary conditions requires some discussion.

For a semi-infinite column BERNER (1964, 1980a) proposed that

$x \dashrightarrow \infty$; $G \dashrightarrow 0$; $C \dashrightarrow C_\infty$ (B9a)

or equivalent

$x \dashrightarrow \infty$; $G \dashrightarrow 0$; $\delta C/\delta x = 0$ (B9b).

With the boundary conditions B8 and B9 the solution of E13 is:

$$C = C_\infty + \frac{(v^2 F L G_0)}{(D_s k + v^2)} \exp(-\frac{k}{v} x) \qquad (E14a)$$

or

$$C = C_\infty + (C_0 - C_\infty) \exp(-\frac{k}{v} x) \qquad (E14b)$$

For normal marine sediments metabolizable organic matter disappears before all sulphate is reduced and C_∞ is positive. However, in many organic-carbon-rich sediments,

$$\frac{(v^2 F L G_0)}{(D_s k + v^2)} > C_0$$

and all sulphate is consumed before all metabolizable organic matter disappears. This condition applies to all marine environments characterized by methane generation. For these sediments, the model predicts negative sulphate concentrations at depth. For instance, in Kau Bay sediments the asymptotic sulphate concentrations approached are about -77, -48 and -30 mM for stations K3, K4 and K11 respectively.

In order to remove this physical impossibility of negative sulphate concentrations, LASAGA and HOLLAND (1976) proposed to multiply the rate term in E13 by a parameter Ψ which has value one when $C > 0$ and zero if $C <= 0$.

It is also possible to consider a finite layer model with the lower boundary condition:

$x = z$; $C = 0$ (B10),

where z is the depth where dissolved sulphate disappears. The solution of equation E13 with boundary conditions B8 and B10 is:

$$C = \frac{(v^2 FLG_0)}{(D_s k + v^2)} \exp(-\frac{k}{v}x) \quad - \quad (E15)$$

$$\frac{(v^2 FLG_0)}{(D_s k + v^2)} \exp(-\frac{k}{v}x) \exp(\frac{v(x-z)}{2D_s}) \frac{\sinh(Rx)}{\sinh(Rz)}$$

$$+ [C_0 - \frac{(v^2 FLG_0)}{(D_s k + v^2)}] \exp(\frac{vx}{2D_s}) \frac{\sinh(R(z-x))}{\sinh(Rz)}$$

where

$$R = \frac{v}{2D_s}$$

BOUDREAU and WESTRICH (1984) have shown that the solution proposed by LASAGA and HOLLAND (1976) does not behave properly as C --> 0; i.e. mass is not preserved. A similar comment can be made for equation E15. As an alternative, BOUDREAU and WESTRICH (1984) advocate the use of the following lower boundary condition:

$$C = 0; \delta C/\delta x = 0 \qquad (B11).$$

The solution of equation E13 with boundary conditions B8 and B11 is:

$$C = \frac{(v^2 FLG_0)}{(D_s k + v^2)} [\exp(-\frac{k}{v}x) \quad + \quad (E16)$$

$$\frac{kD_s}{v^2} \exp(-\frac{k}{v}z + \frac{vz}{D_s})(1-\exp(\frac{vz}{D_s})]$$

where z is the depth of zero sulphate.

The distribution of dissolved sulphate has been modelled using both the finite layer model (E15) and the so-called "modified Berner" model (E16) of BOUDREAU and WESTRICH (1984). Application of these models requires accurate establishment of the depth (z) of zero dissolved sulphate.

This depth (z) is not controlled by external processes but by the internal processes of sulphate reduction. With the data available for Kau Bay sediments this is not an easy task, in particular at stations K3 and K11 (see Figure 4.3). In the finite layer approach it was assumed that the rate constants for sulphate reduction and ammonium generation are equal. After that the dissolved sulphate data were fitted with the concentration (C_o) of sulphate at the sediment-water interface (hence implicitly with G_o) and the depth of zero sulphate as fit parameters. In the BOUDREAU and WESTRICH (1984) approach the depth of zero sulphate was fixed at values obtained from the finite layer approach. Equation E16 has been fitted to the dissolved sulphate concentration versus depth profiles using the concentration of metabolizable organic carbon (G_o) and the first order rate constant (k) for sulphate reduction as fit parameters. At station K4 the depth of zero sulphate and the fit parameters were tuned using a trial-and-error procedure similar to the one advocated by BOUDREAU and WESTRICH (1984). No such approach was adopted for stations K3 and K11 because of the low depth resolution of the data. Results of the modelling efforts are shown in Figure 4.3 and tabulated in Table 4.4.

TABLE 4.4 Parameters used for modelling of dissolved sulphate

	K3		K4		K11	
	E15	E16	E15	E16	E15	E16
D_s ($cm^2\ yr^{-1}$)	218	218	218	218	218	218
v ($cm\ kyr^{-1}$)	600	600	71	71	85	85
F ($gr\ cm^{-3}$)	0.65	0.65	0.65	0.65	0.65	0.65
L	0.5	0.5	0.5	0.5	0.5	0.5
k ($*10^{-3}\ yr^{-1}$)	2.1[1]	10[2]	0.21[1]	0.28[4]	0.255[1]	0.6[2]
G_o ($\mu mol\ C\ gr^{-1}$)	160[1]	500[2]	870[1]	1130[4]	640[1]	1300[2]
z (cm)	60[2]	60[3]	250[2]	233[4]	120[2]	120[3]

1 Assumed similar to organic matter decomposition (see Table 4.3).
2 Obtained by curve fitting.
3 Assumed to be similar for E15 and E16.
4 Obtained by an iterative fit, see text for explanation.

Although the dissolved sulphate data can be described equally well with both models (Figure 4.3), there are large differences in the first order rate constants and the initial amount of metabolizable organic matter. Both the first order rate constant and the initial amount of metabolizable organic

matter are much higher in the modified-Berner model (E16) than in the finite layer model (E15) (Table 4.4). This shows the important issue of choosing the appropriate boundaries in diagenetic models. If the finite layer model (E15) is chosen, it would appear that rates of sulphate reduction are similar to rates of ammonium generation. In contrast, the first-order rate constants extracted with the modified-Berner model (E16) are much higher than the first order rate constants for ammonium production (i.e. organic matter decomposition). This is not surprising since the first-order rate constant for sulphate consumption is actually the result of at least two reactions, namely bacterial sulphate reduction by decomposing organic matter and sulphate reduction by anoxic methane oxidation. On the basis of differences in k and G_o values (Table 4.4) it appears that anoxic methane oxidation is more important at stations K3 and K11 than at station K4. It will be clear that the models presented in this section should be considered as highly simplistic since they do not explicitly include the consumption of sulphate by upward diffusing methane.

4.4.7 KINETIC MODELLING OF PHOSPHATE

Studies of organic-carbon rich sediments have shown that the distribution of dissolved phosphate is very similar to that of dissolved ammonium (e.g. SHOLKOVITZ, 1973; HARTMANN et al., 1973; BERNER, 1977; MARTENS et al., 1978 and many others). There are however some differences. Phosphate is released to anoxic pore waters not only by the decomposition of organic matter, but also by the reduction of ferric hydrous oxides (e.g. BERNER, 1973; FROELICH et al., 1979; KROM and BERNER, 1981; DE LANGE 1986a) and by the dissolution of fish debris (SUESS, 1981). In addition, phosphate is removed from the pore water not only by adsorption, but also by precipitation of minerals such as apatite and struvite (e.g. MARTENS et al., 1978; JAHNKE et al., 1983; FROELICH et al., 1983; 1988; VAN CAPPELLEN and BERNER, 1988). The dissolved phosphate data can be described by:

$$D_P\frac{\delta^2 C}{\delta x^2} - v(1+K)\frac{\delta C}{dx} + FkP - k_m(C - C_{eq}) = 0 \qquad (E17)$$

where C is the concentration of dissolved phosphate, K_P is the dimensionless sorption constant for phosphate, P is the initial amount of metabolizable organic P, k_m is the first order rate constant for phosphate removal and C_{eq} is the concentration at saturation with the authigenic precipitate. The assumptions made to arrive at this equation are similar to those made for dissolved ammonium, except that a few additional assumptions were made:

1 Phosphate is not liberated by any other process than organic matter decomposition.
2 Precipitation of phosphate to form authigenic minerals occurs via first order kinetics. As discussed in section 4.4.3, the assumption of first-order kinetics for authigenic mineral formation is probably not correct. This assumption must be made since fundamental kinetic information on apatite crystallization at conditions relevant to those found in marine pore waters is not available (e.g. VAN CAPPELLEN and BERNER, 1988).
3 Removal of phosphate occurs by means of precipitation of disseminated apatite, struvite and alike compounds, rather than by preferent precipitation in certain layers.

The upper boundary for dissolved phosphate is very similar to that of dissolved ammonium:

$$x = 0;\ P = P_o;\ C = C_o \qquad \text{(B12)},$$

where C_o is the concentration of phosphate at the sediment-water interface and P_o is the initial amount of metabolizable organic P.

For the lower boundary it is possible to consider either a semi-infinite column:

$$x \dashrightarrow \infty;\ P \dashrightarrow 0;\ C \dashrightarrow C_{eq} \qquad \text{(B13)}$$

or a column of finite length:

$$x = L;\ C = C_{eq} \qquad \text{(B14)}.$$

The solutions of equation E17 with these boundary conditions are:

$$C = C_{eq} - \frac{v^2 F k P_0}{(D_p k^2 + (1+K_p) v^2 k - k_m v^2)} [1 - \exp(-\frac{k}{v} x)] \qquad (E18)$$

$$+ [\frac{v^2 F k P_0}{(D_p k^2 + (1+K_p) v^2 k - k_m v^2)} + (C_0 - C_{eq})] \exp(\frac{(1+K_p) v x}{2 D_p} - R x)$$

and

$$C = C_{eq} - \frac{v^2FkP_0}{(D_pk^2 + (1+K_p)v^2k - k_mv^2)}[1-\exp(-\frac{k}{v}x)] \qquad (E19)$$

$$+ [\frac{v^2FkP_0}{(D_pk^2 + (1+K_p)v^2k - k_mv^2)} + (C_0 - C_{eq})]\exp(\frac{(1+K_p)vx}{2D_p})\frac{\sinh(R(L-x))}{\sinh(RL)}$$

respectively, where

$$R = \sqrt{\frac{v^2(1+K_p)^2}{4D^2} + \frac{k_m}{D}}$$

The distribution of dissolved phosphate has been modelled at all stations with equation E18 and at station K11 also with equation E19. The modelling strategy involved the assumption that the generation of dissolved phosphate could be calculated independently using the interstitial water concentrations of ammonium and appropriate stoichiometric constants. An order of magnitude estimate for the first order rate constant for phosphate removal, the only remaining unknown, was then obtained by curve-fitting. The results of the modelling efforts are shown in Figure 4.5 and the parameters used are tabulated in Table 4.5. In order to be instructive the modelling results will be discussed separately for each station.

At station K3 the dissolved phosphate data can be described using organic matter with a N/P ratio of 48 (curves 2 and 3), but not by organic matter with a N/P ratio of 16 (curve 1). This N/P ratio is consistent with the results of the stoichiometric models (see section 4.4.4). The slight difference between the stoichiometric model (N/P = 58) and the kinetic model (N/P = 48) is not significant and may be due to scatter in data and the precipitation of authigenic minerals. A first order rate constant for phosphate removal smaller than 10^{-3} does not seem to influence the distribution of dissolved phosphate (curves 2 and 3).

At station K4 the dissolved phosphate data can be described either by organic matter with a N/P ratio of about 320 (i.e. P_o = 1) and slow phosphate removal (curve 5) or by organic matter with a N/P ratio of 48 (i.e. P_o = 6.69) and significant removal of phosphate (curve 6), but not by organic matter with a N/P ratio of 48 and first order rate constants of 10^{-3} or less (curve 4). The latter conditions are similar to those found at station K3. Hence, at station K4 either the organic matter is more depleted in P or the removal of phosphate is more rapid than at station K3. The N/P ratio of

TABLE 4.5 Parameters used for modelling dissolved phosphate

	C_o (mM)	v (cm/yr)	C_{eq} (mM)	P_o (μmol gr^{-1})	k (*10^3) (yr^{-1})	$logk_m$ (cm)	h (cm)
K3							
1	0.05	0.6	0.32	5.43	2.1	-6	-
2	0.05	0.6	0.32	1.81	2.1	-6	-
3	0.05	0.6	0.32	1.81	2.1	-3	-
K4							
4	0.02	0.071	0.05	6.69	0.21	-3	-
5	0.02	0.071	0.05	1.00	0.21	-3	-
6	0.02	0.071	0.05	6.69	0.21	-1	-
K11							
7	0.03	0.085	0.01	4.96	0.255	-3	-
8	0.03	0.085	0.01	4.96	0.255	-2	-
9	0.03	0.085	0.01	4.96	0.255	-1	-
10	0.03	0.085	0.01	4.96	0.255	-2	220
11	0.03	0.085	0.01	4.96	0.255	-1	220

D_p = 162 cm^2 yr^{-1}; F = 0.65 (gr cm^{-3}); K_p = 1.8 (KROM and BERNER, 1980).

marine organic matter may show considerable variation due to preferential mineralization of P relative to N and the formation of benthic biomass enriched in P. However, the N/P ratio of 320 required to fit the phosphate data at station K4 without invoking substantial precipitation is far beyond the range of published N/P ratios (10-82; e.g. KROM and BERNER, 1981; VAN CAPPELLEN and BERNER, 1988; FROELICH et al., 1988 and references therein). Moreover, in Kau Bay sediments the C/N ratio of decomposing organic matter is fairly similar at various stations (Table 7.1) Therefore, it would appear logical that the same would apply to N/P ratios. Accordingly, the N/P ratio of decomposing organic matter at station K4 is about 48 and consequently the depletion in dissolved phosphate must be due to the precipitation of authigenic P-bearing minerals.

At station K11 the N/P ratio is assumed to be 48 and model curves for various values of the first order rate constant for phosphate removal are presented. Figure 4.5 shows that neither the curves (7, 8 and 9) with equation E18 nor the curves (10 and 11) with equation E19 can adequately describe the dissolved phosphate data. For instance, the model curves with equation E18, i.e. the semi-infinite model, can not reproduce the constant phosphate data below about 2 m. This is probably due to the inadequacy of the model since it is assumed that phosphate removal is occurring at all depths, whereas phosphate precipitates at certain discrete sites only (e.g. see

JAHNKE et al., 1983). Part of this discrepancy between model curves and data can be removed by considering only depths above about 2.2 m. The model curves for the finite layer approach (10 and 11) do indeed provide a somewhat better fit. It should, however, be realized that both models are very simple and may not be suited to describe dissolved phosphate versus depth profiles properly.

Models that describe dissolved phosphate in anoxic sediments should:
1) allow preferential precipitation of authigenic minerals in a limited layer of the sediment as observed for apatite by JAHNKE et al. (1983) and for dolomite at station K4 (chapter 6).
2) incorporate higher order precipitation kinetics.
3) allow other sources for dissolved phosphate than organic matter decomposition. At all stations the concentration of dissolved phosphate close to the sediment-water interface (C_o in Table 4.5) is much higher than the concentration of phosphate in bottom water (see Figure 2.4). This indicates that other sources for phosphate such as dissolution of fish debris (SUESS, 1981) and the release of adsorbed phosphate from dissolving ferric (hydrous) oxides (KROM and BERNER, 1981; DE LANGE, 1986a) are important in Kau Bay sediments. Any release at depth from these sources should be incorporated in models for dissolved phosphate.

4.4.8 ALKALINITY

Alkalinity is defined as the amount of protons required to neutralize the excess of proton acceptors over proton donors. The alkalinity of anoxic pore waters may be affected by a number of processes (e.g. BERNER et al., 1970; SHOLKOVITZ, 1973; BEN-YAAKOV, 1973; MURRAY et al., 1978; GIESKES, 1983; BOUDREAU and CANFIELD, 1988 and others): bacterial sulphate reduction, anoxic methane oxidation, methane generation, the production of ammonium, phosphate and hydrogen sulphide by organic matter decomposition, the production of organic acids and ion-exchange processes. It has, however, been shown that changes in the alkalinity in anoxic pore water can be predicted by taking only bacterial sulphate reduction, ammonium production and authigenic carbonate minerals formation into account (BERNER et al., 1970; SHOLKOVITZ, 1973; BEN-YAAKOV, 1973; SUESS, 1976; MURRAY et al., 1978). According to these authors there should be a two-fold increase in alkalinity for each equivalent of sulphate reduced unless some alkalinity is produced by ammonium production or removed by precipitation of authigenic carbonates. In addition to these reactions, BERNER et al. (1970) included Mg removal, represented by Mg-aluminosilicate formation, as a process which decreases alkalinity.

The inclusion of Mg removal to predict alkalinity changes is somewhat controversial since SHOLKOVITZ (1973) found that the diagenetic reactions responsible for the pore water depletions of Mg are not associated with changes in alkalinity, whereas MURRAY et al. (1978) found that these reactions have to be included to predict alkalinity changes. These discrepancies are probably related to the complex behaviour of Mg in marine pore water (e.g. VON BREYMANN et al., 1991). For instance, in Kau Bay sediments Mg is affected by two type of ion-exchange reactions, and by dolomite and struvite formation among other processes. Because of this complex behaviour of Mg in pore waters of Kau Bay sediments, Mg is not included in the alkalinity model.

The following equation is used to predict the alkalinity of pore water in Kau Bay:

$$Alk = Alk_o + 2*eq.E15 + (1+K_N)*eq.E11 - St*eq.E4 \quad (E20),$$

where Alk_o is the alkalinity of bottom waters ($\approx$ 2.5 mM) and St is a stoichiometric coefficient depending on the carbonate mineral formed (calcite:2; dolomite:4). The second term on the right in E20 represents the alkalinity produced by bacterial sulphate reduction. The third term on the right involves the alkalinity produced by the reaction:

$$NH_3 + H_2CO_3 \text{ --> } NH_4^+ + HCO_3^- \quad (R6)$$

and is corrected for the amount of ammonium in exchangeable positions. The final term on the right in this equation refers to the amount of alkalinity consumed by reactions of the form:

$$Ca/Mg^{2+} + 2\,HCO_3^- \text{ ---> } Ca/MgCO_3 + CO_2 + H_2O \quad (R7).$$

This alkalinity model is not intended to be quantitatively correct, but may provide limits on the number of processes involved. Any proper model for the alkalinity should incorporate a system of coupled differential equations for all components that affect either directly or indirectly the alkalinity (e.g. see BOUDREAU, 1987; BOUDREAU and CANFIELD, 1988). No attempt has been made to apply such a model to the pore waters of Kau Bay because the data available are not comprehensive enough to support such a model. Moreover, the factors that determine the alkalinity must be recognized before they can be modelled.

The results of the alkalinity model are shown in Fig. 4.6. The parameters used for predicting the alkalinity are essentially the same as

those used for modelling sulphate (Table 4.4), ammonium (Table 4.3) and calcium (Table 4.1). For simplicity, it was assumed that alkalinity diffuses in the form of bicarbonate (D_a = 260 $cm^2\ yr^{-1}$).

Figure 4.6 shows that the agreement between model predicted and observed pore water alkalinities is very poor. This discrepancy is too large to be due to the simplistic "semi-open system" calculation procedure. It appears that the a priori assumption that alkalinity can be predicted by taking only bacterial sulphate reduction, ammonium production and authigenic carbonate mineral formation into account, is incorrect. The alkalinity data for interstitial waters in Kau Bay indicate that at least a few other processes must be considered.

At all three stations the alkalinity levels predicted in the sulphate reduction zone are much higher than the levels observed. This is interpreted to be due to anoxic methane oxidation (R5). During the bacterial reduction of sulphate two equivalents of alkalinity are produced for each equivalent of sulphate reduced (R1), whereas during anoxic methane oxidation there is only one equivalent of alkalinity produced for each equivalent of sulphate reduced (R5). Accordingly, the model will predict more alkalinity than is actually formed if anoxic methane oxidation is excluded.

The predicted alkalinity at depths more than 4 m at station K3 is significantly lower than the observed alkalinity. The discrepancy is on the order of 27 mM and can not readily be explained. However, a few comments can be made. Firstly, this discrepancy is not the result of the exclusion of anoxic methane oxidation since correcting for this process would enhance the difference. Secondly, this difference between observed and predicted alkalinities can be reduced to about 10 mM if Ca is not removed by formation of authigenic carbonates but by another process which does not result in changes in alkalinity. Thirdly, this difference between predicted and observed alkalinities can be resolved if the concentrations of exchangeable and fixed ammonium are together six times higher than the concentration of dissolved ammonium. The data in Figure 4.10 show, however, that the amount of exchangeable and dissolved ammonium are almost equal. Similarly, Kau Bay sediments have concentrations of fixed ammonium that are similar to concentrations of exchangeable ammonium and thus of dissolved ammonium. Hence, at station K3 the distribution coefficient between dissolved and solid phase ammonium is on the order of 2 at most. This is a maximum estimate since it requires complete dynamic equilibrium between dissolved, exchangeable and fixed ammonium. Accordingly, the sorption constant required to match predicted and observed alkalinities ($\approx$ 6) is much higher than the sorption constant observed in Kau Bay and is also far outside the range of published values (0.4-1.7; MACKIN and ALLER,

1984). Fourthly, part of the difference between predicted and measured alkalinity could be due to non-carbonate alkalinity which is contributed by borate, silicate, phosphate, ammonia, sulphide and organic acids. Calculations indicate, however, that inorganic non-carbonate alkalinity is on the order of a few mM. The contribution of organic alkalinity is unknown but it is unlikely that it can account for the difference observed. Fifthly, in Kau Bay sediments the concentration of sulphidized iron is on the order of 1.3 to 2.5 wt % (Table 7.2). Depending on the reactions involved, this sulphidization of iron compounds may have affected the alkalinity. If iron is liberated by ion-exchange reactions of the form:

Fe^{2+}-mineral + cation --> cation-mineral + Fe^{2+} (R8),

this would not affect the alkalinity. However, the alkalinity will increase if iron is liberated by reactions of the form:

$2\ FeOOH + HS^- + 5\ H^+ \rightarrow 2\ Fe^{2+} + 4\ H_2O + S^o$ (R9)

or

$Mg_2Fe_3Al_2Si_3O_{10}(OH)_8 + 10\ H^+ \rightarrow$ (R10)
$2\ Mg^{2+} + 3\ Fe^{2+} + Al_2Si_2O_5(OH)_4 + H_4SiO_4 + 5\ H_2O.$

Finally, in the pore waters at depth at station K3 the partial pressure of carbon dioxide in solution is about $10^{-0.75}$. This enhanced carbon dioxide pressure may have promoted silicate weathering reactions which cause an increase in alkalinity; e.g.

$3\ KAlSi_3O_8 + 2\ CO_2 + 14\ H_2O \rightarrow$ (R11)
$KAl_3Si_3O_{10}(OH)_2 + 2\ K^+ + 6\ H_4SiO_4 + 2\ HCO_3^-.$

The sediments in Kau Bay are in particular sensitive to this kind of weathering reactions since they have undergone a relatively short weathering/erosion cycle (see section 2.8). It is therefore likely that various minerals will be altered upon burial when they are exposed to agressive solutions.

The predicted alkalinity at stations K4 and K11 is significantly higher than the observed alkalinity (Fig. 4.6). Part of this overestimation is probably due to the ommission of anoxic methane oxidation in the model. Another part of this difference between predicted and observed alkalinity can be explained by the incomplete description of alkalinity removal by authigenic carbonate precipitation. At these stations alkalinity is removed not only by calcite precipitation, but also by dolomite precipitation (e.g. see chapter 6

and section 4.4.1.2). Figure 4.6 shows that the curves representing alkalinity removal by dolomite precipitation (4,5) provide a better description than the curves representing alkalinity removal by calcite precipitation (2,3). However, even in the case that alkalinity is consumed by dolomite only, there remains a significant discrepancy between predicted and observed alkalinity. It should, however, be realized that at these two stations the amount of calcite and dolomite formed cannot easily be calculated from observed depletions in Ca since there is additional supply of Ca from the underlying fresh-water sediments (see sections 4.4.2.2 and 4.4.3). This implies that more alkalinity is removed by authigenic carbonate precipitation than is calculated by the simple alkalinity model. This is shown by curve 6 in Figure 4.6. This curve is based on the assumptions that dolomite is the dominant carbonate mineral involved and that the present-day flux of Ca from below provides an average estimate for the supply of Ca from the fresh-water sediments. The lowered pH values at depth at these two stations (Figure 4.7) provides additional evidence that more carbonates have precipitated at these two stations than at station K3.

4.4.9 AUTHIGENIC MINERAL FORMATION

In the preceding sections several indications for the formation of various authigenic minerals were presented. Thermodynamic calculations have indicated that the pore waters reach saturation with respect to calcite, aragonite, dolomite, struvite, hydroxy-apatite and alike substances. In addition, there are clear indications for removal of Ca, Mg, Sr, phosphate and alkalinity from the pore waters. Is there solid-phase evidence of the actual formation of these phases? Evidence of the formation and occurrence of authigenic carbonates and ironsulphides is presented in chapters 6 and 7 respectively and will not be repeated here.

There is little evidence of the formation and occurrence of authigenic apatite. Bulk analyses of more than 200 samples provided no indications for phosphorus concentrations above background values (i.e. excess P). Excess phosphorus might be indicative for the presence of authigenic apatite. In addition, it has not been possible to identify authigenic apatite by X-ray diffraction techniques although more than 30 samples were selected for investigation. The identification of authigenic apatite is further complicated by the fact that apatite occurs not only as a authigenic phase, but also as a detrital phase. These phases can, however, be separated by wet-chemical extraction techniques. Simple laboratory experiments have shown that detrital apatite is relatively insoluble in acetic acid, whereas authigenic apatite dissolves in acetic acid. A selection of samples has been investigated

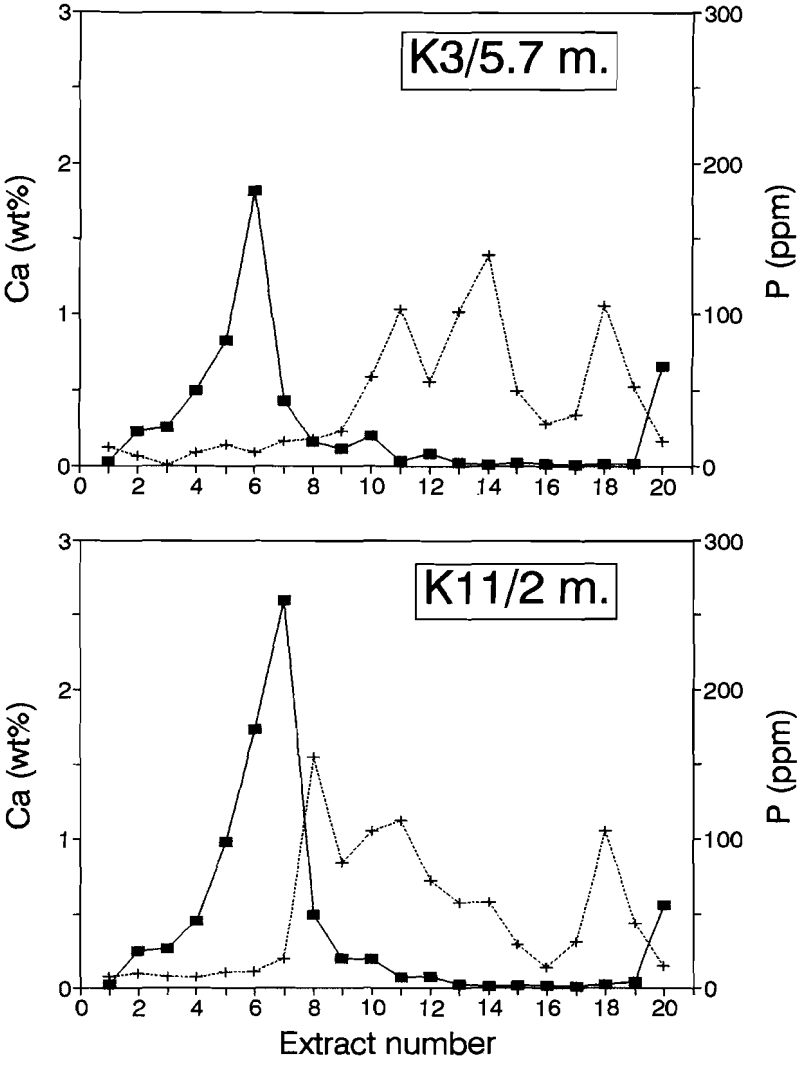

Figure 4.15 The distribution of Ca (squares) and P (crosses) over the various leach fractions. The numbers on the abscissa indicate the various fractions: (1) distilled water, (2) 0.1 N NH_4Ac, (3) 10% 0.1 N HAc/90% 0.1 N NaAc, (4) 20% 0.1 N HAc/80% 0.1 N NaAc, (5) 35% 0.1 N HAc/65% 0.1 N NaAc, (6) 65% 0.1 N HAc/35% 0.1 N NaAc, (7) 80% 0.1 N HAc/20% 0.1 N NaAc, (8) 90% 0.1 N Hac/10% 0.1 N NaAc, (9) 0.1 N HAc, (10) 1 N Hac, (11) 3.3 N HAc, (12) 0.05 N HCl, (13) 0.1 N HCl, (14) 0.5 N HCl, (15) 1 N HCl, (16) 2 N HCl, (17) 6 N HCl, (18) 10 N HF, (19) HNO_3 and (20) residue by $HClO_4/HNO_3/HF$.

by a 20 steps acid-gradient leaching technique (see section 4.2 and chapter 7). The leach patterns for Ca and P in a sample at a depth of 5.7 m at station K3 and a sample at a depth of about 2 m at station K11 are presented in Figure 4.15. The leach patterns show some interesting features. Firstly, there is not a large difference between the leach patterns of Ca for the two samples. Secondly, both samples show the presence of P-phases that dissolve in concentrated acetic acid, HCl and HF (step >10). Thirdly, the sample from station K11 shows the presence of an additional P-phase that dissolves in dilute acetic acid (steps 8,9). No such phase can be recognized in the samples investigated from station K3. This additional P-phase is interpreted to be a diagenetic P-phase. There are a few factors that may explain the fact that an authigenic P-bearing phase can be recognized at station K11, but not at station K3. The sediment accumulation rate at station K11 is almost an order of magnitude lower than at station K3. Authigenic minerals will therefore be less diluted at station K11. In addition, phosphate is removed faster at station K11 than it is at station K3 (see section 4.4.7).

4.5. CONCLUSIONS

1) The two features that characterize Kau Bay, namely its semi-euxinic nature and the presence of fresh-water sediments at depth, have their implications for the composition of Kau Bay pore waters.
2) The presence of fresh-water sediments below marine sediments has resulted in the downward diffusion of Cl and other major components of seawater.
3) Two types of ion-exchange reactions occur in Kau Bay sediments. Firstly, the diffusion of seawater ions to the fresh-water sediments has resulted in ion-exchange processes between the fresh-water clays and the saline-to-brackish pore waters. The increase of Ca and Sr with depth at stations K4 and K11 is the result of this type of ion-exchange reactions. Secondly, the production of ammonium by the anoxic decomposition of organic matter has caused ion-exchange reactions between dissolved ammonium and adsorbed cations. This type of ion-exchange reactions may explain the K and Mg enrichment of the interstitial water at station K3.
4) The distribution of dissolved calcium, strontium, ammonium, sulphate and phosphate can be described by simple mathematical models. The rate parameters derived are, however, strongly dependent on the assumptions made. Future models should address problems related to higher order reaction kinetics, preferential precipitation of authigenic minerals in certain layers (see also chapter 6) and the proper choice of the (lower) boundary.
5) It is not possible to model the distribution of alkalinity in the pore

water of Kau Bay sediments by considering only the alkalinity produced by bacterial sulphate reduction and ammonium formation and the alkalinity consumed by authigenic carbonate precipitation. Additional processes that should be incorporated in the alkalinity model include anoxic methane oxidation, the weathering of various silicates and the precipitation of 'excess' carbonates due to the supply of Ca from below.

6) Thermodynamic calculations show that the pore waters approach equilibrium with calcite, dolomite, struvite, apatite and alike substances.

7) There are clear indications for the removal of calcium, strontium, magnesium, phosphate and alkalinity from the pore waters by precipitation of authigenic minerals. Details of the processes involved in the formation of authigenic minerals will be discussed in chapters 6, 7 and 8.

CHAPTER 5: A SIMPLE RATE MODEL FOR ORGANIC MATTER DECOMPOSITION IN MARINE SEDIMENTS

ABSTRACT

A model is presented for the decomposition of organic matter in marine sediments. The model considers the organic matter as a whole. In this model the first order rate parameters (k) gradually decrease with time (t) according to:

$\log k = -0.95 \log t - 0.81$ ($N = 140$; $r = 0.987$).

This equation is found to be valid over 8 orders of magnitude and is based on organic carbon versus depth profiles of well dated cores and laboratory experiments. The predicted continuous decrease in the reactivity of organic matter is consistent with multi-G models and in situ measurements of sulphate reduction.

Although all organic carbon versus depth profiles follow the same reactivity decrease with time, their reactivity at the sediment-water interface (i.e. 'apparent initial age') is different. Apparent initial ages calculated on the basis of various experiments and field measurements show consistent trends.

5.1 INTRODUCTION

Many of the reactions and processes that occur in the water column and sediments are related either directly or indirectly to the degradation of organic matter. Knowledge of the rate of decomposition of organic matter is therefore of the utmost importance (e.g. BERNER, 1980 a,b; EMERSON et al., 1987; MARTIN and BENDER, 1988; McNICHOL et al., 1988). Rates of organic matter degradation are known to vary over orders of magnitude due to variations in the amount and the lability of the organic matter being degraded (e.g. TOTH and LERMAN, 1977, WESTRICH and BERNER, 1984; HENRICHS and DOYLE, 1986; EMERSON and HEDGES, 1988).

The overall process of organic matter decomposition is thought to be a bacterial food chain in which fermenting micro-organisms hydrolyse the initial detritus and produce low molecular weight species, which are then used by aerobic organisms or sulphate-reducing bacteria (JØRGENSEN, 1982; WESTRICH, 1983). However, very few data are available concerning the nature and amount of labile compounds and the rate and mechanisms of the various reactions that are involved in the degradation of sedimentary organic matter. For this reason the overall process of organic matter decomposition is generally described by simple models (e.g. BERNER, 1980 a). In this paper previous rate models will be briefly evaluated and then an alternative model

will be presented. In this model the reactivity of organic matter gradually decreases with time.

5.2 PREVIOUS MODELS

The first kinetic model describing the degradation of organic matter in marine sediments was the first-order (G) model developed by BERNER (1964). In this model it was assumed that reactive organic matter decomposes at an overall rate directly proportional to its own concentration (i.e. by first- order kinetics):

$$\frac{dG_m}{dt} = -kG_m \qquad (1)$$

where G_m is the concentration of metabolizable organic carbon, k is the first-order decay constant, and t is time. According to this model the concentration of reactive organic matter and the rate of organic matter decomposition both decrease exponentially with time. The first order rate constant (k), or the reactivity of organic matter, is assumed to be constant. However, the assumption that decomposing organic matter has a constant reactivity is not consistent with field and laboratory studies. It has been shown that microbial communities tend to sequentially utilize organic substrates, the more reactive substrates being consumed first (e.g. STUMM-ZOLINGER, 1968; MATELES and CHIAN, 1969; WESTRICH, 1983; EMERSON and HEDGES, 1988; TEGELAAR et al., 1989). As a result of the preferential consumption of reactive components the reactivity of sedimentary organic material decreases with time (BERNER, 1980b).

On the basis of actual rate measurements JØRGENSEN (1978) proposed that organic matter could be divided into various groups of compounds of different reactivity, each of which undergoes first order decomposition. This multi-G model can be expressed as (BERNER, 1980 b; WESTRICH and BERNER, 1984):

$$G_{Tm} = \sum G_i \qquad (2)$$

$$\frac{dG_i}{dt} = -k_i G_i \qquad (3)$$

$$\frac{dG_{Tm}}{dt} = -\sum k_i G_i \qquad (4)$$

where G_i is the concentration of organic carbon in each group, G_{Tm} is the concentration of total metabolizable organic carbon, k_i is the first-order decay constant for each group, and t is time. Selective removal according to the reactivity of each group accounts for the change in the reactivity and the amount of organic matter with time. This multi-G model is consistent with the well-established sequential utilization principle mentioned above.

However, to apply this model successfully, one needs to know the number of labile groups and the relative amount and reactivity of each of these groups. Because this information is far from complete two hybrid models have been developed. The first model considers an infinite number of groups and consequently the variable k becomes a continuously varying parameter. The second model considers a finite number of groups with fixed first-order decay constants (i.e. the quantum-G model of WESTRICH (1983)). Because the quantum-G model is only an approximation, the number of groups to be considered depends on the accuracy of the data to be described and on the time scale under consideration. For instance, in rate models that cover tens of years only two or three components are needed, whereas models for time-scales on the order of 10^4-10^7 yr need up to eight components.

The determination of the amount and reactivity of these components usually involves a graphical analysis (e.g. WESTRICH and BERNER, 1984; WESTRICH, 1983). The graphical separation of experimental processes can, however, be misleading. VAN LIEW (1962) showed clearly that by graphical analysis of a curve representing a continuum of exponential processes one usually obtains only two or three rather similar components. The derived reactivity and quantity of certain groups should therefore be regarded as model-fit parameters rather than true or apparent decay constants and fractions. The rough agreement between decay constants derived for different environments does not invalidate this conclusion. Nevertheless, the quantum-G model has been found to provide a fairly good simulation of natural processes (e.g. JØRGENSEN, 1978; BERNER, 1980 a,b; WESTRICH, 1983; WESTRICH and BERNER, 1984; EMERSON et al., 1987; REIMERS, 1988; JUMARS et al., 1988).

5.3 POWER MODEL

In the G-type models evaluated above the organic matter is considered to be composed of a refractory fraction and one or more labile fractions. This partitioning between labile and refractory compounds is very subjective and

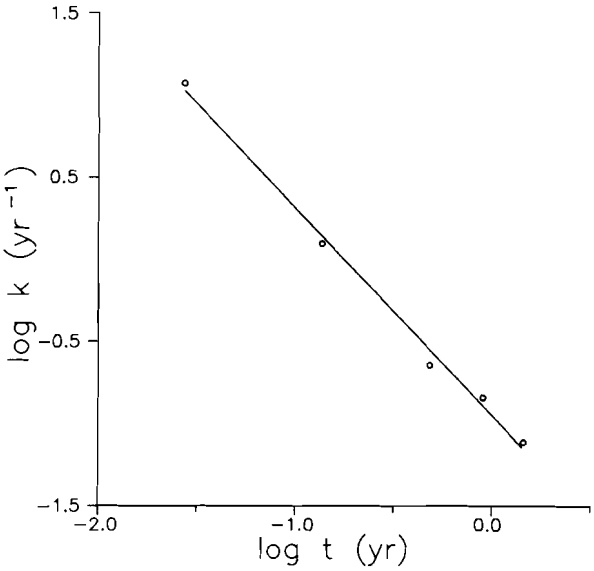

Figure 5.1. The reactivity of organic carbon (k) as a function of time (t) in aerobic plankton decompostion experiments of WESTRICH and BERNER (1984). First order rate parameters have been calculated using equation 6.

dependent on the time scale and environment under consideration. Part of the seemingly refractory organic matter from environments with high sediment accumulation rates is labile when the organic matter is transported to an oxygenated environment with a low accumulation rate (DE LANGE, 1986a, 1988; WILSON et al., 1986). In addition, the results of the DSDP and ODP legs have shown that organic matter is reactive at all sedimentary depths (e.g. TOTH and LERMAN, 1977; GIESKES, 1983). It is therefore necessary to consider the organic matter in total. Another constraint on the model is that the reactivity of organic matter must decrease with time (JØRGENSEN, 1978; BERNER, 1980b). In the model that follows we assume that total organic matter decomposes according to first-order kinetics:

$$\frac{dG_T}{dt} = -k(t)\, G_T \qquad (5)$$

where G_T is the concentration of total organic carbon and k is the time dependent first-order rate parameter. Assuming that k is constant over an interval Δt, k can be calculated by:

$$k = \frac{1}{\Delta t} \ln \frac{G_t}{G_{(t+\Delta t)}} \qquad (6)$$

where G_t is the organic matter concentration at a certain time.

The results of the oxic plankton decomposition experiment of WESTRICH and BERNER (1984) were used to calculate k values for subsequent time intervals. Sampling intervals were taken for Δt and the midpoint of each interval for t. The calculated rate parameters are plotted versus time in Fig. 5.1. The trend in Fig. 5.1 illustrates the gradual decrease in the reactivity of organic matter when it is decomposing. The least squares fit to these data produces a correlation coefficient of 0.997 and fits the equation

$$\log k = -1.26\ (\pm 0.05)\log t - 0.95\ (\pm 0.04) \qquad (7),$$

where t is time in years.

Notice that the same data were used by WESTRICH and BERNER (1984) to support their quantum-G model. Because the reactivity of organic matter decreases on the time-scale of experiments, it is very interesting to see what happens on a geological time scale. We used organic carbon concentration versus depth profiles of cores with a known sedimentation rate to derive rate parameters according to eq. 6. By taking this approach we assume that bioturbation, pressure, temperature and redox conditions are of secondary importance only. Here intervals Δt represent depth intervals between samples and t the depth to the midpoint of each interval. The rate parameters calculated from field data as well as laboratory results are plotted in Fig. 5.2. The data base on which these rate parameters are based is given in the figure caption. This database is not complete, but is a tabulation that is representative of a wide range of oceanic conditions. When plotted on log-log paper, rate parameters based on experimental and field data versus time are described by a single straight line with a correlation coefficient of 0.987 (N = 140):

$$\log k = -0.95(\pm 0.01)\ \log t - 0.81\ (\pm 0.04) \qquad (8a)$$

$$\text{or} \quad k = 0.16\ t^{-0.95} \qquad (8b).$$

This result implies that there is a continuous decrease in the reactivity of organic matter over more than 8 orders of magnitude. This strong relationship also suggests that there is no significant discrepancy between rate parameters derived from laboratory experiments or field data, or oxic and anoxic environments. Moreover, the least square fits to the data derived from laboratory experiments

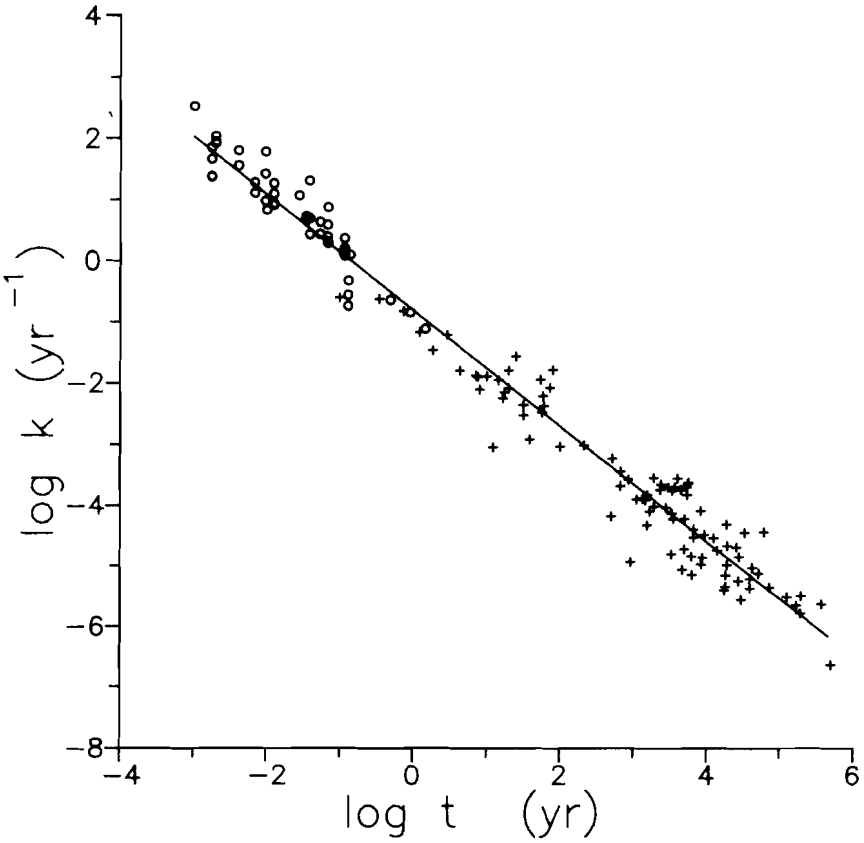

Figure 5.2. The reactivity of organic carbon (k) versus time (t). First order decay parameters have been calculated using equation 6. Dots and crosses represent data from laboratory experiments and organic carbon versus depth profiles of well dated cores respectively. Data from experiments were obtained from: GARBER (1984), GRUNSEICH and DUEDALL (1978), WESTRICH and BERNER (1984) and HENRICHS and DOYLE (1986). Field data were used from: SHOLKOVITZ (1973), MULLER and MANGINI (1980), REIMERS and SUESS (1983), MARTENS and KLUMP (1984), HENRICHS and FARRINGTON (1987), HAMILTON and HEDGES (1988), MURRAY et al. (1978), JOHNSON et al. (1982), HEGGIE et al (1987) and THOMSON et al (1989). Data were rejected where errors or non-steady state phenomena were suspected; i.e. in case of organic carbon concentration increases with time. This compilation is far from complete, but covers a wide range of natural environments.

$$\log k = -1.00\ (\pm 0.06) \log t - 0.84\ (\pm 0.10) \qquad (9a)$$
$$r = 0.93\ N = 46$$

and to those derived from field measurements

$$\log k = -0.88\ (\pm 0.03) \log t - 1.05\ (\pm 0.10) \qquad (9b)$$
$$r = 0.95\ N = 94$$

are very similar. It is surprising that the data fit so well considering that the variance could be caused by varying temperature, pressure and redox conditions, differences in physical, chemical and biological nature of the media, and bioturbation.

Although all field data follow the same reactivity decrease with time, their starting point (i.e. apparent initial "age") is different. For instance, rate parameters derived for Cape Lookout Bight as well as for Pacific Ocean sediments both follow eq. 8, but start with a different k value which is a function of age. This can be accounted for by the introduction of an apparent initial age (JANSSEN, 1984):

$$k = 0.16\ (a+t)^{-0.95} \qquad (10).$$

where a is the apparent initial age and t is the time since the beginning of the decomposition process. Because, in general $t >> a$ this apparent initial age can be approximated by:

$$G_{t1} = G_{t0} \exp 3.2\ (a^{0.05} - (a+t_1)^{0.05}) \qquad (11)$$

where G_{t0} is the concentration of organic carbon at the start of the experiment or at the sediment-water interface and G_{t1} is the concentration of organic carbon at time t_1 (e.g. the first sample below the sediment- water interface). Equation 11 is obtained after substitution of eq. 10 into eq. 5, followed by integration. Some calculated apparent initial ages (a) are shown in Table 5.1.

5.4 EVALUATION OF THE POWER MODEL

The model presented above describes the decrease of the reactivity of organic matter with a power function. According to reaction stoichiometry this power functional decrease with time or depth of the reactivity of organic matter should be followed by a power functional decrease of sulphate reduction rate. This type of depth variation of sulphate reduction rates has indeed been observed in sediments at sites in Limfjorden, Solar Lake and Kattegat

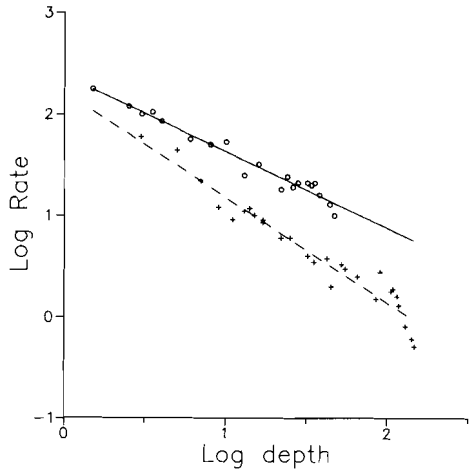

Figure 5.3. Double logarithmic plot of sulphate reduction rates (mM/yr) versus depth (cm). Dots and crosses represent data from Long Island Sound sites SACHEM and NWC respectively (WESTRICH, 1983).

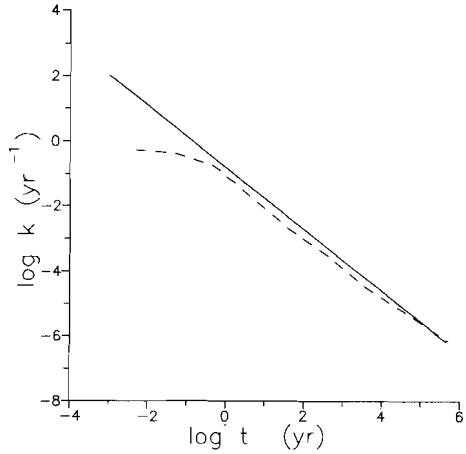

Figure 5.4. Comparison between the power model (solid line) and 8-G model (dashed line). The dashed line is calculated from a theoretical organic carbon concentration versus time curve obtained by integration of the 8-G model using the decay constant compilation of WESTRICH (1983).

(JØRGENSEN, 1978, 1982), and at stations NWC, SACHEM and FOAM in Long Island Sound (Fig. 5.3). This consistency may be taken as a support for the applicability of the power model.

The power model is also consistent with the multi-G model, namely a multi-G model with an infinite number of fractions gives a power function decrease of organic matter reactivity with time (JØRGENSEN, 1978). This can also be demonstrated for a quantum-G model based on 8 fractions (WESTRICH, 1983). The 7 labile fractions are assumed to have an initial concentration of 0.4 wt % organic carbon and the refractory fraction is taken to be 0.05 wt % organic carbon. Rate constants are compiled by WESTRICH (1983) and are based on laboratory experiments, in situ sulphate reduction rate measurements and modelling of sulphate pore water profiles. The calculated theoretical evolution of organic matter is then used as input data for the power model estimates and the results are compared in Fig. 5.4.

Figure 5.4 shows that the distribution is almost identical to the power model distribution of Fig. 5.2. The major difference between the two models

is the higher reactivity predicted by the power model at very short times. This discrepancy is outside the range of field data and may be corrected for by the introduction of a very reactive fraction. Finally, it should be mentioned that the parameters of the power model are deduced from organic carbon profiles, whereas those for the quantum-G model are based on in situ sulphate reduction rate measurements and pore water modelling. Similarity is therefore not inherited from the databases used for calibration.

TABLE 5.1. INITIAL AGES FOR SOME SEDIMENT SITES AND LABORATORY EXPERIMENTS. INITIAL AGES ARE CALCULATED FROM eq. 11.

Experimental Material	**a (day)**	**Reference**
Fresh Plankton	0.09	WESTRICH and BERNER (1984)
Algae	0.68	HENRICHS and DOYLE (1986)
Bacteria	1.69	HENRICHS and DOYLE (1986)
SewageSludge	4.20	GRUNSEICHand DUEDALL (1978)
Sediment Site	**a (year)**	**Reference**
Cape Lookout Bight	0.26	MARTENS and KLUMP (1984)
Saanich Inlet	2.5	MURRAY et al. (1978)
Buzzards Bay	6.3-9.5	HENRICHS and FARRINGTON (1987)
Southwest Pacific	93-1400	REIMERS and SUESS (1983)
Hatteras Ab. Plain	780-5300	HEGGIE et al. (1987)
Central Pacific	14000-35000	MULLER and MANGINI (1980)

Calculated apparent initial ages (Table 5.1) show some consistent trends. First of all, organic material used in experiments has a lower apparent initial age than that found at the sediment-water interface. This is probably caused by the decomposition of organic matter at or above the sediment-water interface prior to burial or by the mixing of fresh and partly degraded organic matter. Secondly, fresh plankton has a lower apparent initial age than pre-treated sewage sludge. Thirdly, the apparent initial ages of organic matter at the sediment-water interface at various sites follow the sequence expected from the water depths and the sediment accumulation rates.

CHAPTER 6: DOLOMITE FORMATION IN ANOXIC SEDIMENTS OF KAU BAY

ABSTRACT

Authigenic dolomite layers occur in the organic-matter-rich sediments of Kau Bay, Indonesia. Dolomite formation is related to the anaerobic decomposition of organic matter which causes depletion of pore-water sulphate and increase in interstitial water alkalinity. X-ray diffractograms of Kau Bay dolomites show sharply defined peaks including the superstructure reflections. Carbon isotopes indicate that a significant portion of the carbon is derived from the degradation of organic matter. The pore waters are highly supersaturated with respect to dolomite, but at greater depths pore waters are undersaturated or are near saturation with respect to calcite and aragonite. Dolomite seems to have formed by direct precipitation from solution. The formation of dolomite is believed to be initiated by the high alkalinity levels found in the zone of anoxic methane oxidation. The rate of dolomite formation is controlled by the supply of Ca and is on the order of a few centimetres per 1 kyr.

6.1 INTRODUCTION

Chemical conditions that favour the formation of sedimentary dolomite have been debated ever since this mineral was discovered by DE DOLOMIEU (1791). The so-called dolomite problem exists primarily because this mineral does not easily precipitate at low temperatures (LIPPMANN, 1973). Possible reasons for this have been summarized (MACHEL and MOUNTJOY, 1986) and are generally referred to as kinetic factors (HARTMAN, 1982; HARDIE, 1987; SIBLEY et al., 1987).

The discovery of Holocene dolomitization in hypersaline environments and brackish waters has directed studies toward these environments (e.g., see MORROW, 1982). However, it is generally accepted that there is no unique environment for dolomitization (LAND, 1980; HARDIE, 1987). Rhombohedral dolomite has been found in various marine sediments for decades (e.g., BONATTI, 1966), but interest in the formation of dolomite in deep-sea cores revived only recently (PISCIOTTO and MAHONEY, 1981; KELTS and McKENZIE, 1982; GARRISON et al., 1984; BAKER and BURNS, 1985). The occurrence of significant amounts of authigenic dolomite in the deep-sea environment appears to be related to organic-carbon-rich sediments (KELTS and McKENZIE, 1982; GARRISON et al., 1984; BAKER and BURNS, 1985, COMPTON and SIEVER, 1986; COMPTON, 1988; SUESS, VON HUENE et al., 1988). Such organogenic dolomites are characterized by carbon-13 isotope

values that deviate strongly from those of normal marine carbonates and by their occurrence as layers and concretions (SPOTTS and SILVERMAN, 1966; GARRISON et al., 1984).

Here we report the occurrence of authigenic dolomite layers in recent organic-carbon-rich sediments of Kau Bay (island of Halmahera, eastern Indonesia). Collateral pore-water and solid-phase data are used to demonstrate that these dolomites did form in situ. Our data link processes that occur in modern anoxic sediments with diagenetic features found in ancient organic-carbon-rich sediments such as the Miocene Monterey Formation of California (GARRISON et al., 1984) and the Lower Jurassic Jet Rock Formation, England (RAISWELL, 1987, 1988a, 1988b).

6.2 KAU BAY

Kau Bay (island of Halmahera, eastern Indonesia) is 470 m deep and covers an area 60 by 30 km. It is separated from the Pacific Ocean by a flat-floored 30-km-wide sill that is only 40 m below sea level. This sill restricts water exchange with the Pacific Ocean. As a consequence, there is a delicate balance between the rate at which oxygenated water is supplied and the rate at which oxygen is consumed by organic-matter decomposition. During the Snellius II expedition (1985) oxygen was found at all depths in the water column, but concentrations were as low as 8 μmol/l just above the bottom (MIDDELBURG et al., 1988a), whereas during the Snellius I expedition (1930) no oxygen was found at depths greater than about 350 m (VAN RIEL, 1943).

Sediments are reducing (Fig. 6.1, chapters 4, 7 and 8) and rich in organic carbon of mixed terrigeneous and marine origin. Sections younger than 10 kyr in the deep Kau Bay comprise uniform greenish hemipelagic muds and thin silty turbidite interbeds. The presence of deep-water benthic foraminifers tolerant of low-oxygen conditions indicates that bottom-water conditions over the past 10 kyr had persistent low oxygen content (BARMAWIDJAJA et al., 1989). The Holocene Kau Bay sediments typically contain 1%-5% S, 1%-8% Fe, 2%-8% organic carbon and 10%-15% calcium carbonate (calcite and aragonite). Within these sediments a range of authigenic minerals has been identified and include dolomite, calcite, pyrite and apatite (e.g. see chapters 4 and 7).

Dark-coloured indurated clays underlying these sediments are characterized by the absence of marine microfossils, extremely low percentages of mangrove pollen and the presence of a fresh-water diatom assemblage (BARMAWIDJAJA et al., 1989). These sediment characteristics along with the low chlorinity of the interstitial water indicate that Kau Bay was a fresh-water lake during Weichselian time (MIDDELBURG and DE LANGE, 1989; see chapters 3 and 4).

This study focuses on the results from one piston core recovered during the Snellius II expedition (VAN DER LINDEN et al., 1989). Core K4P3 was taken at a water depth of 414 m and shows a fairly uniform sedimentation rate of about 71 cm/1 kyr (chapter 2).

6.3 COMPOSITION OF THE SEDIMENTS

The Ca and Mg content of the bulk sediments in core K4P3 are shown in Figure 6.1. Major and trace elements were determined by routine Inductively Coupled Plasma Emission Spectrometry following digestion in a mixture of hydrofluoric, nitric, and perchloric acids. Depth profiles of Ca and Mg are remarkably similar at all depths and show two layers enriched in Ca and Mg. The first layer is light green and slightly indurated, and occurs at a depth of 348 to 350 cm. The gradual boundaries suggest a diagenetic origin. The second layer is beige, strongly indurated and concretionary, and occurs at a depth of 742-748 cm, just at the interface of marine and fresh-water sediments. The dolomite layer at 742-748 cm was found at similar depth in an adjacent core and corresponds to a distinct 3.5 kHz acoustic reflector horizon that could be traced over long distances (VAN DER LINDEN et al., 1989).

The isotopic composition of selected bulk sediment samples was determined by mass spectrometric analysis of gas evolved during a 4-h H_3PO_4 digestion at 25 °C. The isotopic results are given as parts per thousands deviations from the Peedee Belemnite standard (Fig. 6.1). The two dolomite samples both show distinctly higher $\delta^{18}O$ ($+0.4^{o}/_{oo}$ and $+1.0^{o}/_{oo}$) and lower $\delta^{13}C$ ($-11.4^{o}/_{oo}$ and $-11.7^{o}/_{oo}$) than the average $\delta^{18}O$ of $-4.1^{o}/_{oo}$ and $\delta^{13}C$ of $-2.7^{o}/_{oo}$. The dolomite samples are enriched in $\delta^{18}O$ by about $5^{o}/_{oo}$ relative to the other samples. This difference is consistent with cooler waters and the fractionation differences between calcite and dolomite (LAND, 1980).

The low $\delta^{13}C$ values of these authigenic carbonates can be interpreted as a result from a mixture of marine-derived carbonate and carbonate derived from the decomposition of organic matter. With increasing depth the organic-matter-derived carbonate is successively generated by sulphate reduction,

$$2\ CH_2O + SO_4^{2-} \rightarrow 2\ HCO_3^- + H_2S; \qquad (1)$$

by anoxic methane oxidation,

$$CH_4 + SO_4^{2-} \rightarrow HCO_3^- + HS^- + H_2O; \qquad (2)$$

and by methanogenesis,

$$2\ CH_2O \rightarrow CH_4 + CO_2. \qquad (3)$$

These processes occur in distinct zones and generate carbonate with characteristic $\delta^{13}C$ isotope signatures (e.g., CLAYPOOL and KAPLAN, 1974). However, gradients in the concentration of methane and carbonate cause

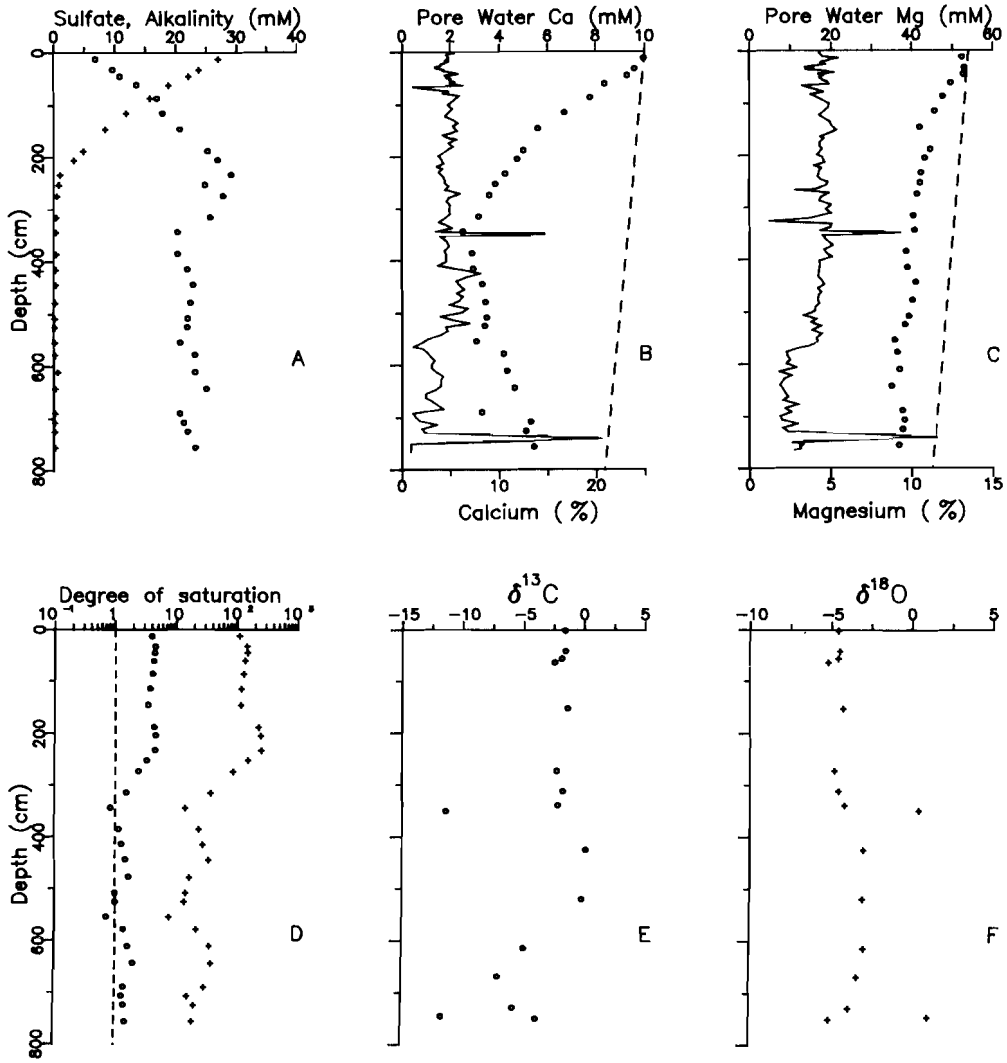

Figure 6.1. Downcore chemical and stable isotope composition of bulk-sediment and pore-water samples in core K4P3. A:) Sulfate (crosses); alkalinity (circles). B: Measured pore water calcium (circles); dashed line = pore water calcium trend expected if no reaction had occurred; solid line = solid phase Ca concentration. C: Measured pore water magnesium (circles); dashed line = pore water magnesium trend expected if no reaction had occurred; solid line = solid phase Mg concentration. D: Degree of saturation for calcite (circles) and dolomite (crosses). Minerals are at equilibrium if the degree of saturation is 1. E: $\delta^{13}C$; F: $\delta^{18}O$.

diffusive exchange by which the $\delta^{13}C$ values of carbonate in a certain zone may change and consequently become less characteristic for that zone. For instance, the radiocarbon age of the upper dolomite layer indicates the involvement of carbon that has migrated. The estimated depositional age is 4.7 kyr, but Accelerator Mass Spectrometry ^{14}C dating yields an age of 6.9 ±0.14 kyr. The excess ^{14}C age indicates that there must be an additional older, and consequently deeper, carbonate source involved. (RITGER et al., 1987). The $\delta^{13}C$ and ^{14}C values provide support for our interpretation that the dolomite layers are formed in the zone of sulphate reduction or the zone of anoxic methane oxidation.

X-ray diffractograms of the two dolomite layers are shown in Figure 6.2 with the hexagonal reference indices (LIPPMANN, 1973). Patterns show sharply defined peaks that are characteristic for well-ordered dolomite. The presence of the (101), (015), (021) and possibly (107) and (009) superstructure reflections is evidence that the samples investigated are dolomites rather than proto-dolomites. These diffractograms are very similar to those for recent dolomite in hemipelagic sediments off Baja California (SHIMMIELD and PRICE, 1984).

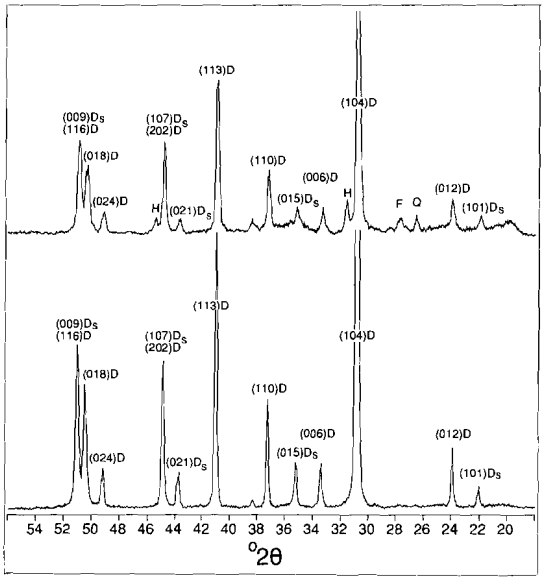

Figure 6.2. X-ray diffractograms of upper dolomite layer (above) and lower concretionary dolomite layer (below). Reflections are indexed on basis of hexagonal reference system. The superstructure reflections (101), (015), (021), (107), and (009) reveal that these samples are ordered dolomites. Within the resolution of our X-ray diffractograms, superstructure reflections (107) and (009) coincide with non-superstructure reflections (202) and (116) respectively. (D = dolomite; D_s = dolomite superstructure reflection; F = feldspar; Q = quartz; H = halite).

6.4 INTERSTITIAL WATER CHEMISTRY

Immediately after recovery of core K4P3, pore water was extracted under high-purity nitrogen in a glove box (DE LANGE, 1986a, 1988). The interstitial water samples were analyzed for nutrients, major elements, and some trace elements by routine ICPES, autoanalyzer, and potentiometric titration techniques.

Anaerobic decomposition of organic matter is the dominant diagenetic process inferred from the pore-water chemistry (Fig. 6.1). Interstitial water sulphate concentrations decrease to zero at a depth of about 250 cm. Alkalinity initially increases to a maximum of 30 mM at a depth of 200-300 cm, then decreases to uniform values of about 22 mM below 350 cm. Calcium initially decreases to a minimum at 350 cm and then increases. Magnesium decreases gradually with depth. These decreases in Ca and Mg are significantly larger than decreases relating to the salinity decrease (Fig. 6.1). On the basis of the pore-water chemical composition, three distinct diagenetic zones can be recognized (e.g., see REEBURGH, 1980): a sulphate reduction zone (0-250 cm; reaction 1), a zone of anoxic methane oxidation (250-300 cm; reaction 2) and a zone of methanogenesis (reaction 3) at depths greater than 300 cm.

The degree of dolomite and calcite saturation was calculated by using the interstitial water composition and punch-in pH data. Equilibria were calculated using an ion-association model (VAN GAANS, 1989) based on WATEQF (PLUMMER et al., 1976). Activity coefficients for all aqueous species were calculated with the ion-pairing model of MILLERO and SCHREIBER (1982).

In the sulphate reduction zone the degree of saturation for aragonite, calcite, and dolomite is more or less constant at 3, 4, and 160 times supersaturation, respectively (Fig. 6.1). The fourfold supersaturation with respect to calcite is similar to other reported values (e.g., COMPTON, 1988). Below the alkalinity maximum there is a significant decrease in the degree of saturation of the pore water with respect to aragonite, calcite, and dolomite. Below 350 cm, interstitial waters are slightly undersaturated with aragonite, are near saturation with calcite, and are about 25 times supersaturated with dolomite.

6.5 NATURE OF DOLOMITIZATION

Dolomite appears to be forming in specific intervals within these sediments. This provides a unique opportunity for observations on depositional environmental conditions and for testing possible mechanisms.

The degradation of organic matter by sulphate reduction may be a prerequisite for the formation of organogenic dolomites. BAKER and

KASTNER (1981) suggested that dissolved sulphate in pore water inhibits dolomite precipitation. LIPPMANN (1973) and MORROW and RICKETTS (1986), however, showed that this inhibitory effect of sulphate on the precipitation of Mg-bearing mixed carbonates is limited. An alternative hypothesis (e.g., LIPPMANN, 1973; HARDIE, 1987) is that the high alkalinity produced during sulphate reduction may be responsible for dolomite precipitation. The distinct low carbon-isotope signature of these organogenic dolomites is evidence of such an organic-matter-derived source of alkalinity.

The pore-water chemical data and the solid-phase isotope data can be used to constrain reaction stoichiometries. The dolomitization reaction can be written either in terms of a supply from solution for all components involved,

$$Ca^{2+} + Mg^{2+} + 4\ HCO_3^- = CaMg(CO_3)_2 + 2\ CO_2 + 2\ H_2O, \qquad (4)$$

or in terms of a calcite or aragonite replacement,

$$2\ CaCO_3 + Mg^{2+} = CaMg(CO_3)_2 + Ca^{2+}. \qquad (5)$$

On the basis of the pore-water chemistry, we suggest that the growth of the dolomite layer at a depth of 348-350 cm is limited by the supply of Ca rather than by the availability of magnesium (Fig. 6.1). According to reaction 4, the consumption of 8 mM of Ca should have concomitant depletion in Mg of 8 mM and depletion in alkalinity of 32 mM. The data presented in Figure 6.1 are consistent with this stoichiometry if we consider the potential alkalinity (i.e., $-2\Delta SO_4 = \Delta HCO_3$; see reaction 1) rather than the measured alkalinity. It seems, therefore, that this dolomite layer is forming according to reaction 4-- i.e. by direct precipitation from solution.

The presence of a minimum in the pore-water concentration of Ca at the same depth as the upper dolomite indicates that this dolomite is actively growing. This observation allows us **(1)** to estimate the distribution coefficient of Sr and Mn for dolomite formation (see section 6.6) and **(2)** to estimate the time required to form this dolomite layer and thus the time and depth of the initiation of the precipitation process. On the basis of the amount of Ca precipitated as dolomite, calculated with equation 3-71 of BERNER (1980a), and the flux of Ca delivered by diffusion from above and below, determined by using Fick's Law, we calculate that the dolomite layer was formed in about 550 yr. With an average sedimentation rate of 71 cm/1 kyr, this would suggest dolomite formation in this layer began at a depth of about 300 cm.

On the basis of its similar isotopic and chemical composition we propose that the concretionary dolomite layer found at a depth of 742-748 cm formed earlier in the same way as the upper dolomite layer is now forming. Following an initial period of rapid growth, further burial led to only limited growth. It should be mentioned that for this concretionary dolomite we cannot rule out the possibility that boundary-layer processes related to the mixing of fresh water and sea water were important.

The data presented in this study are consistent with a two-stage growth process for dolomite layers and concretions. In the first stage there is very rapid growth during the selective precipitation in a narrow zone-- e.g., the upper dolomite layer. Growth rates may be of the order of a few centimetres per 1 kyr. The pore-water calcium profile reveals that the rate of initial precipitation in the organic-carbon-rich sediments is Ca-transport limited, and not surface-reaction controlled as has been suggested by RAISWELL (1988a). The second stage is slow accretion during subsequent burial. KELTS and McKENZIE (1982) calculated growth rates on order of a few tenths of a millimetre per 1 kyr. Our interpretation is consistent with the observation that concretions found at greater depths may retain characteristics of early diagenetic conditions (KELTS and McKENZIE, 1982; GARRISON et al., 1984; RAISWELL, 1988b).

Finally, the problem of what controls initial precipitation sites persists. The low-temperature precipitation kinetics of dolomite seem to be characterized not only by a high nucleation barrier, but also by relatively rapid crystal-growth kinetics. Once nucleation has occurred, the crystal growth of dolomite is very rapid, as suggested by our pore-water data. The precipitation of dolomite is thought to be initiated by high degrees of supersaturation (e.g., SIBLEY et al., 1987). The high degree of supersaturation required for the initiation of precipitation is most likely to be found in the zone of anoxic methane oxidation. This zone is confined upward by the absence of methane and downward by the absence of sulphate and is at or close to the alkalinity maximum. In core K4P3 the zone of anoxic methane oxidation is at a depth of 250-300 cm (Fig. 6.1). Our calculations suggest that dolomite layer formation began at a depth of about 300 cm-- i.e., in a zone of anoxic methane oxidation, at or close to the alkalinity maximum. Under steady-state sedimentation the zone of high alkalinity is continuously moving upward through the sediment column. However, any break or pause in sedimentation stabilizes the zone of excess alkalinity at a certain depth below the sediment surface (RAISWELL, 1987, 1988b). During such an event, alkalinity levels increase as a consequence of the continuing diffusive supply of sulphate from above and of methane from below and their subsequent reaction in this zone (reaction 2). The excess alkalinity may then initiate the dolomitization process. After this initiation, rapid precipitation perturbs the pore-water gradients so that the alkalinity levels and degrees of supersaturation are lowered again.

6.6 APPENDIX: AN ATTEMPT TO ESTIMATE THE DISTRIBUTION COEFFICIENT FOR SR AND MN IN DOLOMITE

The concentrations of Sr and Mn in dolomite have been investigated by numereous authors (e.g. LAND, 1980; HARDIE, 1987; MACHEL and MOUNTJOY, 1986; BAKER and BURNS, 1985; VAHRENKAMP and SWART, 1990; and references therein). The primary objective of these studies has been to use trace element contents to characterize the environment of deposition. These studies rely on the application of a distribution coefficient, which is defined as:

$k^D_{Tr} = (Tr/Ca)_{Dol.}/(Tr/Ca)_{solution}$,

where k^D_{Tr} is the distribution coefficient of trace element Tr in dolomite, $(Tr/Ca)_{Dol.}$ and $(Tr/Ca)_{solution}$ are the the molar ratios of trace element Tr and Ca in dolomite and solution respectively.

It should be realized that this is a highly empirical, and simplistic, approach (e.g. see MORSE and BENDER, 1990). The incorporation of trace elements in carbonate minerals involves a number of processes including sorption, surface precipitation and solid-solution formation (e.g. MIDDELBURG et al., 1987; COMANS and MIDDELBURG, 1987; DAVIS et al., 1987; WERSIN et al., 1989). Distribution coefficients are therefore dependent on factors such as the composition of solid and solution, temperature and the precipitation rate (e.g. see MORSE and BENDER, 1990). Distribution coefficients have nevertheless proven to be very useful in studies of sedimentary rocks. Only a few data for the distribution coefficient of trace elements in dolomite are available, because **(1)** k^D_{Tr} values are very difficult to determine experimentally at low temperatures and **(2)** there are only a few sites of active dolomite formation where both the solution and solid phases are well characterized.

On the basis of the composition of the dolomite layers (Ca = 4394 mmol/kg; Sr = 5.74 mmol/kg and Mn = 21.64 mmol/kg) and the composition of interstitial water at a depth of 350 cm (Ca = 2.51 mM; Sr = 78 μM and Mn = 0.47 μM), distribution coefficients of 0.042 and 26.3 are calculated for Sr and Mn respectively.

This distribution coefficient for Sr in dolomite is within the range of k^D_{Sr} values (0.032 to 0.089) reported for organogenic dolomites at DSDP site 479 (BAKER and BURNS, 1985). It is however slightly higher than the at high temperature (252 to 295 °C) experimentally determined k^D_{Sr} value of about 0.025 (KATZ and MATTHEWS, 1977) and the k^D_{Sr} value of 0.0118 proposed for ancient dolomite by VAHRENKAMP and SWART (1990). Part of this difference may be related to the mode of formation (direct versus replacement), rate of precipitation and composition of solid and solution. It should perhaps

be mentioned that VAHRENKAMP and SWART (1990) assumed a Sr/Ca ratio in solution similar to sea water. This is not necessarily true.

The distribution coefficient for Mn in dolomite obtained in this study (26.3) can not be compared with estimates reported in the literature, because these are not available. However, on the basis of pore-water data for DSDP site 479 at a depth of 170 m (GIESKES et al., 1982) and microprobe analysis of dolomite samples from the same depth interval(KELTS and McKENZIE, 1982), a k^{D}_{Mn} value of about 25 can be calculated. This is in excellent agreement with the value obtained for Kau Bay dolomites.

CHAPTER 7: ORGANIC CARBON, SULPHUR AND IRON IN RECENT SEMI-EUXINIC SEDIMENTS OF KAU BAY

ABSTRACT

Kau Bay (island of Halmahera, Eastern Indonesia) is a 470 m deep basin separated from the Pacific Ocean by a sill that is at present only 40 m below sea-level. During Weichselian time, the sea-level dropped below the depth of the sill and fresh-water sediments were deposited. These sediments are rich in organic matter (C_{org} = 2-6 wt %) with terrigenous characteristics ($\delta^{13}C_{org}$ = -28 to -30 °/$_{oo}$), and are also rich in sulphur (S ≈ 4 wt %). This sulphur enrichment is interpreted to be a late diagenetic feature related to diffusion of dissolved sulphate and sulphide from the marine sediments into the fresh-water sediments ($\delta^{34}S$ = + 15 °/$_{oo}$). The overlying Holocene sediments consist of marine muds deposited in alternating low oxygen and H_2S-bearing bottom waters. The marine sediments are also rich in organic matter (C_{org} = 2-6 wt %), but of mixed terrigenous and marine origin ($\delta^{13}C$ = -25 to -19 °/$_{oo}$). Moreover, their sulphur content is lower (S = 1-2 wt %) and isotopically lighter ($\delta^{34}S$ = -20 °/$_{oo}$).

In addition to pyrite, large amounts of acid volatile sulphur (AVS) compounds accumulate in Kau Bay. The reactive iron content of the sediment limits the amount of iron that is sulphidized, while the supply of oxidants controls the limited conversion of AVS to pyrite. Total and reactive iron contents are strongly correlated with the amount of terrigenous organic matter as a consequence of their common provenance and depositional histories. The marine sediments in Kau Bay show no simple relation between organic carbon and sulphur.

7.1 INTRODUCTION

In sediments the decomposition of organic matter by microbiological sulphate reduction leads to the production of hydrogen sulphide (e.g., JØRGENSEN, 1982). Part of the hydrogen sulphide may react with iron and organic matter and may be buried as iron sulphide (BERNER, 1970a, 1984) and organo-sulphur compounds (KOHNEN et al., 1989). Another part of the hydrogen sulphide may be lost via oxidation in solution or via solid-phase sulphide oxidation (JØRGENSEN, 1977; BERNER and WESTRICH, 1985). The fraction of reduced sulphur that is buried in a sediment varies from 2 to 75 % (JØRGENSEN, 1977, 1982; BERNER and WESTRICH, 1985; CHANTON et al., 1987a; SWIDER AND MACKIN, 1989).

Similarly, the fraction of organic matter that arrives at the sediment

surface, escaping decomposition and becoming buried, varies between 0.5 and about 80 % (HENRICHS and REEBURGH, 1987; CANFIELD, 1989b). It should, however, be realized that normally only a few percent is preserved (EMERSON and HEDGES, 1988). As a result the amounts of reduced sulphur and organic carbon buried in a sediment may represent only a fraction of the total amount produced or delivered.

Despite the dynamical nature of the organic carbon and sulphur cycles, it has been shown that differences in the concentration of organic carbon (C) and reduced sulphur (S) at depth can be used to distinguish between sediments deposited in oxygenated marine, euxinic marine and fresh-water environments (LEVENTHAL, 1983, 1987; BERNER and RAISWELL, 1983, 1984; RAISWELL and BERNER, 1985; ANDERSON et al., 1987; DAVIS et al., 1988; DEAN and ARTHUR, 1989).

This so-called carbon/sulphur method has not been tested extensively on recent euxinic sediments because there are only a few sites where anoxic bottom waters occur. The most important examples of such environments are anoxic silled basins like the Black Sea, the Baltic, Framvaren fjord, Saanich Inlet (ANDERSON and DEVOL, 1987) and Kau Bay (MIDDELBURG et al., 1988a, 1990). Information about the organic carbon, sulphur and iron contents of sediments of these anoxic basins is meagre. In this chapter I report and discuss the solid speciation of iron and sulphur, the isotopic composition of organic carbon and sulphur, and the organic carbon, sulphur and iron content of anoxic sediments of Kau Bay, Indonesia. The objectives of this study are: **(1)** to study the formation of iron sulphides and limiting factors for pyrite formation; **(2)** to interpret the inter-relationships in the C-S-Fe system as indicators of depositional environments; **(3)** to show the importance of reactive iron for pyrite formation and to unravel the link between iron and organic carbon.

7.2 KAU BAY

The study of Kau Bay began during the Snellius I expedition (1929-1930) (KUENEN, 1943; VAN RIEL, 1943) and recommenced during the Snellius II expedition (1984-1985). Kau Bay, which is enclosed by the two northern arms of the island of Halmahera (eastern Indonesia), is 470 m deep and covers an area of 60 by 30 km. It is separated from the Pacific Ocean by a sill that is only 40 m below sea-level. The peculiar submarine morphology of Kau Bay restricts water exchange with the Pacific Ocean and therefore limits the ventilation of deep water. There is a delicate balance between the rate at which oxygenated water is supplied and the rate at which oxygen is consumed by organic matter decomposition. During the Snellius II

expedition (1985) oxygen was found at all depths in the water column, but concentrations were as low as 8 μM just above the bottom (MIDDELBURG et al., 1988; chapter 2), whereas during the Snellius I expedition (1930) no oxygen was found at depths greater than about 350 m and hydrogen sulphide concentrations up to 13 μM were observed (VAN RIEL, 1943).

Therefore, Kau Bay is a typical environment for semi-euxinic or inhospitable bottom conditions, i.e. fluctuating situations where low oxygen, but non-sulphidic bottom waters, alternate with anoxic-sulphidic bottom waters (RAISWELL and BERNER, 1985). Moreover, there is faunal evidence that semi-euxinic conditions have prevailed over the past 10 kyr. The permanent presence of a deep-water low-diversity fauna with a low-oxygen signature indicates that Kau Bay has been poorly ventilated during the Holocene and implies at the same time that anoxic-sulphidic bottom-water conditions are of short duration (chapter 2; BARMAWIDJAJA et al., 1989).

Another interesting feature of Kau Bay is its isolation during periods of low sea-levels. During Weichselian time, the sea level dropped below the depth of the sill and fresh-water sediments were deposited (MIDDELBURG and DE LANGE, 1989; chapters 3, 4 and 8). These sediments are characterized by the absence of marine microfossils, extremely low percentages of mangrove pollen and the presence of a fresh-water diatom assemblage (BARMAWIDJAJA et al., 1989). The fresh-water nature of Weichselien sediments is supported by the low chlorinity of the interstitial water (MIDDELBURG and DE LANGE, 1989; chapters 3 and 4).

7.3 MATERIAL AND METHODS

In the present study results will be discussed of the analyses of cores recovered during the Snellius II expedition in April 1985 (Fig. 2.1). The shipboard routine has been described in detail elsewhere (DE LANGE, 1986a, 1988) and will be summarized briefly below.

Cores were stored at in situ temperature (28 °C) until analysis, which was started within 24 hours of core collection. The core sections of 1 m were split lengthwise into two parts: one part was stored at 4 °C for detailed subsampling at the University laboratory and the other part was immediately transferred to a high-purity nitrogen atmosphere (O_2 < 0.003%). Samples for pore-water extraction were taken with a bone spatula after removal of the top mm of sediment in order to prevent the inclusion of oxidized/contaminated material. The pressure filtration of the sediment in Reeburgh-type squeezers took place in a nitrogen-filled glovebox. The sediment cakes remaining after squeezing were stored under nitrogen in air-

tight jars and kept in the dark at 4 °C during transport.

The recovered pore-water samples were subdivided into three separate portions which were subsequently (1) acidified, (2) used for the determination of alkalinity by potentiometric titration and (3) used for the analyses of ammonium according to the phenol-hypochlorite method (HELDER and DE VRIES, 1979) and of phosphate according to automated STRICKLAND and PARSONS (1968) methods. The acidified portion of pore water was stored at 4 °C and analysed for total S and Fe by Inductively Coupled Plasma Emission Spectrometry (ICPES; ARL 34000). Total sulphur measured in this way is attributed to sulphate. Due to logistic problems only a few samples could be analysed for dissolved sulphide by the method of CLINE (1969).

Prior to analysis, sediment samples for bulk determination were dried at 105 °C and finely ground in an agate mortar. Following digestion in a mixture of hydrofluoric, nitric and perchloric acids, final solutions were made up in 1 N HCl and analysed by ICPES.

All $\delta^{13}C$-C_{org} sediment samples were leached with dilute HCl to eliminate any contribution from inorganic carbon. Following acid leaching the sediment samples were centrifuged and the supernatant was removed. The samples were subsequently dried at 50-60 °C and homogenized. The dried sediment samples were combusted at 900 °C and the gases evolved were subsequently purified by cryogenic vacuum line techniques. The yields were determined manometrically and the collected gases were analysed on a VG SIRA 24 mass spectrometer. The isotope data are reported in $^{o}/_{oo}$ relative to the PeeDee Belemnite standard.

The organic nitrogen content of a few selected samples was determined using methods described in DE LANGE (1988). This involves the separate determination of exchangeable, fixed and total nitrogen and subsequent calculation of organic nitrogen by difference.

Bulk sediment samples for $\delta^{34}S$ measurements were prepared by reducing inorganic sulphur compounds to sulphide with the Kiba reagent (Sn(II)-concentrated phosphoric acid). The sulphide generated was subsequently oxidized to SO_2 at 1000 °C using V_2O_5. The isotopic composition of the SO_2 was measured with a Finnigan MAT 271/45 mass spectrometer equipped with a dual inlet system and a multi-collector system. The $\delta^{34}S$ data are based on duplicate measurements and are reported in $^{o}/_{oo}$ relative to Canyon Diablo.

A selection of sediment samples remaining after squeezing, and stored under nitrogen at 4 °C, was subjected to an acid-gradient extraction technique. These sediment samples were used directly without any pre-treatment. About 1.5 gr of sediment in Teflon (FEP) centrifuge tubes was

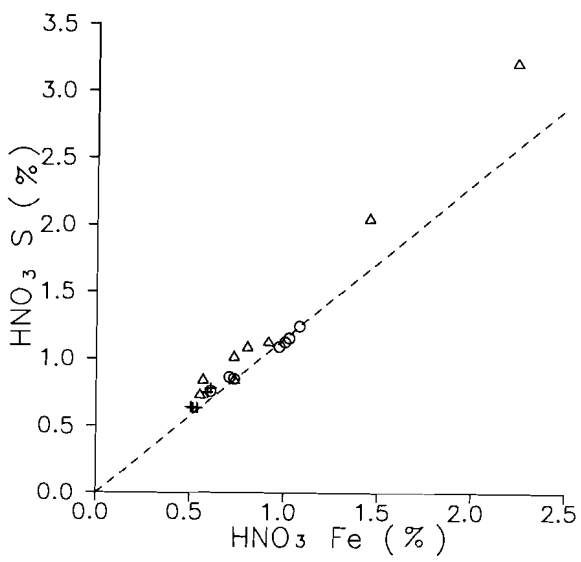

Figure 7.1. The amounts of sulphur and iron extracted by concentrated nitric acid after removal of oxide, silicate and acid-volatile sulphur (AVS) phases. The ideal pyrite stoichiometry is indicated by the dashed line. Dots, triangles and crosses represent data from stations K3, K4 and K11 respectively.

sequentially leached for 3 hours with 20 ml each of : (1) distilled water, (2) 0.1 N NH_4Ac, (3) 10% 0.1 N HAc/90% 0.1 N NaAc, (4) 20% 0.1 N HAc/80% 0.1 N NaAc, (5) 35% 0.1 N HAc/65% 0.1 N NaAc, (6) 65% 0.1 N HAc/35% 0.1 N NaAc, (7) 80% 0.1 N HAc/20% 0.1 N NaAc, (8) 90% 0.1 N Hac/10% 0.1 N NaAc, (9) 0.1 N HAc, (10) 1 N Hac, (11) 3.3 N HAc, (12) 0.05 N HCl, (13) 0.1 N HCl, (14) 0.5 N HCl, (15) 1 N HCl, (16) 2 N HCl and (17) 6 N HCl. After each step the samples were centrifuged, and the supernatant was carefully removed and stored after addition of appropriate amounts of HCl. The residue was subsequently extracted for 24 hours with 20 ml of 10 N HF (18) and concentrated nitric acid (19). After each of these two steps the samples were centrifuged and the supernatant was carefully transferred into a teflon vessel. In the teflon vessel the solutions were evaporated to dryness and the final solutions were made up in 1 N HCl. The final residue left after these 19 steps was digested in a mixture of hydrofluoric, nitric and perchloric acids, subsequently evaporated and taken up in 1 N HCl. All 20 fractions were analysed by ICPES. The sum of the various fractions for Fe was compared with the independently determined total iron content and the difference was found to be less than 10%. This agreement indicates that there was no significant sample loss due to the sequential nature of the extraction procedure.

It should be realized that this acid-gradient leaching technique is only operationally defined and is not intended to be selective. However, for Kau

Bay sediments the amount of iron extracted by 6 N HCl at room temperature for hours is equal to that soluble in hot HCl for one minute. The latter technique has been used by various workers (e.g. BERNER, 1970a; RAISWELL et al., 1988) and our results can therefore be compared with theirs. Moreover, LORD (1982), MORSE and CORNWELL (1987) and HUERTA-DIAZ and MORSE (1990a,b) have shown that iron extracted by concentrated nitric acid after removal of oxide, silicate and acid-volatile sulphur (AVS) phases provides a quantitative measure for iron and trace element concentrations in pyrite. The trace element content of pyrite in Kau Bay sediments is presented in section 7.7.

Figure 7.1 shows that the amounts of sulphur and iron extracted by concentrated nitric acid closely follow the ideal pyrite stoichiometry. The sulphur and iron in the HNO_3 leaches are therefore assumed to represent pyrite-S and pyrite-Fe. Knowledge of the amount of total sulphur and pyrite sulphur allows AVS-sulphur to be calculated by difference; i.e. $AVS\text{-}S = S_{total} - S_{HNO3}$. In this partitioning scheme organic-S compounds are included either in the pyrite-S or in the AVS-S pool depending on their solubility in HCl. However, in view of the organic matter and pyrite contents of marine sediments, the contribution of organic-S will be very small. Sedimentary iron is partitioned into (1) a "non-reactive" fraction (sum of HF and residual fractions), (2) AVS-Fe (calculated by assuming that FeS can represent AVS-Fe; i.e. Fe_3S_4 is only a minor component of AVS), (3) pyrite-Fe (HNO_3 leach) and (4) "potentially reactive" iron (all fractions soluble in 6 N HCl minus AVS-Fe).

7.4 RESULTS

In this study results will be presented from three sites in Kau Bay, namely K3, K4 and K11 (Fig. 2.1). Station K3 is positioned in the deepest part of the basin. The presence of numerous turbidites and high percentages of reworked planktonic foraminifera at station K3 indicate that high amounts of mass-transported sediments are trapped. This is reflected in a high sedimentation rate of 0.6 cm/yr (chapter 2). In contrast to station K3, sediment accumulation rates at stations K4 and K11 are only 0.071 cm/yr and 0.085 cm/yr respectively (chapter 2). This difference in sedimentation rate between the deep water stations K4 and K3 can most probably be attributed to the difference in elevation (VAN DER LINDEN et al., 1989). Similarly, large amounts of sediment may be expected to bypass station K11 which is situated in rather an isolated position, on a ledge.

The sediments in Kau Bay can be divided into three distinct units representing different sedimentary facies (chapter 8). These different units

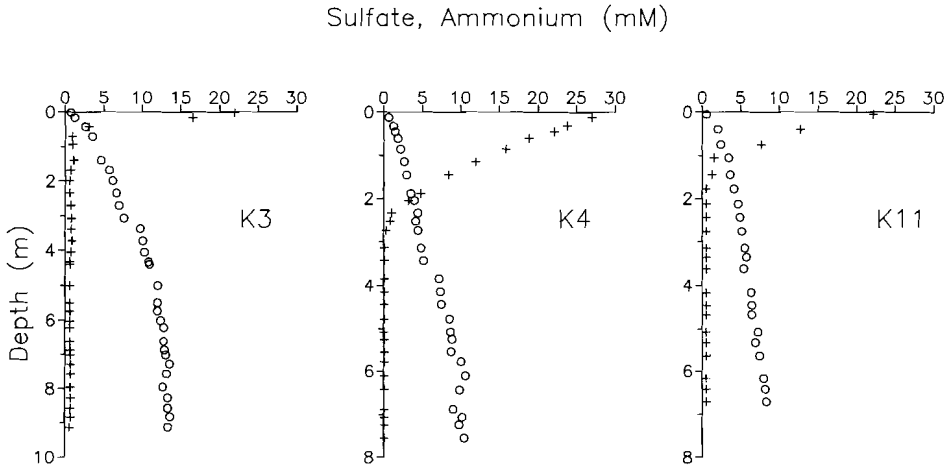

Figure 7.2. The pore water concentration of sulphate (crosses) and ammonium (dots) versus depth in sediments of Kau Bay.

represent the response of Kau Bay to the change from a Pleistocene fresh-water lake to the modern marine basin as a consequence of the post-glacial sea-level rise and the reconnection of the basin to the Pacific. The Holocene sediments (unit 1) consist of uniform greenish hemipelagic marine mud with thin silty interbeds and typically contain 10-15 % carbonate. Within these sediments a range of authigenic minerals has been identified, including dolomite, calcite, pyrite and apatite (chapters 4 and 6 and MIDDELBURG et al., 1990). At station K4 two piston cores penetrated through the greenish marine mud into the underlying dark-coloured fresh-water sediments of unit 3. The sediments of unit 2 comprise the transition from fresh-water to marine conditions.

7.4.1 Pore water chemistry

Figure 7.2 shows dissolved sulphate and ammonium as a function of depth. The general aspects of trends with depth are similar to those reported for other anoxic sediments (e.g. SHOLKOVITZ, 1973; MURRAY et al., 1978). Interstitial water sulphate concentrations decrease to zero at depths

TABLE 7.1. C/N ratio of decomposing organic matter

	K3	K4	K11
D_N ($cm^2\ yr^{-1}$)	436	436	436
D_S ($cm^2\ yr^{-1}$)	218	218	218
K_N[a]	0.9	1.6	0.8
w ($cm\ yr^{-1}$)	0.6	0.071	0.085
k[b] ($yr^{-1} * 10^{-3}$)	2.1	0.21	0.26
$\delta SO_4/\delta NH_4$	8.2	7.5	6.5
C/N ratio	8.4	7.3	6.5

a Determined from plots of exchangeable versus dissolved ammonium.
b Obtained by fitting ammonium versus depth profiles. The rate constants for ammonium production and sulphate reduction are assumed to be similar. This is not necessarily true (see chapter 4).

of about 0.6, 2.2 and 1.2 m for stations K3, K4 and K11 respectively. These decreases in sulphate are significantly larger than decreases relating to the salinity decrease, which accounts for no more than 5 % (MIDDELBURG and DE LANGE, 1989). The depths of dissolved sulphate depletions follow the sequence expected from the sedimentation rates (BERNER, 1978).

These decreases in sulphate are accompanied by large enrichments in ammonium (Fig. 7.2), alkalinity (MIDDELBURG et al., 1990) and phosphate (chapter 4). The continuing downward increase of ammonium below the depth of sulphate depletion implies that ammonium is produced not only by sulphate reducing bacteria, but also by micro-organisms which are active after interstitial water sulphate has been exhausted. Similar observations have been made in Loch Duich (PRICE, 1976), Saanich Inlet (MURRAY et al., 1978), Long Island Sound (ROSENFELD, 1981) and at various DSDP and ODP sites (GIESKES, 1983).

In the zones of sulphate reduction, there are linear relationships between sulphate depletions and ammonium enrichments with slopes varying between 6.5 and 8.2 (chapter 4). This allows us to calculate the carbon/nitrogen ratio of the organic matter undergoing decomposition using the steady-state equation given by BERNER (1977):

$$\frac{C}{N} = \frac{2\Delta SO_4}{\Delta NH_4} \frac{(\omega^2 + kD_S)}{(\omega^2(1+K_N) + kD_N)}$$

where ΔSO_4 is the sulphate depletion, ΔNH_4 is the ammonium enrichment, k is the first order rate constant, D_S and D_N are the diffusion coefficients of SO_4 and NH_4 corrected for tortuosity effects, K_N is the linear sorption coefficient and ω is the sediment accumulation rate. The carbon/nitrogen molar ratios of the decomposing organic matter in Kau Bay vary from 6.5 to 8.4 (Table 7.1), which are close to the ideal Redfield ratio of 6.6. For comparison, the carbon/nitrogen molar ratio of total organic matter varies between 20 and 25. This might indicate preferential decomposition of nitrogen-rich organic matter.

7.4.2 Solid phase chemistry

Before the depth distribution of Kau Bay sediment characteristics is presented, it is instructive to present the results of the acid-gradient leaching technique. The distribution of iron over the various leach fractions is shown in Figure 7.3 and Table 7.2. The leach patterns for the marine sediments show some interesting features. Firstly, there are no major differences between the leach patterns for various samples. This indicates that Kau Bay sediments are rather homogeneous and that the acid-leach technique provides consistent results. Secondly, the distilled water, 0.1 N NH_4Ac and NaAc/HAC buffer leaches together contain less than 1 % of the total iron. In addition, the acetic acid leaches account together for about 2-7 % of the total iron. This low yield indicates that iron-containing carbonates and phosphates are not present in significant amounts, because partial dissolution of acid volatile sulphide minerals by acetic acid (CORNWELL and MORSE, 1987) may account for the iron liberation. Thirdly, pyrite-Fe accounts for about 10 to 17 % of the iron. Fourthly, about 30-40 % of the iron is leachable by HF and about 1 % of the iron is found in the residual fraction. These two fractions are probably "non-reactive" (CORNWELL et al., 1990). Finally, about half of the iron is associated with compounds that dissolve in HCl. This fraction is often referred to as being "reactive" (e.g. BERNER, 1970a, 1984; HUERTA-DIAZ and MORSE, 1990a).

BERNER (1970a) reported that iron released by HCl treatment reflects maximum possible reactivity towards H_2S. It has been shown that the reactivity of sediments towards H_2S is mainly determined by the amount of Fe-oxides (CANFIELD, 1989a; CORNWELL et al., 1990), although clay minerals show some reactivity towards H_2S during burial diagenesis (DREVER, 1971). However, treatment by HCl removes not only Fe-oxides and AVS, but also significant amounts of Fe-bearing silicates. This is shown in Figure 7.3 by the amounts of Si, Al and Mg that are leached along with iron. This release of significant amounts of Si, Al and Mg in addition to Fe

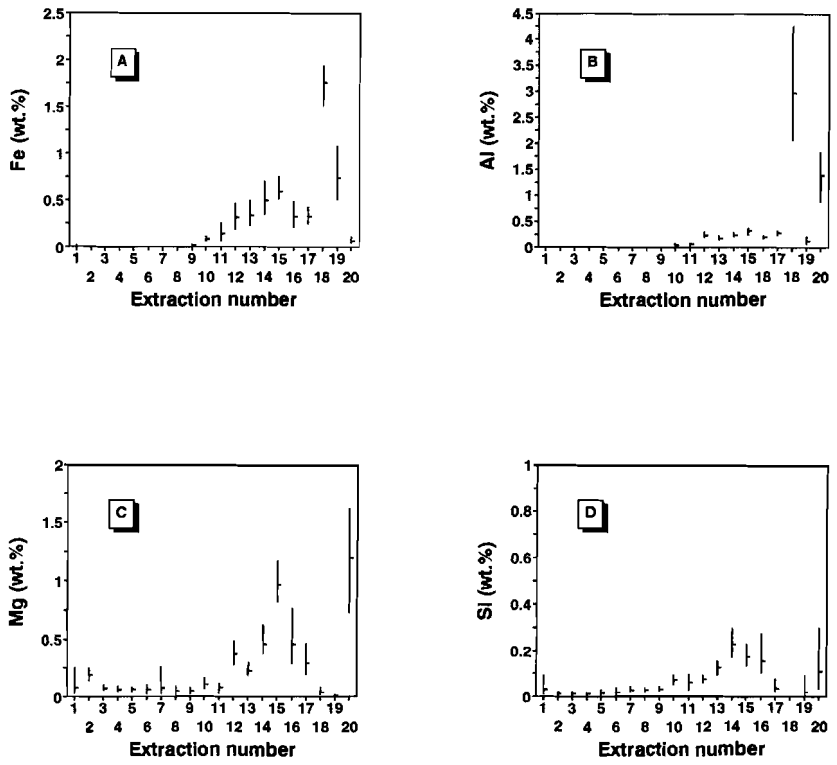

Figure 7.3. The distribution of iron (A), aluminium (B) and magnesium (C) and silicium (D) over the various leach fractions. In order to simplify presentation only the range and average of samples are shown (N=18). The numbers on the abscissa indicate the various fractions: (1) distilled water, (2) 0.1 N NH_4Ac, (3) 10% 0.1 N HAc/90% 0.1 N NaAc, (4) 20% 0.1 N HAc/80% 0.1 N NaAc, (5) 35% 0.1 N HAc/65% 0.1 N NaAc, (6) 65% 0.1 N HAc/35% 0.1 N NaAc, (7) 80% 0.1 N HAc/20% 0.1 N NaAc, (8) 90% 0.1 N Hac/10% 0.1 N NaAc, (9) 0.1 N HAc, (10) 1 N Hac, (11) 3.3 N HAc, (12) 0.05 N HCl, (13) 0.1 N HCl, (14) 0.5 N HCl, (15) 1 N HCl, (16) 2 N HCl, (17) 6 N HCl, (18) 10 N HF, (19) HNO_3 and (20) residue by $HClO_4/HNO_3/HF$.

TABLE 7.2. Iron speciation of Kau Bay sediments

Depth (cm)	Ac.[a] (r%)	HAc[b] (r%)	HCl[c] (r%)	HF[d] (r%)	HNO_3[e] (r%)	Res.[f] (r%)	Tot.[g] (wt%)	Reac.[h] (wt%)	Sul.[i] (wt%)	FeS/FeS_2[j]
K3										
2	0.4	4.8	46.4	34.1	13.3	1.0	5.14	3.60	1.53	1.1
43	0.7	6.4	45.6	30.6	15.6	1.1	5.76	4.10	1.78	0.9
169	0.9	6.5	43.4	34.8	13.6	0.7	4.81	3.32	1.50	1.1
373	0.8	4.2	47.5	29.8	16.6	1.0	6.25	4.50	1.90	0.8
575	0.6	3.3	48.3	30.0	16.7	1.2	5.71	4.24	1.71	0.7
730	0.5	5.6	44.7	35.7	12.7	0.9	4.34	3.05	1.33	1.1
913	0.6	3.9	47.4	30.9	16.1	1.1	5.61	4.25	1.52	0.5
K4										
13	0.4	3.9	43.7	34.8	15.6	1.6	4.40	2.99	1.65	1.2
62	0.4	4.2	43.0	33.9	16.4	2.0	5.07	3.59	1.75	0.8
189	0.5	6.3	41.9	35.4	15.2	0.8	4.49	3.09	1.59	1.0
274	0.4	4.9	41.2	35.3	17.1	1.2	4.44	3.01	1.72	1.0
344	0.3	6.8	45.4	35.6	10.7	1.3	5.08	3.28	2.54	3.1
444	0.3	6.1	42.0	38.4	12.1	1.2	4.05	2.86	1.96	1.9
708[2]	0.3	5.2	22.9	37.1	32.7	1.8	4.32	2.72	2.95	0.8
756[3]	0.1	2.4	24.8	31.0	33.3	8.3	6.77	4.08	3.69	0.5
K11										
5	0.5	5.0	51.6	30.1	11.9	1.0	4.12	2.75	1.14	1.1
75	0.3	3.6	46.6	36.8	11.6	1.1	4.13	2.71	1.15	1.2
178	0.3	3.4	52.5	32.3	10.7	1.0	4.45	3.22	1.26	1.4
276	0.2	3.9	45.6	37.0	12.1	1.3	4.63	3.43	1.37	1.2
447	0.4	4.5	46.8	34.0	13.2	1.1	4.18	3.00	1.57	1.4

a = iron released during steps 1-8 (H_2O; NH_4Ac; Acetate buffers) as a percentage of total iron; b = iron released during steps 9-11 (Acetic acids) as a percentage of total iron; c = iron released during steps 12-17 (HCl) as a percentage of total iron; d = iron released during step 18 (HF) as a percentage of total iron; e = iron released during step 19 (HNO_3) as a percentage of total iron; f = residual iron as a percentage of total iron; g = total iron concentration (wt %); h = sum of pyritic and HCl soluble iron (wt %); i = sulphide bound iron (wt %); j = molar FeS/FeS_2 ratio.

[2,3] Sediment from unit 2 and 3 respectively.

indicates that the determination of 'reactive iron' by HCl digestion results in an overestimation of the reactivity of these sediments towards H_2S. Moreover, all iron phases reactive towards H_2S have been sulphidized in the Kau Bay sediments (see below). Hence, actually sulphidized iron is the best measure of the reactive iron content. For the marine sediments the sulphide-bound iron ranges from 1.3 to 2.5 wt % (Table 7.2) which is only a fraction of the sum of HCl-soluble Fe and pyritic-Fe (3.0 to 4.5 wt %). The amount of reactive iron in recent sediments may often be overestimated, because dissolution of Fe-bearing silicates occurs already when very low concentrations of hydrochloric or acetic acids (Fig. 7.3) or dithionite and oxalate extractants are used (ROBBINS et al., 1984; CANFIELD, 1989a).

7.4.2.1 Bulk sediment composition

The depth distributions of total iron, sulphur and organic carbon contents, and of the isotopic composition of sulphur and organic carbon of sediments in core P3 at station K4 are shown in Figure 7.4. The different lithological units are indicated. In this core sediments from unit 2 are anomalously thick due to slumping and mixing (BARMAWIDJAJA et al., 1989). Therefore, results from this unit will not be discussed in detail.

Depth profiles of iron and sulphur are remarkably similar. Samples from depths of 348-350 cm and 742-748 cm are depleted in both Fe and S due to the presence of dolomite-rich layers (MIDDELBURG et al., 1990; chapter 6). In the youngest unit (1) organic carbon, $\delta^{13}C$ and $\delta^{34}S$ vary from 2 to 5 wt %, -25 to -20 $^{o}/_{oo}$, -24 to -17 $^{o}/_{oo}$, respectively. Iron sulphide forms at the surface or in the top layer of the sediment, because the amount of sulphur does not increase and its isotopic composition does not become heavier with depth in unit I. The difference between the sulphur isotopic composition of the bulk sediment and sea-water sulphate (+ 20 $^{o}/_{oo}$), i.e. the apparent isotope fractionation, varies from -37 to -44 $^{o}/_{oo}$. The apparent sulphur isotope fractionation of about -40 $^{o}/_{oo}$ falls in the middle of the wide range of $\Delta^{34}S$ values reported in the literature for modern and ancient sediments (GOLDHABER and KAPLAN, 1974; CHAMBERS, 1982).

Although the fresh-water sediments from unit 3 have about the same organic carbon content as sediments from the other two units, they have strongly deviating organic carbon ($\delta^{13}C \approx -29$ $^{o}/_{oo}$) and sulphur ($\delta^{34}S \approx +15$ $^{o}/_{oo}$) isotope characteristics and are richer in sulphur and iron (Figure 7.4). It is striking that sediments from unit 3 were deposited in sulphate-poor water and yet are the most enriched in sulphur.

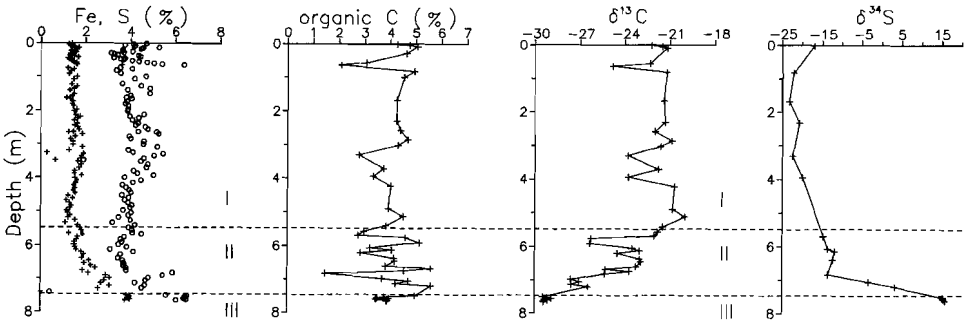

Figure 7.4. The distribution of iron (dots) , sulphur (crosses), organic carbon, $\delta^{13}C_{org}$ and $\delta^{34}S$ versus depth in core K4P3. The three lithological units are indicated: (I) marine, (II) transitional and (III) freshwater sediments.

7.4.2.2 Distribution of sediment characteristics

The distributions of organic carbon, of $\delta^{13}C_{org}$ and of various forms of solid-phase sulphur and iron are shown versus depth for stations K3, K4 and K11 (Figure 7.5). For station K4 the different units are indicated, for the other stations only sediments from unit 1 were recovered. Presented in Figure 7.5 are the cumulative amounts of iron and sulphur for the various fractions. The distance between the curves reflects the amount of that fraction present.

Both the amount and the speciation of solid-phase sulphur are constant from the sediment surface down to sediments from unit 2. The two major sulphur pools in Kau Bay sediments are AVS-S (30-40 %) and pyrite-S (60-70 %). It seems that major amounts of acid volatile sulphur compounds are accumulating in Kau Bay.

Solid phase iron is partitioned into "non-reactive" Fe, AVS-Fe, pyrite-Fe and "potentially reactive" Fe (i.e. 6 N HCl soluble Fe minus AVS-Fe). As in the case of sulphur, both the amount and the speciation of solid-phase Fe are constant from the sediment surface down to sediments from unit 2. The two major Fe fractions are the "non-reactive" and "potentially reactive" fraction that each account for about 35 % of the total iron. The AVS-Fe and pyrite-Fe fractions each comprise about 15 % of the total iron. Figures 7.4 and 7.5 show that for sediments from unit 1 depletions in organic carbon are

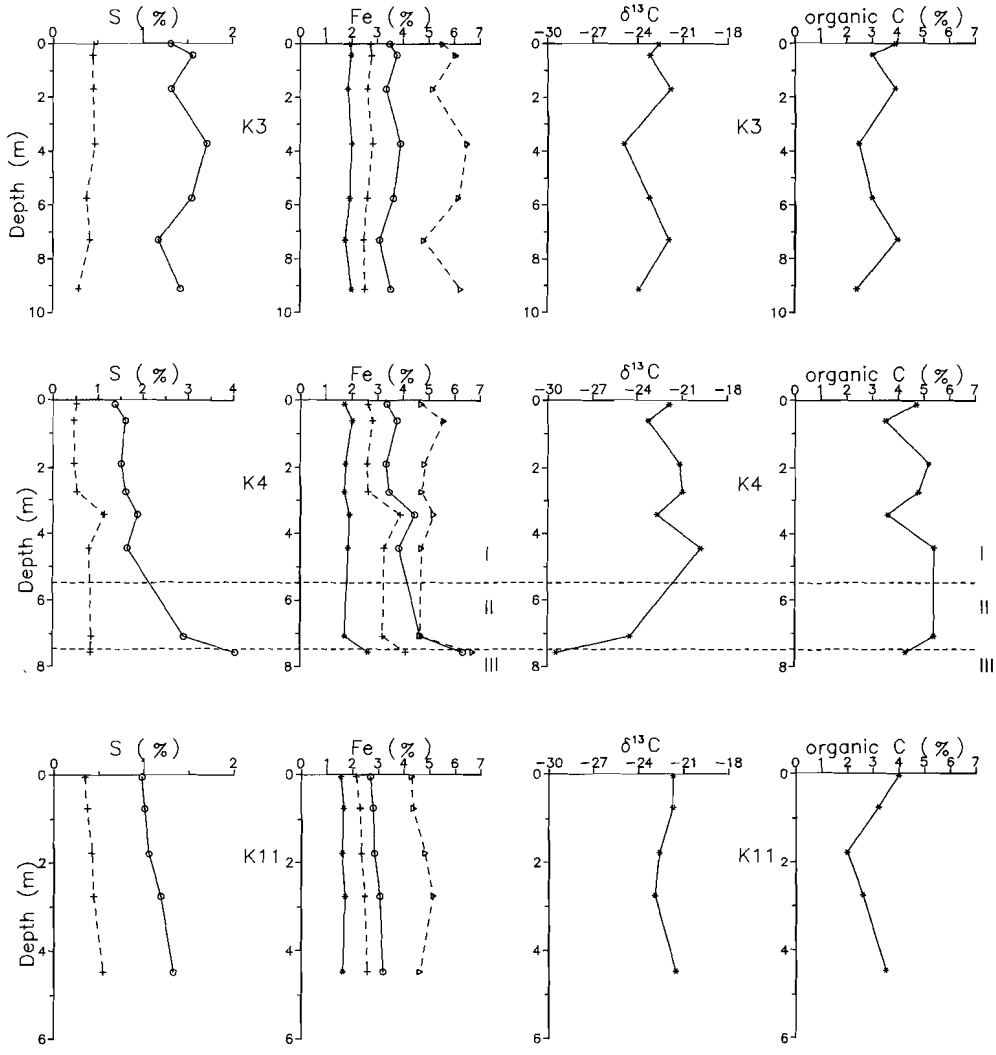

Figure 7.5. The depth distribution of organic carbon, $\delta^{13}C_{org}$ and of various forms of sulphur and iron in sediments from stations K3, K4 and K11. The various pools of sulphur and iron are shown cumulatively. Sulphur: crosses, AVS-S and dots; AVS-S + pyrite-S. Iron: stars, "non-reactive " (i.e. HF and residual Fe); crosses, "non-reactive"+ AVS-Fe; dots, "non-reactive" + AVS-Fe + pyrite Fe; triangles, "non-reactive" + AVS-Fe + pyrite Fe + "potentially reactive iron". For definition of these fractions see text. The lithological units are indicated.

generally accompanied by depletions in its isotopic composition and by enrichments in the total content of iron and sulphur.

Sediments from units 2 and 3 have higher pyrite and lower "potentially reactive" iron contents than those from unit 1 (Figure 7.5). It appears therefore that pyrite forms at the expense of "potentially reactive" iron.

7.5 DISCUSSION

Concentrations of reduced sulphur and organic carbon buried in sediments have been shown to be only a fraction of the total amount produced in or delivered to the sediments: 2 to 75 % for S (JØRGENSEN, 1977, 1982; BERNER and WESTRICH, 1985; CHANTON et al., 1987a; SWIDER AND MACKIN, 1989) and 0.5 to 80 % for organic C (HENRICHS and REEBURGH, 1987; CANFIELD, 1989b). Before interpreting the concentration of sulphur and organic carbon in Kau Bay sediment, it is instructive to determine these fractions by using sedimentary budget calculations.

For S the simplest mass balance approach is to balance the burial of total S against the sources of S which include sulphate, supplied by diffusion and pore water burial, and detrital S. Mathematically:

$$\Phi D_s \frac{\delta SO_4}{\delta x} + \Phi \omega \rho_{sed} SO_{4o} + (1-\Phi)\omega \rho_{sed} S_{detrital} = (1-\Phi)\omega \rho_{sed} S_{total}$$

where Φ is the sediment porosity, D_s is the sediment diffusion coefficient for sulphate, $\delta SO_4/\delta x$ is the sulphate concentration gradient, ω is the sediment accumulation rate, SO_{4o} is the bottom water sulphate concentration, ρ_{sed} is the density of solids, $S_{detrital}$ is solid phase sulphur input and S_{total} is the sulphur concentration that is buried. For detrital S a value of 1 wt% S of the organic matter fraction of carbohydrate composition is assumed (e.g. see CHANTON et al., 1987a). The sulphide retention is calculated by dividing the observed burial by the expected burial of sulphur. The sulphur mass balance is summarized in Table 7.3.

For organic carbon the degree of recycling is expressed in the organic carbon burial efficiency. Following CANFIELD (1989b) the fraction of organic carbon that becomes buried is calculated by dividing the organic carbon burial flux by the delivery flux. The delivery flux is assumed to equal the sum of the burial flux and the depth-integrated rates of organic carbon oxidation by sulphate reduction. The depth-integrated rates of organic carbon oxidation are calculated from the depth integrated sulphate reduction rates. The organic carbon balance is summarized in Table 7.4.

TABLE 7.3. Sulphur mass balance

	K3	K4	K11
(1) supply by diffusion ($\Phi D\ \delta SO_4/\delta x$: $\mu mol/cm^2yr$)	82.0	24.4	36.6
(2) supply by burial (ΦwSO_{4o} : $\mu mol/cm^2yr$)	13.1	1.7	1.9
(3) integrated sulphate reduction rate[a] ($\mu mol/cm^2yr$)	95.1	26.0	38.5
(4) iron sulphide burial expected (wt %)[b]	0.97	2.25	2.79
(5) detrital S (wt %)	0.08	0.11	0.08
(6) total S burial expected (wt %)	1.05	2.26	2.87
(7) total S burial observed (wt %)	1.26	1.48	1.02
(8) S retention (%)	120	65	36
(9) openness to sulphate diffusion (%)[c]	86	94	95

a: integrated rate = $\Phi D\delta SO_4/\delta x + \Phi wSO_{4o}$
b: S burial = (integrated rate * 32)/($p_{sed}(1-\Phi)$*w)
c: openness = dif. flux/(dif. + burial flux)

Both the sulphide retention and the burial efficiency of organic matter of Kau Bay sediments are relatively high compared to reported data (CHANTON et al., 1987a; HENRICHS and REEBURGH, 1987). It seems that the burial efficiency and sulphide retention data are correlated and vary systematically with the sediment accumulation rate, water depth (i.e. oxygen content of bottom water) and hence degree of bioturbation (Table 7.5). Such a correlation between the burial efficiency and sulphide retention has been observed before by BERNER and WESTRICH (1985) and is consistent with

TABLE 7.4 Organic carbon burial

	K3	K4	K11
sediment burial rate (g/cm^2yr)	0.305	0.0369	0.0442
mean organic carbon (wt %)	3.24	4.25	3.06
carbon burial ($g/cm^2yr * 10^{-4}$)[a]	98.8	15.7	13.5
carbon consumed by sulphate reduction ($g/cm^2yr * 10^{-4}$)[b]	22.8	6.23	9.24
burial efficiency (%)	81	72	59

a: sediment burial rate * organic carbon
b: integrated sulph. reduc. rate * 2 * 12

the correlation between reduced sulphur and organic carbon found in normal marine sediments (BERNER, 1984). On the basis of data presented in Table 7.5 it is not possible to draw conclusions regarding the influence of the oxygen content of bottom waters or bioturbation on the preservation of organic carbon and reduced sulphur compounds since these changes coincide with changes in the sedimentation rate.

7.5.1 Organic matter

Both the amount and type of organic matter are important factors that may control the rate of sulphate reduction, and hence the amount of iron sulphide formed. The fraction of organic matter that becomes buried is an extensively modified version of the organic matter supplied and does not necessarily have the same characteristics because of preferential preservation or decomposition (MIDDELBURG, 1989; TEGELAAR et al, 1989; see chapter 5). For instance, in Kau Bay the decomposing organic matter has a molar C/N ratio of 7.4 which is much lower than the molar C/N ratio of bulk organic matter (20 to 25).

Organic matter is often considered to be a composite of residual

TABLE 7.5 Sulphide retention and organic carbon burial

	K3	K4	K11
S retention (%)	117	65	36
organic carbon burial efficiency (%)	81	72	59
sedimentation rate (cm/yr)	0.6	0.071	0.085
water-depth (m)	457	414	260
Oxygen (μmol/l; 1985)	8	50	55
Oxygen (μmol/l; 1930)	H_2S	H_2S	12

materials derived from marine and terrestrial sources. Differentiation of marine and terrestrial organic matter inputs can be based on microscopic, elemental, isotopic and molecular biomarker parameters. It should be realized that each method has its restrictions due to factors such as the representativity of the small fraction of total organic matter that is analysed and the choice of the number and composition of the end-members (KENNICUTT et al., 1987; PRAHL and MUEHLHAUSEN, 1989). In this study we will use the $\delta^{13}C$ of organic matter to characterize its source and distribution. In the interpretation it is assumed that no diagenetic changes in the $\delta^{13}C$ of organic carbon occur although this has been reported (SPIKER and HATCHER, 1984; SCHOLTEN and KREULEN, 1990). This may bias our interpretation in favour of terrestrial organic carbon. Furthermore, the contribution of organic matter derived from bacterial sources is assumed to be quantitatively unimportant.

In figure 7.6, the isotopic composition of organic carbon is plotted versus its concentration. The marine sediments are readily distinguishable from the underlying fresh-water sediments on the basis of the $\delta^{13}C$ of organic matter. The fresh-water sediments are characterized by $\delta^{13}C$ values of -28 to -30 $^{o}/_{oo}$ and show a tendency to lower $\delta^{13}C$ values with increasing organic carbon concentrations. This trend may be due to mixture of terrigenous organic matter with $\delta^{13}C$ of -28 and organic matter derived from fresh-water plankton (-29 to -31 $^{o}/_{oo}$; DEGENS, 1969). However, due to the small difference in end-member compositions (which possibly overlap), the scatter

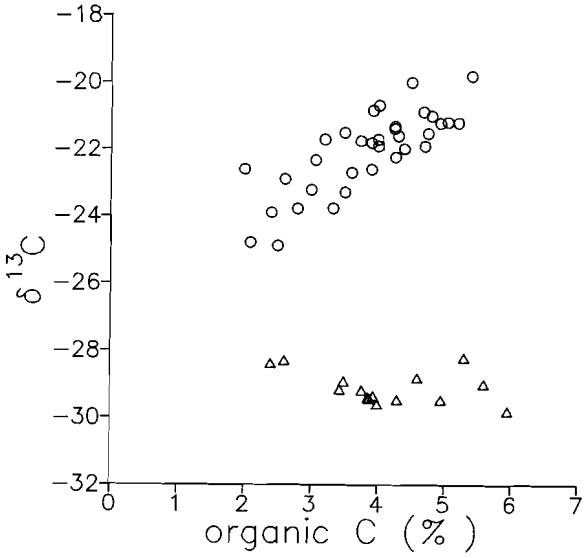

Figure 7.6. Plot of organic carbon isotopic composition versus concentration of organic carbon. Dots and triangles represent data from the marine and freshwater sediments respectively.

in the data and the limited number of samples, it is not possible to constrain this trend better.

The marine sediments are characterized by $\delta^{13}C$ values of -25 to -19 °/$_{oo}$. There is a clear correlation between the amount and isotopic composition of organic carbon (Fig. 7.6). This trend can be interpreted as arising from a mixture of terrigenous organic matter ($\delta^{13}C$ = -26 °/$_{oo}$) and organic matter derived from marine plankton ($\delta^{13}C$ = -21 to -18 °/$_{oo}$; DEGENS, 1969). The terrestrial $\delta^{13}C$ end-member of about -26 °/$_{oo}$ is consistent with the $\delta^{13}C_{org}$ of a wood fragment recovered from station K3 (-25.6 °/$_{oo}$). An obvious interpretation of this relationship is that the quantity of marine organic matter is directly proportional to the quantity of total organic matter. Accordingly, the amount of total organic matter preserved may be used as an indication for paleoproductivity. The good preservation of marine organic carbon is consistent with the high burial estimates presented above (Table 7.5).

Finally, it seems that the $\delta^{13}C_{org}$ of the terrigenous end-member in the fresh-water sediments ($\delta^{13}C \approx$ -28 °/$_{oo}$) is significantly different from that in the marine sediments ($\delta^{13}C \approx$ -26 °/$_{oo}$). This difference in isotopic composition is probably related to a difference in organic matter sources. The terrigenous end-member during the marine stage includes land-derived and mangrove-derived organic matter, whereas during the fresh-water stage mangrove-derived organic matter was negligible since there was no mangrove vegetation at that time (BARMAWIDJAJA et al., 1989).

7.5.2 Factors limiting pyrite formation

The major steps involved in the formation of sedimentary pyrite have been summarized by various researchers (e.g. BERNER, 1970a, 1984; GOLDHABER and KAPLAN, 1974, 1975, 1980; MORSE et al., 1987) and include the reduction of sulphate to hydrogen sulphide, followed by the reaction of hydrogen sulphide with reactive iron minerals to form iron sulphide compounds and subsequent reaction of these metastable iron sulphide compounds with elemental sulphur or polysulphides (hereafter zerovalent sulphur) to form pyrite. Accordingly the amount of pyrite that is formed in a sediment can be limited by: **(1)** the concentration of sulphate, **(2)** the amount and reactivity of organic matter, **(3)** the concentration and reactivity of iron minerals, **(4)** the production of zerovalent sulphur and **(5)** the period of time during which these reactions take place.

In order to reveal the possible limiting factors for pyrite formation in Kau Bay it is necessary to determine where the formation takes place. The majority of pyrite is formed at, above, or close to, the sediment-water interface, because the speciation, total concentration and isotopic composition of sulphur are very constant from the sediment-water interface down to the sediments from unit 2 (Figs. 7.4 and 7.5). Thus, below the top layer, very little S is added to the sediment or transformed into another form during diagenesis. This conclusion concurs with the general observation that pyrite formation is virtually completed very close to the sediment-water interface (KAPLAN et al., 1963; HARTMANN and NIELSEN, 1969; BERNER, 1970a, 1984; GOLDHABER and KAPLAN, 1974, 1980; LEIN et al., 1982; BOESEN and POSTMA, 1988).

For ancient semi-euxinic and euxinic environments it is well established that reactive iron is generally the limiting factor for the amount of iron sulphide formed (BERNER, 1984; RAISWELL and BERNER, 1985). There are several indications that this may also apply to the recent marine semi-euxinic sediments of Kau Bay:

Firstly, the availability of sulphate is not a limiting factor for pyrite formation because there is still abundant sulphate in the pore water at depths where pyrite formation is virtually completed. Moreover, the Kau Bay sediments are very open to sulphate diffusion (> 86 %; Table 7.3) and the $\delta^{34}S$ values are indicative of sulphate reduction in an infinite reservoir. Secondly, pyrite formation in organic-rich sediments is not limited by reactive organic carbon. Although iron sulphide formation is almost complete in the top layers of the sediment, the decomposition of organic matter by sulphate reduction is continuing to greater depths (Fig. 7.2; see also chapter 4). Moreover, after the pore water sulphate has been used up

completely, organic matter is still being decomposed by methane-generating bacteria. This indicates that there is abundant reactive organic matter available. Thirdly, the amount of sulphide-bound-iron does not increase with depth, although sulphate reduction, hence sulphide production, continues to greater depth. Therefore, all iron available for iron sulphide formation reacts in the top layer of the sediment and very little additional iron is sulphidized during diagenesis. Finally, if iron is not limiting one would expect an increase in pore water iron concentrations or the formation of authigenic Fe-bearing carbonates and phosphates in the methane-generating zone. However, pore-water data show that dissolved iron is very low at all depths investigated and we also have no evidence for the formation of Fe-bearing carbonates or phosphates. These points together provide a strong argument for an iron control on the amount of iron sulphide minerals formed.

Whereas reactive iron constrains the amount of iron that is sulphidized, it does not control the incomplete conversion of metastable iron sulphides to pyrite. The incomplete conversion of AVS-compounds to pyrite as found by extraction (Fig. 7.5) is not an analytical artefact since bulk sediment determinations confirm the presence of high concentrations of AVS-compounds (Fig. 7.7).

The transformation of iron monosulphide to pyrite occurs through the addition of sulphur and not by the removal of iron (e.g. VOLKOV, 1961; BERNER, 1970a; RICKARD, 1975; SWIDER and MACKIN, 1989):

$$\text{"FeS"} + S \dashrightarrow FeS_2 \qquad (R1)$$

In the presence of zerovalent sulphur there is complete transformation of FeS to pyrite on a time scale of years (e.g., BERNER, 1970a; BERNER et al., 1979). The incomplete transformation of FeS to pyrite in Kau Bay sediments therefore seems to be due to a shortage of zerovalent sulphur during pyrite formation. Zerovalent sulphur may form as a result of the oxidation of H_2S and FeS by oxidants such as O_2, NO_3, MnO_2 and FeOOH. Accordingly the amount of zerovalent sulphur that is formed depends on **(1)** the amount of sulphides available to be oxidized or **(2)** the amount of oxidants supplied by diffusion or bioturbational processes.

It has been suggested (BERNER, 1970b, 1974a; BERNER et al., 1979; BOESEN and POSTMA, 1988) that the lack of zerovalent sulphur is due to exhaustion of H_2S from the interstitial water as a consequence of low interstitial water sulphate concentrations. The limited amount of sulphate was attributed to a combination of bottom waters with a low salinity (BERNER, 1970b; BOESEN and POSTMA, 1988) and high sedimentation

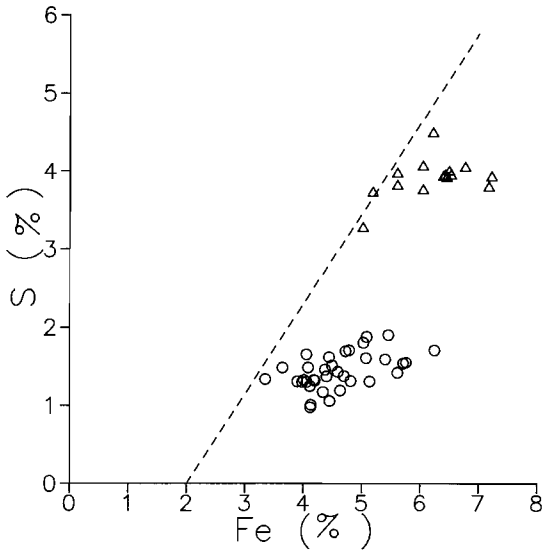

Figure 7.7. Plot of iron versus sulphur concentration. Symbols as in Fig. 7.6. The dashed line represents the ideal pyrite stoichiometry assuming a "non-reactive" iron content of 2 wt% (cf Fig. 7.5).

rates (BERNER, 1974a; BERNER et al., 1979). However, below the top layer of sediments in Kau Bay, there is no further transformation of FeS to pyrite although dissolved sulphate is present down to depths of 200 cm. The few measurements available for pore-water sulphide show concentrations of the order of 1 mM. This suggests that for Kau Bay sediments the limited conversion of FeS to pyrite is due to a lack of oxidants rather than to the availability of sulphate or hydrogen sulphide.

Laboratory and theoretical work (BERNER, 1970a; RICKARD, 1975) and anoxic incubations (WESTRICH, 1983; SWIDER and MACKIN, 1989) have shown that the introduction of oxidants is mandatory for the transformation of FeS to pyrite. For normal marine sediments zerovalent sulphur is not limiting since it is readily produced by the oxidation of FeS or H_2S by dissolved (oxygen and nitrate) and solid-phase (manganese and iron hydroxides) oxidants. However, for euxinic sediments there is no supply of dissolved oxidants by diffusion. Accordingly the only oxidants available are Fe and Mn hydroxides:

$$MnO_2 + HS^- + H_2O \text{ ----> } Mn^{2+} + S^\circ + 3\ OH^- \qquad (R2)$$

$$2\ FeOOH + 3\ HS^- \text{ -----> } 2\ FeS + S^\circ + H_2O + 3\ OH^-. \qquad (R3)$$

The FeS and S° so formed will react and produce pyrite according to reaction (R1). Since Fe-hydroxides are over 15 times more abundant than Mn-oxides the overall reaction can be approximated by:

$$2\ FeOOH + 3\ HS^- \text{-----}> FeS + FeS_2 + H_2O + 3\ OH^- \quad (R4)$$

and nearly equal amounts of FeS and FeS_2 should be formed.

For the recent marine sediments of Kau Bay there appears to be no major oxidant other than ironhydroxides since the average molar FeS/FeS_2 ratio is about 1.1 (Table 7.2). This is not a phenomenon unique to Kau Bay, but may also apply to other euxinic sediments. For the anoxic sediments of the Orca Basin and Skan Bay MORSE and CORNWELL (1987) reported a FeS/FeS_2 ratio close to 1. Similarly, large amounts of AVS have been found to accumulate in the anoxic sediments of Black Hole (Connecticut, USA; WESTRICH, 1983) and the Eastern Scheldt (The Netherlands; OENEMA, 1990). In the sediments of the Eastern Scheldt high concentrations of AVS are found at depths exceeding 150 cm without significant transformation into pyrite. This was attributed to the low concentrations and formation rate of zerovalent sulphur species (OENEMA, 1990). Recent determinations of sulphur speciation in various anoxic environments have shown that the concentrations of elemental sulphur and polysulphides species are very low and therefore may be limiting in pyrite formation (LUTHER et al., 1986; THODE-ANDERSEN and JØRGENSEN, 1989; HENNEKE et al., 1991).

So far it has been assumed that reactions are sufficiently fast to reach completion before burial. This assumption may perhaps not be strictly valid for the sulphidization of slowly reacting Fe-bearing minerals and for the conversion of AVS to pyrite. The time available for reactions is mainly determined by the sediment accumulation rate. In rapidly accumulating sediments reactive iron minerals quickly move through the zone containing sulphidic pore waters. Moreover, this zone is relatively thin due to high rates of sulphate reduction (Figure 7.2; BERNER, 1978). Accordingly, the time available for reaction between H_2S and Fe-compounds is relatively short. Maximum preservation of reactive Fe-compounds, i.e. minimal sulphidization is, therefore, favoured by rapid sediment accumulation.

Relatively little is known about the dissolution kinetics of iron-bearing minerals under anoxic conditions (POSTMA and BROCKENHUUS-SCHACK, 1987; CANFIELD and BERNER, 1987; CANFIELD, 1989a). Minerals such as ferrihydrite, lepidocrocite, goethite and hematite are reactive on a laboratory time-scale (CANFIELD, 1989a), whereas iron-silicates and minerals such as magnetite and ilmenite react more slowly. For instance the "half-life" for magnetite dissolution in anoxic marine sediments ranges from 50 to 1000 years (CANFIELD and BERNER, 1987), which is very similar to its residence time in the sulphate reduction zone (80 to 3000 years for Kau Bay). Hence, due to rapid deposition there may be insufficient time to complete reactions and excess potentially reactive iron may be

buried in Kau Bay (cf. Figure 7.5).

The incomplete conversion of AVS to pyrite is another consequence of high sediment accumulation rates. In rapidly deposited sediments there may be a shortage of elemental sulphur due to short exposure to oxidizing conditions near the sediment-water interface or limited availability of sulphate and sulphide (BERNER, 1974a; BERNER et al., 1979). The incomplete conversion of AVS to pyrite as observed in Kau Bay may therefore be related to the high sediment accumulation rate. Other environments with appreciable AVS-compounds at depth are also characterized by high sedimentation rates (Black Hole, WESTRICH (1983); Eastern Scheldt, OENEMA (1990)). In fact, GOLDHABER and KAPLAN (1975) have shown that there is a fair correlation between the amount of sulphur present as AVS-S and the sedimentation rate.

Finally, sediments from unit 2 and 3 have higher pyrite and lower "potentially reactive" iron contents than those from unit 1 (Figure 7.5; Table 7.2). It appears therefore that pyrite has formed at the expense of "potentially reactive" iron. This additional pyrite may have formed either because of the longer reaction time for these older sediments, or because of historical changes in the degree of bottom water oxygenation, the sedimentation rate or the reactive iron input. We have no data to support or reject any of these possibilities.

7.5.3 Iron-carbon coupling

Various researchers (BAAS BECKING and MOORE, 1959; BERNER, 1970a, 1984; RAISWELL and BERNER, 1985, RAISWELL and AL-BIATTY, 1989) have shown that there may be a good correlation between organic carbon and reactive iron. This relation between organic carbon and iron may be either a diagenetic or a depositional feature.

The covariance of iron with total organic matter and type of organic matter (as revealed by $\delta^{13}C_{org}$ values) is shown in Figure 7.8. Since reactive iron forms a constant amount of total quantity of iron (Figure 7.5, Table 7.2), similar trends were obtained for plots of reactive iron versus organic carbon and $\delta^{13}C_{org}$ (not shown). Figure 7.8a shows that there is a negative correlation between iron and total organic carbon both for the marine and for the fresh-water sediments, but not for the two sediments together. The amount of iron is, however, strongly positively correlated with the amount of terrigenous organic carbon as revealed by $\delta^{13}C_{org}$ values (Fig. 7.8b). These correlations are not due to fluctuations in the carbonate content.

This coupling between organic carbon and iron is interpreted to be a depositional feature. Firstly, higher relative contributions of terrestrial

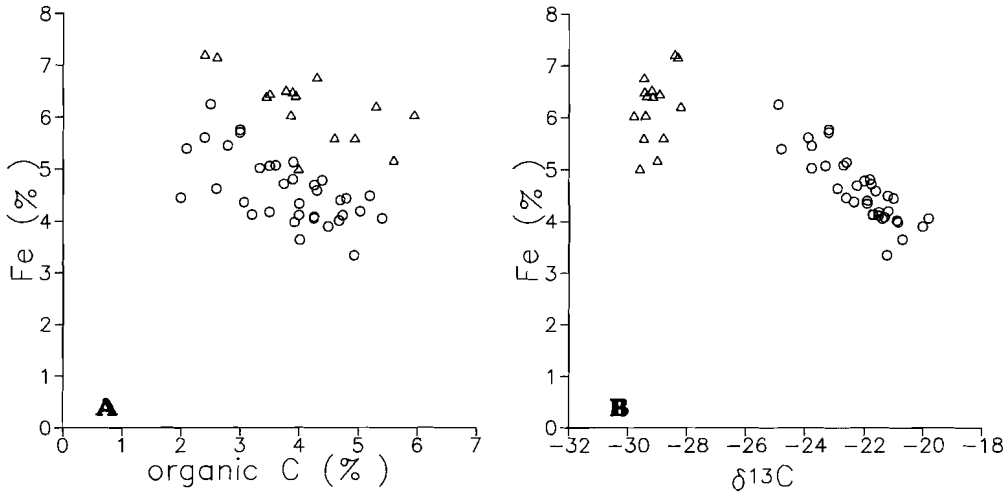

*Figure 7.8. **A.** Iron versus organic carbon; **B.** Iron versus isotopic composition of organic carbon. Dots and triangles represent data from the marine and freshwater sediments respectively.*

organic carbon are accompanied by higher concentrations of iron and thus larger relative contributions of continental debris. This suggests that the coupling between terrestrial organic carbon and iron may be explained by their common provenance and depositional histories. Secondly, in an iron-limited system the concentration of dissolved iron in the pore water is very low and the diagenetic mobility of iron is expected to be minimal. Therefore, iron enrichments are not likely to be formed by diagenetic processes.

The negative correlation between iron and total organic carbon as observed in Kau Bay (Fig. 7.8) may seem to contradict the positive correlations which have been observed for Long Island Sound sediments (BERNER, 1970a, 1984), for the Jet Rock formation (RAISWELL and BERNER, 1985) and for Cambrian-Silurian normal marine sediments (RAISWELL and AL-BIATTY, 1989). It should however be realized that plots of iron versus total organic carbon may show either positive, negative or even no correlation for a coupled deposition of terrestrial organic carbon and iron. The type of correlation is dependent on the relationship between terrestrial organic matter and total organic matter. For instance, if the amount of terrestrial organic matter correlates with the amount of total organic matter, then iron would show a positive correlation with total

organic matter. Alternatively, if marine organic matter correlates with total organic matter, iron would show a negative correlation with total organic matter. The sediments of Kau Bay are an example of the latter type. It will be clear that future studies on Fe-C coupling should consider not only the amount of organic matter, but also the type of organic matter.

7.5.4 Sulphidization of fresh-water sediments

Although the fresh-water sediments in Kau Bay were deposited in sulphate-poor water, they are enriched in sulphur compared to the overlying marine sediments (Figures 7.4, 7.9). This sulphur enrichment is interpreted to be a diagenetic feature related to the diffusion of dissolved sulphide and sulphate from the marine sediments into the fresh-water sediments.

During the deposition of the fresh-water sediment the little amount of sulphate available was rapidly exhausted and only small amounts of sulphides were formed. After the re-establishment of marine conditions abundant sulphate could diffuse into the fresh-water sediments and was used by sulphate reducing bacteria. The hydrogen sulphide produced in the marine sediments first reacted with reactive iron compounds and after reactive iron had become limiting, it started to diffuse into the underlying fresh-water sediments. Since almost all the sulphide that precipitated in the fresh-water sediment was delivered by diffusion of sea water sulphate through the sediment-water interface, the final $\delta^{34}S$ values of these sulphides should be close to the $\delta^{34}S$ values of initial sulphate diffusing into the sediments (e.g. CHAMBERS and TRUDINGER, 1978). The $\delta^{34}S$ values of fresh-water sediments (+ 15 $^{o}/_{oo}$) are consistent with the $\delta^{34}S$ values expected if all the sulphate delivered is quantitatively reduced to sulphide (about + 20 $^{o}/_{oo}$) and are much heavier than the $\delta^{34}S$ values of overlying marine sediments (-24 to -17 $^{o}/_{oo}$).

The difference between the values found (+ 15 $^{o}/_{oo}$) and expected (+ 20 $^{o}/_{oo}$) can be explained by a number of factors. Firstly, the $\delta^{34}S$ value of sulphate diffusing into Kau Bay sediments is probably lower than the $\delta^{34}S$ of sea water (+20 $^{o}/_{oo}$) as a consequence of preferential diffusion of ^{32}S (JØRGENSEN, 1979; CHANTON et al., 1987b). Secondly, part of the sulphide may originate from fresh-water sulphate which has an unknown $\delta^{34}S$ value. Thirdly, the isotopic composition of the residual sulphur pool (about 0.1 wt %) is not known. Fourthly, isotope exchange reactions may have weakened the isotope signal (FOSSING and JØRGENSEN, 1990).

The closed system nature of the reaction between hydrogen sulphide and iron in the fresh-water sediments is also supported by the presence of almost equal amounts of FeS and pyrite (Figs. 7.5, 7.7). The reaction of

sulphides with iron oxide in the absence of other oxidants according to reaction R4, should result in equal amounts of FeS and pyrite.

The diffusion of sulphate and sulphide and their quantitative fixation in iron sulphide compounds may explain the sulphidization of the fresh-water sediments, but it does not explain why the fresh-water sediments are richer in S than the marine sediments. The sulphur enrichment of the fresh-water sediments is a direct consequence of the abundance of reactive iron in these sediments (Figs. 7.4 and 7.8).

Finally, similar observations have been made for sediments in the Baltic and Black Seas (see chapter 8). In the Baltic Sea the fresh-water sediments underlying the marine muds are presently sulphidized by downward H_2S diffusion (BOESEN and POSTMA, 1988). This sulphidization process could be described quantitatively as an iron-limited system in which in situ sulphidization of iron in the fresh-water sediments occurs as a response to the downward diffusion of H_2S. For the Black Sea the situation is more complex because more than one transition exists and the marine sediments overlie brackish-water sediments rather than fresh-water sediments (BERNER, 1970b, 1974a). However, there are still various similarities such as the presence of major amounts of FeS in the brackish-water sediments (BERNER, 1970b, 1974a) and the sulphur isotope enrichment of these brackish-water sediments (VINOGRADOV et al., 1962; Figure 8.1). Accordingly, these similarities indicate that in iron-limited euxinic sediments diffusion of hydrogen sulphide may result in the accumulation of large amounts of iron sulphide compounds in the absence of sulphate or organic matter. This may have major implications for the interpretation of C/S ratios in the sedimentary record.

7.5.5 Organic-carbon/sulphur/iron relationships and sedimentary environments

The relationships between organic carbon, sulphur and iron have been used to characterize the paleoenvironment of ancient rocks. The relationships in the form of sulphur versus organic carbon plots have proved very powerful for distinguishing between sediments deposited in oxygenated marine, euxinic marine and fresh-water environments (BERNER and RAISWELL, 1983, 1984; RAISWELL and BERNER, 1985). The relationships can also be used to recognize the degree of bottom water oxygenation on the basis of the degree of pyritization, which is the ratio of pyritic Fe to pyritic Fe + HCl-soluble Fe (RAISWELL et al., 1988). These methods have not been tested extensively on recent euxinic sediments because there are only a few sites where anoxic sediments occur.

7.5.5.1 C/S-method

Constraints on the C/S method originate from the factors which determine how much iron sulphide can form in a sediment. In normal marine sediments there is a good correlation between organic carbon and pyrite sulphur with a constant C/S ratio of about 2.8 (BERNER, 1970a, 1984; GOLDHABER and KAPLAN, 1974). According to BERNER (1984) the origin of the constant C/S ratio in normal marine sediments is that constant fractions of organic carbon and reduced sulphur are preserved in the sediment and that labile organic matter limits the amount of iron sulphide formed. For fresh-water sediments the availability of sulphate limits the amount of iron sulphide formed and the organic-carbon/reduced-sulphur ratio is much higher than that in normal marine sediments (BERNER and RAISWELL, 1984). In euxinic sediments reactive iron determines the amount of iron sulphide formed. There should consequently be no relation between organic carbon and reduced sulphur. Organic-carbon/reduced-sulphur ratios may be either lower or higher than that in normal marine sediments. The ratio will depend on the relation between organic carbon and iron.

The sulphur versus organic carbon plot for Kau Bay sediments is shown in Fig 7.9. For comparison the trend for normal marine sediments (BERNER, 1984) is also included. The fresh-water sediments in Kau Bay show no relation between organic carbon and sulphur and are highly enriched in sulphur compared to normal marine sediments. On the basis of these data alone the fresh-water sediments in Kau Bay could be interpreted to be euxinic marine sediments. Accordingly, before applying the C/S method to alternating marine and fresh-water sediments one should be certain that diffusion of hydrogen sulphide has not resulted in sulphur enrichment. This enrichment of sulphur may occur in the absence of sulphate and organic matter provided there is abundant reactive iron.

The marine sediments in Kau Bay show no relation between organic carbon and sulphur, which is in good agreement with the expected decoupling of organic carbon and sulphur in euxinic sediments (RAISWELL and BERNER, 1985). A separation into syngenetic and diagenetic iron sulphide formation following the reasoning of LEVENTHAL (1983) would suggest that all iron sulphides are formed syngenetically. This is in agreement with the very constant depth distribution of the speciation, concentration and isotopic composition of sulphur (Figs. 7.4, 7.5). It will be clear that a fossil equivalent of the Kau Bay marine sediments can be recognized using the C/S method.

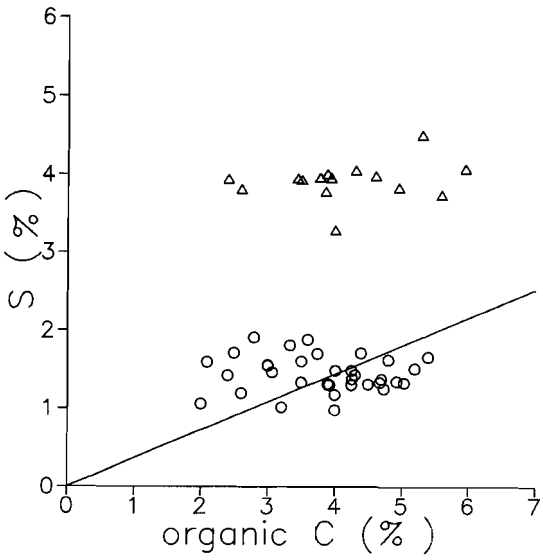

Figure 7.9. Relation between sulphur and organic carbon in Kau Bay sediments. Symbols as in Fig. 7.6. The full line represents the trend for normal marine sediments (slope = 0.36).

7.5.5.2 DOP

It has been suggested that degree of pyritization values are more effective than C/S ratios for discriminating normal marine from semi-euxinic and euxinic sediments (RAISWELL et al., 1988). These authors have shown that normal marine sediments have DOP values < 0.42 and that semi-euxinic and euxinic sediments have DOP values varying from 0.46 to 0.8 and from 0.55 to 0.93, respectively. However, the dataset on which this method is based includes only ancient sediments. If DOP is to be a reliable criterion for determining the degree of bottom-water oxygenation of sedimentary rocks, it should be tested in recent semi-euxinic and euxinic settings. It is particularly important to determine whether differences in sedimentation rates have a major or minor influence on DOP values.

For Kau Bay sediments DOP values are obtained by:

$$DOP = \frac{\text{Pyritic Fe}}{\text{Pyritic Fe + HCl-soluble Fe}}$$

where HCl-soluble Fe refers to iron which dissolves in 6 N HCl at room temperature for hours. For sediments rich in acid-volatile sulphur compounds BOESEN and POSTMA (1988) introduced the degree of sulphidization (DOS) which is here calculated as:

$$DOS = \frac{\text{Pyritic Fe + AVS-Fe}}{\text{Pyritic Fe + HCl-soluble Fe.}}$$

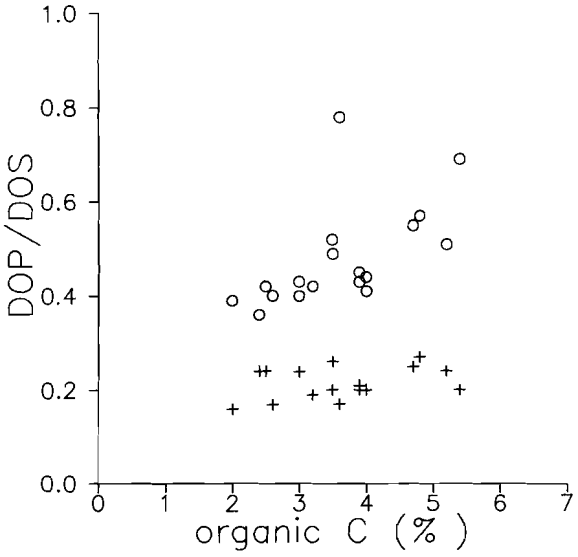

Figure 7.10. Plot of DOP (crosses) and DOS (dots) values versus organic carbon in marine sediments of Kau Bay.

For sediments low in AVS-Fe, DOP and DOS give similar results. The recent marine sediments of Kau Bay have DOP and DOS values that range from 0.16 to 0.27 and 0.36 to 0.78 respectively. Figure 7.10 shows a plot of DOP and DOS versus organic carbon. There is no simple relationship between organic carbon and DOP/DOS. DOP values are constant (0.22±0.03), whereas DOS values show a weak correlation ($r=0.6$; $N=18$) with organic carbon. DOS values for recent semi-euxinic sediments of Kau Bay (0.36-0.78) agree very well with DOP values of ancient semi-euxinic sediments (0.46 to 0.8; RAISWELL et al., 1988). Hence, data from Kau Bay provide a useful test for the DOP model.

Similarly, recent euxinic sediments from the Black Sea have DOP values that vary from 0.46 to 0.85 (CALVERT and KARLIN, 1990) and from 0.55 to 0.80 (LYONS and BERNER, 1990). Again, results from a modern euxinic setting (i.e. the Black Sea) agree very well with ancient-sediment studies. On the basis of results from Kau Bay and Black Sea it may, therefore, be concluded that DOP values may indicate the degree of bottom water oxygenation and that specific depositional conditions are only of secondary importance.

Finally, the recent sediments form the euxinic Gotland and semi-euxinic Bornholm Deeps in the Baltic have DOS values that range from 0.35 to 0.7 and from 0.2 to 0.55 respectively (BOESEN and POSTMA, 1988). These DOS values are based on total iron rather than on the sum of pyritic-Fe and HCL-soluble-Fe and are therefore not directly comparable with data from Kau Bay, the Black Sea or ancient sediment studies. However, the

euxinic Gotland Deep has higher DOS values than the semi-euxinic Bornholm Deep. These data are thus consistent with the DOP model of RAISWELL et al. (1988).

7.6 CONCLUSIONS

1) The determination of 'iron reactive towards H_2S' by HCl digestion results in an overestimation of the reactivity of the sediments, because various Fe-bearing compounds that are soluble in HCL do not react with H_2S. This overestimation of reactive iron leads to an underestimation of the degree of pyritization values.

2) For Kau Bay sediment, reactive iron limits the amount of sulphide-bound iron, and the availability of oxidants controls the production of zerovalent sulphur and hence the FeS/FeS_2 ratio.

3) There is a strong correlation between iron and terrestrial organic carbon in Kau Bay sediments. This coupling between organic carbon and iron is interpreted to be a depositional feature. Future studies on Fe-C coupling should consider not only the amount, but also the type of organic matter.

4) There is a clear correlation between the quantity of total organic matter and marine organic matter. The amount of total organic matter preserved can therefore be used as a proxy for paleoproductivity in Kau Bay.

5) The fresh-water sediments underlying the marine sediments can be recognized on the basis of their $\delta^{13}C_{org}$ characteristics, but not by the C/S method. The fresh-water sediments are enriched in sulphur and $\delta^{34}S$ due to the high concentration of reactive iron and the diffusion of sulphide from the marine sediments. Therefore care should be taken when applying the C/S method to alternating fresh-water and euxinic marine deposits.

6) The marine sediments in Kau Bay show no relation between organic carbon and sulphur; this finding is in good agreement with the expected decoupling of organic carbon and sulphur in iron-limited euxinic environments.

7) DOS data from the semi-euxinic Kau Bay agree well with ancient sediment studies and provide a useful test for the DOP model of RAISWELL et al. (1988).

7.7 APPENDIX: Trace elements in pyrite phase of Kau Bay

Element	Molar ratio[1] * 10^5 Mean[4]	SDev	Range	Lit[2]	Enrichmment Factor[3]
As	30	17	7- 75	63- 328	1.82
Co	33	20	< 1- 76	81- 281	0.59
Cr	261	212	60- 963	19- 410	0.35
Cu[5]	295	103	105- 491	148- 4005	2.65
Mn	1644	646	645-2789	275-47000	0.0
Mo	25	20	4- 89	1- 54	1.30
Ni	260	110	93- 438	110- 1730	0.70
Zn	40	13	16- 60	26- 2030	0.35

1 Ratio expressed on a molar basis as trace-el_{pyr}/ Fe_{pyr}

2 HUERTA-DIAZ and MORSE (1990b)

3 Enrichment factor defined as (trace-el_{pyr}/trace-el_{bulk})/(Fe_{pyr}/Fe_{bulk})

4 Based on HNO_3-step of 20 samples

5 Part of Cu can be attributed to organic matter (HUERTA-DIAZ and MORSE, 1990a).

CHAPTER 8: ORGANIC-RICH TRANSITIONAL FACIES IN SILLED BASINS: RESPONSE TO SEA-LEVEL CHANGE

ABSTRACT

High-resolution profiles of organic carbon, $\delta^{13}C_{org.}$, sulphur, $\delta^{34}S$ and some trace elements in cores from two silled basins, namely Kau Bay (Indonesia) and the Black Sea, are reported. For both Kau Bay and Black Sea, the sedimentary record can be divided into three distinct units representing a Pleistocene fresh/brackish water (Unit 3), a Holocene transitional (Unit 2) and a recent fully marine facies (Unit 1). The geochemical characteristics of these units are strikingly similar for both basins.

The sediments from Unit 3 are characterized by the predominance of terrestrial organic matter, by Mo and U concentrations at crustal abundance and positive $\delta^{34}S$ values. The transitional sediments (Unit 2) are strongly enriched in marine organic matter, Mo, V and U and have intermediate $\delta^{34}S$ values. Sediments from the modern marine facies (Unit 1) are moderately organic-carbon rich, slightly enriched in Mo and U and have negative $\delta^{34}S$ values.

The organic-carbon rich sediments from Unit 2 were formed by increased production during the transition from the Pleistocene isolated fresh/brackish water environment to the modern open marine facies. This temporary higher productivity was caused by displacement of nutrients from the deep water into the euphotic zone due to the gradual infilling by marine waters.

8.1 INTRODUCTION

Some marine basins or seas are partially isolated from the open ocean or from an adjacent sea due to the presence of a sill which restricts water exchange between the enclosed basins and the adjacent areas of the open ocean. As a consequence, these silled basins have a distinctive hydrography, chemistry and biology (RICHARDS, 1960; DEUSER, 1975; GRASSHOFF, 1975; ANDERSON and DEVOL, 1987).

On the basis of the water balance, silled basins can be divided into two main groups (GRASSHOFF, 1975). The first group comprises those basins located in arid zones having a negative water balance. Since evaporation exceeds the total input of fresh water, there is a constant inflow of shallow nutrient-depleted oceanic water and a loss of deep waters to the open ocean.

The bottom waters in these basins are both oxygenated and nutrient depleted. Typical examples of this category are the Mediterranean and the Red Sea (GRASSHOFF, 1975; DEMAISON and MOORE, 1980). The second group comprises silled basins with a positive water balance which are located in humid zones. This type of basin may act as a nutrient trap which thus may stimulate higher primary productivity. If deep-water renewal is relatively slow, anoxic conditions usually develop in the bottom waters. Typical examples of this category are Kau Bay, Indonesia, the Black Sea, the Baltic Sea and some Norwegian and Canadian fjords (e.g., GRASSHOFF, 1975; DEUSER, 1975; DEMAISON and MOORE, 1980; ANDERSON and DEVOL, 1987).

The restricted nature of these basins also makes them sensitive to eustatic sea-level fluctuations. During periods of low global sea level, some silled basins will become isolated from the open ocean. For those basins with a negative water balance, this isolation will cause an increase in salinity and eventually the deposition of evaporites. The Messinian salinity crisis in the Mediterranean is the best example (HSÜ et al., 1977). In contrast, for silled basins with a positive water balance, isolation may result in a decrease in salinity or even the conversion of the marine basin into a fresh-water lake. For example, the deposition of late Miocene fresh-water deposits in the Sea of Japan was due to the isolation of this silled basin with a positive water balance from the open ocean (BURCKLE and AKIBA, 1978). Similarly, the low global sea level associated with the Weichselian glaciation caused the isolation of various silled basins and the deposition of fresh-water or brackish-water sediments in Kau Bay (MIDDELBURG and DE LANGE, 1989; BARMAWIDJAJA et al., 1989), the Baltic Sea (SUESS, 1976, 1979, 1982; BOESEN and POSTMA, 1988) and the Black Sea (ROSS et al., 1970; ROSS and DEGENS, 1974).

In this paper we describe the response of two silled basins with a positive water balance to the transgression following the last glaciation. Both Kau Bay (island of Halmahera, Indonesia) and the Black Sea have changed from a Weichselian fresh-water/brackish water lake to a Holocene anoxic marine basin. Special attention will be given to the distribution of organic carbon, sulphur, molybdenum and uranium. We show that the trends shown by these constituents in the various facies are strikingly similar in both basins and are also similar to trends observed in some ancient transgressive systems.

8.2 KAU BAY

Kau Bay is 470 m deep and covers an area of 60 by 30 km. It is separated from the Pacific Ocean by a flat-floored 30 km-wide sill which is only 40 m below sea level. At present, Kau Bay is a semi-euxinic marine basin wherein low oxygen, but non-sulphidic, bottom waters alternate with periods of anoxic sulphidic bottom waters (MIDDELBURG et al., 1988a; chapter 2). However, during Weichselian time, sea level dropped below the sill depth, Kau Bay was isolated, and fresh-water sediments were deposited. These sediments are characterized by the absence of marine microfossils, extremely low percentages of mangrove pollen and the presence of a fresh-water diatom assemblage (BARMAWIDJAJA et al., 1989).

The late Pleistocene and Holocene sediment sequence in the bay can be divided into three distinct units. From the surface down these are: a Holocene semi-euxinic marine facies (Unit 1), a transitional facies (Unit 2) and a Weichselian fresh-water unit (Unit 3). These different units represent the response of Kau Bay to the change from a Pleistocene fresh-water lake to the modern marine basin as a consequence of the post-glacial sea-level rise and the reconnection of the basin to the Pacific Ocean.

The three sedimentary units can be readily distinguished by their organic carbon (C_{org}) and minor metal contents and $\delta^{13}C_{org}$ and $\delta^{34}S$ characteristics (Figure 8.1). The fresh-water sediments from Unit 3 have 2 to 6 % by weight C_{org} and are depleted in $\delta^{13}C_{org}$ (-30 to -28 $^{o}/_{oo}$), but enriched in $\delta^{34}S$ (+15 $^{o}/_{oo}$) relative to the overlying units. Sediments from the transitional Unit 2 are strongly enriched in C_{org} (up to 10 weight %), Mo (353 ppm) and some other trace elements (Table 8.1), and show a dramatic change in $\delta^{13}C_{org}$ to values of -22 $^{o}/_{oo}$ (Figure 8.1). Marine sediments from Unit 1 have 3 to 5 % by weight C_{org}, background (i.e. crustal abundance) Mo values and $\delta^{13}C_{org}$ values as heavy as -21 $^{o}/_{oo}$. The concentration of organic matter correlates closely with its isotopic composition in Units 1 and 2; the total quantity of organic matter is directly proportional to the proportion of marine organic matter and may thus be used as a proxy for palaeoproductivity (chapter 7).

In order to decipher the processes that produced the marked C_{org} enrichment in unit 2, it is necessary to consider the environmental changes that took place during the filling of Kau Bay by seawater after sea-level rise. Figure 8.2 shows the distribution of organic matter in the context of environmental changes. The process started with the spilling of saline water over the sill; this influx probably sank to the bottom. Surface waters, however, remained fresh, as indicated by the diatom flora (BARMAWIDJAJA et al., 1989). As a consequence of the continuous inflow of oceanic waters, the interface between the saline and overlying fresh

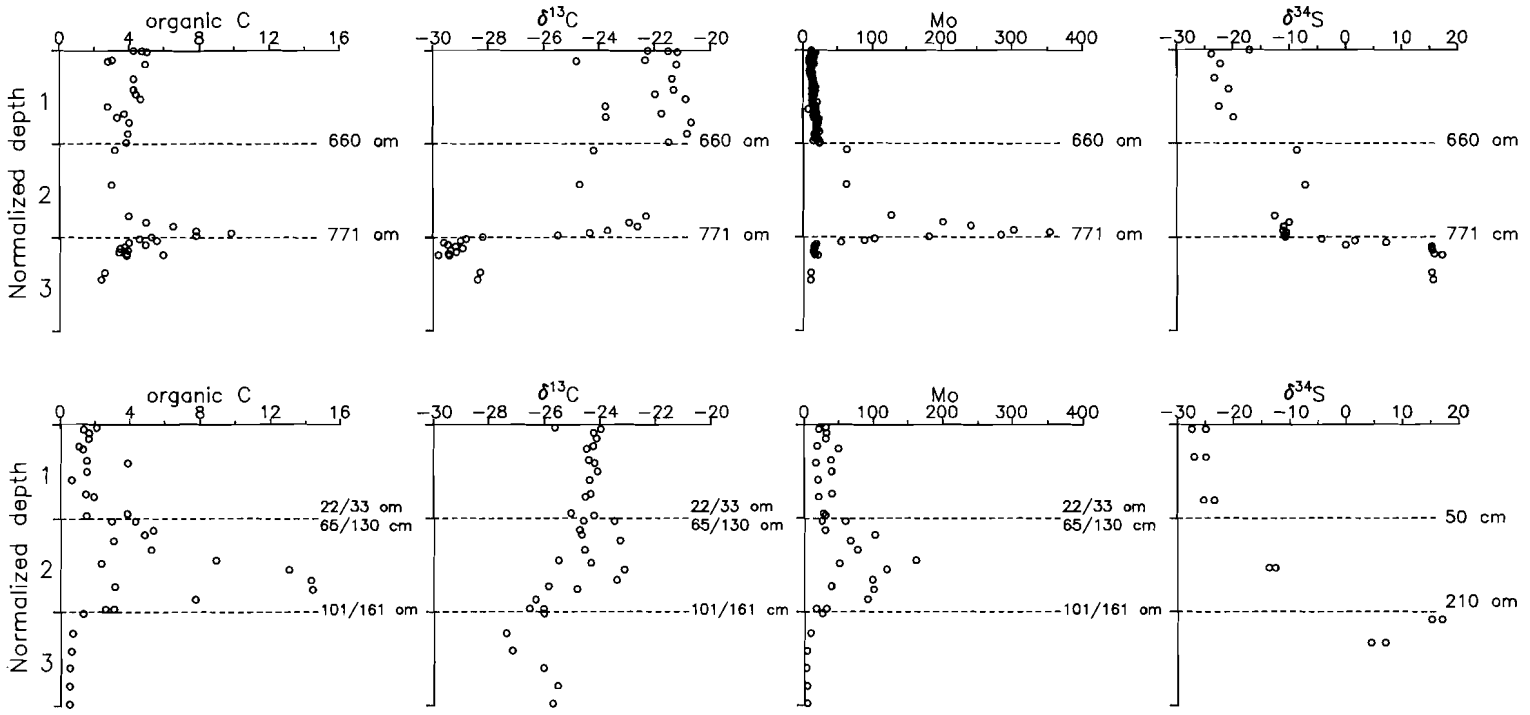

Figure 8.1. Organic carbon, $\delta^{13}C_{org}$, molybdenum and $\delta^{34}S$ distributions in the Late Pleistocene and Holocene sections in Kau Bay (upper) and the Black Sea (lower). Units 1 to 3 are lithological units explained in text. The ordinate in each plot is the normalized depth ((sample depth - depth of the upper boundary of the lithological unit)/thickness of unit). The depth in core of each lithological unit is indicated. For Kau Bay data were obtained using methods described in chapter 7. For the Black Sea organic carbon, $\delta^{13}C$ and Mo were obtained from CALVERT and FONTUGNE (1987) and CALVERT (1990), and $\delta^{34}S$ was obtained from VINOGRADOV et al. (1962).

waters rose through the water column and the surface waters gradually became more saline, as is recorded by the presence of marine diatoms, pteropods and planktonic foraminifera in Unit 1 (BARMAWIDJAJA et al., 1989).

The micropalaeontological evidence shows that the increase in organic carbon coincides with the change from fresh to saline surface waters (Figure 8.2). This enrichment in marine organic carbon is probably the result of higher plankton production brought about by displacement of nutrients from the deep waters into the euphotic zone. After the establishment of marine conditions, the rate of upward displacement of saline nutrient-rich water decreased and this was followed by a decrease in productivity. This productivity increase in response to the infilling of a lake by marine waters is not limited to Kau Bay, but applies also to the Black Sea (STRAKHOV, 1971).

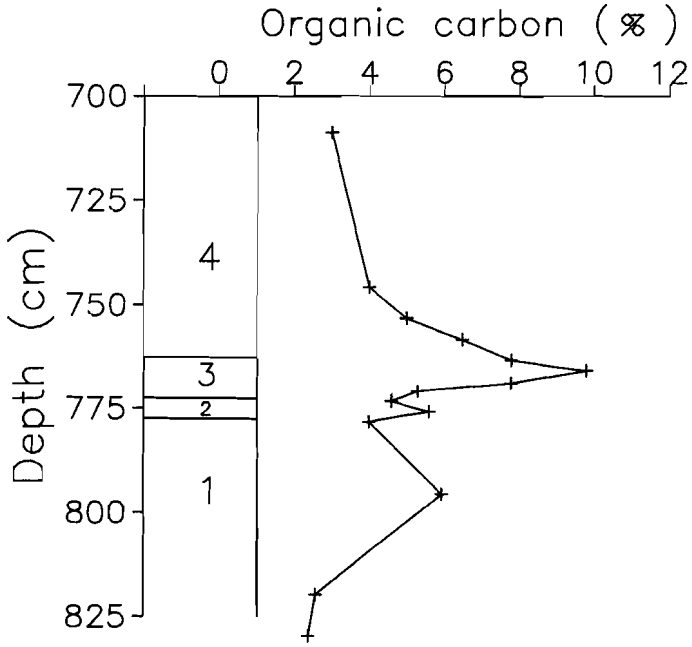

Figure 8.2. The transgressive sequence in Kau Bay and the distribution of organic carbon. Stages during the transgression: 1 fresh-water conditions; 2 saline bottom waters, but fresh surface waters; 3 surface waters change from fresh to saline; 4 gradual establishment of full marine conditions. These stages are based on faunal analysis reported by BARMAWIDJAJA et al. (1989).

8.3 BLACK SEA

The Black Sea is the world's largest permanently anoxic basin, with a maximum water depth of 2200 m. The oxic/anoxic boundary lies at 100 to 150 m depth (MURRAY et al., 1989), and the sill connecting the basin with the Mediterranean is 35 m deep. The stratigraphy of the deep-water sediments of the Black Sea has been established by ROSS et al. (1970) and ROSS and DEGENS (1974). VINOGRADOV et al. (1962), CALVERT (1990), CALVERT and FONTUGNE (1987) and CALVERT et al. (1987) have presented information on the geochemical and isotopic responses to the changing environment in this basin. The modern facies (Unit 1) is a finely-laminated, coccolith marl. A sapropel underlies Unit 1, and this in turn overlies freshwater sediment (Unit 3). These three units reflect the response of the basin to the large changes in environmental conditions consequent upon the re-connection of the basin with the Mediterranean approximately 9,000 years ago (ROSS et al., 1970).

As in the case of Kau Bay, the three units can be readily distinguished by their geochemical and isotopic properties (Figure 8.1 and Table 8.1). Unit 1 contains a few weight % C_{org} with a $\delta^{13}C_{org}$ value of -24 $^{o}/_{oo}$ and light $\delta^{34}S$ values (-25 to -29 $^{o}/_{oo}$). Molybdenum concentrations range from 19 to 50 ppm. The sapropel contains up to 14 weight % C_{org} with the heaviest $\delta^{13}C_{org}$ values (-23 $^{o}/_{oo}$); molybdenum concentrations reach 162 ppm. Unit 3 sediments have the lowest C_{org} contents of the three units (<1 weight %), the lightest $\delta^{13}C_{org}$ values (-27 $^{o}/_{oo}$) and the heaviest $\delta^{34}S$ values (+15 $^{o}/_{oo}$); Mo values are at crustal abundance levels. CALVERT and FONTUGNE (1987) have interpreted the carbon isotopic data as reflecting a terrestrial source of the organic matter in Unit 3 and a predominance of marine organic matter input to the sapropel during the change from the freshwater to the marine phase of the basin. CALVERT (1990) has also used the behaviour of Br, I and Mn to show that the basin was actually oxygenated to the bottom during the accumulation of the sapropel, and that anoxic conditions were established when the laminated sediments of Unit 1 began to accumulate.

8.4 A SEAWATER SOURCE FOR MO, S, U AND V

In both Kau Bay and the Black Sea, the change from fresh/brackish water to marine conditions resulted not only in a temporary higher productivity, but also in a shift from an environment low in sulphate, Mo, V and U to an environment with higher concentrations of these constituents. How are these changes reflected in the behaviour of these elements in the sediments? Table

TABLE 8.1. AVERAGE COMPOSITION OF THE SEDIMENTARY UNITS IN KAU BAY, THE BLACK SEA AND THE LOWER CRETACEOUS SHAFTESBURY FORMATION, ALBERTA

Basin or Formation	C_{org}	S	Fe	Mo	V	U
Kau Bay[1]						
Unit 1	4.2	1.4	4.3	18	132	5.9
Unit 2	5.7	3.4	4.7	182	257	15.6
Unit 3	3.7	3.9	6.4	13	217	3.9
Black Sea[2]						
Unit 1	1.8	1.3	3.9	30	123	3.9
Unit 2	6.3	1.4	4.0	71	231	11.5
Unit 3	0.6	0.7	3.8	5	138	3.6
Shaftesbury Formation[3]						
Unit 1	1.6	0.8	--	25	236	4.3
Unit 2	4.3	2.3	--	182	321	5.7
Unit 3	0.9	1.3	--	86	244	6.6
Average Shale[4]	0.9	0.4	4.7	3	130	3.7

1 this study; 2 CALVERT (1990); U data from CAGATAY et al. (1990); 3 LECKIE et al. (1990); 4 HOLLAND (1984)
(C_{org}, S, Fe in wt%; Mo, V and U in ppm).

8.1 provides the information on both basins that can be used to answer this question.

In Kau Bay, the marine sediments (Unit 1) are slightly enriched in Mo and U compared with the fresh/brackish water sediments (Unit 3). In contrast to Units 1 and 3, however, the organic-rich sediments from Unit 2 are significantly enriched in Mo, V and U. In the Black Sea, Unit 1 has higher concentrations of S and Mo but similar concentrations of U and V compared with Unit 3. Once again, the organic-rich unit (Unit 2) has significantly higher concentrations of Mo, U and V.

Parallel enrichments of Mo, V and U with C_{org} in anoxic organic-carbon-rich sediments have been found in various ancient (HOLLAND, 1984) and modern sediments (CALVERT, 1976; FRANCOIS, 1988). These enrichments have been attributed to reduction followed by scavenging of the reduced species by Fe-sulphides (Mo) or organic matter (Mo, V and U) or to reduction followed by formation of insoluble compounds such as Mo-sulphides and V(IV) and U(IV) hydroxides (CALVERT, 1976, 1990; VAN DER WEIJDEN et al., 1990).

Although most sedimentary sulphur is ultimately derived from seawater

sulphate, this is not necessarily reflected in its distribution since the amount of S in euxinic sediments is determined by the reactive iron content (RAISWELL and BERNER, 1985; BOESEN and POSTMA, 1988; CALVERT and KARLIN, 1990; LYONS and BERNER, 1990; chapter 7). After the establishment of marine conditions, abundant sulphate would have become available for the microbiological formation of sulphide. The sulphide produced in the marine sediments first reacted in situ with the available reactive iron compounds; after Fe became limiting, the dissolved sulphide then started to diffuse into the underlying sediments, where, because of the limited amount of pyrite formation in the fresh-water conditions, abundant reactive iron was still present. In Kau Bay, the reactive iron contents were so high that the S contents of Unit 3 are actually higher than in the other units (Table 8.1 ; see also chapter 7). Most of the S found in the sediments from Unit 3 is therefore derived from seawater sulphate. In the Black Sea, the fresh/brackish-water sediments of Unit 3 also have moderately high S concentrations, and these are probably due to diffusion of unreacted dissolved sulphide from the overlying sapropel.

Since all the sulphate diffusing into the fresh-water horizons in Kau Bay and the Black Sea is quantitatively reduced and fixed as iron sulphide compounds (closed system), the $\delta^{34}S$ value of the solid phase sulphides buried should approach the $\delta^{34}S$ value of the sulphate diffusing into the sediments. The $\delta^{34}S$ characteristics of unit 3 sediments in Kau Bay and Black Sea are +15 and +13 $^{o}/_{oo}$, respectively (Figure 8.1), distinctly different from the values characteristic of sulphide phases formed in an open system (GOLDHABER and KAPLAN, 1974), but close to that of seawater ($\delta^{34}S$ = + 20 $^{o}/_{oo}$). The small difference between the $\delta^{34}S$ value of seawater and that of Unit 3 sediments can be explained by preferential diffusion of ^{32}S (JØRGENSEN, 1979; CHANTON et al., 1987b) and the presence of sulphur compounds formed during the fresh or brackish water stage of the basins (BERNER, 1970b; see also chapter 7).

8.5 GEOCHEMICAL RECORD DURING A MARINE TRANSGRESSION

The data presented in this study indicate that sediments deposited in a silled basin during a marine transgression can be recognized using geochemical and isotopic criteria. For both Kau Bay and Black Sea, the sedimentary record can be divided into three distinct units representing a lacustrine (Unit 3), a transitional (Unit 2) and a fully marine facies (Unit 1). The sediments from Unit 3 are characterized by the predominance of terrestrial organic matter, by Mo and U concentrations similar to those of

average shale, and by heavy $\delta^{34}S$ values as a consequence of sulphate reduction and iron sulphide formation under conditions closed to sulphate. The transitional sediments (Unit 2) are strongly enriched in marine planktonic organic matter, Mo, V and U, and have intermediate $\delta^{34}S$ values. Sediments from the modern marine facies (Unit 1) are moderately organic-rich, slightly enriched in Mo and U, and have negative $\delta^{34}S$ values (Kau Bay: -17 to -24 $^{o}/_{oo}$; Black Sea: - 25 to -29 $^{o}/_{oo}$) as a consequence of sulphate reduction in an environment open to sulphate. Sediments from Unit 1 may either be calcareous ooze, as in the Black Sea (ROSS and DEGENS, 1974), or organic carbon-rich muds with carbonate concretions, as in Kau Bay (MIDDELBURG et al., 1990; chapter 6).

The unusual geochemical and isotopic characteristics of the transitional facies (Unit 2) in both Kau Bay and the Black Sea appear to be duplicated in some organic carbon-rich shale units that commonly form during marine transgressions (e.g. LECKIE et al., 1990; LEEDER et al., 1990; MYERS and WIGNALL, 1987). The basal shale of the Late Albian Shaftesbury Formation from Alberta (Canada), for example, may be used as an example of such a transitional facies preserved in the geological record (LECKIE et al., 1990). The Formation can be divided into three distinct units: a brackish water/estuarine shale (Unit 3), a radioactive shale (Unit 2) and an open-marine shale (Unit 1). The radioactive shale is enriched in organic matter, S and some minor elements (Table 8.1) and was formed during an algal bloom period (LECKIE et al., 1990). Although the Shaftesbury Formation was deposited in a relatively shallow, open marine environment, the chemical signatures in the radioactive shale are very similar to those found in two modern silled basins discussed here (Table 8.1). This suggests that the transgressive sequence preserved in silled basins may have a wider application.

REFERENCES

AKEN H.M. VAN and VERBEEK H. (1988) The hydrography and ventilation of Kau Bay in Halmahera. *Neth. J. Sea Res.* **22**, 403-413.

ALLER R.C. (1980) Diagenetic processes near the sediment-water interface of Long Island Sound. I. Decomposition and nutrient element geochemistry (S,N,P). *Adv. Geophys.* **22**, 237-250.

ALLER R.C. and MACKIN J.E. (1984) Preservation of reactive organic matter in marine sediments. *Earth Plan. Sci. Let.* **70**, 260-266.

ALLER R.C., MACKIN J.E. and COX R.T. Jr. (1986) Diagenesis of Fe and S in Amazon inner shelf muds: apparent dominance of Fe reduction and implications for the genesis of ironstones. *Contin. Shelf. Sci.* **6**, 263-289.

ANDERSON J.J. and DEVOL A.H. (1987) Extent and intensity of the anoxic zone in basins and fjords. *Deep Sea Res.* **34**, 927-944.

ANDERSON T.F., KRUGER J. and RAISWELL R. (1987) C-S-Fe relationships and the isotopic composition of pyrite in the New Albany Shale of the Illinois Basin, U.S.A. *Geochim. Cosmochim. Acta* 51, 2795-2805.

ANDERSON R.F., LEHURAY A.P., FLEISHER M.Q. and MURRAY J.W. (1989) Uranium deposition in Saanich Inlet sediments, Vancouver Islands. *Geochim. Cosmochim. Acta* **53**, 2205-2213.

ANDREAE M.O. (1978) Distribution and speciation of arsenic in natural waters and some marine algae. *Deep-Sea Res.* **25**, 391-402.

ANDREAE M.O. (1979) Arsenic speciation in seawater and interstitial waters: The influence of biological-chemical interactions on the chemistry of a trace element, *Limnol. Oceanogr.* **24**, 440-452.

ANDREAE M.O. (1983) The determination of the chemical species of some of the "hydride elements" (arsenic, antimony, tin and germanium) in seawater: methodology and results. In *Trace Metals in Seawater* (eds. C.S. Wong, E.A. Boyle, K.W. Bruland, J.D. Burton and E.D. Goldberg), pp 1-19, Plenum Press, New York.

ANDREAE M.O., ASMODE J.-F., FOSTER P. and VAN'T DACK L. (1981). Determination of Antimony(III), Antimony(V), and Methylantimony Species in Natural Waters by Atomic Absorption Spectrometry with Hydride Generation. *Anal. Chem.* **53**, 1766-1771.

APPLEBY P.A. and OLDFIELD F. (1978) The calculation of lead-210 dates assuming a constant rate of supply of unsupported ^{210}Pb to the sediment. *Catena* 5, 1-8

BAAS BECKING L.G.M. and MOORE D. (1959) The relation between iron and organic matter in sediments. *J. Sediment. Petrol.* **29**, 454-458.

BAKER P.A. and KASTNER M. (1981) Constraints on the formation of sedimentary dolomite. *Science* **213**, 214-216.

BAKER P.A. and BURNS S.R. (1985) Occurrence and formation of dolomite in organic-rich continental margin sediments. *Amer. Ass. Petr. Geol. Bull.* **69**, 1917-1930.

BARD E., HAMELIN B., FAIRBANKS R.G. and ZINDLER A. (1990) Calibration of the ^{14}C timescale over the past 30,000 years using mass spectrometric U-Th ages from Barbados corals. *Nature* **345**, 405-410.

BARMAWIDJAJA D.M., DE JONG A.F.M., VAN DER BORG K., VAN DER KAARS W.A. and ZACHARIASSE W.J. (1989) Kau Bay, Halmahera, a late Quaternary palaeoenvironmental record of a poorly ventilated basin. *Netherlands Journal of Sea Research* **24**, 591-605.

BARMAWIDJAJA D.M., DE JONG A.F.M., VAN DER BORG K., VAN DER KAARS W.A., VAN DER LINDEN W.J.M. and ZACHARIASSE W.J. (1990) The timing of the post-glacial marine invasion of Kau Bay, Halmahera, Indonesia. *Radiocarbon* **31**, 201-210.

BARNES C.E. and COCHRAN J.K. (1990) Uranium removal in oceanic sediments and the oceanic U balance. *Earth Planet. Sci. Lett.* **97**, 94-101.

BENNEKOM, A.J. VAN (1988) Deep-water transit times in the eastern Indonesian basins, calculated from dissolved silica in deep and interstitial waters. *Nether. J. Sea Res.* **22**, 341-354.

BEN-YAAKOV S. (1973) pH buffering of pore water of recent anoxic marine sediments. *Limnol. Oceanogr.* **18**, 86-94.

BERNER R.A. (1964) An idealized model of dissolved sulfate distribution in recent sediments. *Geochim. Cosmochim. Acta* **28**, 1497-1503.

BERNER R.A. (1970a) Sedimentary pyrite formation. *Amer. J. Sci.* **268**, 1-23.

BERNER R.A. (1970b) Pleistocene sea levels possibly indicated by buried black sediments in the Black Sea. *Nature* **227**, 700.

BERNER R.A. (1973) Phosphate removal from sea water by adsorption on volcanogenic ferric oxides. *Earth Planet. Sci. Lett.* **18**, 77-86.

BERNER R.A. (1974a) Iron sulfides in pleistocene deep Black Sea Sediments and their paleoceanographic significance in E.T. Degens and D.A. Ross, eds., The Black Sea-geology, chemistry and biology. *AAPG Mem.* **20**, 524-531.

BERNER R.A. (1974b) Kinetic models for the early diagenesis of nitrogen, sulfur, phosphorus and silicon in anoxic marine sediments, p. 427-449. In: E.D. Goldberg, ed., The Sea, v. 5, Wiley.

BERNER R.A. (1977) Stoichiometric models for nutrient regeneration in anoxic sediment. *Limnol. Oceanogr.* **22**, 781-786.

BERNER R.A. (1978) Sulfate reduction and the rate of deposition of marine sediments. *Earth Planet. Sci. Lett.* **37**, 492-498.

BERNER R.A. (1980a) *Early Diagenesis. A theoretical approach.* Princeton University Press, 241 p.

BERNER R.A. (1980b) A rate model for organic matter decomposition during bacterial sulfate reduction in marine sediments. In *Biogeochimie de la mattere organique'a l'interface eau-sediment marin.* Colloq. Int. CNRS **293**, 35-44.

BERNER R.A. (1981) Authigenic mineral formation resulting from organic matter decomposition in modern sediments. *Fortschr. Miner.* **59**, 117-135.

BERNER R.A. (1984) Sedimentary pyrite formation: An update. *Geochim. Cosmochim. Acta* **48**, 605-615.

BERNER R.A. and RAISWELL R. (1983) Burial of organic carbon and pyrite sulfur in sediments over Phanerozoic time: A new theory. *Geochim. Cosmochim. Acta* **47**, 855-862.

BERNER R.A. and RAISWELL R. (1984) C/S method for distinguishing freshwater from marine sedimentary rocks. *Geology* **12**, 365-368.

BERNER R.A. and WESTRICH J.T. (1985) Bioturbation and the early diagenesis of carbon and sulfur. *Amer. J. Sci.* **285**, 193-206.

BERNER R.A., M.R. SCOTT and C. THOMLINSON (1970) Carbonate alkalinity in the pore waters of anoxic marine sediments. *Limnol. Oceanogr.* **15**, 544-549.

BERNER R.A., BALDWIN T. and HOLDREN G.R. Jr. (1979) Authigenic iron sulfides as paleosalinity indicators. *Jour. Sed. Pet.* **49**, 1345-1350.

BERTINE K.K. and LEE D.S. (1983) Antimony content and speciation in the water column and interstitial waters of Saanich Inlet. In *Trace Metals in Seawater* (eds. C.S. Wong, E.A. Boyle, K.W. Bruland, J.D. Burton and E.D. Goldberg), pp 21-38, Plenum Press, New York.

BLOOM, A.L., BROECKER, W.S., CHAPPEL, J., MATTHEWS, R.H. and MESOLELLA K.J. (1974). Quaternary Sea Level Fluctuations on a Tectonic Coast: New $^{230}Th/^{234}U$ Dates from the Huon Peninsula, New Guinea. *Quat. Res.* **4**, 185-205.

BLOOMQUIST R.G. (1977) *Chemical characteristics of interstitial water from the southern Baltic Sea.* Ph.D. thesis, Univ. Stockholm, 111 p.

BOESEN C. AND POSTMA D. (1988) Pyrite formation in anoxic sediments of the Baltic. *Amer. J. Sci.* **288,** 575-603.

BONATTI E. (1966) Deep sea authigenic calcite and dolomite. *Science* **153,** 534-537.

BORG VAN DER K., ALDERLIESTEN C., HOUSTON C.M., DE JONG A.F.M. and VAN ZWOL N.A. (1987) Accelaration Mass Spectrometry with ^{14}C and ^{10}Be in Utrecht. *Nuclear Instr. and Methods* **B29,** 143.

BOUDREAU B.P. (1987) A steady-state diagenetic model for dissolved carbonate species and pH in the porewaters of oxic and suboxic sediments. *Geochim. Cosmochim. Acta* **51,** 1985-1996.

BOUDREAU B.P. and WESTRICH J.T. (1984) The dependence of bacterial sulphate reduction on sulphate concentration in marine sediments. *Geochim. Cosmochim. Acta* **48,** 2503-2516.

BOUDREAU B.P. and CANFIELD D.E. (1988) A provisional diagenetic model for pH in anoxic porewaters: Application to the FOAM site. *Jour. Mar. Res.* **46,** 429-455.

BOUDREAU B.P. and RUDDICK B.R. (1991) On a reactive continuum representation of organic matter diagenesis. *Amer. J. Sci.* (submitted).

BROECKER W.S. and PENG T-H. (1983) *Tracers in the Sea* Lamont-Doherty Geological Observatory, New York, 699pp.

BURCKLE L.H. and AKIBA F. (1978) Implications of late Neogene fresh-water sediment in the Sea of Japan. *Geology* **6,**123-127.

CAGATAY M.N., GEDIK A. and SALTOGLU T. (1990) Geochemistry of uranium in the late Pleistocene-Holocene sediments from the southern part of the Black Sea basin. *Chem. Geol.* **82,** 129-144

CALVERT S.E. (1976) The mineralogy and geochemistry of nearshore sediments. *in* Riley, J.P., Chester, R., eds., Chemical Oceanography, v. 6, Academic Press, London, p. 187- 280.

CALVERT S.E. (1990) Geochemistry and Origin of the Holocene Sapropel in the Black Sea: in Ittekkot, V., Kempe, S., Michaelis, W., and Spitzy, A., eds., Facets of Modern Biogeochemistry, Springer Verlag, p. 326-352.

CALVERT S.E. and FONTUGNE M.R. (1987) Stable carbon isotopic evidence for the marine origin of the organic matter in the Holocene Black Sea sapropel. *Isot. Geosc.* **66,** 315-322.

CALVERT S.E. and KARLIN R. (1990) Sulphur/carbon relationships in Black Sea sediment. *Geochim. Cosmochim. Acta* (submitted).

CALVERT S.E., VOGEL J.S. and SOUTHON J.R. (1987) Carbon accumulation rates and the origin of the Holocene sapropel in the Black Sea. *Geology* **15**, 918-921.

CANFIELD D.E. and BERNER R.A. (1987) Dissolution and pyritization of magnetite in anoxic marine sediments. *Geochim. Cosmochim. Acta* **51**, 645-659.

CANFIELD D.E. (1989a) Reactive iron in marine sediments. *Geochim. Cosmochim. Acta* **53**, 619-632.

CANFIELD D.E. (1989b) Sulfate reduction and oxic respiration in marine sediments: implications for organic carbon preservation in euxinic sediments. *Deep Sea Res.* **36**, 121-138.

CARPENTER A.B. (1980) The chemistry of dolomite formation I: the stability of dolomite. *SEPM Spec. Publ.* **28**, 111-122.

CARSLAW H.S. and JAEGER J.C. (1959) Conduction of Heat in Solids, 2nd ed., Oxford University Press, London, England, 1-510.

CHAMBERS L.A. (1982) Sulfur isotope study of a modern intertidal environment, and the interpretation of ancient sulfides. *Geochim. Cosmochim. Acta* **46**, 721-728.

CHAMBERS L.A. and TRUDINGER P.A. (1979) Microbiological fractionation of stable sulfur isotopes: a review and critique. *Geomicrobiol. J.* **1**, 249-294.

CHANDER S. and FUERSTENAU D.W. (1984) Solubility and interfacial properties of hydroxyapatite: a review. In: D.N. Misra, ed., Adsorption and surface chemisty of hydroxyapatite, Plenum Press, pp. 13-28.

CHANTON J.P., MARTENS C.S., and GOLDHABER M.B. (1987a) Biogeochemical cycling in an organic-rich coastal marine basin. 7. Sulfur mass balance, oxygen uptake, and sulfide retention. *Geochim. Cosmochim. Acta* **51**, 1187-1199.

CHANTON J.P., MARTENS C.S., and GOLDHABER M.B. (1987b) Biogeochemical cycling in an organic-rich coastal marine basin. 8. A sulfur isotopic budget balanced by differentiall diffusion across the sediment-water interface *Geochim. Cosmochim. Acta* **51**, 1201-1208.

CLAYPOOL G.E. and KAPLAN I.R. (1974) The origin and distribution of methane in marine sediments, *in* Kaplan, I.R., ed., Natural gases in marine sediments: New York, Plenum, p. 97-139.

CLINE J.D. (1969) Spectrophotometric determination of hydrogen sulfide in natural water. *Limnol. Oceanogr.* **14**, 454-458.

COMANS R.N.J. and MIDDELBURG J.J. (1987) Sorption of trace metals on calcite: Applicability of the surface precipitation model. *Geochim. Cosmochim. Acta* **51**, 2587-2591.

COMANS R.N.J, MIDDELBURG J.J., ZONDERHUIS J., WOITTIEZ J.R.W., DE LANGE G.J., DAS H.A. and VAN DER WEIJDEN C.H. (1989) Mobilization of radiocaesium in pore water of lake sediments. *Nature* **339**, 367-369.

COMPTON J.S. (1988) Degree of supersaturation and precipitation of organogenic dolomite. *Geology* **16**, 318-321.

COMPTON J.S. and SIEVER R. (1986) Diffusion and mass balance of Mg during early dolomite formation, Monterey Formation. *Geochim. Cosmochim. Acta* **50**, 125-135.

CORNWELL J.C. and MORSE J.W. (1987) The characterization of iron sulfide minerals in anoxic marine sediments. *Mar. Chem.* **22**, 193-206.

CORNWELL J.C., LIN S., HUERTA-DIAZ M. and MORSE J.W. (1990) Iron sulfide mineral formation and diagenesis in the sediments of Laguna Madre and adjacent basins. *Mar. Chem.* (submitted).

CRANK J. (1975) The Mathematics of Diffusion, 2nd ed., Pergamon Press, Oxford, 1-414.

DAVIS J.A., FULLER C.C. and COOK A.D. (1987) A model for trace metal sorption processes at the calcite surface: Adsorption of Cd^{2+} and subsequent solid solution formation. *Geochim. Cosmochim. Acta* **51**, 1477-1490.

DAVIS H.R., BYERS C.W. and DEAN W.E. (1988) Pyrite formation in the lower Cretaceous Mowry shale: effect of organic matter type and reactive iron content. *Amer. J. Sci.* **288**, 873-890.

DE LANGE G.J. (1983) Geochemical evidence of a massive slide in the southern Norwegian Sea. *Nature* **305**, 420-422.

DE LANGE G.J. (1984) Shipboard pressure-filtration system for interstitial water extraction. *Meded. Rijks. Geol. Dienst* **38**, 209-214.

DE LANGE G.J. (1986a) Early diagenetic reactions in interbedded pelagic and turbiditic sediments in the Nares Abyssal Plain (western North Atlantic): Consequences for the composition of sediment and interstitial water. *Geochim. Cosmochim. Acta* **50**, 2543-2561.

DE LANGE G.J. (1986b). Chemical composition of interstitial water in cores from the Nares Abyssal Plain (Western North Atlantic). *Oceanol. Acta* **9**, 159-168.

DE LANGE G.J. (1988) *Geochemical and early diagenetic aspects of interbedded pelagic/turbiditic sediments in two N. Atlantic Abyssal Plains.* Ph.D. thesis, University of Utrecht, Geologica Ultraiectina, no. 57, 190pp.

DEAN W.E. and ARTHUR M.A. (1989) Iron-sulfur-carbon relationships in organic-carbon-rich sequences 1: Cretaceous western interior seaway. *Amer. J. Sci.* **289**, 708-743.

DEGENS E. (1969) Biogeochemistry of stable carbon isotopes. In *Organic Geochemistry* (editors, E. Eglinton and M.T.J. Murphy), Springer-Verlag, Berlin, pp. 304-325.

DEGENS E.T. and ROSS D.A. (1972) Chronology of the Black Sea over the last 25,000 years. *Chem. Geol.* **10**, 1-16.

DELIBRIAS G. (1989) Carbon-14, ch. 15 in Roth E. and Poty B., eds. Nuclear mehods of Dating, 399-436, Kluwer Academic Publ., Dordrecht.

DEMAISON G.J. and MOORE G.T. (1980) Anoxic environments and oil source bed genesis. *Amer. Ass. Petr. Geol. Bull.* **64**, 1179-1209.

DEVOL A.H., ANDERSON J.J., KUIVILA K. and MURRAY J.W. (1984) A model for coupled sulfate reduction and methane oxidation in the sediments of Saanich Inlet. *Geochim. Cosmochim. Acta* **48**, 993-1004.

DEUSER W.G. (1975) Reducing environments: in Riley, J.P., Chester, R., eds., Chemical Oceanography, v. 3, Academic Press, London, p. 1-37.

DOLOMIEU D. de (1791) Sur un genre de pierres trés-peu effervescentes avec les acides, & phosphorescents par la collision. *Observation et mèmoire sur la physique, sur l'histoire naturelle, et sur les arts et mètiers (Journal Physique)* **39**, 3-10.

DREVER J.I. (1971) Magnesium-iron replacement in clay minerals in anoxic marine sediments. *Science* **172**, 1334-1336.

ELDERFIELD H. and TRUESDALE V.W. (1980) On the biophilic nature of iodine in seawater. *Earth Planet. Sci. Lett.* **50**, 105-114.

ELDERFIELD H., MC CAFFREY R.J., LUEDTKE N., BENDER M. and TRUESDALE V.W. (1981) Chemical diagenesis in Narragansett Bay sediments. *Amer. J. Sci.* **281**, 1021-1055.

EMERSON S and HEDGES J.I. (1988) Processes controlling the organic carbon content of open ocean sediments. *Paleoceanography*, **3**, 621-634.

EMERSON S., CRANSTON R.E. and LISS P.S. (1979). Redox species in a reducing fjord: equilibrium and kinetic considerations. *Deep-Sea Res.* **26**, 859-878.

EMERSON S., KALHORN S., JACOBS L., TEBO B.M., NEALSON K.H. and ROSSON R.A. (1982). Environmental oxidation rate of manganese(II): bacterial catalysis. *Geochim. Cosmochim. Acta* **46**, 1073-1079.

EMERSON S., STUMP C., GROOTES P.M., STUIVER M., FARWELL G.W. and SCHMIDT F.H. (1987) Estimates of degradable organic carbon in deep-sea surface sediments from ^{14}C concentrations. *Nature* **329**, 51-53.

EVENSEN N.M, HAMILTON P.J and O'NIONS R.K. (1978) Rare-earth abundances in chondritic meteorites. *Geochim. Cosmochim. Acta* **42**, 1199-1212.

FOSSING H. and JØRGENSEN B.B. (1990) Isotope exchange reactions with radiolabelled sulfur compounds in anoxic seawater. *Biogeochem.* **9**, 233-245.

FRANCOIS R. (1988) A study on the regulation of the concentrations of some trace metals (Rb, Sr, Zn, Pb, Cu, V, Cr, Ni, Mn and Mo) in Saanich Inlet Sediments, British Columbia, Canada. *Mar. Geol.* **83**, 285-308.

FROELICH P.N., KLINKHAMMER G.P., BENDER M.L., LUEDTKE N.A., HEATH G.R., CULLEN D., DAUPHIN P., HAMMOND D., HARTMAN B. and MAYNARD V. (1979) Early oxidation of organic matter in pelagic sediments of the eastern equatorial Atlantic: suboxic diagenesis. *Geochim. Cosmochim. Acta* **43**, 1075-1090.

FROELICH P.N., KIM K.-H., JANHKE R., BURNETT W.C., SOUTAR A. and DEAKIN M. (1983) Pore water fluoride in Peru continental margin sediments: uptake from seawater. *Geochim. Cosmochim. Acta* **47**, 1605-1612.

FROELICH P.N., ARTHUR M.A., BURNETT W.C., DEAKIN M., HENSLEY V., JANHKE R., KAUL L., KIM K.-H., ROE K., SOUTAR A. and VATHAKANON C. (1988) Early diagenesis of organic matter in Peru continental margin sediments: Phosphorite precipitation. *Mar. Geol.* **80**, 309-343.

GAANS van P.F.M. (1989) WATEQX-- A restructured, generalized and extended Fortran 77 computer code and database format for the WATEQ aqueous chemical model for element speciation and mineral saturation, for use on personal computers and mainframes. *Computers and Geoscience* **15**, 843-887.

GARBER J.H. (1984) Laboratory study of nitrogen and phosphorus remineralization during the decomposition of coastal plankton and seston. *Estuar. Coast. Shelf Sci.* **18**, 685-702.

GARRELS R. M. and THOMPSON M.E. (1962) A chemical model for seawater at 25°C and one atmosphere total pressure. *Amer. J. Sci.* **260**, 57-66.

GARRELS R. M. and CHRIST C.L. (1965) *Solutions, Minerals and Equilibria*, Harper, New York, 450 p.

GARRISON R.E., KASTNER M. and ZENGER D.H., editors (1984) Dolomites of the Monterey Formation and other organic-rich units. *Society of Economic Paleontologists and Mineralogists Pacific Section Special Publication* **41**, 215 p.

GIESKES J.M. (1983) The chemistry of interstitial waters of deep-sea sediments: Interpretation of Deep Sea drilling data In Riley J.P., Chester, R., eds., Chemical Oceanography, v.8., Academic Press, London, p. 221-269.

GIESKES J.M., ELDERFIELD H., LAWRENCE J.R., JOHNSON J., MEYERS B. and CAMPBELL A. (1982) Geochemistry of interstitial waters and sediments, Leg 64, Gulf of California. *Init. Rep. DSDP* **64**, Washington, DC, U.S., Government Printing Office, pp. 675-694.

GLENN C.R. and ARTHUR M.A. (1985) Sedimentary and geochemical indicators of productivity and oxygen contents in modern and ancient basins: The Holocene Black Sea as the "type" anoxic basin. *Chem. Geol.* **48**, 325-354.

GOLDHABER M.B. and KAPLAN I.R. (1974) The sulfur cycle. In *The Sea* (ed. E.D. GOLDBERG), Vol. 5, pp. 569-655. J. Wiley & Sons.

GOLDHABER M.B. and KAPLAN I.R. (1975) Controls and consequences of sulfate reduction in recent marine sediments. *Soil Sci.* **119**, 42-55.

GOLDHABER M.B. and KAPLAN I.R. (1980) Mechanisms of sulfur incorporation and isotope fractionation during early diagenesis in sediments of the Gulf of California. *Mar. Chem.* **9**, 95-143.

GRASSHOFF K. (1975) The hydrochemistry of landlocked basins and fjords: in Riley, J.P., Chester, R., eds., Chemical Oceanography, v. 2, Academic Press, London, p. 456-598.

GRUNSEICH G.S. and DUEDALL I.W. (1978) The decomposition of sewage sludge in seawater. *Water Res.* **12**, 535-545.

HAMILTON S.E. and HEDGES J.I. (1988) The comparative geochemistries of lignins and carbohydrates in an anoxic fjord. *Geochim. Cosmochim. Acta* **52**, 129-142.

HARDIE L.A. (1987) Dolomitization: A critical view of some current views. *Jour. Sed. Pet.* **57**, 166-183.

HARTMAN P. (1982) On the growth of dolomite and kaolinite crystals. *Neues Jahrbuch fur Mineralogie Monatshefte* **2**, 84-92.

HARTMANN M. and NIELSEN H. (1969) δ^{34}S-Werte in rezenten Meeressedimenten und ihre Deutung am Beispiel einiger Sedimentprofile aus der westlichen Ostsee. *Geol. Rundsch.* **58**, 621-655.

HARTMANN M., MüLLER P., SUESS E. and VAN DER WEIJDEN C.H. (1973) Oxidation of organic matter in recent marine sediments. *Meteor. Forsch.-Ergebnisse* **12**, 77-86.

HEGGIE D., MARIS C., HUDSON A., DYMOND J., BEACH R. and CULLEN J. (1987) Organic carbon oxidation and preservation in NW Atlantic continental margin sediments. In Weaver P.P.E. and Thomson J. (eds.), *Geology and Geochemistry of Abyssal Plains*, Geological Society Special Publ. No. 31. Blackwell Scientific Publications, London, pp 167-177.

HELDER W. (1989) Early diagenesis and sediment-water exchange in the Savu Basin (eastern Indonesia). *Neth. J. Sea Res.* **24**, 555-572.

HELDER W. and DE VRIES R.T.P. (1979) An automated phenol-hypochlorite method for the determination of ammonia in sea- and brackish waters. *Neth. J. Sea Res.* **13**, 154-160.

HENNEKE E., LUTHER, G.W. III and DE LANGE G.J. (1991) Determination of inorganic sulphur speciation in recent hypersaline anoxic sediments with polarographic techniques. *Mar. Geol.* (in press)

HENRICHS S.M. and REEBURGH W.S. (1987) Anaerobic mineralization of marine sediment organic matter: Rates and the role of anaerobic processes in the oceanic carbon economy. *Geomicrobiol. J.* **5**, 191-237.

HENRICHS S.M. and DOYLE A.P. (1986) Decomposition of ^{14}C-labeled organic substances in marine sediments. *Limnol. Oceanogr.* **31**, 765-778.

HENRICHS S.M. and FARRINGTON J.W. (1987) Early diagenesis of amino acids and organic matter in two coastal marine sediments. *Geochim. Cosmochim. Acta* **51**, 1-15.

HOLLAND H.D. (1984) The chemical evolution of the atmosphere and oceans, Princeton University Press, Princeton, 582p.

HSÜ K.J., MONTADERT L., BERNOULLI D., et al (1977), History of the Mediterranean salinity crisis. *Nature* **267**, 399-403.

HUERTA-DIAZ M.A. and MORSE J.W. (1990a) A quantitative method for determination of trace metal concentrations in sedimentary pyrite. *Mar. Chem.* **29**, 119-144.

HUERTA-DIAZ M.A. and MORSE J.W. (1990b) Pyritization of trace metals in anoxic marine sediments. *Geochim. Cosmochim. Acta* (submitted).

IRGOLIC K.J. and STOCKTON R.A. (1987) Element-specific detectors for liquid chromatography: the determination of arsenic compounds. *Mar. Chem.* **22**, 265- 278.

JAKOBSEN R. and POSTMA D. (1989) Formation and solid solution of Ca-rhodochrosites in marine muds of the Baltic deeps. *Geochim. Cosmochim. Acta.* 53, 2639-2648.

JAHNKE R.A. (1984) The synthesis and solubility of carbonate fluoroapatite. *Amer. J. Sci.* **284**, 58-78.

JAHNKE R.A., EMERSON S.R., ROE K.K. and BURNETT W.C. (1983) The present day formation of apatite in Mexican continental margin sediments. *Geochim. Cosmochim. Acta* **47**, 259-266.

JANSSEN B.H. (1984) A simple method for calculating decomposition and accumulation of 'young' soil organic matter. *Plant and Soil* **76**, 297-304.

JEANDEL C., CAISSO M. and MINSTER J.F.(1987) Vanadium behaviour in the global ocean and in the Mediterranean Sea. *Mar. Chem.* 21, 51-74.

JOHNSON T.C., EVANS J.E. and EISENREICH S.J. (1982) Total organic carbon in Lake Superior sediments: Comparisons with hemipelagic and pelagic marine environments. *Limnol. Oceanogr.* **27**, 481-491.

JØRGENSEN B.B. (1977) The sulfur cycle of a coastal marine sediment (Limfjorden, Denmark). *Limnol. Oceanogr.* **22**, 814-832.

JØRGENSEN B.B. (1978) A comparison of methods for the quantification of bacterial sulfate reduction in coastal marine sediments. II Calculation from mathematical models. *Geomicrobiol. J.* **1**, 29-47.

JØRGENSEN B.B. (1979) A theoretical model of the stable sulfur isotope distribution in marine sediments. *Geochim. Cosmochim. Acta* **43**, 363-374.

JØRGENSEN B.B. (1982) Mineralization of organic matter in the sea bed - The role of sulphate reduction. *Nature* **296**, 643-645.

JØRGENSEN B.B. (1983) Processes at the sediment-water interface. In: The major Biogeochemical cycles and their interactions, eds. Bolin B. and Cook R.B., SCOPE 21, John Wiley & Sons, Chicester, 477-515.

JUMARS P.A., ALTENBACH A.V., DE LANGE G.J., EMERSON S.R., HARGRAVE B.T., MULLER P.J., PRAHL F.G., REIMERS C.E., STEIGER T. and SUESS E. (1988) Transformation of seafloor-arriving fluxes into the sedimentary record. In *Productivity of the ocean: Present and Past.*, eds., W.H. Berger, Y. Smetaceh and D. Wefer, Life Sciences Res. Rpt. 44, pp. 291-311, J. Wiley & Sons.

KAPLAN I.R., EMERY K.O. and RITTENBERG S.C. (1963) The distribution and isotopic composition of sulphur in recent marine sediments off Southern California. *Geochim. Cosmochim. Acta* **27**, 297-331.

KATZ A. and MATTHEWS A. (1977) The dolomitization of $CaCO_3$: an experimental study at 252-295 °C. *Geochim. Cosmochim. Acta* **41**, 297-308.

KELTS K. and McKENZIE J. (1982) Diagenetic dolomite formation in Quaternary anoxic diatomaceous muds of Deep Sea Drilling Project Leg 64, Gulf of California, *in* Curray, J.R., Moore, D.G., et al., Initial reports of the Deep Sea Drilling Project, Volume 64: Washington, D.C., U.S. Government Printing Office, p. 553-569.

KENNEDY H.A. and ELDERFIELD H. (1987) Iodine diagenesis in pelagic deep-sea sediments. *Geochim. Cosmochim. Acta* **51**, 2489-2504.

KENNETT J.P. (1982). *Marine geology.* Prentice-Hall Inc., Englewood Cliffs, 1-752.

KENNICUTT M.C. II, BARKER C., BROOKS J.M., DEFREITAS D.A. and ZHU G.H. (1987) Selected organic matter source indicators in the Orinoco, Nile and Changjiang deltas. *Org. Geoch.* 11, 41-51.

KINNIBURGH D.G. and JACKSON M.L. (1981) Cation adsorption by hydrous metal oxides and clay. In: *Adsorption of inorganics at solid/liquid interfaces*, eds. Anderson M.A. and Rubin A.J., Ann Arbor Science.

KÖGLER F.C. and LARSEN B. (1979) The West Bornholm basin in the Baltic Sea: Geological structure and quaternary sediments. *Boreas* **8**, 1-22.

KOHNEN M.E.L., SINNINGHE DAMSTE J.S., TEN HAVEN H.L. and DE LEEUW J.W. (1989) Early incorporation of polysulfide in sedimentary organic matter. *Nature*, **341**, 640-641.

KOOP K., BOYNTON W.R., WULFF F. and CARMAN R. (1990) Sediment-water oxygen and nutrient exchanges along a depth gradient in the Baltic Sea. *Mar. Ecol. Prog. Ser.* **63**, 65-77.

KROM M.D. and BERNER R.A. (1980) Adsorption of phosphate in anoxic sediments. *Limnol. Oceanogr.* **25**, 797-806.

KROM M.D. and BERNER R.A. (1981) The diagenesis of phosphorus in a nearshore marine sediment. *Geochim. Cosmochim. Acta* **45**, 207-216.

KUENEN PH. G. (1943) Collection of the samples and some general aspects. *Snellius Exped.* 1929-1930. Vol. V, part 3, E.J. Brill, Leiden, 1-46.

LAND L.S. (1980) The isotopic and trace element geochemistry of dolomite. The state of the art, *in* Zenger, D.H., Dunham, J.B., and Ethington, R.L., editors, Concepts and models of dolomitization: Society of Economic Paleontologists and Mineralogists Special Publication 28, p. 87-110.

LANGE C.B., BERGER W.H., BURKE S.K., CASEY R.E., SCHIMMMELMAN A., SOUTAR A. and WEINHEIMER A.L (1987) El Nino in Santa Barbara Basin: Diatom, radiolarian and foraminiferan responses to the 1983 El Nino event. *Mar. Geol.* **78**: 153-160.

LASAGA A.C. and HOLLAND H.D. (1976) Mathematical aspects of non-steady- state diagenesis. *Geochim. Cosmochim. Acta* **40**, 257-266.

LECKIE D.A., SINGH C., GOODARZI F. and WALL J.H. (1990) Organic-rich, radioactive marine shale: a case study of a shallow-water condensed section, Cretaceous Shaftesbury Formation, Alberta, Canada. *Jour. Sed. Petr.* **60**, 101-117.

LEEDER M., RAISWELL R., AL-BIATTY H., McMAHON A. and HARDMAN M. (1990) Carboniferous stratigraphy, sedimentation and correlation of well 48/3-3 in the southern North Sea Basin: integrated use of palynology, natural gamma/sonic logs and carbon/sulphur geochemistry. *Jour. Geol. Soc. London* **147**, 287-300.

LEIN A.Y., VAYNSHTEYN M.B., NAMSARAYEH B.B., KASHPARRORA Y.E., MATROSOV A.G., BONDAR V.A. and IVANOV M.V. (1982) Biogeochemistry of anaerobic diagenesis of recent Baltic sediments. *Geoch. Int.* **19**, 90-103.

LERMAN A. (1975) Maintenance of steady state in oceanic sediments. *Amer. J. Sci* **275**,

LERMAN A. (1979) *Geochemical Processes: Water and Sediment Environments*, John Wiley & Sons, New York, 1-481.

LERMAN A. and WEILER R.R. (1970) Diffusion and accumulation of chloride and sodium in Lake Ontario sediment. *Earth Planet. Sci. Lett.* **10**, 150-156.

LERMAN A. and JONES B.F. (1973) Transient and steady-state salt transport between sediments and brine in closed lakes. *Limnol. Oceanogr.* **18**, 72-85.

LEVENTHAL J.S. (1983) An interpretation of carbon and sulfur relationships in Black Sea sediments as indicators of environments of deposition. *Geochim. Cosmochim. Acta* **47**, 133-138.

LEVENTHAL J.S. (1987) Carbon and sulfur relationships in Devonian shales from the Appalachian Basin as an indicator of environment of deposition. *Amer. J. Sci.* **287**, 33-49.

LI Y.-H. and GREGORY S. (1974) Diffusion of ions in seawater and in deep-sea sediments. *Geochim. Cosmochim. Acta* **38**, 703- 714.

LI Y.-H., BURKHARDT L., BUCHHOLTZ M., O'HARA P. and SANTSCHI P.H. (1984) Partition of radiotracers between suspended particles and seawater. *Geochim. Cosmochim. Acta* **48**, 2011-2019.

LINDEN W.J.M. VAN, HARTOSUKOHARDJO S. and SUKARDJONO H. (1989) Kau Bay, Halmahera, regional setting, physiography and shallow structure. *Neth. J. Sea Res.* **24**, 573-581.

LIPPMANN F. (1973) *Sedimentary carbonate minerals*, New York, Springer-Verlag, 228 p.

LORD C.J. III (1982) A selective and precise method for pyrite determination in sedimentary materials *J. Sed. Pet.* **52**, 664-666.

LUTHER G.W. III, CHURCH T.M. GIBLIN A.E. and HOWARTH R.W. (1986) Speciation of dissolved sulfur in salt marshes by polarographic methods. In: M. Sohn (editor), Organic Marine Geochemistry, ACS Symp. Ser., **305**, 339-355.

LUTHER G.W. III and COLE H. (1988) Iodine speciation in Chesapeake Bay waters. *Mar. Chem.* **27**, 315-325.

LUTHER G.W. III, SWARTZ C.B. and ULLMAN W.J. (1988) Direct determination of Iodide in Seawater by Cathodic Stripping Square Wave Voltammetry. *Anal. Chem.* **60**, 1721-1724.

LYONS T.W. and BERNER R.A. (1990) Reactive iron in Black Sea sediments. *EOS* **71**, 173.

MAES A. and CREMERS A. (1986) Highly selective ion-exchange in clay minerals and zeolites. In: *Geochemical Processes at Mineral Surfaces*, eds. J.A. Davis and K.F. Hayes, ACS **323**, 254-295.

MACHEL H.G. and MOUNTJOY E.W. (1986) Chemistry and environments of dolomitization - A reappraisal. *Earth-Science Reviews* **23**, 175-222.

MACKIN J.E. and ALLER R.C. (1984) Ammonium adsorption in marine sediments. *Limnol. Oceanogr.* **29**, 250-257.

MANHEIM F.T. (1961) A geochemical profile of the Baltic Sea. *Geochim. Cosmochim. Acta* **25**, 52-71.

MANHEIM F.T. (1982) Geochemistry of manganese carbonates in the Baltic Sea. *Stockholm Contrib. Geol.* **37**, 145-149.

MANHEIM F.T. and CHAN K.M. (1974) Interstitial waters of Black Sea sediments: New Data and review, in: Degens, E.T. and Ross, D.A., eds., The Black Sea-geology, chemistry and biology. - American Association of Petroleum Geologists Memoir **20**: 155-180.

MARTENS C.S. and KLUMP J.V. (1984) Biogeochemical cycling in an organic- rich marine basin. 4. An organic carbon budget for sediments dominated by sulfate reduction and methanogenesis. *Geochim. Cosmochim. Acta* **48**, 1987- 2004.

MARTENS C.S., BERNER R.A. and ROSENFELD J.K. (1978) Interstitial water chemistry of anoxic Long Island Sound sediment. 2. Nutrient regeneration and phosphate removal. *Limnol. Oceanogr.* **23**, 605-617.

MARTIN W.R. and BENDER M.L. (1988) The variability of benthic fluxes and sedimentary remineralization rates in response to seasonally variable organic carbon rain rates in the deep sea: A modelling study. *Amer. J. Sci.* **288**, 561-574.

MATELES R.I. and CHIAN S.K. (1969) Kinetics of substrate uptake in pure and mixed culture. *Envir. Sci. Technol.*, **3**, 569-574.

McLENNAN S.M. (1989) Rare Earth Elements in sedimtary rocks: Influence of provenance and sedimentary processes. *Rev. in Mineral.* **21**, 169-200.

McNICHOL A.P., LEE C. and DRUFFEL E.R.M. (1988) Carbon cycling in coastal sediments: 1 A quantitative estimate of the remineralization of organic carbon in the sediments of Buzzards Bay, MA. *Geochim. Cosmochim. Acta* **52**, 1531-1543.

MIDDELBURG J.J. (1989) A simple rate model for organic matter decomposition. *Geochim. Cosmochim. Acta* **53**, 1566-1571.

MIDDELBURG J.J. (1991) Organic matter decomposition in the marine environment. In: *Encyclopedia of Earth System Science*, ed., W. A. Nierenberg, Academic Press, San Diego, (in press).

MIDDELBURG J.J. and DE LANGE G.J. (1989) The isolation of Kau Bay during the last glaciation: direct evidence from interstitial water chlorinity. *Neth. J. Sea Res.* **24**, 615-622.

MIDDELBURG J.J., DE LANGE G.J. and VAN DER WEIJDEN C.H. (1987) Manganese solubility control in marine pore waters. *Geochim. Cosmochim. Acta* **51**, 759-763.

MIDDELBURG J.J., DE LANGE G.J., VAN DER SLOOT H.A., VAN EMBURG P.R. and SHOFIYAH S. (1988a) Particulate manganese and iron framboids in Kau Bay, Halmahera (eastern Indonesia). *Mar. Chem.* **34**, 353-364.

MIDDELBURG J.J., HOEDE D., VAN DER SLOOT H.A., VAN DER WEIJDEN C.H. and WIJKSTRA J.W. (1988b) Arsenic, antimony and vanadium in the North Atlantic Ocean. *Geochim. Cosmochim. Acta* **52**, 2871-2878.

MIDDELBURG J.J., DE LANGE G.J., VAN DER WEIJDEN C.H. and SHOFIYAH S. (1989) Sediment chemistry of Kau Bay, Halmahera (eastern Indonesia). *Neth. J. Sea Res.* **24**, 607-613.

MIDDELBURG J.J., DE LANGE G.J. and KREULEN R. (1990) Dolomite formation in anoxic sediments of Kau Bay, Indonesia. *Geology* **18**, 399-402.

MILLERO F.J. and SCHREIBER D.R. (1982) Use of the ion pairing model to estimate activity coefficients of the ionic components of natural waters. *American Journal of Science* **282**, 1508-1540.

MORRIS A.W. (1975) Dissolved molybdenum and vanadium in the northeast Atlantic Ocean. *Deep-Sea Res.* **22**, 49-54.

MORROW D.W. and RICKETTS B.D. (1986) Chemical controls on the precipitation of mineral analogues of dolomite: The sulfate enigma. *Geology* **14**, 408-410.

MORROW D.W. (1982) Diagenesis 2. Dolomite - Part 2, Dolomitization models and ancient dolostones. *Geoscience Canada* **9**, 95-107.

MORSE J.W. (1983) The kinetics of calcium carbonate dissolution and precipitation. In: *Carbonates: Mineralogy and Chemistry*, ed. J. Reeder, *Rev. in Miner.* **11**, 227-264.

MORSE J.W. and CORNWELL J.C. (1987) Analysis and distribution of iron sulfide minerals in recent anoxic marine sediments. *Mar. Chem.* **22**, 55-69.

MORSE J.W. and CASEY W.H. (1988) Ostwald processes and mineral paragenesis in sediments. *Amer. J. Sci.* **288**, 537-560.

MORSE J.W. and BENDER M.L. (1990) Partition coefficients in calcite: Examination of factors influencing the validity of experiments and their applications to natural systems. *Chem. Geol.* **82**, 265-277.

MORSE J.W., MILLERO F.J., CORNWELL J.C. and RICKARD D. (1987) The chemistry of hydrogen sulfide and iron sulfide systems in natural waters. *Earth-Science Rev.* **24**, 1-42.

MUCCI A. (1988) Manganese uptake during calcite precipitation from seawater: Conditions leading to the formation of pseudo-kutnahorite. *Geochim. Cosmochim. Acta* **52**, 1859-1868.

MÜLLER P.J. and MANGINI A. (1980). Organic carbon decomposition rates in sediments of the Pacific Manganese Nodule belt dated by ^{230}Th and ^{231}Pa. *Earth Planet. Sci. Lett.* 51, 94-114.

MURRAY J.W., GRUNDMANIS V. and SMETHIE W.M. (1978) Interstitial water chemistry in the sediments of Saanich Inlet. *Geochim. Cosmochim. Acta* **42**, 1011-1026.

MURRAY J.W., JANNASCH H.W., HONJO S., ANDERSON R.F., REEBURGH W.S., TOP Z., FRIEDERICH G.E., CODISPOTI L.A. and IZDAR, E. (1989) Unexpected changes in the oxic/anoxic interface in the Black Sea. *Nature* **338**, 411-413.

MYERS K.J. and WIGNALL P.B. (1987) Understanding Jurassic Organic-rich Mudrocks - New concepts using gamma-ray spectrometry and palaeoecology: Examples from the Kimmeridge Clay of Dorset and the Jet Rock of Yorkshire: in Legget, J.K., and Zuffa, G.G., Marine Clastic Sedimentology, Graham and Trotman, p. 172-189.

NEEB G.A. (1943) The composition and distribution of the samples. Snellius Exped. 1929-1930, Vol. V, part 3, section II, E.J. Brill, Leiden: 1-268.

OENEMA O. (1990) Sulfate reduction in fine-grained sediments in the Eastern Scheldt, southwest Netherlands. *Biogeochem.* **9**, 53-74.

PAULL C.K., MARTENS C.S., CHANTON J.P., NEUMANN A.C., COSTON J., JULL A.J.T. and TOOLIN L.J. (1990) Old carbon in living organisms and young $CaCO_3$ cements from abyssal brine seeps. *Nature* **342**, 166-168.

PEDERSEN T.F. and SHIMMIELD G.B. (1990) Interstitial water chemistry, Leg 117: Contrasts with the Peru Margin. In: *Proc. ODP Sci. Results* **117** (in press)

PETERSON M.L. and CARPENTER R. (1983) Biogeochemical processes affecting total arsenic and arsenic species distributions in an intermittently anoxic fjord. *Mar. Chem.* 12, 295-321.

PISCIOTTO V.A. and MAHONEY J.J. (1981) Isotopic survey of diagenetic carbonates, Deep Sea Drilling Project Leg 63, *in* R. Yeats, B. Haq, et al., Initial Reports of the Deep Sea Drilling Project, v. 63, p. 595-609.

PLUMMER L.N., JONES B.F. and TRUESDELL A.H. (1976) WATEQF-A FORTRAN IV version of WATEQ, a computer program for calculating chemical equilibrium of natural waters: U.S. Geological Survey Water Resources Investigation 76-13.

POSTMA D. (1982) Pyrite and siderite formation in brackish and freshwater swamp sediments. *Amer. J. Sci.*, **282**, 1151-1183.

POSTMA D. and BROCKENHUUS-SCHACK B.S. (1987) Diagenesis of iron in proglacial sand deposits of late- and post-Weichselian age. *J. Sed. Pet.* 57, 1040-1053.

PRAHL F.G. and MUEHLHAUSEN L.A. (1989) Lipid biomarkers as geochemical tools for paleoceanographic study. in Berger, W.H., Smetacek, V.S. and Wefer G., eds. Productivity of the Ocean: Present and Past, John Wiley & Sons, pp. 271-284.

PRICE N. B. (1976) Chemical diagenesis in sediments. *in:* Riley J.P., Chester, R., eds., *Chemical Oceanography,* v.6., Academic Press, London, p. 1-59

PRICE N.B. and CALVERT S.E. (1973) A study of the geochemistry of suspended particulate matter in coastal waters. *Mar. Chem.* **1**, 169-189.

PRICE N.B. and SKEI J.M. (1975) Areal and seasonal variations in the chemistry of suspended particulate matter in a deep fjord. *Estuarine and Coastal Mar. Sci.* **3**, 349-369.

RAISWELL R. (1987) Non-steady state microbiological diagenesis and the origin of concretions and nodular limestones, *in* Marshall, J.D., editor, The diagenesis of sedimentary sequences. *Geological Society of London Special Publication* **36**, 41-54.

RAISWELL R. (1988a) Evidence for surface reaction-controlled growth of carbonate concretions in shales. *Sedimentology* **35**, 571-575.

RAISWELL R. (1988b) Chemical model for the origin of minor limestone-shale cycles by anaerobic methane oxidation. *Geology* **16**, 641-644.

RAISWELL R. and BERNER R.A. (1985) Pyrite formation in euxinic and semi-euxinic sediments. *Amer. J. Sci.* **285**, 710-724.

RAISWELL R. and AL-BIATTY H.J. (1989) Depositional and diagenetic C-S-Fe signatures in early Paleozoic normal marine shales. *Geochim. Cosmochim. Acta* **53**, 1147-1152.

RAISWELL R., BUCKLEY F., BERNER R.A. and ANDERSON T.F. (1988) Degree of pyritization of iron as a paleoenvironmental indicator of bottom water oxygenation. *J. Sediment. Petrol.* **58**, 812-819.

REEBURGH W.S. (1967) An improved interstitial water sampler. - *Limnol. Oceanogr.* **12**: 163-170.

REEBURGH W.S. (1976) Methane consumption in Cariaco Trench waters and sediments. *Earth Planet. Sci. Lett.* **28**, 337-344.

REEBURGH W.S. (1980) Anaerobic methane oxidation: Rate depth distributions in Skan Bay sediments. *Earth Plan. Sci. Lett.* **47**, 345-352.

REIMERS C.E. (1988) The control of benthic fluxes by particulate supply. In: *Productivity of the ocean: Present and Past.*, eds., W.H. Berger, Y. Smetaceh and D. Wefer, Life Sciences Res. Rpt. 44, pp. 291-311, J. Wiley & Sons.

REIMERS C.E. and SUESS E. (1983) The partitioning of organic carbon fluxes and sedimentary organic matter decomposition rates in the ocean. *Mar. Chem.* **13**, 141-168.

RICHARDS F.A. (1960) Some chemical and hydrographic observations along the north coast of South America - I. Cabo Tres Puntas to Curacao including the Cariaco Trench and the Gulf of Cariaco. *Deep-Sea Res.* 7, 163-182.

RICKARD D.T. (1975) Kinetics and mechanism of pyrite formation at low temperatures. *Amer. J. Sci* **275**, 636-652.

RIEL P.M. VAN (1943) The bottom water, introductory remarks and oxygen content. *Snellius Exped.* 1929-1930. Vol. II, part 5, E.J. Brill, Leiden, 1-62.

RITGER S., CARSON B. and SUESS E. (1987) Methane-derived authigenic carbonates formed by subduction-induced pore-water expulsion along the Oregon/Washington margin. *Geol. Soc. Amer. Bull.* **98**, 147-156.

ROBBINS J.M., LYLE M. and HEATH G.R. (1984) A sequential extraction procedure for partitioning elements among co-existing phases in marine sediments. *Oregon State Univ. Report 84-3.*

ROSENFELD J.K. (1981) Nitrogen diagenesis in Long Island Sound sediments. *Amer. J. Sci.* **281**, 436-462.

ROSS D.A. and DEGENS E.T. (1974) Recent sediments of the Black Sea. In: Degens, E.T. and Ross, D.A. eds., The Black Sea-Geology, chemistry and biology. *Amer. Ass. Petr. Geol. Mem.* 20, p. 183-199.

ROSS D.A., DEGENS E.T. and MACILVAINE J. (1970) Black Sea: Recent sedimentary history. *Science* **170**, 163-165.

ROTH E. and POTY B. (1989) *Nuclear Methods of Dating.* Kluwer Academic Publ., 600p.

SADIQ M. (1988) Thermodynamic solubility relationships of inorganic vanadium in the marine environment. *Mar. Chem.* **23**, 87-96.

SAYLES F.L. (1979) The composition and diagenesis of interstitial solutions - I. Fluxes across the seawater-sediment interface in the Atlantic Ocean. *Geochim. Cosmochim. Acta* **43**, 527-545.

SAYLES F.L. and MANGELSDORF P.C. (1977) The equilibration of clay minerals with seawater: exchange reactions. *Geochim. Cosmochim. Acta* **41**, 951-960.

SCHOLTEN S.O. and KREULEN R. (1990) Early diagenetic changes in nitrogen and carbon isotopes of marine sediments. (submitted).

SHAFFER G. (1987) Redfield ratios, primary production, and organic carbon burial in the Baltic Sea. *Deep-Sea Res.* **34**, 769-784.

SHAW T.J., GIESKES J.M. and JAHNKE R.A. (1990) Early diagenesis in differing depositional environments: The response of transition metals in pore water. *Geochim. Cosmochim. Acta* **54**, 1233-1246.

SHERREL R.M. and BOYLE E.A. (1988) Zinc, Chromium, Vanadium and Iron in the Mediterranean Sea. *Deep-Sea Res.* **35**, 1319-1334.

SHILLER A.M. and BOYLE E.A. (1987) Dissolved vanadium in rivers and estuaries. *Earth Planet. Sci. Lett.* **86**, 214-224.

SHILLER A.M., GIESKES J.M. and PRICE N.B. (1985) Particulate iron and manganese in the Santa Barbara Basin, California. *Geochim. Cosmochim. Acta* **49**, 1239-1249.

SHIMMIELD G.B. and PRICE N.B. (1984) Recent dolomite formation in hemi-pelagic sediments off Baja California, Mexico, *in* Garrison, R.E., Kastner, M., and Zenger, D.H., editors, 1984, Dolomites of the Monterey Formation and other organic-rich units. *Society of Economic Paleontologists and Mineralogists Pacific Section Special Publication* 41, 5-18.

SHOLKOVITZ E. (1973) Interstitial water chemistry of the Santa Barbara Basin sediments. *Geochim. Cosmochim. Acta* **37**, 2043-2073.

SHOLKOVITZ E.R. (1988) Rare Earth elements in the sedimentsof the North Atlantic Ocean, Amazon Delta and East China Sea: reinterpretation of terrigenous input patterns to the oceans. *Amer. J. Sci.* **288**, 236-281.

SIBLEY D.F., DEDOES R.E. and BARTLETT R. (1987) Kinetics of dolomitization. *Geology* **15**, 1112-1114.

SKEI J.M. and MELSOM S. (1982) Seasonal and vertical variation in the chemical composition of suspended particulate matter in an oxygen-deficient fjord. *Estuarine and Coastal Mar. Sci.* **14**, 61-78.

SPENCER D.W. and SACHS P.L. (1970) Some aspects of the distribution, chemistry and mineralogy of suspended matter in the Gulf of Maine. *Mar. Geol.* **9**, 117-136.

SPENCER D.W., BREWER P.G. and SACHS P.L. (1972) Aspects of the distribution and trace element composition of suspended matter in the Black Sea. *Geochim. Cosmochim. Acta* **36**, 71-86.

SPIKER E.C. and HATCHER P.G. (1984) Carbon isotope fractionation of sapropelic organic matter during early diagenesis. *Org. Geochem.* **5**, 283-290.

SPOSITO G. (1984) *The surface chemistry of soils.* Oxford University Press, New York.

SPOTTS J. and SILVERMAN S. (1966) Organic dolomite from Point Fermin, California. *Amer. Miner.* **51**, 1144-1155.

STATHAM P.J., BURTON J.D. and MAHER, W.A. (1987) Dissolved arsenic in waters of the Cape Basin. *Deep-Sea Res.* **34**, 1353-1359.

STRAKHOV N.M. (1971) Geochemical evolution of the Black Sea in the Holocene. *Lithology and Mineral Resources*, **3**, 263-274.

STRICKLAND J.D.H. and PARSONS T.R. (1968) A practical handbook of seawater analysis. *Fish. Board. Canada Bull.* **167**, 311p.

STUMM-ZOLLINGER E. (1968) Substrate utilization in heterotrophic bacterial communities. *J. Water Pollut. Control Fed.* **40**, 213-229.

STUMM W. and MORGAN J.J. (1981) Aquatic chemistry. New York, John Wiley & Sons, 780p.

SUESS E. (1976) *Porenlösungen mariner Sedimente - Ihre chemische Zusammensetzung als Audruck frühdiagenetischer Vorgänge.* Habilitationsschrift. Universitat Kiel, 193p.

SUESS E. (1979) Mineral phases formed in anoxic sediments by microbial decomposition of organic matter. *Geochim. Cosmochim. Acta* **43**, 339-352.

SUESS E. (1981) Phosphate regeneration from sediments of the Peru continental margin by dissolution of fish debris. *Geochim. Cosmochim. Acta* **45**, 577-588.

SUESS E. (1982) Authigenic barite in varved clays: Result of marine transgression over freshwater deposits and associated changes in interstitial water chemistry. In: *The dynamic environment of the ocean floor*, eds. Fanning and Manheim, Lexington Books, 339-355.

SUESS E., VON HUENE R., et al. (1988) Ocean Drilling Program Leg 112, Peru continental margin: Part 2, Sedimentary history and diagenesis in a coastal upwelling environment. *Geology* **16**, 939-943.

SWIDER K.T. and MACKIN J.E. (1989) Transformations of sulfur compounds in marsh-flat sediments. *Geochim. Cosmochim. Acta* **53**, 2311-2323.

TAYLOR A.W., FRAZIER A.W. and GURNEY E.L. (1963) Solubility products of magnesium ammonium and magnesium potassium phosphate. *Trans. Faraday Soc.* **59**, 1580-1589.

TEBO B.M. (1983) *The Ecology and Ultrastructure of Marine Manganese Oxidizing Bacteria.* Ph.D. Thesis. University of California, San Diego.

TEBO B.M., NEALSON K.H., EMERSON S. and JACOBS L. (1984) Microbial mediation of Mn(II) and Co(II) precipitation at the O_2/H_2S interface in two anoxic fjords. *Limnol. Oceanogr.* **29**, 1247-1258.

TEGELAAR E.W., DE LEEUW J.W., DERENNE S. and LARGEAU C. (1989) A reappraisal of kerogen formation. *Geochim. Cosmochim. Acta* **53**, 3103-3106.

TERRAIN HANDBOOK 31 (1944) Kaoe Baai (Bay), Allied General Headquarters, Geographic Section, Southwest Pacific Area.

THODE-ANDERSEN S. and JØRGENSEN B.B. (1989) Sulfate reduction and the formation of ^{35}S-labeled FeS, FeS_2 and S° in coastal marine sediment. *Limnol. Oceanogr.* **34**, 793-806.

THOMSON J., HIGGS N.C. and COLLEY S. (1989) A geochemical investigation of reduction haloes developed under turbidites in brown clay. *Mar. Geol.* **89**, 315-330.

TOTH D.J. and LERMAN A. (1977) Organic matter reactivity and sedimentation rates in the ocean. *Amer. J. Sci.* **277**, 465-485.

TRUESDALE V.W. (1975) "Reactive" and "unreactive" iodine in seawater - A possible indication of an organically bound iodine fraction. *Mar. Chem.* **3**, 111-119.

TSUNOGAI S. (1971) Iodine in the deep water of the ocean. *Deep-Sea Res.* **18**, 913-919.

TURNER D.R., WHITFIELD M. and DICKSON A.G (1981) The equilibrium speciation of dissolved components in freshwater and seawater at 25° C and 1 atmosphere pressure. *Geochim. Cosmochim. Acta* **45**, 855-881.

ULLMAN W.J. and ALLER R.C. (1980). Dissolved iodine flux from estuarine sediments and implications for the enrichment of iodine at the sediment-water interface. *Geochim. Cosmochim. Acta* **44**, 1177-1184.

ULLMAN W.J. and ALLER R.C. (1983). Diffusion coefficients in nearshore marine sediments. *Limnol. Oceanogr.* **27**: 552-556.

ULLMAN W.J., LUTHER G.W. III, DE LANGE G.J. and WOITTIEZ J.R.W. (1990) Iodine chemistry in deep anoxic basins and overlying waters of the Mediterranean Sea. *Mar. Chem.* **31** (in press).

VAHRENKAMP V.C. and SWART P.K. (1990) New distribution coefficient for the incorporation of strontium into dolomite and its implications for the formation of ancient dolomites. *Geology* **18**, 387-391.

VAN CAPPELLEN P. and BERNER R.A. (1988) A mathematical model for the early diagenesis of phosphorus and fluorine in marine sediments: apatite precipitation. *Amer. J. Sci.* **288**, 289-333.

VAN DER SLOOT H.A. (1976) Neutron activation analysis of trace elements in water samples after preconcentration on active carbon. Ph.D. dissertation, Free University of Amsterdam: Netherlands Energy Research Foundation Report ECN-1: 218 pp.

VAN DER SLOOT H.A. and ZONDERHUIS J. (1979) Instrumental Neutron Activation Analysis of 37 Geochemical Reference Samples. *Geost. Newsl.* **3**, 185-193.

VAN DER SLOOT H.A., HOEDE D., HAMBURG G., DE LANGE G.J., MIDDELBURG J.J. and SOPHIAH S. (1988) Suspended manganese micro-nodules in Kau Bay, Halmahera (eastern Indonesia). *Mar. Geol.* **82**, 251-259.

VAN DER WEIJDEN C.H., DE LANGE G.J, MIDDELBURG J.J, VAN DER SLOOT H.A, HOEDE D. and S. SHOFIYAH (1989) Geochemical characteristics of Kau Bay water. *Neth. J. Sea Res.* **24**, 583-589.

VAN DER WEIJDEN C.H., MIDDELBURG J.J, DE LANGE G.J, VAN DER SLOOT H.A, HOEDE D. and WOITTIEZ J.R.W. (1990) Profiles of the redox-sensitive trace elements As, Sb, V, Mo, and U in the Tyro and Bannock Basins (eastern Mediterranean). *Mar. Chem.* **31** (in press).

VAN GENUCHTEN, M.Th. (1981) Analytical solutions for chemical transport with simultaneous adsorption, zero-order production and first-order decay. *Jour. of Hydrology*, **49**, 213-233.

VAN LIEW H.D. (1962) Semilogarithmic plots of data which reflect a continuum of exponential processes. *Science* **138**, 682-683.

VERBEEK H. (1987) Hydrography and renewal of the Kau Bay. The Snellius II expedition. Report R87-7. Institute of Meteorology and Oceanography, University of Utrecht.

VINOGRADOV A.P., GRINENKO V.A. and USTINOV V.I. (1962) Isotopic composition of sulphur compounds in the Black Sea. *Geokhimiya* **10**, 973-997.

VOLKOV I.I. (1961) Iron sulfides, their interdependence and transformation to the bottom sediments of the Black Sea. *Akad. Nauk. SSSR Inst. Okeanologii Trudy* **50**, 68-92.

VON BREYMANN M.T., COLLIER R. and SUESS E. (1991) Magnesium adsorption and ion exchange in marine sediments: a multi-component model. *Geochim. Cosmochim. Acta* (submitted).

WANGERSKY P.J. (1986) Biological control of trace metal residence time and speciation: a review and synthesis. *Mar. Chem.* **18**, 269-297.

WEDEPOHL K.H. (1968) Chemical fractionation in the sedimentary environment. In: *Origin and distribution of the elements*, ed., L.H. Ahrens, Pergamon Press, 999-1016.

WEHRLI B. (1987) Vanadium in der Hydrosphäre; Oberflächenkomplexe und Oxidationskinetik. Ph.D. dissertation, ETH Zürich, 129 pp.

WERSIN P., CHARLET L., KARTHEIN R. and STUMM W. (1989) From adsorption to precipitation: Sorption of Mn^{2+} on $FeCO_3$ (s). *Geochim. Cosmochim. Acta* **53**, 2787-2796.

WESTRICH J.T. (1983) *The consequences and controls of bacterial sulfate reduction in marine sediments.* Ph.D. thesis, Yale University, 530 p.

WESTRICH J.T. and BERNER R.A. (1984) The role of sedimentary organic matter in bacterial sulfate reduction: The G-model tested. *Limnol. Oceanogr.* **29**, 236-249.

WHITFIELD, M and TURNER, D.R. (1987) The role of particles in regulating the composition of sea water. In *Aquatic Surface Chemistry* (ed. W. Stumm), pp 457-493, Wiley, New York.

WILSON T.R.S. (1986). Vertical porewater advection in deep-ocean sediments investigated by means of a general diagenetic model. *The Science of the Total Environment* **49**: 163-173.

WILSON T.R.S., THOMSON J., HYDES D.J., COLLEY S., CULKIN F. and SORENSEN J. (1986) Oxidation fronts in pelagic sediments: Diagenetic formation of metal-rich layers. *Science* **232**, 972-975.

WINKLER W.L. (1916) Der Jodid and Jodat Iongehalt des Meerwassers. *Z. Angew. Chem.* **29**, 205-207.

WOITTIEZ J.R.W., WALS G.D., NIEUWENDIJK B.J.T., ZONDERHUIS, J and VAN DER SLOOT H.A. (1991) The determination of iodide, iodate, total inorganic iodine and filterable iodine in seawater. *Mar. Chem.* (submitted).

WONG G.T.F. and BREWER P.G. (1977) The marine chemistry of iodine in anoxic basins. *Geochim. Cosmochim Acta* **41**, 151-159.

WULFF, F and STIGEBRANDT, A. (1989) A time-dependent budget model for nutrients in the Baltic Sea. *Glob. Biogeoch. Cycl.* **3**, 63-78.

CURRICULUM VITAE

Jacobus Bernardus Maria Middelburg werd geboren op 6 mei 1963 te Twello. In 1981 behaalde hij het diploma Atheneum B aan het Geert Grootte College te Deventer. In augustus van dat jaar begon hij met de studie Geologie aan de Rijksuniversiteit te Groningen. In april 1984 werd het kandidaatsexamen met lof afgelegd. De studie werd voortgezet aan de Rijksuniversiteit te Utrecht. In januari 1987 studeerde hij met lof af als geochemicus, met als bijvakken Mariene Geochemie en Sedimentologie. Van februari tot december 1987 was hij werkzaam als toegevoegd onderzoeker bij de afdeling Geochemie van het Instituut voor Aardwetenschappen (IVAU) van de Rijksuniversiteit te Utrecht (RUU). Vervolgens was hij als onderzoeker-in-opleiding in dienst van de Nederlandse organisatie voor wetenschappelijk onderzoek (NWO), werkzaam bij de afdeling Geochemie van het IVAU van de RUU.